https://doi.org/10.5194/essd-2019-128
Preprint. Discussion started: 19 August 2019

Open Access Earth System Science Data Discussions

The Global Methane Budget 2000-2017

Marielle Saunois[1], Ann R. Stavert[2], Ben Poulter[3], Philippe Bousquet[1], Josep G. Canadell[2], Robert B. Jackson[4], Peter A. Raymond[5], Edward J. Dlugokencky[6], Sander Houweling[7,8], Prabir K. Patra[9,10], Philippe Ciais[1], Vivek K. Arora[11], David Bastviken[12], Peter Bergamaschi[13], Donald R. Blake[14], Gordon Brailsford[15], Lori Bruhwiler[6], Kimberly M. Carlson[16,17], Mark Carrol[3], Simona Castaldi[18,19,20], Naveen Chandra[9], Cyril Crevoisier[21], Patrick M. Crill[22], Kristofer Covey[23], Charles L. Curry[24], Giuseppe Etiope[25,26], Christian Frankenberg[27,28], Nicola Gedney[29], Michaela I. Hegglin[30], Lena Höglund-Isaksson[31], Gustaf Hugelius[32], Misa Ishizawa[33], Akihiko Ito[33], Greet Janssens-Maenhout[13], Katherine M. Jensen[34], Fortunat Joos[35],Thomas Kleinen[36], Paul B. Krummel[37], Ray L. Langenfelds[37], Goulven G. Laruelle[38], Licheng Liu[39], Toshinobu Machida[33], Shamil Maksyutov[33], Kyle C. McDonald[34], Joe McNorton[40], Paul A. Miller[41], Joe R. Melton[42], Isamu Morino[33], Jurek Müller[35], Fabiola Murguia-Flores[43], Vaishali Naik[44], Yosuke Niwa[33,45], Sergio Noce[20], Simon O'Doherty[46], Robert J. Parker[47], Changhui Peng[48], Shushi Peng[49], Glen P. Peters[50], Catherine Prigent[51], Ronald Prinn[52], Michel Ramonet[1], Pierre Regnier[38], William J. Riley[53], Judith A. Rosentreter [54], Arjo Segers[55], Isobel J. Simpson[14], Hao Shi[56], Steven J. Smith[57,58], Paul L. Steele[37], Brett F. Thornton[22], Hanqin Tian[56], Yasunori Tohjima[33], Francesco N. Tubiello[59], Aki Tsuruta[60] Nicolas Viovy[1], Apostolos Voulgarakis[61], Thomas S. Weber[62], Michiel van Weele[63], Guido R. van der Werf[8], Ray F. Weiss[64], Doug Worthy[65], Debra Wunch[66], Yi Yin[1,27], Yukio Yoshida[33], Wenxin Zhang[41], Zhen Zhang[67], Yuanghong Zhao[1], Bo Zheng[1], Qing Zhu[53], Qiuan Zhu[68], and Qianlai Zhuang[39]

[1]Laboratoire des Sciences du Climat et de l'Environnement, LSCE-IPSL (CEA-CNRS-UVSQ), Université Paris-Saclay 91191 Gif-sur-Yvette, France
[2]Global Carbon Project, CSIRO Oceans and Atmosphere, Aspendale, VIC 3195, and Canberra, ACT 2601, Australia
[3]NASA Goddard Space Flight Center, Biospheric Science Laboratory, Greenbelt, MD 20771, USA

https://doi.org/10.5194/essd-2019-128
Preprint. Discussion started: 19 August 2019

Open Access Earth System Science Data Discussions

[4]Department of Earth System Science, Woods Institute for the Environment, and Precourt Institute for Energy, Stanford University, Stanford, CA 94305-2210, USA
[5]School of Forestry and Environmental Studies, Yale University, New Haven, CT 06511, USA.
[6]NOAA ESRL, 325 Broadway, Boulder, CO 80305, USA
[7]SRON Netherlands Institute for Space Research, Sorbonnelaan 2, 3584 CA Utrecht, the Netherlands
[8]Vrije Universiteit Amsterdam, Department of Earth Sciences, Earth and Climate Cluster, VU Amsterdam, Amsterdam, the Netherlands
[9]Research Institute for Global Change, JAMSTEC, 3173-25 Showa-machi, Kanazawa, Yokohama, 236-0001, Japan
[10] Center for Environmental Remote Sensing, Chiba University, Chiba, Japan
[11]Canadian Centre for Climate Modelling and Analysis, Climate Research Division, Environment and Climate Change Canada, Victoria, BC, V8W 2Y2, Canada
[12]Department of Thematic Studies – Environmental Change, Linköping University, 581 83 Linköping, Sweden
[13]European Commission Joint Research Centre, Via E. Fermi 2749, 21027 Ispra (Va), Italy
[14]Department of Chemistry, University of California Irvine, 570 Rowland Hall, Irvine, CA 92697, USA
[15]National Institute of Water and Atmospheric Research, 301 Evans Bay Parade, Wellington, New Zealand
[16] Institute on the Environment, University of Minnesota, Saint Paul, Minnesota 55108, USA
[17] Department of Natural Resources and Environmental Management, University of Hawai'i, Honolulu, Hawai'i 96822, USA.
[18]Dipartimento di Scienze Ambientali, Biologiche e Farmaceutiche, Università degli Studi della Campania Luigi Vanvitelli, via Vivaldi 43, 81100 Caserta, Italy
[19]Department of Landscape Design and Sustainable Ecosystems, RUDN University, Moscow, Russia
[20]Impacts on Agriculture,Forests, and Ecosystem Services Division, Centro Euro-Mediterraneo sui Cambiamenti Climatici, Via Augusto Imperatore 16, 73100 Lecce, Italy
[21]Laboratoire de Météorologie Dynamique, LMD-IPSL, Ecole Polytechnique, 91120 Palaiseau, France
[22]Department of Geological Sciences and Bolin Centre for Climate Research, Svante Arrhenius väg 8, 106 91 Stockholm, Sweden
[23]Program in Environmental Studies and Sciences, Skidmore College, Saratoga Springs, NY 12866, USA
[24]School of Earth and Ocean Sciences, University of Victoria, P.O. Box 1700 STN CSC, Victoria, BC, Canada V8W 2Y2
[25]Istituto Nazionale di Geofisica e Vulcanologia, Sezione Roma 2, via V. Murata 605 00143 Rome, Italy
[26] Faculty of Environmental Science and Engineering, Babes Bolyai University, Cluj-Napoca, Romania
[27] Division of Geological and Planetary Sciences, California Institute of Technology, Pasadena, CA, United States
[28]Jet Propulsion Laboratory, California Institute of Technology, Pasadena, CA, United States
[29]Met Office Hadley Centre, Joint Centre for Hydrometeorological Research, Maclean Building, Wallingford OX10 8BB, UK

https://doi.org/10.5194/essd-2019-128
Preprint. Discussion started: 19 August 2019

Open Access Earth System Science Data Discussions

[30]Department of Meteorology, University of Reading, Earley Gate, Reading RG6 6BB, United Kingdom
[31]Air Quality and Greenhouse Gases Program (AIR), International Institute for Applied Systems Analysis (IIASA), 2361 Laxenburg, Austria
[32]Department of Physical Geography and Bolin Centre for Climate Research, Stockholm University, 106 91 Stockholm, Sweden
[33]Center for Global Environmental Research, National Institute for Environmental Studies (NIES), Onogawa 16-2, Tsukuba, Ibaraki 305-8506, Japan
[34]Department of Earth and Atmospheric Sciences, City College of New York, City University of New York, New York, NY 10031, USA
[35]Climate and Environmental Physics, Physics Institute and Oeschger Centre for Climate Change Research, University of Bern, Sidlerstr. 5, 3012 Bern, Switzerland
[36]Max Planck Institute for Meteorology, Bundesstraße 53, 20146 Hamburg, Germany
[37]Climate Science Centre, CSIRO Oceans and Atmosphere, Aspendale, Victoria 3195, Australia
[38]Department Geoscience, Environment & Society, Université Libre de Bruxelles, 1050-Brussels, Belgium
[39]Department of Earth, Atmospheric, Planetary Sciences, Department of Agronomy, Purdue University, West Lafayette, IN 47907, USA
[40]Research Department, European Centre for Medium-Range Weather Forecasts, Reading, UK
[41]Department of Physical Geography and Ecosystem Science, Lund University, Sölvegatan 12, 223 62, Lund, Sweden
[42]Climate Research Division, Environment and Climate Change Canada, Victoria, BC, V8W 2Y2, Canada
[43]School of Geographical Sciences, University of Bristol, Bristol, BS8 1SS, UK
[44]NOAA/Geophysical Fluid Dynamics Laboratory (GFDL), 201 Forrestal Rd., Princeton, NJ 08540, USA
[45]Meteorological Research Institute (MRI), Nagamine 1-1, Tsukuba, Ibaraki 305-0052, Japan
[46]School of Chemistry, University of Bristol, Cantock's Close, Clifton, Bristol BS8 1TS, UK
[47]National Centre for Earth Observation, University of Leicester, Leicester, LE1 7RH, UK
[48]Department of Biology Sciences, Institute of Environment Science, University of Quebec at Montreal, Montreal, QC H3C 3P8, Canada
[49]Sino-French Institute for Earth System Science, College of Urban and Environmental Sciences, Peking University, Beijing 100871, China.
[50]CICERO Center for International Climate Research, Pb. 1129 Blindern, 0318 Oslo, Norway
[51]CNRS, Sorbonne Université, Observatoire de Paris, Université PSL, Lerma, Paris, France
[52]Department of Earth, Atmospheric and Planetary Sciences, Massachusetts Institute of Technology (MIT), Building 54-1312, Cambridge, MA 02139, USA
[53]Climate and Ecosystem Sciences Division, Lawrence Berkeley National Lab, 1 Cyclotron Road, Berkeley, CA 94720, US
[54]Centre for Coastal Biogeochemistry, School of Environment, Science and Engineering, Southern Cross University, Lismore, NSW 2480, Australia
[55]TNO, dep. of Climate Air & Sustainability, P.O. Box 80015, NL-3508-TA, Utrecht,The Netherlands
[56]International Center for Climate and Global Change Research, School of Forestry and Wildlife

https://doi.org/10.5194/essd-2019-128
Preprint. Discussion started: 19 August 2019

Open Access Earth System Science Data Discussions

Sciences, Auburn University, 602 Duncan Drive, Auburn, AL 36849, USA
[57]Joint Global Change Research Institute, Pacific Northwest National Lab, College Park, MD, USA
[58]Department of Atmospheric and Oceanic Science, University of Maryland, College Park, MD, USA
[59]Statistics Division, Food and Agriculture Organization of the United Nations (FAO), Viale delle Terme di Caracalla, Rome 00153, Italy
[60]Finnish Meteorological Institute, P.O. Box 503, FI-00101, Helsinki, Finland
[61]Department of Physics, Imperial College London, London SW7 2AZ, UK
[62]Department of Earth and Environmental Sciences, University of Rochester, Rochester, NY 14627, USA
[63]KNMI, P.O. Box 201, 3730 AE, De Bilt, the Netherlands
[64]Scripps Institution of Oceanography (SIO), University of California San Diego, La Jolla, CA 92093, USA
[65]Environnement Canada, 4905, rue Dufferin, Toronto, Canada
[66]Department of Physics, University of Toronto, 60 St. George Street, Toronto, Ontario, Canada
[67]Department of Geographical Sciences, University of Maryland, United States of America
[68]College of Hydrology and Water Resources, Hohai University, Nanjing, 210098, China

Correspondence to: Marielle Saunois (marielle.saunois@lsce.ipsl.fr)

Abstract. Understanding and quantifying the global methane (CH_4) budget is important for assessing realistic pathways to mitigate climate change. Atmospheric emissions and concentrations of CH_4 are continuing to increase, making CH_4 the second most important human-influenced greenhouse gas in terms of climate forcing, after carbon dioxide (CO_2). Assessing the relative importance of CH_4 in comparison to CO_2 is complicated by its shorter atmospheric lifetime, stronger warming potential, and atmospheric growth rate variations over the past decade, the causes of which are still debated. Two major difficulties in reducing uncertainties arise from the variety of geographically overlapping CH_4 sources and from the destruction of CH_4 by short-lived hydroxyl radicals (OH). To address these difficulties, we have established a consortium of multi-disciplinary scientists under the umbrella of the Global Carbon Project to synthesize and stimulate new research aimed at improving and regularly updating the global methane budget. Following Saunois et al. (2016), we present here the second version of the living review paper dedicated to the decadal methane budget, integrating results of top-down studies (atmospheric observations within an atmospheric inverse-modelling framework) and bottom-up estimates (including process-based models for estimating land surface emissions and atmospheric chemistry, inventories of anthropogenic emissions, and data-driven extrapolations).

For the 2008-2017 decade, global methane emissions are estimated by atmospheric inversions (top-down approach) to be 572 Tg CH_4 yr^{-1} (range 538-593, corresponding to the minimum and maximum estimates of the ensemble), of which 357 Tg CH_4 yr^{-1} or ~60% are attributed to anthropogenic sources (range 50-

https://doi.org/10.5194/essd-2019-128
Preprint. Discussion started: 19 August 2019

65%). This total emission is 27 Tg CH_4 yr^{-1} larger than the value estimated for the period 2000-2009 and 24 Tg CH_4 yr^{-1} larger than the one reported in the previous budget for the period 2003-2012 (Saunois et al. 2016). Since 2012, global CH_4 emissions have been tracking the carbon intensive scenarios developed by the Intergovernmental Panel on Climate Change (Gidden et al., 2019). Bottom-up methods suggest larger global emissions (737 Tg CH_4 yr^{-1}, range 583-880) than top-down inversion methods, mostly because of larger estimated natural emissions from sources such as natural wetlands, other inland water systems, and geological sources. However the strength of the atmospheric constraints on the top-down budget, suggest that these bottom-up emissions are overestimated. The latitudinal distribution of atmospheric-based emissions indicates a predominance of tropical emissions (~65% of the global budget, <30°N) compared to mid (~30%, 30°N-60°N) and high northern latitudes (~4%, 60°N-90°N). Our analyses suggest that uncertainties associated with estimates of anthropogenic emissions are smaller than those of natural sources, with top-down inversions yielding larger uncertainties than bottom-up inventories and models.

The most important source of uncertainty in the methane budget is attributable to natural emissions, especially those from wetlands and other inland waters. Some global source estimates are smaller compared to the previously published budgets (Saunois et al. 2016; Kirschke et al. 2013), particularly for vegetated wetland emissions that are lower by about 35 Tg CH_4 yr^{-1} due to efforts to partition vegetated wetlands and inland waters. Emissions from geological sources are also found to be smaller by 7 Tg CH_4 yr^{-1}, and wild animals by 8 Tg CH_4 yr^{-1}. However the overall discrepancy between bottom-up and top-down estimates has been reduced by only 5% compared to Saunois et al. (2016), due to a higher estimate of freshwater emissions resulting from recent research and the integration of emissions from estuaries. Priorities for improving the methane budget include: i) a global, high-resolution map of water-saturated soils and inundated areas emitting methane based on a robust classification of different types of emitting habitats; ii) further development of process-based models for inland-water emissions; iii) intensification of methane observations at local scales (e.g., FLUXNET-CH4 measurements and urban monitoring to constrain bottom-up land surface models, and at regional scales (surface networks and satellites) to constrain atmospheric inversions; iv) improvements of transport models and the representation of photochemical sinks in top-down inversions, and v) development of a 3D variational inversion system using isotopic and/or co-emitted species such as ethane.

The data presented here can be downloaded from ICOS (https://doi.org/10.18160/GCP-CH4-2019; Saunois et al., 2019) and the Global Carbon Project.

https://doi.org/10.5194/essd-2019-128
Preprint. Discussion started: 19 August 2019

1 Introduction

The surface dry air mole fraction of atmospheric methane (CH_4) reached 1850 ppb in 2017 (Fig. 1), approximately 2.6 times greater than its estimated pre-industrial equilibrium value in 1750. This increase is attributable in large part to increased anthropogenic emissions arising primarily from agriculture (e.g., livestock production, rice cultivation, biomass burning), fossil fuel production and use, waste disposal, and alterations to natural methane fluxes due to increased atmospheric CO_2 concentrations and climate change (Ciais et al., 2013). Atmospheric CH_4 is a stronger absorber of Earth's emitted thermal infrared radiation than carbon dioxide (CO_2), as expressed by the global warming potential (GWP). For a 100-yr time horizon and without considering climate feedbacks GWP(CH_4)=28 (IPCC AR5, Myhre et al., 2013). Although global anthropogenic emissions of CH_4 are estimated at around 366 Tg CH_4 yr^{-1} (Saunois et al., 2016), representing only 3% of the global CO_2 anthropogenic emissions in units of carbon mass flux, the increase of atmospheric CH_4 concentrations has contributed ~23% (~0.62 $W.m^{-2}$) to the additional radiative forcing accumulated in the lower atmosphere since 1750 (Etminan et al., 2016). Changes in other chemical compounds (such as nitrogen oxides (NO_x) or carbon monoxide (CO)) also influence the forcing of CH_4 through changes to its atmospheric lifetime. From an emission point of view, the total radiative forcing attributable to anthropogenic CH_4 emissions is currently about 0.97 W m^{-2} (Myhre et al., 2013). This is because emission of CH_4 contributes to the production of ozone, stratospheric water vapour, and CO_2, and most importantly affects its own lifetime (Myhre et al., 2013; Shindell et al., 2012). CH_4 has a short lifetime in the atmosphere (about 9 years for the year 2010 (Prather et al., 2012)) hence a stabilization or reduction of CH_4 emissions leads rapidly to a stabilization or reduction of its atmospheric concentration and therefore its radiative forcing. Reducing CH_4 emissions is therefore recognized as an effective option for climate change mitigation, especially on shorter, decadal timescales (Shindell et al., 2012). Moreover, CH_4 is a precursor of important air pollutants, and, as such, its emissions are covered by two international conventions: the United Nations Framework Convention on Climate Change (UNFCCC) and the Convention on Long Range Transport of Air Pollution (CLRTAP).

Changes in the magnitude and temporal variation (annual to inter-annual) of methane sources and sinks over the past decades are characterized by high uncertainties (Kirschke et al., 2013; Saunois et al., 2017; Turner et al., 2019), with relative uncertainties (hereafter reported as min-max ranges) of 20-35% for inventories of anthropogenic emissions in specific sectors (e.g., agriculture, waste, fossil fuels), 50% for biomass burning and natural wetland emissions, and reaching 100% or more for other natural sources (e.g. inland waters, geological sources). The uncertainty in the chemical loss of methane by OH, the predominant sink of atmospheric methane, is estimated between 10% (Prather et al., 2012) and 15% (Saunois et al., 2016), representing, in relation to top-down methods, the minimum uncertainty associated

https://doi.org/10.5194/essd-2019-128
Preprint. Discussion started: 19 August 2019

with global methane emissions, as other sinks are much smaller and the atmospheric growth rate is well-defined (Dlugokencky et al., 2009). Globally, the contribution of natural CH_4 emissions to total emissions is reasonably well quantified, for instance by combining lifetime estimates with reconstructed pre-industrial atmospheric methane concentrations from ice cores (e.g. Ehhalt et al., 2001). Uncertainties in emissions may reach 40-60% at regional scales (e.g. for South America, Africa, China and India, Saunois et al., 2016). Beyond the intrinsic value of characterizing the biogeochemical cycle of methane, understanding the evolution of the methane budget has strong implications for developing credible future climate emission scenarios. Worryingly, the current anthropogenic methane emissions trajectory is estimated to lie between the two warmest IPCC-AR5 scenarios (Nisbet et al., 2016; Nisbet et al., 2019), i.e., the RCP8.5 and RCP6.0, corresponding to temperature increases above 3°C by the end of this century. This trajectory implies that large reductions of methane emissions are necessary in order to meet the 1.5-2°C target of the Paris Agreement (Collins et al., 2013; Nisbet et al., 2019).

In order to verify such reductions, sustained and long-term monitoring of atmospheric methane is needed for more precise estimation of trends, and the uncertainties in major emission sources also need to be reduced (Pacala et al., 2010; Bergamaschi et al., 2018a). Reducing uncertainties in individual methane sources and thus in the overall methane budget is not an easy task for at least four reasons. Firstly, methane is emitted by a variety of processes that need to be understood and quantified separately, including both natural and anthropogenic sources, point and diffuse sources, and sources associated with three main emission processes (i.e., biogenic, thermogenic and pyrogenic). These multiple sources and processes require the integration of data from diverse scientific communities. The fact that anthropogenic emissions result from unintentional leakage from fossil fuel production or agriculture further complicates production of accurate bottom-up emission estimates. Secondly, atmospheric methane is removed by chemical reactions in the atmosphere involving radicals (mainly OH) that have very short lifetimes (typically ~1s). Although OH can be measured locally, its spatio-temporal distribution remains uncertain at regional to global scales, in part because of a lack of direct measurements. Thirdly, only the net methane budget (sources minus sinks) is constrained by precise observations of atmospheric growth rates (Dlugokencky et al., 2009), leaving the sum of sources and the sum of sinks uncertain. One simplification for CH_4 compared to CO_2 is that the oceanic contribution to the global methane budget is small (~1-3%), making source estimation predominantly a continental problem (USEPA, 2010a). Finally, we lack observations to constrain 1) process models that produce estimates of wetland extent (Stocker et al., 2014; Kleinen et al., 2012) and wetland emissions (Melton et al., 2013; Poulter et al., 2017; Wania et al., 2013), 2) other inland water sources (Bastviken et al., 2011;Wik et al., 2016a), 3) inventories of anthropogenic emissions (Höglund-Isaksson, 2012; Höglund-Isaksson, 2017; Janssens-Maenhout et al., 2019; USEPA, 2012), and 4) atmospheric inversions, which aim to represent or estimate methane emissions from global to regional

https://doi.org/10.5194/essd-2019-128
Preprint. Discussion started: 19 August 2019

scales (Bergamaschi et al., 2013; Bergamaschi et al., 2018b; Bohn et al., 2015; Houweling et al., 2014; Kirschke et al., 2013; Saunois et al., 2016; Spahni et al., 2011; Thompson et al., 2017; Tian et al., 2016).

The global methane budget inferred from atmospheric observations relies on regional constraints from atmospheric sampling networks, which are relatively dense for northern mid-latitudes, with a number of high-precision and high-accuracy surface stations, but are sparser at tropical latitudes and in the Southern Hemisphere (Dlugokencky et al., 2011). Recently the atmospheric observation density has increased in the tropics due to satellite-based platforms that provide column-average methane mixing ratios. Despite continuous improvements in the precision and accuracy of space-based measurements (Buchwitz et al., 2016), systematic errors greater than several ppb on total column observations may limit the usage of such data to constrain surface emissions (Alexe et al., 2015; Locatelli et al., 2015; Bousquet et al., 2018; Chevallier et al., 2017). The development of robust bias corrections on existing data can help overcome this issue (e.g., Inoue et al., 2016), and satellite based inversions have already proven useful to reduce global an regional flux uncertainties over surface based inverions (Fraser et al., 2013).

The Global Carbon Project (GCP) seeks to develop a complete picture of the carbon cycle by establishing common, consistent scientific knowledge to support policy debate and actions to mitigate greenhouse gas emissions to the atmosphere (www.globalcarbonproject.org). The objective of this paper is to analyse and synthesize the current knowledge of the global methane budget, by gathering results of observations and models in order to better understand and quantify the main robust features of this budget and its remaining uncertainties. We combine results from a large ensemble of bottom-up approaches (e.g., process-based models for natural wetlands, data-driven approaches for other natural sources, inventories of anthropogenic emissions and biomass burning, and atmospheric chemistry models), and top-down approaches (including methane atmospheric observing networks, atmospheric inversions inferring emissions and sinks from atmospheric observations and models of atmospheric transport and chemistry). The focus of this work is on decadal budgets and to update the previous assessment made for the period 2003-2012 to the recent period 2008-2017, while leaving in-depth analysis of trends and year-to-year changes to other publications. This paper is a living review, published at two- to three-year intervals, to provide an update and new synthesis of available observational, statistical and model data in order to refine state-of-the-art estimates of the overall CH_4 budget and its individual components.

Kirschke et al. (2013) was the first CH_4 budget synthesis and was followed by Saunois et al. (2016). Kirschke et al. (2013) reported decadal mean CH_4 emissions and sinks from 1980 to 2009 based on bottom-up and top-down approaches. Saunois et al. (2016) reported methane emissions for three time periods: 1) the last calendar decade (2000-2009), 2) the last available decade (2003-2012), and 3) the last available year (2012). Here, we update this same approach reporting methane emissions and sinks for 2000-2009 decade, for the most recent 2008-2017 decade where data are available, and, preliminarily, for the year

https://doi.org/10.5194/essd-2019-128
Preprint. Discussion started: 19 August 2019

2017, reducing the time lag between the last reported year and analysis. The methane budget is presented here at global and latitudinal scales and can be downloaded from ICOS (https://doi.org/10.18160/GCP-CH4-2019; Saunois et al., 2019) .

290 . Further insight into regional budgets will be provided in (Stavert et al., 2019).

Five sections follow this introduction. Section 2 presents the methodology followed to treat and analyse the data streams. Section 3 presents the current knowledge about methane sources and sinks based on the ensemble of bottom-up approaches reported here (models, inventories, data-driven approaches). Section 4 reports atmospheric observations and top-down atmospheric inversions gathered for this paper. Section 5,

295 based on Sect. 3 and 4, provides the updated analysis of the global methane budget. Finally, Section 6 discusses future developments, missing components, and the most critical remaining uncertainties based on this update to the global methane budget.

2 Methodology

Unless specified, fluxes relevant to the methane budget are expressed in teragrams of CH_4 per year (1Tg

300 CH_4 yr^{-1}=10^{12} gCH_4 yr^{-1}), while atmospheric methane concentrations are expressed as dry air mole fractions, in parts per billion (ppb), with atmospheric methane annual increases, G_{ATM}, expressed in ppb yr^{-1}. In the tables, we present mean values and ranges for the two decades 2000-2009, and 2008-2017, together with results for the most recent available year (2017). Results obtained from previous syntheses (i.e., Saunois et al., 2016)) are also given for the decade 2000-2009. Following Saunois et al. (2016) and

305 considering the relatively small and variable number of studies generally available for individual estimates, uncertainties are reported as minimum and maximum values of the available studies, in brackets. In doing so, we acknowledge that we do not take into account the uncertainty of the individual estimates, but rather we express uncertainty as the range of available mean estimates, i.e., the standard error across measurements/methodologies considered. This means that the actual uncertainty range may be larger than

310 the range provided here. These minimum and maximum values are those calculated using the boxplot analysis presented in Section 2.2 and thus exclude identified outliers.

The CH_4 emission estimates are provided with up to three digits, for consistency across all budget flux components and to ensure the accuracy of aggregated fluxes. Nonetheless, the uncertainties involved in the global budget do not justify the use of more than two significant digits.

315 ### 2.1 Processing of emission maps

Common data analysis procedures have been applied to the different bottom-up models, inventories and atmospheric inversions whenever gridded products exist. The monthly or yearly fluxes (emissions and

https://doi.org/10.5194/essd-2019-128
Preprint. Discussion started: 19 August 2019

sinks) provided by different groups were processed in the same way. They were either provided on a 1°x1° grid or re-gridded to 1°x1°, before converting into the common unit of Tg CH_4 per grid cell. For land fluxes in coastal pixels, misallocation to the ocean was avoided by reallocating the land emissions to the neighbouring land pixel. The opposite was done for ocean fluxes. Monthly, annual and decadal means were computed from the gridded 1°x1° maps.

2.2 Definition of the boxplots

Most budgets are presented as boxplots, which have been created using routines in the IDL programming language using the classical convention of presenting quartiles (25%, median, 75%), outliers, and minimum and maximum values without outliers. Outliers were determined as values below the first quartile minus three times the inter-quartile range, or values above third quartile plus three times the inter-quartile range. Outliers were identified separately in relevant plots. The mean values reported in the tables are represented as "+" symbols in the corresponding figures.

2.3 Definition of regions and source categories

Geographically, emissions were reported globally and for three latitudinal bands (90°S-30°N, 30-60°N, 60-90°N, only for gridded products). When extrapolating emission estimates forward in time (see Sect. 3.1.1), and for the regional budget presented in (Stavert, 2019), a set of 19 regions (oceans and 18 continental regions, see supplementary Fig. S1) were used. As anthropogenic emissions are often reported by country, we define these regions based on a country list (Table S1). This approach was compatible with all top-down and bottom-up approaches considered. The number of regions was chosen to be close to the widely used TransCom inter-comparison map (Gurney et al., 2004), but with subdivisions to separate the contribution from important countries or regions for the methane cycle (China, South Asia, Tropical America, Tropical Africa, USA, and Russia). The resulting region definition is the same as used for the GCP N_2O budget (Tian et al., 2019).

Following Saunois et al. (2016), we report emissions depending on their anthropogenic or natural origin and for five main GCP categories for both bottom-up and top-down approaches. The natural emissions include two main GCP categories: "natural wetlands", and "other natural emissions" (e.g., other inland waters, wild animals, wildfires, termites, land geological sources, geological and biogenic oceanic sources and terrestrial permafrost). Anthropogenic emissions include three main GCP categories: "agriculture and waste emissions", "fossil fuel emissions", "biomass and biofuel burning emissions". In the summary tables (Tab. 3 and 6), all types of fires are included as anthropogenic sources, although they are partly of natural origin, as shown on the infographic Fig. 6 (Van der Werf et al., 2010).

https://doi.org/10.5194/essd-2019-128
Preprint. Discussion started: 19 August 2019

Bottom-up estimates of methane emissions for some processes are derived from models (e.g., biogeochemical models for wetlands, models for termites), inventories (agriculture and waste emissions, fossil fuel emissions, biomass and biofuel burning emissions), satellite based products (large scale biomass burning), or observation based upscaling for other sources (e.g., inland water, geological sources…). From these bottom-up approaches, it is possible to provide estimates for more detailed source categories inside each main GCP category (see budget in Table 3). However, the total methane emission derived from the combination of independent bottom-up estimates is unconstrained.

For the atmospheric inversion (top-down) approach the situation is different. Atmospheric observations provide a constraint on the global source, given a fairly strong constraint on the global sink derived from methyl chloroform (Montzka et al., 2011; Rigby et al., 2017). The inversions reported in this work solve either for a total methane flux (e.g. Pison et al., 2013), or for a limited number of flux categories (e.g. Bergamaschi et al., 2013). In most of the inverse system the atmospheric oxidant concentrations are prescribed and thus the atmospheric sink is not solved. Indeed, the assimilation of CH_4 observations alone, as reported in this synthesis, can help to separate sources with different locations or temporal variations but cannot fully separate individual sources as they often overlap in space and time in some regions. Global and regional methane emissions per source category were obtained directly from the gridded optimized fluxes, wherever an inversion had solved for the relevant five main GCP categories. Alternatively, if the inversion solved for total emissions (or for different categories other than the five main GCP ones), then the prior contribution of each source category at the spatial resolution of the inversion was scaled by the ratio of the total (or embedding category) optimized flux divided by the total (or embedding category) prior flux (Kirschke et al., 2013). The soil uptake was provided separately in order to report total gross surface emissions instead of net fluxes (sources minus soil uptake).

In summary, bottom-up models and inventories are presented for all source processes and for the five main categories defined above globally. Top-down inversions are reported globally only for the five main emission categories.

3 Methane sources and sinks

Here we provide a synthesis of methane sources and sinks based on an ensemble of bottom-up emission estimation methods: process-based models, statistical databases, and data-driven methods. For each source category, a description of the relevant emitting processes is given, together with a brief description of the original data sets (measurements, models) and the related methodology. Then, the estimate for the global source and its range is given and analysed. More detailed descriptions of the data sets can be found

https://doi.org/10.5194/essd-2019-128
Preprint. Discussion started: 19 August 2019

elsewhere (see references of each component in the different subsections and tables) and in the supplementary material of this paper.

Methane sources can be organized by emitting process (i.e., biogenic, thermogenic, or pyrogenic) or by anthropogenic versus natural origin. Biogenic methane is the final product of the decomposition of organic matter by methanogenic *Archaea* in anaerobic environments, such as water-saturated soils, swamps, rice paddies, marine sediments, landfills, sewage and wastewater treatment facilities, or inside animal digestive systems. Thermogenic methane is formed on geological time scales by the breakdown of buried organic matter due to heat and pressure deep in the Earth's crust. Thermogenic methane reaches the atmosphere through marine and land geological gas seeps. These methane emissions are increased by human processes, for instance the exploitation and distribution of fossil fuels (e.g., coal mining, natural gas production, gas transmission and distribution, oil production and refinery). Pyrogenic methane is produced by the incomplete combustion of biomass and other organic material. Peat fires, biomass burning in deforested or degraded areas, wildfires and biofuel burning are the largest sources of pyrogenic methane. Methane hydrates, ice-like cages of trapped methane found in continental shelves and slopes and below sub-sea and land permafrost, can be of either biogenic or thermogenic origin. Each of the three process categories has both anthropogenic and natural components. In the following, we present the different methane sources depending on their anthropogenic or natural origin (see Sect. 2.3 for definition of the categories), which seems more relevant for planning climate mitigation activities. However this choice does not correspond exactly to the definition of anthropogenic and natural used by UNFCCC and IPCC guidelines (IPCC, 2006), where, for pragmatic reasons, all emissions from managed land are reported as anthropogenic, which is not the case here. For instance, we consider all wetlands in the natural emissions category, despite some wetlands being actively managed.

3.1 Anthropogenic methane sources

Various human activities emit methane to the atmosphere. Agricultural processes under anaerobic conditions, such as enteric fermentation in ruminant livestock, manure management and applications, and rice cultivation, emit biogenic CH_4, as does the decomposition of municipal solid waste. Methane is also emitted during the production and distribution of natural gas and petroleum, and is released as a by-product of coal mining and incomplete fossil fuel and biomass combustion (USEPA, 2016).

Available statistical emission databases typically apply the IPCC methodologies resulting in bottom-up estimates of sector-specific emissions using country-specific activity data and emission factors.

https://doi.org/10.5194/essd-2019-128
Preprint. Discussion started: 19 August 2019

410 **3.1.1 Reported global inventories**

The main bottom-up global inventory datasets covering anthropogenic emissions from all sectors are those from the United States Environmental Protection Agency, USEPA (2012), the Greenhouse gas and Air pollutant Interactions and Synergies (GAINS) model developed by the International Institute for Applied Systems Analysis (IIASA) (Gómez-Sanabria et al., 2018; Höglund-Isaksson, 2012; Höglund-Isaksson,
415 2017) and the Emissions Database for Global Atmospheric Research (EDGAR, Janssens-Maenhout et al., 2019) compiled by the European Commission Joint Research Centre (EC-JRC) and Netherland's Environmental Assessment Agency (PBL). Also included in this budget analysis is the Community Emissions Data System for historical emissions (CEDS) (Hoesly et al., 2018) developed for use by the climate modelling community in the Coupled Model Inter-comparison Project Phase 6 (CMIP6). The Food
420 and Agriculture Organization (FAO) dataset emission database (Tubiello et al., 2019) is included but only covers emissions from agriculture and land use (including peatland and biomass fires).

These inventory datasets report the major sources of anthropogenic methane emissions: fossil fuel production, transmission and distribution; livestock enteric fermentation; livestock manure management and application; rice cultivation; solid waste and wastewater. Since the level of detail provided by country
425 and by sector varies among inventories, the data used for this analysis were reconciled into common categories (see Table S2). For example, agricultural and waste burning emissions treated as a separate category in EDGAR, GAINS and FAO, are included in the biofuel sector in the USEPA inventory and in the agricultural sector in CEDS. The GAINS, EDGAR and FAO estimates of agricultural waste burning were excluded from this analysis (these amounted to 1-3 Tg CH_4 yr^{-1} in recent decades). Excluding
430 agricultural waste burning estimates also prevents any inadvertent overlap with separate estimates of biomass burning emissions (e.g. GFEDv4.1s). In these inventories, methane emissions for a given region/country and a given sector are usually calculated following standard IPCC methodology (IPCC, 2006), for instance as the product of an activity factor and an emission factor for this activity. An abatement coefficient is used additionally, to account for any regulations implemented to control emissions
435 (see, e.g., Höglund-Isaksson et al., 2015). The USEPA integrated emission inventory model provides estimates every five years for both past and future periods, with projections after 2005. GAINS provides annual data for past emissions and a projection for 2020; FAOSTAT (Tubiello et al., 2019) provides data for the period 1961-2016 plus projections to 2030 and 2050; and CEDS and EDGAR provide annual estimates only for past emissions. These datasets differ in their assumptions and the data used for the
440 calculation; however, they are not completely independent because they follow the same IPCC guidelines (IPCC, 2006), and, at least for agriculture, use the same FAOSTAT activity data. While the USEPA inventory adopts the emissions reported by the countries to the UNFCCC, other inventories (FAOSTAT,

https://doi.org/10.5194/essd-2019-128
Preprint. Discussion started: 19 August 2019

EDGAR and the GAINS model) produce their own estimates using a consistent approach for all countries. These other inventories need large amounts of country-specific activity data and emission factor information or, if not available, may adopt IPCC default factors or emission factors reported to UNFCCC (Höglund-Isaksson, 2012;Janssens-Maenhout et al., 2019; Olivier and Janssens-Maenhout, 2012; Tubiello et al., 2019). CEDS takes a different approach starting from pre-existing default emission estimates; for methane, a combination of EDGAR and FAO estimates are used, scaled to match other individual or region-specific inventory values when available. This process maintains the spatial information in the default emission inventories while preserving consistency with the country level data. The FAOSTAT was used to provide estimates of methane emissions at the country level but was limited to agriculture (enteric fermentation, manure management, rice cultivation, energy usage, burning of crop residues and prescribed burning of savannahs) and land-use (biomass burning). It will hereafter be referred as FAO-CH_4. FAO-CH_4 uses activity data mainly from the FAOSTAT crop and livestock production database, as reported by countries to FAO (Tubiello et al., 2013), and apply mostly the Tier 1 IPCC methodology for emissions factors (IPCC, 2006), which depend on geographic location and development status of the country. Finally, we note that, for manure, the necessary country-scale temperature was obtained from the FAO global agro-ecological zone database (GAEZv3.0, 2012). Although, country emissions are reported annually to the UNFCCC by annex I countries, and episodically reported by non-annex I countries, data gaps in national greenhouse gas inventories do not allow the inclusion of these estimates in this analysis, although the USEPA inventory includes those available from UNFCCC.

We use the following versions of these databases:

- EDGARv4.3.2 which provides yearly gridded emissions by sectors from 1970 to 2012 (Janssens-Maenhout et al., 2019),
- the GAINS model scenario ECLIPSE v6 (Gómez-Sanabria et al., 2018;Höglund-Isaksson, 2012;Höglund-Isaksson, 2017) which provides both annual sectorial totals by country for 1990 to 2015 and a projection for 2020 (that assumes current emission legislation for the future) and an annual sectorial gridded product for 1990 to 2015,
- USEPA (USEPA, 2012), which provides 5-year sectorial totals by country for 1990 to 2020 (estimates from 2005 onward are a projection), with no gridded distribution available,
- the CEDS emission estimates version 2017-05-18 which provides both gridded monthly and annual country based emissions by sectors for 1970 to 2014 (Hoesly et al., 2018),
- FAO-CH_4 (database accessed in February 2019, FAO (2019)) containing annual country level data for the period 1961-2016, for rice, manure, and enteric fermentation; and 1990 to 2016 for burning savannah, crop residue and non-agricultural biomass burning.

https://doi.org/10.5194/essd-2019-128
Preprint. Discussion started: 19 August 2019

Further details of the datasets used in this study are provided in Table 1. The recent expansion in the number of gridded data sets available, including EDGARv4.3.2, CEDS and GAINS, has greatly increased the input options for inverse and climate modelling. However, these inventories are not all regularly updated, whereas the FAOSTAT database provides methane emission estimates up to year 2016. As our study aimed to report emissions for the period 2000-2017, it was necessary to extend and interpolate some of the datasets to cover this period. The estimates from USEPA were linearly interpolated to provide yearly values. The FAO-CH_4 dataset was extrapolated to 2017 using a linear fit for the 2014-2016 data. We have also extrapolated the EDGARv4.3.2 up to 2017 using the extended FAO-CH_4 emissions for CH_4 emissions from enteric fermentation, manure management and rice cultivation, and using BP statistical review of fossil fuel production and consumption (BP Statistical Review of World Energy, 2019) to update CH_4 emissions from coal, oil and gas sectors. In this extrapolated inventory, called EDGARv4.3.2$_{EXT}$, methane emissions for year *t* are set equal to the 2012 EDGAR CH_4 emissions ($E_{EDGARv4.3.2}$) times the ratio between the FAO-CH_4 emissions (or BP statistics) of year *t* ($E_{FAO\text{-}CH4}(t)$) and FAO-CH_4 emissions (or BP statistics) of 2012 ($E_{FAO\text{-}CH4}(2012)$). For each emission sector, the region-specific emissions ($E_{EDGARv4.3.2ext}$) in year (*t)* are estimated following Eq. (1):

$$E_{EDGARv4.3.2ext}(t) = E_{EDGARv4.3.2}(2012) \times E_{FAO-CH4}(t)/E_{FAO-CH4}(2012) \quad (1)$$

Transport, industrial, waste and biofuel sources were linearly extrapolated based on the last three years of data while other sources are kept constant at the 2012 level. This extrapolation approach is necessary, and often performed by top-down approaches to define prior emissions because, up to now, global inventories such as sector-specific emissions in the EDGAR database are not updated on a regular basis. To allow comparisons through 2017, the CEDS dataset has also been extrapolated in an identical method creating CEDS$_{EXT}$. However, in contrast to the EDGARv4.3.2 dataset, the CEDS dataset provides only a combined oil and gas sector; hence, it was necessary to extend this dataset using the sum of BP oil and gas emissions. The by-country GAINS dataset was linearly projected by sector for each country using the trend between the historic 2015 and projected 2020 values. These by-country projections were then aggregated to the 19 global regions (Section 2.3 and Fig. S1) and used to extrapolate the GAINS gridded dataset in a similar manner to that described in Equation 1. For ease of reading, all further references in this paper will be to the extended inventories CEDS$_{EXT}$, EDGARv4.3.2$_{EXT}$ and GAINS$_{EXT}$ although the "EXT" suffix will be dropped hereafter.

3.1.2 Total anthropogenic methane emissions

In order to avoid double counting and ensure consistency with each inventory, the range (min-max) and mean values of the total anthropogenic emissions were not calculated as the sum of the mean and range of the three upper-level anthropogenic categories ("Agriculture and waste", "Fossil fuels" and "Biomass

https://doi.org/10.5194/essd-2019-128
Preprint. Discussion started: 19 August 2019

burning & biofuels"). Instead, we calculated separately the total anthropogenic emissions for each inventory by adding its values for "Agriculture and waste", "Fossil fuels" and "biofuels" with the range of available large-scale biomass burning emissions. This approach was used for the EGDARv4.3.2, CEDS and GAINS inventories, where as we kept the USEPA inventory as originally reported because it includes its own estimates of biomass burning emissions. As a result, FAO-CH_4 estimates are not included in the range derived for the total anthropogenic emissions, but they are included in the values reported for the "Agriculture and waste" category. For the latter, we calculate the range and mean value as the sum of the mean and range of the three anthropogenic subcategory estimates "Enteric fermentation and Manure", "Rice", and "Landfills and Waste". The values reported for the upper-level anthropogenic categories ("Agriculture and waste", "Fossil fuels" and "Biomass burning & biofuels") are therefore consistent with the sum of their subcategories, although there might be small percentage differences between the reported total anthropogenic emissions and the sum of the three upper-level categories. This approach provides a more accurate representation of the range of emission estimates, avoiding an artificial expansion of the uncertainty attributable to subtle differences in the definition of sub-sector categorisations between inventories.

Based on the ensemble of databases detailed above, total anthropogenic emissions were 366 [348-392] Tg CH_4 yr^{-1} for the decade 2008-2017 (Table 3, including biomass and biofuel burning) and 334 [325-357] Tg CH_4 yr^{-1} for the preceding decade 2000-2009. Our estimate for the preceding decade is statistically consistent with the findings of Saunois et al. (2016) (338 Tg CH4 yr-1 [329-342]) and of Kirschke et al. (2013) (331 Tg CH4 yr-1 [304-368]) for the same period. The slightly larger range reported herein with respect to our previous findings is mainly due to a larger range in the biomass burning estimates, as more biomass burning products are included in our new budget. The range associated with our estimates (~10-12%) is smaller than the range reported in the Arctic Monitoring And Assessment Programme (AMAP) report (Höglund-Isaksson et al., 2015) (~20%), perhaps both because the latter analysed data from a wider range of inventories and projections, and because the AMAP was referenced to one year only (2005) rather than averaged over a decade, as done here.

Figure 2 summarizes the global methane emissions of anthropogenic sources (including biomass and biofuel burning) estimated and projected by the different datasets between 2000 and 2050. The datasets consistently estimate total anthropogenic emissions of ~300 Tg CH_4 yr^{-1} in 2000. The main discrepancy between the inventories is observed in their trend after 2005, with the lowest emissions projected by GAINS and the largest emissions estimated by CEDS. Despite relatively good agreement between the inventories for total emissions from year 2000 onwards, large differences were found at the sector and country level (IPCC, 2014). Some of these discrepancies are detailed in the following sections and in (Stavert et al., 2019). For the Sixth Assessment report of the IPCC, seven main Shared Socioeconomic

https://doi.org/10.5194/essd-2019-128
Preprint. Discussion started: 19 August 2019

Pathways (SSPs) have been defined to provide climate projections in the Coupled Model Intercomparison Project 6 (CMIP6) (Gidden et al., 2019) ranging from 1.9 to 8.5 W m^{-2} radiative forcing by the year 2100 (as shown by the number in the SSP names). For the 1970-2014 period, the historical emissions used in CMIP6 combine anthropogenic emissions from Hoesly et al. (2018) (CEDS) and a climatological value from the GFEDv4.1s biomass burning inventory (van Marle et al., 2017). The CEDS anthropogenic emissions estimates, based on EDGARv4.2, are 10-20 Tg higher than the more recent EDGARv4.3.2 (van Marle et al., 2017). Methane emissions continue to track emissions from RCP8.5, indicating that climate policies have not been sufficient to change the emissions trajectory substantially to date (Nisbet et al., 2019). In the future, the SSP storylines span a range of future outcomes, and it appears likely that higher-emission trajectories will be realised.

This shows the tremendous challenge of climate mitigation that lies ahead to reach the goals of the Paris agreement Despite the offset of the SSP scenarios compared to the recent inventories, it will be crucial to monitor the trends estimated in the reported inventories in the following years and compare them to the SSP's.

3.1.3 Methane emissions from fossil fuel production and use

Most anthropogenic methane emissions related to fossil fuels come from the exploitation, transportation, and usage of coal, oil, and natural gas. Additional emissions reported in this category include small industrial contributions such as production of chemicals and metals, fossil fuel fires (underground coal mine fires and the Kuwait oil and gas fires), and transport. Methane emissions from the oil industry (e.g. refining) and production of charcoal are estimated to be a few Tg CH_4 yr^{-1} only (EDGARv4.2, 2011) and are included in the transformation industry sector in the inventory. Fossil fuel fires are included in the sub-category "Oil & Gas". For our budget, emissions from industries and transport are reported apart from the two main sub-categories "Oil & Gas" and "Coal". Each amounts to about 5 Tg CH_4 yr^{-1}. The large range (0-12 Tg CH_4 yr^{-1}) is attributable to difficulties allocating some sectors to specific GCP sub-categories consistently among the different inventories (See Table S2). In Saunois et al. (2016), these emissions were included in the sub-category "Oil & Gas" or "Coal". The spatial distribution of methane emissions from fossil fuels is presented in Fig. 3 based on the mean gridded maps provided by CEDS, EDGARv4.3.2 and GAINS for the 2008-2017 decade; USEPA lacks a gridded product.

Global emissions of methane from fossil fuels, other industries and transport are estimated from four global inventories yielding 127 [111-154] Tg CH_4 yr^{-1} for the 2008-2017 decade (Table 3), but with large differences in the rate of change during this period across inventories. The sector accounts on average for 35% (range 30-42%) of the total global anthropogenic emissions.

https://doi.org/10.5194/essd-2019-128
Preprint. Discussion started: 19 August 2019

Coal mining. During mining, methane is emitted from ventilation shafts, where large volumes of air are pumped into the mine to keep the CH_4 mixing ratio below 0.5% to avoid accidental ignition, and attributable to dewatering operations. In countries of the Organization for Economic Co-operation and Development (OECD), methane released from ventilation shafts is used as fuel, but in many countries it is still emitted into the atmosphere or flared, despite efforts for coalmine recovery under the UNFCCC Clean Development Mechanisms (http://cdm.unfccc.int). Methane emissions also occur during post-mining handling, processing, and transportation. Some CH_4 is released from coal waste piles and abandoned mines, however emissions from these sources are believed to be low (IPCC, 2000).

Almost 40% (IEA, 2018) of the world's electricity is still produced from coal. This contribution indeed grew in the 2000s at the rate of several per cent per year, driven by Asian economic growth where large reserves exist, but global coal consumption has been fairly stable since 2011. In 2018, the top ten largest coal producing nations accounted for ~90% of total world emissions for coal mining; among them, the top three producers (China, USA and India) produced almost two thirds (64%) of the world's coal (CIA, 2016; BP 2019).

Global estimates of CH_4 emissions from coal mining show a large variation, in part due to the lack of comprehensive data from all major producing countries. The range of coal mining emissions is estimated at 29-60 Tg of methane for 2008-2017, the highest value coming from the CEDS inventory and the lowest from USEPA.

As outlined in Sect. 3.1.2, coal mining is the main source explaining the differences between inventories globally (Fig. 2). Indeed, these differences are explained mainly by the different CH_4 emission factors used for calculating fugitive emissions from coal mining in China. Coal mining emission factors depend strongly on the type of coal extraction (underground mining emitting up to 10 times more than surface mining), the geological underground structure, which is region-specific, history (basin uplift), and the quality of the coal (brown coal emitting more than hard coal). CEDS seems to have overestimated coal mining emissions from China by almost a factor of 2, most likely due to its dependence on the EDGARv4.2 emission inventory. As highlighted by Saunois et al. (2016) a county-based inventory of Chinese methane emissions also confirms the overestimate of about +38% with total anthropogenic emissions estimated at 43±6 Tg CH_4 yr^{-1} (Peng et al., 2016). A study using $^{13}CH_4$ data by (Thompson et al., 2015) showed that their prior (based on EDGARv4.2FT2010) also overestimated the Chinese methane emissions by 30%, however they found no significant difference in the coal sector estimates between prior and posterior. EDGARv4.2 inventory followed the IPCC guidelines and used the European averaged emission factor for CH_4 from coal production to substitute missing data for China, which was a factor of two too high. These differences highlight significant errors resulting from the inappropriate use of emission factors, and that applying "Tier 1" approaches for coal mine emissions is not accurate enough as stated by the IPCC guidelines. The newly

https://doi.org/10.5194/essd-2019-128
Preprint. Discussion started: 19 August 2019

released version of EDGARv4.3.2 revises China emission factors down and distributes the fugitive CH_4 from coal mining to more than 80 times more coal mining locations in China.

For the 2008-2017 decade, methane emissions from coal mining are estimated at 33% of total fossil fuel related emissions of methane (42 Tg CH_4 yr^{-1}, range of 29-60). An additional very small source corresponds to fossil fuel fires (mostly underground coal fires, ~0.15 Tg yr^{-1} in 2012, EDGARv4.3.2).

Oil and natural gas systems.

This category includes emissions from conventional oil and gas exploitation and from shale gas exploitation. Natural gas is comprised primarily of methane, so both fugitive and planned emissions during the drilling of wells in gas fields, extraction, transportation, storage, gas distribution, end use, and incomplete combustion of gas flares emit methane (Lamb et al., 2015; Shorter et al., 1996).

For the 2008-2017 decade, methane emissions from upstream and downstream natural oil and gas sectors are estimated to represent about 63% of total fossil CH_4 emissions (76 Tg CH_4 yr^{-1}, range of 66-92, Table 3), with a lower uncertainty range than for coal emissions for most countries.

a. Conventional oil and gas. Persistent fugitive emissions (e.g., due to leaky valves and compressors) should be distinguished from intermittent emissions due to maintenance (e.g. purging and draining of pipes). During transportation, fugitive emissions can occur in oil tankers, fuel trucks and gas transmission pipelines, due to corrosion, manufacturing, welding, etc. According to Lelieveld et al. (2005), the CH_4 fugitive emissions from gas pipelines should be relatively low, however distribution networks in older cities have higher rates, especially those with cast-iron and unprotected steel pipelines. Measurement campaigns in cities within the USA and Europe also revealed that significant emissions occur in specific locations (e.g. storage facilities, city gates, well and pipeline pressurization/depressurization points) along the distribution networks (e.g. Jackson et al., 2014a; McKain et al., 2015; Wunch et al., 2016). However, methane emissions can vary significantly from one city to another depending, in part, on the age of city infrastructure and the quality of its maintenance, making urban emissions difficult to scale-up. In many facilities, such as gas and oil fields, refineries and offshore platforms, venting of natural gas is now replaced by flaring with almost complete conversion to CO_2; these two processes are usually considered together in inventories of oil and gas industries. Also, single-point failure of natural gas infrastructure can leak methane at high rate for months, such as at the Aliso Canyon blowout in the Los Angeles, CA, basin, thus hampering emission control strategies (Conley et al., 2016).

Methane emissions from oil and natural gas systems also vary greatly in different global inventories (69 to 97 Tg yr^{-1} in 2017, Table 3). The inventories generally rely on the same sources and magnitudes for the activity data, with the derived differences therefore resulting primarily from different methodologies and parameters used, including both emission and emission factors. Those factors are country- or even site-specific and the few field measurements available often combine oil and gas activities (Brandt et al., 2014)

https://doi.org/10.5194/essd-2019-128
Preprint. Discussion started: 19 August 2019

and remain largely unknown for most major oil- and gas-producing countries. Depending on the country, the reported emission factors may vary by two orders of magnitude for oil production and by one order of magnitude for gas production (Table SI-5.1 of (Höglund-Isaksson, 2017). The GAINS estimate of methane emissions from oil production, for instance, is twice as high as the estimate from EDGARv4.3.2. For natural gas, the uncertainty is of a similar order of magnitude. During oil extraction, the gas generated can be either recovered (re-injected or utilized as an energy source) or not recovered (flared or vented to the atmosphere). The recovery rates vary from one country to another (being much higher in the USA, Europe and Canada than elsewhere), and, could lead to an amount of gas released into the atmosphere during oil production two times higher accounting for country-specific rates of generation and recovery of associated gas than when using default values (Höglund-Isaksson, 2012). This difference in methodology explains, in part, why GAINS estimates are higher than those of EDGARv4.3.2. Another challenge lies in determining the amount of flared or vented unrecovered gas, as venting emits CH_4 whereas flaring converts all or most methane (usually >99%) to CO_2. The balance of flaring and venting also depends on the type of oil: flaring is less common for heavy oil wells than for conventional ones (Höglund-Isaksson et al., 2015). Satellite images can detect flaring (Elvidge et al., 2009; 2016) and may be used to verify country estimates, but such satellites can not currently be used to estimate the efficiency of CH_4 conversion to CO_2.

b. **Shale gas.** Production of natural gas from the exploitation of hitherto unproductive rock formations, especially shale, began in the 1980s in the US on an experimental or small-scale basis, then, from early 2000s, exploitation started at large commercial scale. Two techniques developed and often applied together are horizontal drilling and hydraulic fracturing. The shale gas contribution to total dry natural gas production in the United States reached 62% in 2017, growing rapidly from 40% in 2012, with only small volumes produced before 2005 (EIA, 2019). Indeed, the practice of high-volume hydraulic fracturing (fracking) for oil and gas extraction is a growing sector of methane and other hydrocarbon production, especially in the U.S. Most studies (Alvarez et al., 2018; Brandt et al., 2014; Howarth et al., 2011b; Jackson et al., 2014b; Karion et al., 2013; Moore et al., 2014; Olivier and Janssens-Maenhout, 2014; Pétron et al., 2014; Zavala-Araiza et al., 2015) albeit not all (Peischl et al., 2015; Allen et al., 2013; Cathles et al., 2012), suggest that methane emissions from oil and gas industry are underestimated by inventories and agencies, including the USEPA. For instance, the recent synthesis of (Alvarez et al., 2018) suggests that methane emissions from the U.S. oil and gas supply chain are ~60% higher than the USEPA estimate (13±2 Tg yr-1 against 8±2 Tg yr-1), corresponding to 2.3% of US gas production. They propose that existing inventory methods are most likely missing emissions released during abnormal operating conditions, such as those observed across the rapidly expanding shale gas sector. Zavala-Araiza et al. (2015) showed that a few high-emitting facilities, i.e., super-emitters, neglected in the inventories, dominated emissions. For instance, they estimate that 2% of the facilities of the Barnett region are responsible for 50% of the methane emissions.

https://doi.org/10.5194/essd-2019-128
Preprint. Discussion started: 19 August 2019

These high emitting points, located on the conventional part of the facility, could be avoided through better operating conditions and repair of malfunctions. Their result also suggests that the emission factors of conventional and non-conventional gas facilities might not be as different as originally thought by Howarth et al. (2011a,b). Indeed, the possibly larger emission factors from the unconventional gas as compared to the conventional one have been widely debated (e.g. Cathles et al., 2012; Howarth et al., 2011a,b). However, the latest studies tend to infer similar emission factors in a narrow range of 1-3% (Alvarez et al.; 2018; Zavala-Araiza, 2015; Peischl et al., 2015), different from the widely spread rates of 3-17% from previous studies (e.g. Caulton et al., 2014; Schneising et al., 2014).

The global implications of the rapidly growing shale gas activity in the US remains to be determined precisely. Schwietzke et al. (2017) proposed that the underestimation found in the U.S. might exist on a global scale for the same reasons (operating processes and malfunctioning equipment). Extending the work of Saunois et al. (2016), Bruhwiler et al. (2017) and Lan et al. (2019) found no evidence of a contribution of North American CH_4 emissions to the increasing global atmospheric trend over the past decade. Still, as U.S. production increases, absolute methane emissions almost certainly increase, as well. U.S. crude oil production doubled over the last decade to reach record levels of 11 million barrels per day in 2018; natural gas production rose more than 50% to 83.4 billion cubic feet per day, also a U.S. record (EIA 2019)

3.1.4 Agriculture and waste

This main category includes methane emissions related to livestock production (i.e., enteric fermentation in ruminant animals and manure management), rice cultivation, landfills, and wastewater handling. Of these, globally and in most countries livestock is by far the largest source of CH_4, followed by waste handling and rice cultivation. Conversely, field burning of agricultural residues is a minor source of CH_4 reported in emission inventories. The spatial distribution of methane emissions from agriculture and waste handling is presented in Fig. 3 based on the mean gridded maps provided by CEDS, EDGARv4.3.2 and GAINS over the 2008-2017 decade.

Global emissions from agriculture and waste for the period 2008-2017 are estimated at 206 Tg CH_4 yr^{-1} (range 191-223, Table 3), representing 56% of total anthropogenic emissions. This total is ~60% greater than the estimated 127 Tg yr-1 emitted through fossil fuel production and use (see Section 3.1.3 above and Table 3).

Livestock: Enteric fermentation and manure management. Domestic ruminant such as cattle, buffalo, sheep, goats, and camels emit large amounts of methane as a by-product of the anaerobic microbial activity in their digestive systems (Johnson et al., 2002). The very stable temperatures (about 39°C) and pH (6.5-6.8) values within in the rumen of domestic ruminants, along with a constant plant matter flow from grazing (cattle graze many hours per day), allow methanogenic *Archaea* residing within the rumen to

https://doi.org/10.5194/essd-2019-128
Preprint. Discussion started: 19 August 2019

produce methane. Methane is released from the rumen mainly through the mouth of multi-stomached ruminants (eructation, ~87% of emissions) or absorbed in the blood system. The methane produced in the intestines and partially transmitted through the rectum is only ~13%.

The total number of livestock continues to grow steadily. There are currently about 1.4 billion cattle globally, 1 billion sheep, and nearly as many goats (http://www.fao.org/faostat/en/#data/GE). Livestock numbers are linearly related to CH_4 emissions in inventories using the Tier 1 IPCC approach such as FAOSTAT. In practice, some non-linearity may arise due to dependencies of emissions on total weight of the animals and their diet, which are better captured by Tier 2 and higher approaches. Cattle, due to their large population, large size, and particular digestive characteristics, account for the majority of enteric fermentation CH_4 emissions from livestock worldwide (Tubiello et al., 2019), particularly in intensive agricultural systems in developed and emerging economies, including the United States (USEPA, 2016). Methane emissions from enteric fermentation also vary from one country to another as cattle may experience diverse living conditions that vary spatially and temporally, especially in the tropics (Chang and al., 2019).

Anaerobic conditions often characterize manure decomposition in a variety of manure management systems throughout the world (e.g., liquid/slurry treated in lagoons, ponds, tanks, or pits), with the volatile solids component in manure producing CH_4 as a result. In contrast, when manure is handled as a solid (e.g., in stacks or dry-lots) or deposited on pasture, range, or paddock lands, it tends to decompose aerobically and produce little or no CH_4. Ambient temperature, moisture, and manure storage or residency time affect the amount of CH_4 produced because they influence the growth of the microorganisms responsible for CH_4 formation. For non-liquid-based manure systems, moist conditions (which can be induced by rainfall and humidity) can promote CH_4 production. Manure composition, which varies with animal diet, growth rate, and type, including the animal's digestive system, also affects the amount of CH_4 produced. In general, the potential for CH_4 emissions grows with the energy contents of the feed. However, some higher-energy feeds also are more digestible than lower quality forages, which can result in less overall waste excreted from the animal (USEPA, 2006). Despite these complexities, most global datasets used herein apply a simplified IPCC Tier 1 approach, where amounts of manure treated depend on animal numbers and simplified climatic conditions by country.

Global methane emissions from enteric fermentation and manure management are estimated in the range of 99-115 Tg CH_4 yr^{-1}, for the year 2010, in the GAINS model and CEDS, USEPA, FAO-CH_4 and EDGARv4.3.2 inventories. These values are slightly higher than the IPCC Tier II estimates of Dangal et al (2017) (i.e., 87.5 and 95.7 Tg CH_4/yr for 2000 and 2010 respectively) and the IPCC Tier III estimates of Herrero et al (2013) (83.2 Tg CH_4 yr^{-1} for 2000).

https://doi.org/10.5194/essd-2019-128
Preprint. Discussion started: 19 August 2019

For the period 2008-2017, we estimated total emissions of 111 [106-116] Tg CH_4 yr^{-1} for enteric fermentation and manure management, about one third of total global anthropogenic emissions.

Rice cultivation. Most of the world's rice is grown in flooded paddy fields (Baicich, 2013). Under these shallow-flooded conditions, aerobic decomposition of organic matter gradually depletes most of the oxygen in the soil, resulting in anaerobic conditions and methane production. Most of this methane is oxidized in the overlying soil, while some is dissolved in the floodwater and leached away. The remaining methane is released to the atmosphere, primarily by diffusive transport through the rice plants, but methane also escapes from the soil via diffusion and bubbling through floodwaters (USEPA, 2016; Bridgham et al., 2013).

The water management systems used to cultivate rice are one of the most important factors influencing CH_4 emissions and is one of the most promising approaches for CH_4 emission mitigation (e.g. periodical drainage and aeration not only causes existing soil CH_4 to oxidize, but also inhibits further CH_4 production in soils (Simpson et al., 1995;USEPA, 2016;Zhang et al., 2016b). Upland rice fields are not flooded, and therefore are not a significant source of CH_4. Other factors that influence CH_4 emissions from flooded rice fields include fertilization practices (i.e. the use of urea and organic fertilizers), soil temperature, soil type (texture and aggregated size), rice variety and cultivation practices (e.g., tillage, seeding, and weeding practices) (USEPA, 2011, 2016; Kai et al., 2011; Yan et al., 2009; Conrad et al., 2000). For instance, methane emissions from rice paddies increase with organic amendments (Cai et al., 1997) but can be mitigated by applying other types of fertilizers (mineral, composts, biogas residues, wet seeding) (Wassmann et al., 2000).

The geographical distribution of rice emissions has been assessed by global (e.g., Tubiello, 2019; USEPA, 2006, 2012; Janssens-Maenhout et al., 2019) and regional (e.g. Peng et al., 2016; Chen et al., 2013; Chen and Prinn, 2006; Yan et al., 2009; Castelán-Ortega et al., 2014; Zhang and Chen, 2014) inventories or land surface models (Spahni et al., 2011; Zhang et al., 2016a; Ren et al., 2011; Tian et al., 2010; Tian et al., 2011; Li et al., 2005; Pathak et al., 2005). The emissions show a seasonal cycle, peaking in the summer months in the extra-tropics associated with the monsoons and with land management. Similar to emissions from livestock, emissions from rice paddies are influenced not only by extent of rice field area (equivalent to the number of livestock), but also by changes in the productivity of plants (Jiang et al., 2017) as these alter the CH_4 emission factor used in inventories. Nonetheless, the databases considered herein are largely based on IPCC Tier 1 methods, which largely scale with cultivated area but include regional specificities in emission factors.

The largest emissions are found in Asia (Hayashida et al., 2013), with China (5-11 Tg CH_4 yr^{-1}, Chen et al., 2013; Zhang et al., 2016a) and India (~3-5 Tg CH_4 yr^{-1}, Bhatia et al., 2013) accounting for 30 to 50% of global emissions (Fig. 3). This contrasts with the work of (Carlson et al., 2016) who suggested that India

https://doi.org/10.5194/essd-2019-128
Preprint. Discussion started: 19 August 2019

contributed a larger flux, 7.4 Tg CH_4/yr, than China, 6.2 Tg CH_4/yr around the year 2000. The lower emissions in China were linked to paddy drainage practises. The decrease of CH_4 emissions from rice cultivation over the past decades is confirmed in most inventories, because of the decrease in rice cultivation area, the change in agricultural practices, and a northward shift of rice cultivation since 1970s as in China (e.g. Chen et al., 2013)).

Based on the global inventories considered in this study, global methane emissions from rice paddies are estimated to be 30 [25-38] Tg CH_4 yr^{-1} for the 2008-2017 decade (Table 3), or about 8% of total global anthropogenic emissions of methane. These estimates are consistent with the 29 Tg CH_4 yr^{-1} estimated for the year 2000 by Carlson et al (2016).

Waste management. This sector includes emissions from managed and non-managed landfills (solid waste disposal on land), and wastewater handling, where all kinds of waste are deposited. These can emit significant amounts of methane through the anaerobic decomposition of organic material by microorganisms. Methane production from waste depends on pH, moisture and temperature. The optimum pH for methane emission is between 6.8 and 7.4 (Thorneloe et al., 2000). The development of carboxylic acids leads to low pH, which limits methane emissions. Food or organic waste, leaves and grass clippings ferment quite easily, while wood and wood products generally ferment slowly, and cellulose and lignin even more slowly (USEPA, 2010b).

Waste management is responsible for about 11% of total global anthropogenic methane emissions in 2000 at global scale (Kirschke et al., 2013). A recent assessment of methane emissions in the U.S. found landfills to account for almost 26% of total U.S. anthropogenic methane emissions in 2014, the largest contribution of any single CH_4 source in the United States (USEPA, 2016). In Europe, gas control is mandatory on all landfills from 2009 onwards, following the ambitious objective raised in the EU Landfill Directive (1999) to reduce the landfilling of biodegradable waste to 65% below the 1990 level by 2016. This is attempted through source separation and treatment of separated biodegradable waste in composts, bio-digesters, and paper recycling. This approach is assumed more efficient in terms of reducing methane emissions than the more usual gas collection and capture. Collected biogas is either burned by flaring, or used as fuel if it is pure enough (i.e. the content of methane is > 30%). Many managed landfills have the practice to apply cover material (e.g. soil, clay, sand) over the waste being disposed of in the landfill to prevent odour, reduce risk to public health, but also promote microbial communities of methanotrophic organisms (Bogner et al., 2007). In developing countries, very large open landfills still exist, with important health and environmental consequences in addition to methane emissions (André et al., 2014).

Wastewater from domestic and industrial sources is treated in municipal sewage treatment facilities and private effluent treatment plants. The principal factor in determining the CH_4 generation potential of

https://doi.org/10.5194/essd-2019-128
Preprint. Discussion started: 19 August 2019

wastewater is the amount of degradable organic material in the wastewater. Wastewater with high organic content is treated anaerobically and that leads to increased emissions (André et al., 2014). The large and fast urban development worldwide, and especially in Asia and Africa, could enhance methane emissions from waste unless adequate policies are designed and implemented rapidly.

The GAINS model and CEDS and EDGAR inventories give robust emission estimates from solid waste in the range of 29-41 Tg CH_4 yr^{-1} in the year 2005, and wastewater in the range 14-33 Tg CH_4 yr^{-1}1.

In this study, the global emission of methane from waste management is estimated in the range of 60-69 Tg CH_4 yr^{-1} for the 2008-2017 period with a mean value of 65 Tg CH_4 yr^{-1}, about 12% of total global anthropogenic emissions.

3.1.5 Biomass and biofuel burning

This category includes methane emissions from biomass burning in forests, savannahs, grasslands, peats, agricultural residues, as well as, from the burning of biofuels in the residential sector (stoves, boilers, fireplaces). Biomass and biofuel burning emits methane under incomplete combustion conditions, i.e., when oxygen availability is insufficient for complete combustion, for example in charcoal manufacture and smouldering fires. The amount of methane that is emitted during the burning of biomass depends primarily on the amount of biomass, the burning conditions, and the material being burned. At the global scale, during the period 2008-2017, biomass and biofuel burning generated methane emissions of 30 [26-40] Tg CH_4 yr^{-1} (Table 3), of which 30-50 % is biofuel burning.

In this study, we use the large-scale biomass burning (forest, savannah, grassland and peat fires) from specific biomass burning inventories (GFEDv4.1s, QFEDv2.5, GFASv1.3, FINNv1.5, FAO-CH_4 see below for details) and the biofuel burning contribution from anthropogenic emission inventories (EDGARv4.3.2, CEDS, GAINS and USEPA).

The spatial distribution of methane emissions from biomass burning over the 2008-2017 decade is presented in Fig. 3 and is based on the mean gridded maps provided by CEDS, EDGARv4.3.2 and GAINS for biofuel burning, and the mean gridded maps provided by the biomass burning inventories presented thereafter.

Biomass burning. Fire is the most important disturbance event in terrestrial ecosystems at the global scale (van der Werf et al., 2010), and can be of either natural (typically ~10%, ignited by lightning strikes or started accidentally) or anthropogenic origin (~90%, human initiated fires) (USEPA (2010a) chapter 9.1). Anthropogenic fires are concentrated in the tropics and subtropics, where forests, savannahs and grasslands may be burned to clear land for agricultural purposes or to maintain pastures and rangelands. Small fires associated with agricultural activity, such as field burning and agricultural waste burning, are often not well

https://doi.org/10.5194/essd-2019-128
Preprint. Discussion started: 19 August 2019

detected by remote sensing methods and are instead estimated based on cultivated area. As it is among the species emitted during biomass burning, carbon monoxide is a pertinent tracer for biomass burning emissions (Yin et al., 2015;Pechony et al., 2013).

Usually the biomass burning emissions are estimated using IPCC methodology, as:

$$E(x,t) = A(x,t,) * B(x) * FB * EF \quad (2)$$

where *A(x,t)* is the area burned, *B(x)* the biomass loading (depending on the biomes) at the location, *FB* the fraction of the area burned (or the efficiency of the fire depending on the vegetation type and the fire type) and *EF* the emissions factor (mass of the considered species / mass of biomass burned). Depending on the approach, these parameters can be derived using satellite data and/or biogeochemical model, or through simpler, IPCC default approaches.

The Global Fire Emission Database (GFED) is the most widely used global biomass burning emission dataset and provides estimates from 1997. In this review, we use GFEDv4.1s (van der Werf et al., 2017). GFED is based on the Carnegie-Ames-Stanford-Approach (CASA) biogeochemical model and satellite derived estimates of burned area, fire activity and plant productivity. From November 2000 onwards, these three parameters are inferred from the MODerate resolution Imaging Spectroradiometer (MODIS) sensor. For the period prior to MODIS, burned area maps are derived from the Tropical Rainfall Measuring Mission (TRMM) Visible and Infrared Scanner (VIRS) and Along-Track Scanning Radiometer (ATSR) active fire data and estimates of plant productivity derived from Advanced Very High Resolution Radiometer (AVHRR) observations during the same period. GFEDv4.1s (with small fires) is available at a 0.25° resolution and on a daily basis from 1997 to 2017. The particularity of the GFEDv4.1s burned area is that small fires are better accounted for as detected by MODIS (Randerson et al., 2012), increasing carbon emissions by approximately 35% on the global scale. However, interestingly, global methane emissions are 25% lower in GFEDv4 than in the previous version GFEDv3 because of new emission factors updated from Akagi et al. (2011).

The Quick Fire Emissions Dataset (QFED) is calculated using the fire radiative power (FRP) approach, in which the thermal energy emitted by active fires is converted to an estimate of methane flux using biome specific emissions factors and a unique method for accounting for cloud cover. FRP is estimated using the MODIS satellite and combined with vegetation maps from the International Geosphere-Biosphere Programme (IGBP) database. The resulting emissions factors are scaled to match GFEDv2. Further information related to this method and the derivation of the biome specific emission factors can be found in (Darmenov and da Silva, 2015). Here we use the historical QFEDv2.5 product available daily on a 0.1x0.1 grid for 2000 to 2017. Comparisons of an earlier version, QFEDv2.2, to other fire products (including GFEDv1.0 and GFASv3.1), (Darmenov and da Silva, 2015) found that the QFED database was well

https://doi.org/10.5194/essd-2019-128
Preprint. Discussion started: 19 August 2019

correlated with the other datasets, particularly GFAS (see after, R^2 = 0.96), with QFED typically showing similar seasonality but slightly larger global emissions than both GFED and GFAS.

The Fire Inventory from NCAR (FINN, Wiedinmyer et al., 2011) provides daily, 1km resolution estimates of gas and particle emissions from open burning of biomass (including wildfire, agricultural fires and prescribed burning) over the globe for the period 2002-2018. FINNv1.5 uses MODIS satellite observations for active fires, land cover and vegetation density. The emission factors are from Akagi et al. (2011), the estimated fuel loading are assigned using model results from Hoelzemann et al. (2004), and the fraction of biomass burned is assigned as a function of tree cover (Wiedinmyer et al., 2006).

The Global Fire Assimilation System (GFAS, Kaiser et al., 2012) calculates biomass burning emissions by assimilating Fire Radiative Power (FRP) observations from MODIS at a daily frequency and 0.5° resolution and is available for the time period 2000-2016. After correcting the FRP observations for diurnal cycle, gaps etc., it is linked to the dry matter combustion rate using Wooster et al. (2005) and CH_4 emission factors from Andreae and Merlet (2001). Here we use GFASv1.3.

The FAO-CH_4 yearly biomass burning emissions are based on the most recent MODIS 6 burned area products, coupled with a pixel level (500m) implementation of the IPCC Tier 1 approach. The FAO-CH_4 dataset has been shown to be consistent with GFED, however it extends the estimation of peatland fires to regions beyond South East Asia (Rossi et al., 2016). FAO-CH_4 biomass burning emissions are available from 1990 to 2016 (Table 1).

The differences in the biomass burning emission estimates arise from various difficulties, among them the ability to represent and know geographical and meteorological conditions and fuel composition, which highly impact combustion completeness and emission factors. The latter also vary greatly according to fire type, ranging from 2.2 g CH_4 kg^{-1} dry matter burned for savannah and grassland fires up to 21 g CH_4 kg^{-1} dry matter burned for peat fires (van der Werf et al., 2010).

Tian et al. (2016) estimated that CH_4 emissions from biomass burning during the 2000s were 23±11 Tg CH_4 yr^{-1} (top-down) and 20±7 Tg CH_4 yr^{-1} (bottom-up). Based on a combination of bottom-up estimates for fire emissions, of burnt area measurements, and of observationally-constrained top-down emissions of CO, (Worden et al., 2017) estimated lower fire emissions at 12.9 ± 3.3 CH_4 yr^{-1} for the time period 2001-2014. In this study, based on the five aforementioned products, biomass burning emissions are estimated at 17 Tg CH_4 yr^{-1} [14-26] for the decade 2008-2017, representing about 5% of total global anthropogenic methane emissions.

Biofuel burning. Biomass that is used to produce energy for domestic, industrial, commercial, or transportation purposes is hereafter called biofuel burning. A largely dominant fraction of methane emissions from biofuels comes from domestic cooking or heating in stoves, boilers and fireplaces, mostly

https://doi.org/10.5194/essd-2019-128
Preprint. Discussion started: 19 August 2019

in open cooking fires where wood, charcoal, agricultural residues, or animal dung are burnt. It is estimated that more than two billion people, mostly in developing countries, use solid biofuels to cook and heat their homes on a daily basis (André et al., 2014), and yet methane emissions from biofuel combustion have not yet received full attention. Biofuel burning estimates are gathered from the CEDS, USEPA, GAINS and EDGAR inventories.

Due to the sectorial breakdown of the EDGAR and CEDS inventories the biofuel component of the budget has been estimated as equivalent to the "RCO - Energy for buildings" sector as defined in (Worden et al., 2017) and Hoesly et al. 2018 (See Table S2). This is equivalent to the sum of the IPCC 1A4a_Commercial-institutional, 1A4b_Residential, 1A4c_Agriculture-forestry-fishing and 1A5_Other-unspecified reporting categories. This definition is consistent with that used in Saunois et al. (2016) and Kirschke et al. (2013). While this sector incorporates biofuel use it also includes the use of other combustible materials (e.g. coal or gas) for small scale heat and electricity generation within residential and commercial premises. Data provided within the GAINS inventory suggests that this approach may overestimate biofuels emissions by between 5 and 50%.

In this study, biofuel burning is estimated to contribute 11 Tg CH_4 yr^{-1} [10-14] to the global methane budget, about 3% of total global anthropogenic methane emissions.

3.1.6 Other anthropogenic sources (not included in the budget)

Other anthropogenic sources not yet directly accounted for here are related to agriculture and land-use management. In particular, increases in global palm oil production have led to the clearing of natural peat forests, reducing natural peatland area and the associated natural CH_4 emissions. While studies have long suggested that CH_4 emissions from peatland drainage ditches are likely to be significant (e.g., Minkkinen and Laine, 2006), CH_4 emissions related to palm oil plantations remain to be properly quantified. Page et al. (2011) and Taylor et al. (2014) have quantified global palm oil wastewater treatment fluxes as 2 ± 21 Tg CH_4 yr^{-1} for 2000-2009 and 4± 32 Tg CH_4 yr^{-1} for 2010-2013. This currently represents a small and highly uncertain source of methane but potentially growing in the future.

Anthropogenic flooded land, including reservoirs, artificial ponds, canals, and ditches, emit CH_4 to the atmosphere. The emission pathways are the same as those described for inland waters below (diffusive flux, ebullition and plant-mediated flux), plus reservoir specific pathways including degassing of CH_4 from turbines (hydropower reservoirs only) and elevated diffusive emissions in rivers downstream of the reservoir - these latter emissions are enhanced if the water outlet comes from anoxic CH_4-rich hypolimnion waters in the reservoir (Bastviken et al., 2004; Guérin et al., 2006; 2016). Methane emissions from reservoirs (mostly larger ones) are estimated along with the natural inland water system (Sect 3.2.2), despite their anthropogenic origin. Small artificial water-bodies have a high surface area to volume ratio,

https://doi.org/10.5194/essd-2019-128
Preprint. Discussion started: 19 August 2019

and shallow depth, and are likely to be a notable source of methane, at least at the regional scale (Grinham et al., 2018; Ollivier et al., 2019). These studies found that emissions varied by pond type (for example: livestock rearing farm dams vs. cropping farm dams vs. urban ponds vs. weirs). A rough estimate of the global impact of this emission source is globally significant, between 3 and 8 Tg CH_4 yr^{-1} (calculated using the mean emission rates from Grinham et al. (2018) and Ollivier et al. (2018) and an estimate of global farm impoundment surface area of 77,000 km^2 (Downing et al., 2006)). Still, this estimate is quite uncertain given uncertainty in both the per-area emission rates (which likely vary by both pond type and by geographic location) and in the surface area of artificial ponds globally. However, this rough estimate does emphasise the potential significance of these sources, although double counting with current uncertain estimates from natural inland water systems (see next section) is possible (Thornton et al., 2016b). Canals and ditches have recently been highlighted as high areal emitters (e.g., Stanley et al., 2016), and their contribution to large-scale emission are typically included in estimates for overall running waters so far. For an extended discussion on general uncertainties of inland water flux estimates, see the natural inland water section below.

3.2 Natural methane sources

Natural methane sources include vegetated wetland emissions and inland water systems (lakes, small ponds, rivers), land geological sources (gas-oil seeps, mud volcanoes, microseepage, geothermal manifestations and volcanoes), wild animals, wildfires, termites, thawing terrestrial and marine permafrost and oceanic sources (biogenic, geological and hydrate). Many sources have been recognized but their magnitude and variability remain the most uncertain part of the global methane budget (Kirschke et al., 2013; Saunois et al., 2016).

3.2.1 Wetlands

Wetlands are generally defined as ecosystems in which soils or peats are water saturated or where surface inundation (permanent or not) dominates the soil biogeochemistry and determines the ecosystem species composition (USEPA, 2010a). In order to refine such overly broad definition for methane emissions, we define wetlands as ecosystems with inundated or saturated soils or peats where anaerobic conditions lead to methane production (USEPA, 2010a; Matthews and Fung, 1987). Brackish water emissions are discussed separately in Sect. 3.2.6. Our definition includes peatlands (bogs and fens), mineral soil wetlands (swamps and marshes), as well as seasonal or permanent floodplains. It excludes exposed water surfaces without emergent macrophytes, such as lakes, rivers, estuaries, ponds, and reservoirs (addressed in the next section), as well as rice agriculture (see Sect. 3.1.4, rice cultivation paragraph) and wastewater ponds. It also excludes coastal vegetated ecosystems (mangroves, seagrasses, salt marshes) with salinities usually

https://doi.org/10.5194/essd-2019-128
Preprint. Discussion started: 19 August 2019

>0.5 (See Sect. 3.2.6). Even with this definition, parts of the wetlands could be considered as anthropogenic systems, being affected by human-driven land-use changes such as impoundments or even losses due to drainage (Woodward et al., 2012). In the following we keep the generic denomination wetlands for natural and human-influenced wetlands.

Anaerobic conditions are required for acetoclastic or hydrogenotrophic methanogenesis by *Archea*. High-water table or flooded conditions limit oxygen availability and creates suitable redox conditions for methane production (Fiedler and Sommer, 2000) in water saturated soils, peats and sediments. Although recent work suggests modest amounts of methane can also be produced in aerobic tidal freshwater marshsoils (Angle et al., 2017), this process is not integrated in this analysis. The three most important factors influencing methane production in wetlands are the spatial and temporal extent of anoxia (linked to water saturation), temperature and substrate availability (Wania et al., 2010; Valentine et al., 1994; Whalen, 2005). Once produced, methane can reach the atmosphere through a combination of three processes: molecular diffusion limited advection, plant-mediated transport, and ebullition. On its way to the atmosphere, methane can be partly or completely oxidized by a group of bacteria, called methanotrophs, which use methane as their only source of energy and carbon (USEPA, 2010a). Concurrently, methane from the atmosphere can diffuse into the soil column and be oxidized (See Sect. 3.3.4).

Land-surface models estimate CH_4 emissions through a series of processes, including CH_4 production, CH_4 oxidation and transportation and are further regulated by changing environmental factors (Tian et al., 2010; Xu et al., 2010; Melton et al., 2013;Wania et al., 2013; Poulter et al., 2017). Methane emissions originating from wetlands to the atmosphere are computed as the product of an emission flux density and a methane producing area or surface extent (Supplementary Material, Melton et al. (2013); Bohn et al., 2015). Wetland extent appears to be a primary contributor to uncertainties in the absolute flux of methane emissions from wetlands and climate response the main source of uncertainty for seasonal and interannual variability (Bohn et al., 2015; Desai et al., 2015; Poulter et al., 2017).

In this work, following on from Melton et al. (2013) and Poulter et al. (2017), thirteen land surface models computing net CH_4 emissions (Table 2) were run under a common protocol with a 30-year spin-up (1901-1930) followed by a simulation until the end of 2017 forced by CRU-JRA reconstructed climate fields (Harris, 2019). Atmospheric CO_2 influencing NPP was also prescribed in the models, allowing the models to separately estimate carbon substrate availability for methanogenesis. In all models, the same remote sensing based wetland area and dynamics dataset, which we refer to as WAD2M; Wetland Area Dynamics for Methane Modeling) was prescribed. The WAD2M dataset is a monthly global wetland area dataset, which has been developed to address some known issues of previous work, such as inclusion of inland waters (Poulter et al., 2017). WAD2M combines microwave remote sensing data from Schroeder et al. (2015) with various regional inventory datasets to develop a monthly global wetland area dataset (Poulter et

https://doi.org/10.5194/essd-2019-128
Preprint. Discussion started: 19 August 2019

al., 2019). Non-vegetated wetland inland waters (i.e., lakes, rivers and ponds) were subtracted using the Global Surface Waters dataset of (Pekel et al., 2016), assuming that permanent waters were those that were present > 50% of the time within a 32-year observing period. Then, data for the tropics (Gumbricht et al., 2017), high-latitudes (Hugelius et al., 2014) and (Widhalm et al., 2015) and temperate regions (Lehner and Döll, 2004) were used to set the long-term annual mean wetland area, to which a seasonal cycle of fractional surface water was added using data from the Surface WAter Microwave Product Series Version 3.2 (SWAMPS) (Jensen and McDonald, 2019;Schroeder et al., 2015). Rice agriculture was removed using the MIRCA2000 dataset from circa 2000, as a fixed distribution The combined remote-sensing and inventory WAD2M product leads to a maximum wetland area of 14.9 Mkm^2during the peak season (8.4 Mkm^2 on annual average, with a range of 8.0 to 8.9 Mkm^2 from 2000-2017, about 5.5% of the global land surface). The largest wetland areas in the WAD2M are in Amazonia, the Congo Basin, and the Western Siberian Lowlands, which in previous studies have appeared to be strongly underestimated by several inventories (Bohn et al., 2015).

The average emission map from wetlands for 2008-2017 built from the 13 models is plotted in Fig. 3. The zones with the largest emissions reflect the WAD2M database: the Amazon basin, equatorial Africa and Asia, Canada, western Siberia, eastern India, and Bangladesh. Regions where methane emissions are robustly inferred (i.e., regions where mean flux is larger than the standard deviation of the models) represent 61% of the total methane flux due to natural wetlands. This contribution is 80% lower than found in Saunois et al. (2016) probably due to the different ensemble of models gathered here and the more stringent exclusion of inland waters. Over the 13 models, 10 contributed to Saunois et al. (2016), three models newly participated for this release (JSBACH, LPJ-GUESS and TEM-MDM), and SDGVM did not contribute (Table S3). The main primary emission zones are consistent between models, which is clearly favoured by the prescribed common wetland extent. However, the different sensitivities of the models to temperature, vapour pressure, precipitation, and radiation can generate substantially different patterns, such as in India. Some secondary (in magnitude) emission zones are also consistently inferred between models: Scandinavia, Continental Europe, Eastern Siberia, Central USA, and tropical Africa. Using improved regional methane emission data sets (such as studies over North America, Africa, China, and Amazon) can enhance the accuracy of the global budget assessment (Tian et al., 2011; Xu and Tian, 2012; Ringeval et al., 2014; Valentini et al., 2014).

The resulting global flux range for natural wetland emissions is 101-179 Tg CH_4 yr^{-1} for the 2000-2017 period, with an average of 148 Tg CH_4 yr^{-1} and a one-sigma standard deviation of 25 Tg CH_4 yr^{-1}. For the last decade, 2008-2017, the average ensemble emissions were 149 Tg CH_4 yr^{-1} with a range of 102-182 (Table 3). Using a prognostic set of simulations, where models used their own internal approach to estimate wetland area and dynamics, the average ensemble emissions were 161 Tg CH_4 yr^{-1} with a range of 125-218

https://doi.org/10.5194/essd-2019-128
Preprint. Discussion started: 19 August 2019

for the 2008-2017 period. The greater range of uncertainty from the prognostic models is due to unconstrained wetland area, but generally the magnitude and interannual variability agree between diagnostic and prognostic approaches. These emissions represent about 30% of the total (natural plus anthropogenic) methane sources. The large range in the estimates of wetland CH_4 emissions results from difficulties in defining wetland CH_4 producing areas as well as in parameterizing terrestrial anaerobic conditions that drive sources and the oxidative conditions leading to sinks (Poulter et al., 2017; Melton et al., 2013; Wania et al., 2013). The ensemble mean using diagnostic wetland extent in the models is lower by ~35 Tg CH_4 yr^{-1} than the one previously reported (see Table 3, for 2000-2009 with comparison to Saunois et al., 2016). This difference results from a reduction in double counting due to i) decreased wetland area in WAD2M, especially for high-latitude regions where the inland waters, i.e., lakes, small ponds and lakes, were removed, and ii) to some extent, an improved removal of rice agriculture area using the MIRCA-2000 database.

3.2.2 Other inland water systems (lakes, ponds, rivers, reservoirs)

This category includes methane emissions from freshwater systems (lakes, ponds, reservoirs, streams and rivers). Methane emissions to the atmosphere from freshwaters occur through a number of pathways including (1) diffusive loss of dissolved CH_4 across the air-water boundary; (2) ebullition flux from organic rich sediments and (3) flux mediated by emergent aquatic macrophytes (plant transport) in littoral environments. It is very rare that bottom-up emission budgets distinguish among all of these flux types, and many top-down inversion do not have these emissions explicitly represented. Meta-data analyses are hampered for methane due to a mix of methodological approaches, which capture different components of emissions depending on method and time of deployment and data processing (Stanley et al., 2016). The different methods and study designs used also capture different scales in space and time. Altogether, this inconsistency in the data collection makes detailed modelling of fluxes highly uncertain. To date, very few process-based models exist for these fluxes, relying on data driven approaches and extrapolations. For many lakes, particularly smaller shallower lakes and ponds, it is established that ebullition and plant fluxes (in lakes with substantial emergent macrophyte communities) can make up a substantial contribution to fluxes, potentially accounting for 50% to more than 90% of the flux from these water bodies. While contributions from ebullition appear lower from rivers, there are currently insufficient measurements from these systems to determine its role (Stanley et al., 2016; Crawford et al., 2014). Ebullition fluxes are very challenging to measure, due to the high degree of spatiotemporal variability with very high fluxes occurring in parts of an ecosystem over the time frames of seconds followed by long periods without ebullition.

Streams and rivers. Freshwater methane fluxes from streams and rivers were first estimated to be 1.5 Tg CH_4 yr^{-1} (Bastviken et al. 2011). However, this study had measurements from only 21 sites globally. More

https://doi.org/10.5194/essd-2019-128
Preprint. Discussion started: 19 August 2019

recently, Stanley et al. (2016) compiled a data set of 385 sites and estimated a diffusive emission of 27 Tg CH_4 yr^{-1} (5th–95th percentiles: 0.01–160 Tg CH_4 yr^{-1}). Detailed regional studies in the tropics and temperate watersheds (Borges et al., 2015;Campeau and del Giorgio, 2014) support a flux in the range of 27 Tg CH_4 yr^{-1} as opposed to the initial ~1.5 Tg CH_4 yr^{-1}, however the low number of measurements, the lack of clarity on ebullitive fluxes, and the large degree of variance in measurements have precluded an accurate spatial representation of stream and river methane fluxes. No new global estimates have been published since Stanley et al. (2016) and Saunois et al. (2016). As a result, we use here the same estimate for stream and rivers as in Saunois et al. (2016): 27 Tg CH_4 yr^{-1}.

Lakes and ponds. Methane emissions from lakes were first estimated to 1-20 Tg CH_4 yr^{-1} based on measurements in two systems (Great Fresh Creek, Maryland and Lake Erie; Ehhalt (1974)). A subsequent global emission estimate was 11-55 Tg CH_4 yr^{-1} based on measurements from three Arctic lakes and a few temperate and tropical systems (Smith and Lewis, 1992), and 8-48 Tg CH_4 yr^{-1} using extended data from a series of latitudinal bands (73 lakes, Bastviken et al., (2004)). Based on data from 421 lakes and ponds, Bastviken et al. (2011) updated their values to 71.6 Tg CH_4 yr^{-1}, including emissions from non-saline lakes and ponds. High-latitude lakes include both post-glacial and thermokarst lakes (water bodies formed by thermokarst), the latter having larger emissions per square meter but smaller regional emissions than the former because of smaller areal extent (Wik et al., 2016b). Water body depth, sediment type, and eco-climatic region are the key factors explaining variation in methane fluxes from lakes (Wik et al., 2016b). A regional estimate for latitudes above 50° North (Wik et al., 2016b) estimated lake and pond methane emissions to 16.5 Tg CH_4 yr^{-1} (compared to 13.4 Tg CH_4 yr^{-1} in Bastviken et al. (2011), above 54 °N). Tan et al (2016) used atmospheric inversion approaches and estimated that the current pan-Arctic (north of 60 °N) lakes emit 2.4-14.2 Tg CH_4 yr^{-1}, while a process-based lake biogeochemistry model (bLake4Me) estimated the emissions at 11.9 [7.1-17.3] Tg CH_4 yr^{-1} (Tan et al., 2015). These numbers for northern or Arctic lakes need to be considered with regard to the latitudinal area encompassed which differ among studies (Thornton et al. 2016b). Saunois et al. (2016) estimates for emissions from natural lakes and ponds were based on Bastviken et al. (2011), using the emissions from the northern high latitudes above 50°N from Wik et al., (2016b), leading to a rounded mean value of 75 Tg CH_4 yr^{-1}. Thus emissions between 50°N and 54°N were double counted in this previous estimate. Roughly re-distributing Bastviken et al. (2011) latitudinal values over different latitudinal bands leads to lake emissions at 18.8 Tg CH_4 yr^{-1} and 10.1 Tg CH_4 yr^{-1} north of 50°N and north of 60°N respectively, higher than Wik et al. (2016b) and lower than Tan and Zhuang (2015). Combining Bastviken et al. (2011) south of 50°N with the estimate from Wik et al. (2016b) and Bastviken et al. (2011) south of 60°N) with. Tan and Zhuang, 2015) leads to global emissions of 69.3 and 73.4 Tg CH_4 yr^{-1} respectively. Thus we derive here a rounded mean global estimate of 71 Tg CH_4 yr^{-1} close to Bastviken et al. (2011) (71.6 Tg CH_4 yr^{-1}).

https://doi.org/10.5194/essd-2019-128
Preprint. Discussion started: 19 August 2019

Reservoirs. Methane emissions from reservoirs may be considered anthropogenic sources as humans build them. However, reservoir ecosystems are not managed afterwards and methane emissions do not directly depend on human activities. In this budget methane emissions from reservoirs are accounted for in the natural sources. In Saunois et al. (2016), methane emissions from reservoirs were estimated to be 20 Tg CH_4 yr^{-1} using Bastviken et al. (2011), which was based on data from 32 systems. A more recent and extensive review estimated total reservoir emissions to 18 Tg CH_4 yr-1 (95% confidence interval 12-30 Tg CH_4 yr-1; n = 75 (Deemer et al., 2016)), which is used to revise our estimate in this study.

Combination. Combining emissions from lakes and ponds from Bastviken et al. (2011) (71.6 Tg CH_4 yr^{-1}) with the recent estimate of Deemer et al. (2016) for reservoirs and the streams and river estimates from Stanley et al. (2016) leads to total inland freshwater emissions of 117 Tg CH_4 yr^{-1}. Recently, using a new up scaling approach based on size weighting productivity and chlorophyll-A, (DelSontro et al., 2018) provided a combined lake and reservoir estimates of 104 (5th–95th percentiles: 67-165), 149 (5th–95th percentiles: 95-236) and 185 (5th–95th percentiles: 119-295) Tg CH_4 yr^{-1}, using the lake size distributions from Downing et al. (2006), Messager et al. (2016) and Verpooter et al. (2014), respectively. These estimates are higher (by 10%, 57% and almost 100%, respectively) than previously reported in Saunois et al. (2016) (ie, 95 Tg CH_4 yr^{-1} for lakes, ponds and reservoirs). Adding the streams and river estimates from Stanley et al. (2016) to DelSontro et al. (2018) yields total freshwater estimates of 131, 176 and 212 Tg CH_4 yr^{-1}.

Previously, Kirschke et al. (2013) reported a range of 8-73 Tg CH4 yr-1 for this ensemble of emissions and Saunois et al. (2016) a mean value of 122 Tg CH_4 yr^{-1} (75 Tg CH_4 yr^{-1} for lakes and ponds, adding 20 Tg CH_4 yr^{-1} for reservoirs (Bastviken et al., 2011) and 27 Tg CH_4 yr^{-1} for streams and rivers (Stanley et al., 2016)). This mean value was based on a single set of estimates, to which a 50% uncertainty was associated as a range (60-180 Tg CH_4 yr^{-1}). Here the new estimates of DelSontro et al. (2018) allows to calculate a mean estimate of all inland freshwaters at 159 Tg CH_4 yr^{-1} associated to the range 117-212 Tg CH_4 yr^{-1} that reflects the minimum and maximum values of the available studies (see Methodology, Sect. 2). However, it should be noted that this range does not take into account the uncertainty of individual studies. Importantly, these current estimates do not include the smallest size class of lakes or ephemeral streams resulting in a possible misallocation of freshwater fluxes to wetland ecosystems in spite of the attempts to discount open water emissions from the wetland estimate (see above). The present data indicate that lakes or natural ponds, flooded land/reservoirs and streams/rivers account for 70%, 13% and 17% of the average fluxes, respectively (given the large uncertainty the percentages should be seen as approximate relative magnitudes only).

The improvement in quantifying inland water fluxes is highly dependent on the availability of more accurate assessments of their surface area. Yet despite new estimates of surface areas, there are still

https://doi.org/10.5194/essd-2019-128
Preprint. Discussion started: 19 August 2019

important discrepancies between published studies that prevent us from stabilizing estimates of freshwater methane emissions in this update of the global methane budget. For streams and rivers, the 355,000km^2 used in Bastviken et al. (2011) were re-evaluated to 540,000 km^2 by Stanley et al. (2016) due to new surface area estimate from Raymond et al. (2013). Regarding lakes and reservoirs, the three current inventories (Downing et al., 2006;Messager et al., 2016;Verpoorter et al., 2014) show typical differences of a factor 2 to 5 by size-class. Also, it was noted that small ponds, which were not included in either Downing et al. (2006) or Verpoorter et al. (2014), have a diffusive flux higher than any other size class of lakes (Holgerson and Raymond, 2016). Further analysis, and possibly more refined process-based models, are still necessary and urgent to evaluate these global up scaled estimates against regional specific approaches such as Wik et al. (2016b) for the northern high latitude lakes.

It is important to note that the above estimates of all inland water fluxes are not independent. Instead, they represent updates from increasing data quantity and quality. Altogether, these studies consider data from about 1000 systems, of which ~750 are located north of 50°N. In this context we only consider fluxes from open waters assuming that plant-mediated fluxes (estimated at 10.2 Tg CH_4 yr^{-1} in Bastviken et al., 2011) are included in the wetland emission term. It should also be noted that issues regarding spatiotemporal variability are not considered in consistent ways at present (Wik et al., 2016a; Natchimuthu et al., 2015). Given the inconsistencies in the areal flux data and in area estimates, the aim to make frequent updates of the methane emissions is presently not possible for inland water emissions. Even more than for other emission categories, differences in inland water flux values between updates of this paper are more likely to represent differences in what data are used and how the data is processed, rather than reflecting real temporal trends in the environment.

Several aspects will need consideration to reduce the remaining uncertainty in the freshwater fluxes including generating flux measurements that are more representative in time and space, updating surface area databases (e.g. GLOWABO, Verpoorter et al. (2014), HydroLAKES, Messager et al., 2016), and refining our understanding of ebullitive fluxes. Furthermore, it is clear that double accounting between inland waters and wetlands is occuring (Thornton et al., 2016b). As a result, new frontiers include i) concluding the ongoing effort to develop high resolution (further <30m) classification of saturated and inundated continental surfaces, ii) developing systematic flux data collection efforts, capturing spatiotemporal variability, and in turn (iii) the development of process-based models, to include lateral fluxes, for example, for the different inland waters systems avoiding up scaling issues, as recently done by e.g. (Maavara et al., 2019) for N_2O.

https://doi.org/10.5194/essd-2019-128
Preprint. Discussion started: 19 August 2019

3.2.3 Onshore and offshore geological sources

Significant amounts of methane, produced within the Earth's crust, naturally migrate to the atmosphere through tectonic faults and fractured rocks. Major emissions are related to hydrocarbon production in sedimentary basins (microbial and thermogenic methane), through continuous or episodic exhalations from onshore and shallow marine hydrocarbon seeps and through diffuse soil microseepage (after Etiope, 2015). Specifically, five source categories have been considered. Four are onshore sources: gas-oil seeps, mud volcanoes, diffuse microseepage and geothermal manifestations including volcanoes. One source is offshore: submarine seepage, which may include the same types of gas manifestations occurring on land. Based on (i) the acquisition of thousands of land-based flux measurements for various seepage types in many countries, (ii) existing datasets from oil and gas industry and studies on volcanism, and (iii) following the same procedures as for other sources (using the concepts of "point sources", "area sources", "activity data" and "emission factors", EMEP/EEA, 2009), (Etiope et al., 2019) have produced the first gridded maps of geological methane emissions and their isotopic signature for these five categories, with a global total of 37.4 Tg CH_4 yr^{-1} (reproduced in Fig. 4). The grid maps do not represent, however, the actual global geological-CH_4 emission because the datasets used for the spatial gridding (developed for modelling purposes) were not complete or did not contain the information necessary for improving all previous estimates. Combining the best estimates for the five categories of geological sources (from grid maps or from previous statistical and process-based models), the breakdown by category reveals that onshore microseepage dominate (24 Tg CH_4 yr^{-1}), the other categories having similar smaller contributions: as average values, 4.7 Tg CH_4 yr^{-1} for geothermal manifestations, about 7 Tg CH_4 yr^{-1} for submarine seepage and 9.6 Tg CH_4 yr^{-1} for onshore seeps and mud volcanoes. These values lead to a global bottom-up geological emission mean of 45 [27-63] Tg CH_4 yr^{-1} (Etiope and Schwietzke, 2019).

This bottom-up estimate is compatible with top-down estimates derived by combining radiocarbon (^{14}C) and ethane concentrations data in the atmosphere and polar ice-cores and related modelling (Lassey et al., 2007a,b; (Nicewonger et al., 2016); Schwietzke et al., 2016; (Dalsøren et al., 2018), Etiope and Schwietzke, 2019). While all bottom-up and some top-down estimates, following different and independent techniques from different authors consistently suggest a global geo-CH_4 emission in the order of 40-50 Tg yr-1, the radiocarbon (^{14}C-CH_4) data in ice cores reported by (Petrenko et al., 2017) appear to lower the estimate, with a range of 0 (zero) to 18.1 Tg CH_4 yr^{-1} (<15.4 Tg CH_4 yr^{-1}, 95 percent confidence) at least for the atmosphere between 11,000 and 12,000 years ago (Younger-Dryas Preboreal transition). If the Petrenko et al. (2017) estimate is correct and reflects present-day conditions (which is questionable), its range, including zero and near-zero emissions, is lower than any estimates from different authors that do

https://doi.org/10.5194/essd-2019-128
Preprint. Discussion started: 19 August 2019

not go below 18 Tg CH_4 yr^{-1} (Etiope et al., 2019). The discrepancy between Petrenko et al (2017) and all other estimates has opened a new debate and certainly it represents an interesting topic of discussion.

Waiting for further investigation on this topic, we decide to keep the best estimates from Etiope and Shwietzke, (2019) for the mean values, and associate it to the lowest estimates reported in Etiope et al. (2019). Thus we report a total global geological emission of 45 [18-63] Tg CH_4 yr^{-1}, with the following breakdown: offshore emissions 7 [5-10] Tg CH_4 yr^{-1} and onshore emissions 38 [13-53] Tg CH_4 yr^{-1}. The updated bottom-up estimate is slightly lower than the previous budget mostly due to a reduction of estimated emissions of onshore and offshore seeps (see Sect. 3.2.6 for more offshore contribution explanations).

3.2.4 Termites

Termites are an order of insects (isoptera), which occur predominantly in the tropical and subtropical latitudes (Abe et al., 2000). Thanks to their metabolism they play an important role in the decomposition of plant material and C cycling, CO_2 and CH_4 being released during the anaerobic decomposition of plant biomass in their gut (Sanderson, 1996). The uncertainty related to this CH_4 source is very high as CH_4 emissions from termites in different ecosystem types can vary and are driven by a range of factors while the number field measurements both of termite biomass and emissions are relatively scarce (Kirschke et al. 2013).

In Kirschke et al. (2013) (see their supplementary material), a re-analysis of CH_4 emissions from termites at the global scale was proposed. There CH_4 emissions per unit of surface were estimated as the product of termite biomass, termite CH_4 emissions per unit of termite mass and a scalar factor expressing the effect of land use/cover change, the latter two terms estimated from published literature re-analysis (Kirschke et al., 2013, supplementary). For tropical climates, termite biomass was estimated by a simple regression model representing its dependence on GPP (Kirschke et al., 2013, supplementary), whereas termite biomass for forest and grassland ecosystems of the warm temperate climate and for shrub lands of the Mediterranean sub-climate were estimated from data reported by Sanderson (1996). The CH_4 emission factor per unit of termite biomass was estimated as 2.8 mg CH_4 g^{-1} termite h^{-1} for tropical ecosystems and Mediterranean shrublands (Kirschke et al., 2013) and 1.7 mg CH_4 g^{-1} termite h^{-1} for temperate forests and grasslands (Fraser et al., 1986). Emissions were scaled-up in ESRI ArcGIS environment and annual CH_4 fluxes computed for the three periods 1982-1989, 1990-1999 and 2000-2007 representative of the 1980s', 1990s' and 2000s', respectively.

The re-analysis of termite emissions proposed in Saunois et al. (2016), maintained the same approach but data were calculated using climate zoning (following the Koppen-Geiger classification) applied to updated

https://doi.org/10.5194/essd-2019-128
Preprint. Discussion started: 19 August 2019

climate datasets by Santini and di Paola (2015), and was adopted to take into account different combinations of termite biomass per unit area and CH_4 emission factor per unit of termite biomass.

Here, this analysis is extended to cover the period 2000-2007 and 2010-2016. This latest estimate follows the approach outlined above for Saunois et al. (2016). However in order to extend the analysis to 2016, an alternative, MODIS based measure of GPP (Zhang et al., 2017a) rather than (Jung et al., 2009) and (Jung et al., 2011) was used to estimate termite biomass. To have coherent datasets of GPP and land use, the latter variable previously derived from Ramankutty and Foley (1999) was substituted by MODIS maps (Friedl et al., 2010;Channan et al., 2014.). These new estimates covered 2000-2007 and 2010-2016 using 2002 and 2012 MODIS data as an average reference year for each period, respectively.

Termite CH_4 emissions show only little inter-annual and inter-decadal variability (0.1 Tg CH_4 yr^{-1}) but a strong regional variability with tropical South America and Africa being the main sources (23 and 28% of the global total emissions, respectively) due to the extent of their natural forest and savannah ecosystems (Fig. 4). Changing GPP and land use dataset sources had only a minimal impact on the 2000-2007 global termite flux, increasing it from 8.7 Tg CH_4 yr^{-1} as found in the first two re-analyses (Kirschke et al., 2013, Saunois et al. 2016) to 9.9 Tg CH_4 yr^{-1} (present data), well within the estimated uncertainty (8.7±3.1 Tg CH_4 yr^{-1}). But it had a noticeable effect on the spatial distribution of the flux (Fig. S2). These changes, most obviously a halving of the South East Asian flux, aligned with shifts in the underlying GPP product. Previous studies (Zhang et. al 2017a, Mercado et. al 2009) had linked these GPP shifts to a methodological issue with light-use efficiency that drove an underestimate of evergreen broadleaf and evergreen needleleaf forest GPP, biomes which are prevalent in the tropics. This value is close to the average estimate derived from previous up-scaling studies, which report values spanning from 2 to 22 Tg CH_4 yr^{-1} (Ciais et al., 2013).

In this study, we report a decadal value of 9 Tg CH_4 yr^{-1} (range [3-15] Tg CH_4 yr^{-1}, Table 3).

3.2.5 Wild animals

Wild ruminants emit methane through the microbial fermentation process occurring in their rumen, similarly to domesticated livestock species (USEPA, 2010a). Using a total animal population of 100-500 million, (Crutzen et al., 1986) estimated the global emissions of CH_4 from wild ruminants in the range of 2-6 Tg CH_4 yr^{-1}. More recently, (Pérez-Barbería, 2017) lowered this estimate to 1.1-2.7 Tg CH_4 yr^{-1} using a number of total animal population of 214 millions (range [210-219]), arguing that the maximum number of animals (500 million) used in Crutzen et al. (1986) was only poorly justified. Moreover Perez-Barberia (2017) also stated that the value of 15 Tg CH_4 yr^{-1} found in the last IPCC reports is much higher than their estimate because this value comes from an extrapolation of Crutzen work for the last glacial maximum when the population of wild animals was much larger, as originally proposed by (Chappellaz et al., 1993).

https://doi.org/10.5194/essd-2019-128
Preprint. Discussion started: 19 August 2019

Based on these findings, the range adopted in this updated methane budget is 2 [1-3] Tg CH_4 yr^{-1} (Table 3).

3.2.6 Oceanic sources

Oceanic sources comprise coastal ocean and open ocean methane release. Possible sources of oceanic CH_4 include: (1) production from marine (bare and vegetated) sediments or thawing sub-sea permafrost; (2) in situ production in the water column, especially in the coastal ocean because of submarine groundwater discharge (USEPA, 2010a); (3) leaks from geological marine seepage (see also Sect. 3.2.3); (4) emission from the destabilisation of marine hydrates. Once at the seabed, methane can be transported through the water column by diffusion in a dissolved form (especially in the upwelling zones), or by ebullition (gas bubbles, e.g. from geological marine seeps), for instance, in shallow waters of continental shelves. In coastal vegetated habitats methane can also be transported to the atmosphere through the *aerenchyma* of emergent aquatic plants (Ramachandran et al., 2004).

Biogenic emissions from open and coastal ocean. The most common biogenic ocean emission value found in the literature is 10 Tg CH_4 yr^{-1} (Rhee et al., 2009). It appears that most studies rely on the work of Ehhalt (1974), where the value was estimated on the basis of the measurements done by Swinnerton and co-workers (Lamontagne et al., 1973; Swinnerton and Linnenbom, 1967) for the open ocean, combined with purely speculated emissions from the continental shelf. Based on basin-wide observations using updated methodologies, three studies found estimates ranging from 0.2 to 3 Tg CH_4 yr^{-1} (Conrad and Seiler, 1988; Bates et al., 1996; Rhee et al., 2009), associated with super-saturations of surface waters that are an order of magnitude smaller than previously estimated, both for the open ocean (saturation anomaly ~0.04, see Rhee et al. (2009), equation 4) and for continental shelf (saturation anomaly ~0.2). In their synthesis, indirectly referring to the original observations from Lambert and Schmidt (1993), Wuebbles and Hayhoe (2002), they use a value of 5 Tg CH_4 yr^{-1}. Proposed explanations for discrepancies regarding sea-to air methane emissions in the open ocean rely on experimental biases in the former studies of Swinnerton and Linnenbom (Rhee et al., 2009). This may explain why the Bange et al. (1994) compilation cites a global source of 11-18 Tg CH_4 yr^{-1} with a dominant contribution of coastal regions. Here, we report a range of 0-5 Tg CH_4 yr^{-1}, with a mean value of 2 Tg CH_4 yr^{-1} for biogenic emissions from open and coastal ocean (excluding estuaries).

Biogenic emissions from brackish waters (estuaries, coastal wetlands) were not reported in the previous budget (Saunois et al., 2016). Methane emissions from estuaries were originally estimated by Bange et al. (1994), Upstill-Goddard et al. (2000) and Middelburg et al. (2002) to be comprised between 1 and -3 Tg CH_4 yr^{-1}. This range was later revised upwards by Borges and Abril (2011) to about 7 Tg CH_4 yr^{-1} based on a methodology distinguishing between different estuarine types and accounting for the contribution of tidal flats, marshes and mangroves, for a total of 39 systems and a global "inner" estuarine surface area of 1.1

https://doi.org/10.5194/essd-2019-128
Preprint. Discussion started: 19 August 2019

10^6 km^2 (Laruelle et al., 2013). The same methodology as in Laruelle et al. (2013) has been applied here to the same systems using an expanded database of local and regional measurements (72 systems) and suggests however that global estuarine CH_4 emissions were overestimated and may actually not surpass 3-3.5 Tg CH_4 yr^{-1}. Despite this overall reduction, the specific contribution of sediment and water emissions from mangrove ecosystems is however higher and contributes 0.03 to 1.7 Tg CH_4 yr^{-1} globally (Rosentreter et al., 2018). This estuarine estimate does not include the uncertain contribution from large river plumes protruding onto the shelves. Their surface area reaches about 3.7 10^6 km^2 (Kang et al., 2013) but because of significantly lower CH_4 concentration (e.g. Zhang et al., 2008; Osudar et al., 2015) than in inner estuaries, the outgassing associated with these plumes likely does not exceed 1-2 Tg CH_4 yr^{-1}. Seagrass meadows are also not included although they might release 0.09 to 2.7 Tg CH_4 yr^{-1} (Garcias-Bonet and Duarte, 2017). These methane emissions from vegetated coastal ecosystems can partially offset (Rosentreter et al. 2018) their "blue carbon" sink (e.g., Nellemann et al., 2009; McLeod et al., 2011). Note that the latter two contributions might partly overlap with oceanic (open and coastal) sources estimates. The total (inner and outer) estuarine emission flux, which is based on only about 80 systems is thus in the range 4-5 Tg CH_4 yr^{-1} (including marshes and mangrove). High uncertainties in coastal ocean emission estimates can be reduced by better defining the various coastal ecosystem types and their boundaries to avoid double-counting (e.g. estuaries, brackish wetlands, freshwater wetlands), updating the surface area of each of these coastal systems, and better quantifying methane emission rates in each ecosystem type.

As a result, here we report a range of 4-10 Tg CH_4 yr^{-1} for emissions from coastal and open ocean (including estuaries), with a mean value of 6 Tg CH_4 yr^{-1}.

Geological emissions. The production of methane at the seabed is known to be significant. For instance, marine seepages emit up to 65 Tg CH_4 yr^{-1} globally at seabed level (USEPA, 2010a). What is uncertain is the flux of oceanic methane reaching the atmosphere. For example, bubble plumes of CH_4 from the seabed have been observed in the water column, but not detected in the Arctic atmosphere (Westbrook et al., 2009; Fisher et al., 2011). There are several barriers preventing methane to be expelled to the atmosphere. Firstly, starting from the bottom, gas hydrates and permafrost serve as a barrier to fluid and gas migration towards the seafloor (James et al., 2016). On centennial to millennial timescales, trapped gases may be released when permafrost is perturbed and cracks, or through Pingo-like features. Secondly, and most importantly microbial processes control methane emissions from the seabed. Anaerobic methane oxidation, first described by Reeburgh and Heggie (1977), coupled to sulfate reduction controls methane losses from sediments to the overlying water (Reeburgh, 2007; Egger et al., 2018). Methane only escapes marine sediments in significant amounts from rapidly accumulating sedimentary environments or *via* advective processes such as ebullition or groundwater flow in shallow shelf regions. Anaerobic methane oxidation was demonstrated to be able to keep up with the thaw front of thawing permafrost in a region that had been

https://doi.org/10.5194/essd-2019-128
Preprint. Discussion started: 19 August 2019

inundated within the past 1000 years (Overduin et al., 2015). Thirdly, a large part of the seabed CH_4 production and emission is oxidised in the water column and does not reach the atmosphere (James et al., 2016). Aerobic oxidation is a very efficient sink, which allows very little methane; even from established and vigorous gas seep areas or even gas well blowouts such as the Deepwater Horizon, from reaching the atmosphere. Fourthly, the oceanic pycnocline acts as a physical barrier limiting the transport of methane (and other species) towards the surface. Fifthly, the dissolution of bubbles into the ocean water prevents methane from reaching the ocean surface. Although bubbling is the most efficient way to transfer methane from the seabed to the atmosphere, the fraction of bubbles actually reaching the atmosphere is very uncertain and critically depends on emission depths (< 100-200m, McGinnis et al., 2015) and on the size of the bubbles (>5-8 mm, James et al., 2016). Finally, surface oceans are aerobic and contribute to the oxidation of dissolved methane (USEPA, 2010a). However, surface waters can be more supersaturated than the underlying deeper waters, leading to a methane paradox (Sasakawa et al., 2008). Possible explanations involve i) upwelling in areas with surface mixed layers covered by sea-ice (Damm et al., 2015), ii) the release of methane by the degradation of dissolved organic matter phosphonates in aerobic conditions (Repeta et al., 2016), iii) methane production by marine algae (Lenhart et al., 2016), or iv) methane production within the anoxic centre of sinking particles (Sasakawa et al., 2008), but more work is still needed to be conclusive about this apparent paradox.

For geological emissions, the most used value has long been 20 Tg CH_4 yr^{-1}, relying on expert knowledge and literature synthesis proposed in a workshop reported in Kvenvolden et al. (2001), the author of this study recognising that this was a first estimation and needs revision. Since then, oceanographic campaigns have been organized, especially to sample bubbling areas of active seafloor gas seep bubbling. For instance, Shakhova et al. (2010; 2014) infer 8-17 Tg CH_4 yr^{-1} emissions just for the Eastern Siberian Arctic Shelf (ESAS), based on the extrapolation of numerous but local measurements, and possibly related to thawing subseabed permafrost (Shakhova et al., 2015). Because of the highly heterogeneous distribution of dissolved CH_4 in coastal regions, where bubbles can most easily reach the atmosphere, extrapolation of in situ local measurements to the global scale can be hazardous and lead to biased global estimates. Indeed, using very precise and accurate continuous land shore-based atmospheric methane observations in the Arctic region, Berchet et al. (2016) found a range of emissions for ESAS of ~2.5 Tg CH_4 yr^{-1} (range [0-5]), 4-8 times lower than Shakhova's estimates. Such a reduction in ESAS emission estimate has also been inferred from oceanic observations by Thornton et al. (2016a) with a maximum sea-air CH_4 flux of 2.9 Tg CH_4 yr^{-1} for this region. Etiope et al. (2019) suggested a minimum global total submarine seepage emissions of 3.9 Tg CH_4 yr^{-1} simply summing published regional emission estimates for 15 areas for identified emission areas (above 7 Tg CH_4 yr^{-1} when extrapolated to include non-measured areas). These

https://doi.org/10.5194/essd-2019-128
Preprint. Discussion started: 19 August 2019

recent results, based on different approaches, suggest that the current estimate of 20 Tg CH_4 yr^{-1} is too large and needs revision.

Therefore, as discussed in Section 3.2.2, we report here a reduced range of 5-10 Tg CH_4 yr^{-1} for marine geological emissions compared to the previous budget, with a mean value of 7 Tg CH_4 yr^{-1}.

Hydrate emissions. Among the different origins of oceanic methane, hydrates have attracted a lot of attention. Methane hydrates (or sometimes called clathrates) are ice-like crystals formed under specific temperature and pressure conditions (Milkov, 2005). The stability zone for methane hydrates (high pressure, ambient temperatures) can be found in the shallow lithosphere (i.e. <2,000 m depth), either in the continental sedimentary rocks of polar regions, or in the oceanic sediments at water depths greater than 300 m (continental shelves, sediment-water interface) (Kvenvolden and Rogers, 2005; Milkov, 2005). Methane hydrates can be either of biogenic origin (formed in situ at depth in the sediment by microbial activity) or of thermogenic origin (non-biogenic gas migrated from deeper sediments and trapped due to pressure/temperature conditions or due to some capping geological structure such as marine permafrost). The total stock of marine methane hydrates is large but uncertain, with global estimates ranging from hundreds to thousands of Pg CH_4 (Klauda and Sandler, 2005; Wallmann et al., 2012).

Concerning more specifically atmospheric emissions from marine hydrates, Etiope (2015) points out that current estimates of methane air-sea flux from hydrates (2-10 Tg CH_4 yr^{-1} in e.g. Ciais et al. (2013) or Kirschke et al., 2013) originate from the hypothetical values of Cicerone and Oremland (1988). No experimental data or estimation procedures have been explicitly described along the chain of references since then (Lelieveld et al., 1998; Denman et al., 2007; Kirschke et al., 2013; IPCC, 2001). It was estimated that ~473 Tg CH_4 have been released in the water column over 100 years (Kretschmer et al., 2015). Those few Tg per year become negligible once consumption in the water column has been accounted for. While events such as submarine slumps may trigger local releases of considerable amounts of methane from hydrates that may reach the atmosphere (Etiope, 2015; Paull et al., 2002), on a global scale, present-day atmospheric methane emissions from hydrates do not appear to be a significant source to the atmosphere, and at least formally, we should consider 0 Tg CH_4 yr^{-1} emissions.

Estimates of total (biogenic and geological) open and coastal oceanic emissions. Summing biogenic, geological and hydrate emissions from open and coastal ocean (excluding estuaries) leads to a total of 9 Tg CH4 yr-1 (range 5-17). A recent work (Weber et al, 2019) suggests a new robust estimate of the climatological oceanic flux based on the statistical mapping of methane supersaturation measurements collected as part of the MEMENTO project (Kock and Bange, 2015) for the diffusive fluxes. The ebullitive fluxes were estimated by combining previous estimates of seafloor ebullition from various geologic sources (Hornafius et al., 1999;Kvenvolden and Rogers, 2005), observed bubble size distributions (Wang et al., 2016), and a bubble model to estimate the transfer efficiency of methane from the seafloor to atmosphere

https://doi.org/10.5194/essd-2019-128
Preprint. Discussion started: 19 August 2019

(McGinnis et al., 2006). Using these methods, the diffusive flux was estimated as 2-6 Tg CH_4 yr^{-1} and the ebullitive flux as 2-11 Tg CH_4 yr^{-1}, giving a total (open and coastal) oceanic flux estimate of 6-15 Tg CH_4 yr^{-1} (90% confidence interval) when the probability distributions for the two pathways are combined. Another recent estimate based on the biogeochemistry model PlankTOM10 (Le Quéré et al., 2016) calculates an open and coastal ocean methane flux (excluding estuaries) of 8 [-13/ +19] Tg CH_4 yr^{-1} (Buitenhuis et al., in prep, 2019), with a coastal contribution of 44%.

Our estimate agrees well with the estimates of 6-15 Tg CH_4 yr^{-1} by Weber et al. (2019) and 8 Tg CH_4 yr^{-1} (Buitenhuis et al., in prep, 2019). Distribution of open and coastal oceanic fluxes from Weber et al. (2019) is shown in Fig. 4. This more robust estimate took benefit from synthesis of in situ measurements of atmospheric and surface water methane concentrations and of bubbling areas, and of the development of process-based models for oceanic methane emissions. Methane emissions from brackish water were not estimated in Saunois et al. (2016) and additional 4 Tg CH_4 yr^{-1} are reported in this budget, leading to similar total oceanic emissions despite a reduced estimate in geological off shore emissions compared to Saunois et al. (2016).

3.2.7 Terrestrial permafrost and hydrates

Permafrost is defined as frozen soil, sediment, or rock having temperatures at or below 0°C for at least two consecutive years (Harris et al., 1988). The total extent of permafrost in the Northern Hemisphere is about 14 million km^2, or 15% of the exposed land surface (Obu et al., 2019). As the climate warms, large areas of permafrost are also warming and if soil temperatures pass 0°C, thawing of the permafrost occurs. Permafrost thaw is most pronounced in southern, spatially isolated permafrost zones, but also occurs in northern continuous permafrost (Obu et al., 2019). Thaw occurs either as a gradual, often widespread deepening of the active layer or as more rapid localised thaw associated to loss of massive ground ice (thermokarst) (Schuur et al., 2015). A total of 1035 ± 150 Pg of carbon can be found in the upper 3 meters or permafrost regions, or ~1300 Pg of carbon (1100 to 1500) Pg C for all permafrost (Hugelius et al., 2014).

The thawing permafrost can generate direct and indirect methane emissions. Direct methane emissions rely on the release of methane contained in the thawing permafrost. This flux to the atmosphere is small and estimated to be at maximum 1 Tg CH_4 yr^{-1} at present (USEPA, 2010a). Indirect methane emissions are probably more important. They rely on: 1) methanogenesis induced when the organic matter contained in thawing permafrost is released; 2) the associated changes in land surface hydrology possibly enhancing methane production (McCalley et al., 2014); and 3) the formation of more thermokarst lakes from erosion and soil collapsing. Such methane production is probably already significant today and could be more important in the future associated with a strong positive feedback to climate change (Schuur et al., 2015).

https://doi.org/10.5194/essd-2019-128
Preprint. Discussion started: 19 August 2019

1440 However, indirect methane emissions from permafrost thawing are difficult to estimate at present, with very few data to refer to, and in any case largely overlap with wetland and freshwater emissions occurring above or around thawing areas. For instance, based on lake and soil measurements (Walter Anthony et al., 2016) found that methane emissions (~4 Tg CH_4 yr^{-1}) from thermokarst areas of lakes that have expanded over the past 60 years were directly proportional to the mass of soil carbon inputs to the lakes from the
1445 erosion of thawing permafrost.

Here, we choose to report only the direct emission range of 0-1 Tg CH_4 yr^{-1}, keeping in mind that current wetland, thermokarst lakes and other freshwater methane emissions already likely include a significant indirect contribution originating from thawing permafrost. For the next century, it is estimated that 5-15% of the terrestrial permafrost carbon pool is vulnerable to release in the form of greenhouse gases,
1450 corresponding to 130-160 Pg C (Koven et al., 2015). The likely progressive release in the atmosphere of such an amount of carbon as carbon dioxide and methane may have a significant impact on climate change trajectory (Schuur et al., 2015). The underlying methane hydrates represent a substantial reservoir of methane, estimated up to 530 000 Tg of CH_4 (Ciais et al., 2013). Although local to regional studies are conducted (e.g. Kuhn et al., 2018; Kohnert et al., 2017), present and future emissions related to this
1455 reservoir are difficult to assess for all the Arctic at the moment and still require more work.

3.2.8 Vegetation

Three distinct pathways for the production and emission of methane by living vegetation are considered here (see (Covey and Megonigal, 2019) for an extensive review). Firstly, plants produce methane through an abiotic photochemical process induced by stress (Keppler et al., 2006). This pathway was initially
1460 criticized (e.g., Dueck et al., 2007; Nisbet et al., 2009), and although numerous studies have since confirmed aerobic emissions from plants and better resolved its physical drivers (Fraser et al. 2015), global estimates still vary by two orders of magnitude (Liu et al., 2015). This source has not been confirmed in-field however, and although the potential implication for the global methane budget remains unclear, emissions from this source are certainly much smaller than originally estimated in Keppler et al. (2006)
1465 (Bloom et al., 2010; Fraser et al., 2015). Second, and of clearer significance, plants act as "straws", drawing up and releasing microbially produced methane from anoxic soils (Rice et al., 2010; Cicerone and Shetter, 1981). For instance, because in the forested wetlands of Amazonia, tree stems are the dominant ecosystem flux pathway for soil-produced methane, including stem emissions in ecosystem budgets can reconcile regional bottom-up and top-down estimates (Pangala et al., 2017). Third, the stems of both living trees
1470 (Covey et al., 2012) and dead wood (Covey et al., 2016) provide an environment suitable for microbial methanogenesis. Static chambers demonstrate locally significant through-bark flux from both soil- (Pangala et al., 2013; 2015), and tree stem-based methanogens (Wang et al., 2016; Pitz and Megonigal, 2017). A

https://doi.org/10.5194/essd-2019-128
Preprint. Discussion started: 19 August 2019

recent synthesis indicates stem CH_4 emissions significantly increase the source strength of forested wetland, and modestly decrease the sink strength of upland forests (Covey and Megonigal, 2019). The recent but sustained scientific activity about CH_4 dynamics in forested ecosystems reveals a far more complex story than previously thought, with an interplay of, productive/consumptive, aerobic/anaerobic, biotic/abiotic, processes occurring between upland/wetland soils, trees, and the atmosphere. Understanding the complex processes that regulate CH_4 source–sink dynamics in forests and estimating their contribution to the global methane budget requires cross-disciplinary research, more observations, and new models that can overcome the classical binary classifications of wetland versus upland forest and of emitting versus uptaking soils (Barba et al., 2019) ; Covey and Megonigal, 2019). Although we recognize these emissions are potentially large (particularly tree transport from inundated soil), global estimates for each of these pathways remain highly uncertain and/or are currently ascribed here to other flux categories sources (e/g. inland waters, wetlands, upland soils).

3.3 Methane sinks and lifetime

Methane is the most abundant reactive trace gas in the troposphere and its reactivity is important to both tropospheric and stratospheric chemistry. The main atmospheric sink of methane (~90% of the total sink mechanism) is oxidation by the hydroxyl radical (OH), mostly in the troposphere (Ehhalt, 1974). Other losses are by photochemistry in the stratosphere (reactions with chlorine atoms (Cl) and atomic oxygen ($O(^1D)$), oxidation in soils (Curry, 2007; Dutaur and Verchot, 2007), and by photochemistry in the marine boundary layer (reaction with Cl; Allan et al. (2007), Thornton et al. (2010) . Uncertainties in the total sink of methane as estimated by atmospheric chemistry models are in the order of 20-40% (Kirschke et al., 2013). It is much less (10-20%) when using atmospheric proxy methods (e.g. methyl chloroform, see below) as in atmospheric inversions (Kirschke et al., 2013). Methane is a significant source of water vapor in the middle to upper stratosphere, and influences stratospheric ozone concentrations by converting reactive chlorine to less reactive hydrochloric acid (HCl). In the present release of the global methane budget, we estimate bottom-up methane chemical sinks and lifetime based on global model results from the Climate Chemistry Model Initiative (CCMI) (Morgenstern et al., 2017).

3.3.1 Tropospheric OH oxidation

OH radicals are produced following the photolysis of ozone (O_3) in the presence of water vapour. OH is destroyed by reactions with CO, CH_4, and non-methane volatile organic compounds but since OH exists in photochemical equilibrium with HO_2, the net effect of CH_4 oxidation on the HO_x budget also depends on the level of NO_x (Lelieveld et al., 2002) and other competitive oxidants. Considering its very short lifetime (up to a few seconds, Lelieveld et al., 2004), it is not possible to estimate global OH concentrations directly

https://doi.org/10.5194/essd-2019-128
Preprint. Discussion started: 19 August 2019

from observations. Observations are generally carried out within the boundary layer, while the global OH distribution and variability are more influenced by the free troposphere (Lelieveld et al., 2016). Following the Atmospheric Chemistry and Climate Model Intercomparison Project (ACCMIP), which studied the long-term changes in atmospheric composition between 1850 and 2100 (Lamarque et al., 2013), a new series of experiments was conducted by several chemistry-climate models and chemistry-transport models participating in the Chemistry-Climate Model Initiative (CCMI) (Morgenstern et al., 2017). Over the period 2000-2010, the multi-model mean (11 models) global mass-weighted OH tropospheric concentration was 11.7±1.0 x 10^5 molec cm^{-3} (range 9.9-14.4 x 10^5 molec cm^{-3}, (Zhao et al., 2019) consistent with the previous estimates from ACCMIP (11.7±1.0 x 10^5 molec cm^{-3}, with a range of 10.3-13.4 x 10^5 molec cm^{-3}, Voulgarakis et al. (2013) for year 2000) and the estimates of Prather et al. (2012) at 11.2±1.3 x 10^5 molec cm^{-3}. Indeed Lelieveld et al. (2016) suggest that tropospheric OH is buffered against potential perturbations from emissions, mostly due to chemistry and transport connections in the free troposphere, through transport of oxidants such as ozone. (Nicely et al., 2017) attribute the differences in OH simulated by different chemistry transport models to, in decreasing order of importance, different chemical mechanisms, various treatment of the photolysis rate of ozone, and modeled ozone and carbon monoxide. Besides the uncertainty on global OH concentrations, there is an uncertainty in the spatial and temporal distribution of OH. Models often simulate higher OH in the northern hemisphere leading to a NH/SH OH ratio greater than 1 (Naik et al., 2013; Zhao et al., 2019). A methane inversion using a NH/SH OH ratio higher than 1 infers higher methane emissions in the Northern hemisphere and lower in the tropics and in the Southern hemisphere (Patra et al., 2014). However, there is evidence for parity in inter-hemispheric OH concentrations (Patra et al., 2014), which needs to be confirmed by other observational and model-derived estimates.

OH concentrations and their changes can be sensitive to climate variability (e.g. Pinatubo eruption, Dlugokencky et al., 1996 ,Turner et al., 2018), biomass burning (Voulgarakis et al., 2015), and anthropogenic activities. For instance, the increase of the oxidizing capacity of the troposphere in South and East Asia associated with increasing NO_X emissions (Mijling et al., 2013) and decreasing CO emissions (Yin et al., 2015), possibly enhances CH_4 consumption and therefore limits the atmospheric impact of increasing emissions (Dalsøren et al., 2009). Despite such large regional changes, the global mean OH concentration was suggested to have changed only slightly over the past 150 years (Naik et al., 2013). This is due to the compensating effects of the concurrent increases of positive influences on OH (water vapour, tropospheric ozone, nitrogen oxides (NOx) emissions, and UV radiation due to decreasing stratospheric ozone), and of OH sinks (methane burden, carbon monoxide and non-methane volatile organic compound emissions and burden). However the sign and integrated magnitude (from 1850 to 2000) of OH changes is uncertain, varying from -13% to +15% among the ACCMIP models (mean of -1%, Naik

https://doi.org/10.5194/essd-2019-128
Preprint. Discussion started: 19 August 2019

et al., 2013). Dentener et al. (2003) found a positive trend in global OH concentrations of 0.24 ± 0.06% yr^{-1} between 1979 and 1993, mostly explained by changes in the tropical tropospheric water vapor content. Accurate methyl chloroform atmospheric observations together with estimates of its emissions (Montzka and Fraser, 2003) allow an estimate of OH concentrations and changes in the troposphere since the 1980s. Montzka et al. (2011) inferred small inter-annual OH variability and trends (typical OH changes from year to year of less than 3%), and attributed previously estimated large year-to-year OH variations before 1998 (e.g. Bousquet et al. (2005), Prinn et al. (2001) to overly large sensitivity of OH concentrations inferred from methyl chloroform measurements to uncertainties in the latter's emissions. However, Prinn et al. (2005) also showed lower post-1998 OH variability that they attributed to the lack of strong post-1998 El Nino's. CCMI models show OH inter-annual variability ranging from 0.4% to 1.8% (Zhao et al., 2019) over 2000-2010, consistent, albeit lower, than the value deduced from methyl chloroform measurements. However these simulations take into account meteorology variability but not emission interannual variability (e.g., from biomass burning) and thus are expected to simulate lower OH inter annual variability than in reality. Using an empirical model constrained by global observations of ozone, water vapor, methane, and temperature as well as the simulated effects of changing NOx emissions and tropical expansion, Nicely et al. (2017) found an inter-annual variability in OH of about 1.3-1.6 % between 1980 and 2015, in agreement with Montzka et al. (2011). As methyl chloroform has reached very low concentrations in the atmosphere, in compliance with the regulations of the Montreal Protocol and its Amendments, a replacement compound is needed to estimate global OH concentrations. Several HCFCs and HFCs have been tested (Miller et al., 1998; Montzka et al., 2011; Huang and Prinn, 2002; Liang et al., 2017) to infer OH but do not yet provide equivalent results to methyl chloroform.

We report here a climatological range of 553 [476-677] Tg CH_4 yr^{-1} derived from the seven models that contributed to CCMI for the total tropospheric (tropopause height at 200 hPa) loss of methane by OH oxidation over the period 2000-2009, which is slightly higher than the one from the ACCMIP models (528 [454-617] Tg CH_4 yr^{-1} reported in Kirschke et al. (2013) and Saunois et al., 2016).

3.3.2 Stratospheric loss

CH_4 enters the stratosphere primarily via slow ascent through the tropical tropopause region and reaches higher altitudes and latitudes via the stratospheric general circulation - the Brewer-Dobson circulation (Brewer, 1949; M B Dobson et al., 1946). Some troposphere-stratosphere exchange also happens across the extratropical tropopause due to mixing (e.g., Holton et al., 1986; (Hoor et al., 2004). Reeburgh (2007) estimated that approximately 60 Tg CH_4 enters the stratosphere per year, which is likely subject to inter annual variability (e.g., Noël et al., 2018). In the stratosphere, CH_4 is lost through reactions with excited atomic oxygen $O(^1D)$, atomic chlorine (Cl), atomic fluorine (F), and OH (le Texier et al., 1988; Brasseur

https://doi.org/10.5194/essd-2019-128
Preprint. Discussion started: 19 August 2019

and Salomon, 2006). The combined effects of transport and chemical loss lead to the typical CH_4 distributions observed in the stratosphere, which vary with the strength of the Brewer-Dobson circulation on seasonal to interannual timescales (Jones and Pyle, 1984; Randel et al., 1998). Note that strong subsidence in the polar vortex impacts the isotope fractionation of methane in Arctic polar air, leading to high isotope enrichments (Röckmann et al., 2011). This increase in stratospheric water vapour due to methane destruction leads to a positive radiative forcing and stimulates the production of OH through its reaction with atomic oxygen (Forster et al., 2007). Uncertainties in the chemical loss of stratospheric methane are large, due to uncertain inter-annual variability in stratospheric transport as well as its chemical interactions and feedbacks with stratospheric ozone (Portmann et al., 2012). Particularly, the fraction of stratospheric loss due to the different oxidants is still uncertain, with possibly 20-35% due to halons, about 25% due to $O(^1D)$ mostly in the high stratosphere and the rest due to stratospheric OH (McCarthy et al., 2003). In this study, seven chemistry climate models from the CCMI project (Table S4) are used to provide estimates of methane chemical loss, including reactions with OH, $O(^1D)$, and Cl; CH_4 photolysis is also included but occurs only above the stratosphere. Considering a 200 hPa tropopause height, the CCMI models suggest an estimate of 31 [12-37] Tg CH_4 yr^{-1} for the methane stratospheric sink for the period 2000-2010 (Table S4). The 20 Tg difference compared to the mean value reported by Kirschke et al. (2013) and Saunois et al. (2016) for the same period (51 [16-84] Tg CH_4 yr^{-1}), is probably due to the plausible double-counting of $O(^1D)$ and Cl oxidations in our previous calculation, as the chemistry-climate models usually report the total chemical loss of methane (not OH oxidation only).

We report here a climatological range of 12-37 Tg CH_4 yr^{-1} associated to a mean value of 31 Tg CH_4 yr^{-1}.

3.3.3 Tropospheric reaction with Cl

Halogen atoms can also contribute to the oxidation of methane in the troposphere. Allan et al. (2005) measured mixing ratios of methane and $\delta^{13}C$-CH_4 at two stations in the southern hemisphere from 1991 to 2003, and found that the apparent kinetic isotope effect of the atmospheric methane sink was significantly larger than that explained by OH alone. A seasonally varying sink due to atomic chlorine (Cl) in the marine boundary layer of between 13 and 37 Tg CH_4 yr^{-1} was proposed as the explanatory mechanism (Allan et al., 2007; Platt et al., 2004). This sink was estimated to occur mainly over coastal and marine regions, where NaCl from evaporated droplets of seawater react with NO_2 to eventually form Cl_2, which then UV-dissociates to Cl. However significant production of nitryl chloride ($ClNO_2$) at continental sites has been recently reported (Riedel et al., 2014) and suggests the broader presence of Cl, which in turn would expand the significance of the Cl sink in the troposphere. Recently, using a chemistry transport model, (Hossaini et al., 2016) suggest a chlorine sink in the lower range of Allan et al. (2007), ~12-13 Tg CH_4 yr^{-1} (about 2.5 % of the tropospheric sink). They also estimate that $ClNO_2$ yields a 1 Tg yr^{-1} sink of methane. Another

https://doi.org/10.5194/essd-2019-128
Preprint. Discussion started: 19 August 2019

modelling study of (Wang et al., 2019a) produced a more comprehensive analysis of global tropospheric chlorine chemistry and found a chlorine sink of 5 Tg yr^{-1}, representing only 1% of the total methane tropospheric sink. Both the KIE approach and chemistry transport model simulations carry uncertainties (extrapolations based on only a few sites and use of indirect measurements, for the former; missing sources, coarse resolution, underestimation of some anthropogenic sources for the latter). However, (Gromov et al., 2018) found that chlorine can contribute only 0.23% the tropospheric sink of methane (about 1 Tg CH_4 yr^{-1}) in order to balance the global $^{13}C(CO)$ budget.

Awaiting further work to better assess the magnitude of the chlorine sink in the methane budget, we suggest a lower estimate but a larger range than in Saunois et al., (2016) and report the following climatological value for the 2000s: 11 [1-35] Tg CH_4 yr^{-1}.

3.3.4 Soil uptake

Unsaturated oxic soils are sinks of atmospheric methane due to the presence of methanotrophic bacteria, which consume methane as a source of energy. Dutaur and Verchot (2007) conducted a comprehensive meta-analysis of field measurements of CH_4 uptake spanning a variety of ecosystems. Extrapolating to the global scale, they reported a range of 36 ± 23 Tg CH_4 yr^{-1}, but also showed that stratifying the results by climatic zone, ecosystem and soil type led to a narrower range (and lower mean estimate) of 22 ± 12 Tg CH_4 yr^{-1}. Modelling studies, employing meteorological data as external forcing, have also produced a considerable range of estimates. Using a soil depth-averaged formulation based on Fick's law with parameterizations for diffusion and biological oxidation of CH_4, Ridgwell et al. (1999) estimated the global sink strength at 38 Tg CH_4 yr^{-1}, with a range 20-51 Tg CH_4 yr^{-1} reflecting the model structural uncertainty in the base oxidation parameter. Curry (2007) improved on the latter by employing an exact solution of the one-dimensional diffusion-reaction equation in the near-surface soil layer (i.e., exponential decrease in CH_4 concentration below the surface), a land surface hydrology model, and calibration of the oxidation rate to field measurements. This resulted in a global estimate of 28 Tg CH_4 yr^{-1} (9-47 Tg CH_4 yr^{-1}), the result reported by (Zhuang et al., 2013), Kirschke et al. (2013) and Saunois et al. (2016). Ito and Inatomi (2012) used an ensemble methodology to explore the variation in estimates produced by these parameterizations and others, which spanned the range 25-35 Tg CH_4 yr^{-1}. (Murguia-Flores et al., 2018) further refined the Curry (2007) model's structural and parametric representations of key drivers of soil methanotrophy, demonstrating good agreement with the observed latitudinal distribution of soil uptake (Dutaur and Verchot, 2007). Their model simulated a methane soil sink of 32 Tg CH_4 yr^{-1} for the period 2000-2017 (Fig. 4), compared to 38 and 29 Tg CH_4 yr^{-1} using the Ridgwell et al. (1999) and Curry (2007) parameterizations, respectively, under the same meteorological forcing. As part of a more comprehensive model accounting for a range of methane sources and sinks, Tian et al. (2010, 2015, 2016) computed

https://doi.org/10.5194/essd-2019-128
Preprint. Discussion started: 19 August 2019

vertically-averaged CH_4 soil uptake including the additional mechanisms of aqueous diffusion and plant-mediated (*aerenchyma*) transport, arriving at the estimate 30±19 Tg CH_4 yr^{-1} (Tian et al., 2016). The still more comprehensive biogeochemical model of Riley et al. (2011) included vertically resolved representations of the same processes considered by Tian et al. (2016), in addition to grid cell fractional inundation and, importantly, the joint limitation of uptake by both CH_4 and O_2 availability in the soil column. Riley et al. (2011) estimated a global CH_4 soil sink of 31 Tg CH_4 yr^{-1} with a structural uncertainty of 15-38 Tg CH_4 yr^{-1} (a higher upper limit resulted from an elevated gas diffusivity to mimic convective transport; as this is not usually considered, we adopt the lower upper bound associated with no limitation of uptake at low soil moisture). A model of this degree of complexity is required to explicitly simulate situations where the soil water content increases enough to inhibit the diffusion of oxygen, and the soil becomes a methane source (Lohila et al., 2016). This transition can be rapid, thus creating areas (for example, seasonal wetlands) that can be either a source or a sink of methane depending on the season.

The previous Curry (2007) estimate might be revised upward based on subsequent work and the increase in CH_4 concentration since that time, which gives a central estimate of 30.1 Tg CH_4 yr^{-1}. Considering structural uncertainty in the various models' assumptions and parameters, we report here the median and range of Tian et al. (2016): 30 [11-49] Tg CH_4 yr^{-1} for the periods 2000-2009 and 2008-2017.

3.3.5 CH_4 lifetime

The atmospheric lifetime of a given gas in steady state may be defined as the global atmospheric burden (Tg) divided by the total sink (Tg/yr) (IPCC, 2001). At steady state the atmospheric lifetime equals the decay time (e-folding time) of a perturbation. As methane is not in steady state at present, we fit a function that approaches steady state when calculating methane lifetime using atmospheric measurements (Sect. 4.1.1). Global models provide an estimate of the loss of the gas due to individual sinks, which can then be used to derive lifetime due to a specific sink. For example, methane's tropospheric lifetime is determined as global atmospheric methane burden divided by the loss from OH oxidation in the troposphere, sometimes called "chemical lifetime". While its total lifetime corresponds to the global burden divided by the total loss including tropospheric loss from OH oxidation, stratospheric chemistry and soil uptake. The CCMI models (described in Morgenstein et al., 2017) estimate the tropospheric methane lifetime at about 9 years (average over years 2000-2009), with a range of 7.2-10.1 years (see Table S4). While this range agrees with previous values found in ACCMIP (9.3 [7.1-10.6] years, Voulgarakis et al. (2013); Kirschke et al., 2013), the mean value reported here is lower than previously reported, probably due to a smaller and different ensemble of climate models. Adding 35 Tg to account for the soil uptake to the total chemical loss of the CCMI models, we derive a total methane lifetime of 7.8 years (average over 2000-2009 with a range of 6.5-8.8 years). These updated model estimates of total methane lifetime agree with the previous estimates from ACCMIP

https://doi.org/10.5194/essd-2019-128
Preprint. Discussion started: 19 August 2019

(8.2 [6.4-9.2] years for year 2000, Voulgarakis et al., 2013). The model results for total methane lifetime are consistent with, though smaller than, the value estimated by Prather et al. (2012) derived from observations (9.1 ± 0.9 years) and most commonly used in the literature (Ciais et al., 2013), and the steady-state calculation from atmospheric observations (9.3 yr, Sect. 4.1.1). This large spread in methane lifetime (between models, and between models and observation based estimates) needs to be better understood and reduced to 1) close the present-day methane budget and past changes and 2) ensure an accurate forecast of future climate.

4 Atmospheric observations and top-down inversions

4.1 Atmospheric observations

The first systematic atmospheric CH_4 observations began in 1978 (Blake et al., 1982) with infrequent measurements from discrete air samples collected in the Pacific at a range of latitudes from 67°N to 53°S. Because most of these air samples were from well-mixed oceanic air masses and the measurement technique was precise and accurate, they were sufficient to establish an increasing trend and the first indication of the latitudinal gradient of methane. Spatial and temporal coverage was greatly improved soon after (Blake and Rowland, 1986) with the addition of the Earth System Research Laboratory from US National Oceanic and Atmospheric Administration (NOAA/ESRL) flask network (Steele et al. (1987), Fig. 1), and of the Advanced Global Atmospheric Gases Experiment (AGAGE) (Prinn et al, 2000; Cunnold et al., 2002), the Commonwealth Scientific and Industrial Research Organisation (CSIRO, Francey et al., 1999), the University of California Irvine (UCI, Simpson et al., 2012) and other in situ and flask networks (e.g. ICOS network in Europe, https://www.icos-ri.eu/). The combined datasets provide the longest time series of globally averaged CH_4 abundance. Since the early-2000s, CH_4 column averaged mole fractions have been retrieved through passive remote sensing from space (Buchwitz et al., 2005a,b; Frankenberg et al., 2005; Butz et al., 2011; Crevoisier et al., 2009; Hu et al., 2016). Ground-based Fourier transform infrared (FTIR) measurements at fixed locations also provide time-resolved methane column observations during daylight hours, and a validation dataset against which to evaluate the satellite measurements (TCCON network, e.g. Wunch et al., 2011; Bader et al., 2017).

In this budget, in-situ observations from the different networks were used in the top-down atmospheric inversions to estimate methane sources and sinks over the period 2000-2017. Satellite observations from TANSO/FTS instrument on board the satellite GOSAT were used to estimate methane sources and sinks over the period 2009-2017. Other atmospheric data (FTIR, airborne measurements, AirCore…) exist but are not specifically used in this study, however further information is provided in the Supplementary Material. These data are not commonly used to infer fluxes from global inversions (yet), but are used to

https://doi.org/10.5194/essd-2019-128
Preprint. Discussion started: 19 August 2019

verify their performance, see e.g. Bergamaschi et al. (2013). Isotopic atmospheric measurements of $\delta^{13}CH_4$ can help to partition the different methanogenic processes of methane and $\delta D\text{-}CH_4$ provides valuable information on the oxidation by the OH radicals (Röckmann et al., 2011) due to a fractionation of about 300‰. Integrating isotopic information is important to improve our understanding of the methane budget. While box-model studies have used isotopic information to discuss methane source and sinks changes (Rice et al., 2016; Rigby et al., 2017; Schaefer et al., 2016; Turner et al., 2017; Schwietzke et al., 2016; Thompson et al., 2018), such approaches seem more reliable to assess global emission changes than to infer decadal budgets. Also such isotopic constraints have been used in analytical inversion framework (e.g., Milakoff Fletcher et al., 2004; Bousquet et al., 2006), but have not yet been integrated in the inverse systems used in this study to perform top-down inversions (See Supplementary materials).

4.1.1 In situ CH_4 observations and atmospheric growth rate at the surface

Four observational networks provide globally averaged CH_4 mole fractions at the Earth's surface: NOAA/ESRL (Dlugokencky et al., 1994), AGAGE (Prinn et al., 2000; 2018; Cunnold et al., 2002; Rigby et al., 2008), CSIRO (Francey et al., 1999) and the University of California Irvine (UCI, Simpson et al., 2012). The data are archived at the World Data Centre for Greenhouse Gases (WDCGG) of the WMO Global Atmospheric Watch (WMO-GAW) program, including measurements from other sites that are not operated as part of the four networks. The CH_4 in-situ monitoring network has grown significantly over the last decade due to the emergence of laser diode spectrometers which are robust and accurate enough to allow deployments with minimal maintenance enabling the development of denser networks in developed countries (Yver Kwok et al., 2015; Stanley et al., 2018), and new stations in remote environment (Bian et al., 2016; Nisbet et al., 2019).

The networks differ in their sampling strategies, including the frequency of observations, spatial distribution, and methods of calculating globally averaged CH_4 mole fractions. Details are given in the supplementary material of Kirschke et al. (2013). The global average values of CH_4 concentrations presented here are computed using measurements through gas chromatography with flame ionization detection (GC/FID), although chromatographic schemes vary among the labs. Because GC/FID is a relative measurement method, the instrument response must be calibrated against standards. The current WMO reference scale, maintained by NOAA/ESRL, WMO-X2004A (Dlugokencky et al., 2005), was updated in July 2015. NOAA and CSIRO global means are on this scale. AGAGE uses an independent standard scale maintained by Tohoku University (Aoki et al., 1992), but direct comparisons of standards and indirect comparisons of atmospheric measurements show that differences are below 5 ppb (Vardag et al., 2014;Tans and Zellweger, 2014). UCI uses another independent scale that was established in 1978 and is traceable to NIST (Simpson et al., 2012; Flores et al., 2015), but has not been included in standard exchanges with other

https://doi.org/10.5194/essd-2019-128
Preprint. Discussion started: 19 August 2019

networks so differences with the other networks cannot be quantitatively defined. Additional experimental details are presented in the supplementary material from Kirschke et al. (2013) and references therein.

In Fig. 1, (a) globally averaged CH_4 and (b) its growth rate (derivative of the deseasonalized trend curve) through to 2017 are plotted for the four measurement programs using a procedure of signal decomposition described in Thoning et al. (1989). We define the annual increase G_{ATM} as the increase in the growth rate from Jan. 1 in one year to Jan. 1 in the next year. Agreement among the four networks is good for the global growth rate, especially since ~1990. The large differences observed mainly before 1990 reflect probably the different spatial coverage and stations of each network. The long-term behaviour of globally averaged atmospheric CH_4 shows a decreasing but positive growth rate (defined as the derivative of the deseasonalized mixing ratio) from the early-1980s through 1998, a near-stabilization of CH_4 concentrations from 1999 to 2006, and a renewed period with positive but stable growth rates since 2007, slightly larger after 2014. When a constant atmospheric lifetime is assumed, the decreasing growth rate from 1983 through 2006 implies that atmospheric CH_4 was approaching steady state, with no trend in emissions. The NOAA global mean CH_4 concentration was fitted with a function that describes the approach to a first-order steady state ($_{SS}$ index): $[CH_4](t) = [CH_4]_{ss}-([CH_4]_{ss}-[CH_4]_0)e^{-t/\tau}$; solving for the lifetime, τ, gives 9.3 years, which is very close to current literature values (e.g., Prather et al., 2012).

On decadal timescales, the annual increase is on average 2.1±0.3 ppb yr^{-1} for 2000-2009, 6.6±0.3 ppb yr^{-1} for 2008-2017 and 6.1±1.0 ppb yr^{-1} for the year 2017. From 1999 to 2006, the annual increase of atmospheric CH_4 was remarkably small at 0.6±0.1 ppb yr^{-1}. After 2006, the atmospheric growth rate has recovered to a level similar to that of the mid-1990s (~5 ppb yr^{-1}), or even to that of the 1980s for 2014 and 2015 (>10 ppb yr^{-1}).

4.1.2 Satellite data of column average CH_4

In the 2000s, two space-borne instruments sensitive to atmospheric methane in the lower troposphere were put in orbit and have provided atmospheric methane column-averaged dry air mole fraction (XCH_4), using shortwave Infrared spectrometry (SWIR). Satellite data of XCH_4 have been primarily evaluated against the Total Carbon Column Observing Network (TCCON) data (e.g., Butz et al., 2011; Morino et al., 2011). The first space-borne instrument was the Scanning Imaging Absorption spectrometer for Atmospheric CartograpHY (SCIAMACHY). SCIAMACHY was operated on board the ESA ENVIronmental SATellite (ENVISAT) between 2003 and 2012 (Burrows et al., 1995; Buchwitz et al., 2006; Dils et al., 2006; Frankenberg et al., 2011). The use of SCIAMACHY in top-down approaches necessitates important bias correction, especially after 2005. As the mission ended in 2012, we do not report any estimates based on SCIAMACHY data in this budget. In 2006, 2012 and 2018, the Infrared Atmospheric Sounding Interferometer (IASI) on board the European MetOp,A, B and C satellites have started to operate.

https://doi.org/10.5194/essd-2019-128
Preprint. Discussion started: 19 August 2019

Measuring the thermal radiation from Earth and the atmosphere in the TIR, they provide mid-to-upper troposphere columns of methane (representative of the 5-15 km layer) over the tropics using an infrared sounding interferometer (Crevoisier et al., 2009). Despite their sensitivity being limited to the mid-to-upper troposphere, their use in flux inversions has shown consistent results in the tropics with surface and other satellite-based inversions (Cressot et al., 2014). However these satellite data, limited to the tropics and to the mid-to-upper troposphere are not used in this global methane budget.

In January 2009, the JAXA satellite Greenhouse Gases Observing SATellite (GOSAT) was launched (Butz et al., 2011; Morino et al., 2011) containing the TANSO-FTS instrument, which observes in the shortwave infrared (SWIR). Different retrievals of methane based on TANSO-FTS/GOSAT products are made available to the community (e.g. Yoshida et al., 2013; Schepers et al., 2012; Parker et al., 2011) based on two retrieval approaches, Proxy and Full Physics. The proxy method retrieves the ratio of methane column (XCH_4) and carbon dioxide column (XCO_2), from which XCH_4 is derived after multiplication with transport model-derived XCO_2 (Chevallier et al., 2010; Peters et al., 2007; Frankenberg et al., 2006). Computing the ratio between the nearby spectral absorption bands (1.65µm for CH_4 and 1.60µm for CO_2) effectively removes biases due to light scattering from clouds and aerosols. The second approach is the Full Physics algorithm, which retrieves the aerosol properties (amount, size and height) along with CO_2 and CH_4 columns (e.g. Butz et al., 2011). Although GOSAT retrievals still show significant unexplained biases and limited sampling in cloud covered regions and in the high latitude winter, it represents an important improvement compared to SCIAMACHY both for random and systematic observation errors (see Table S2 of Buchwitz et al., 2016). GOSAT-2 was launched in October 2018 with expected improved precision and accuracy (JAXA, 2019).

Atmospheric inversions based on SCIAMACHY or GOSAT CH_4 retrievals have been carried out by different research groups (Fraser et al., 2013; Cressot et al., 2014; Alexe et al., 2015; Bergamaschi et al., 2013; Locatelli et al., 2015; Jacob et al., 2016;Maasakkers et al., 2019;Pandey et al., 2017) and are reported in Saunois et al. (2016) Here, only inversions using GOSAT retrievals are used.

4.2 Top-down inversions used in the budget

An atmospheric inversion is the optimal combination of atmospheric observations, of a model of atmospheric transport and chemistry, and of a prior estimate of methane sources and sinks in order to provide improved estimates of the latter (fluxes and their uncertainty). The theoretical principle of methane inversions is detailed in the Supplementary material (ST2) and an overview of the different methods applied to methane is presented in (Houweling et al., 2017).

We consider here an ensemble of inversions gathering various chemistry transport models, differing in vertical and horizontal resolutions, meteorological forcings, advection and convection schemes, boundary

https://doi.org/10.5194/essd-2019-128
Preprint. Discussion started: 19 August 2019

layer mixing; we assume that this model range is sufficient to cover the range of transport model errors in the estimate of methane fluxes. General characteristics of the inversion systems are provided in Table 4. Further details can be found in the referenced papers and in the Supplementary Material. Each group was asked to provide gridded flux estimates for the period 2000-2017, using either surface or satellite data, but no additional constraints were imposed so that each group could use their preferred inversion setup. A set of prior emission distributions was built from the most recent inventories or model-based estimates (see Supplementary Material), but its use was not mandatory (Table S6). This approach corresponds to a flux assessment, but not to a model inter-comparison. Posterior uncertainty is time and computer resource consuming, especially for the 4D-var approaches that use Monte Carlo methods. Consequently, posterior uncertainty has been provided by only two groups and is found to be lower than the ensemble spread. Indeed, chemistry transport models differ in inter-hemispheric transport, stratospheric methane profiles and OH distribution, which limitations are not fully taken into account in the individual posterior uncertainty. As a result, the reported range for top-down approaches is narrower than expected when fully accounting for the individual estimates uncertainty. In other words, the range minimum is higher than the lowest estimate less its uncertainty, and the range maximum lower than the highest estimate plus its uncertainty.

Nine atmospheric inversion systems using global Eulerian transport models were used in this study compared to eight in Saunois et al. (2016). Each inversion system provided one or several simulations, including sensitivity tests varying the assimilated observations (surface or satellite) or the inversion setup. This represents a total of 22 inversion runs with different time coverage: generally 2000-2017 for surface-based observations, and 2010-2017 for GOSAT-based inversions (Table 4 and Table S6). When multiple sensitivity tests were performed we used the mean of this ensemble as to not to overweight one particular inverse system. It should also be noticed that some satellite-based inversions are in fact combined satellite and surface inversions as they use satellite retrievals and surface measurements simultaneously (Bergamaschi et al., 2013; Alexe et al., 2015; Houweling et al., 2014). Nevertheless, these inversions are still referred to as satellite-based inversions. Bias correction procedures have been developed to assimilate GOSAT data (Monteil et al., 2013; Cressot et al., 2014; Houweling et al., 2014; Locatelli et al., 2015; Alexe et al., 2015). Although partly due to transport model errors, significant to large corrections applied to the satellite total column CH_4 data question the comparably low systematic errors reported in satellite validation studies using TCCON (Dils et al., 2014; CCI-Report, 2016).

Each group provided gridded monthly maps of emissions for both their prior and posterior total and for sources per category (see the categories Sect. 2.3). Results are reported in Sect. 5. Atmospheric sinks from the top-down approaches have been provided for this budget, and are compared with the values reported in Kirschke et al. (2013). Not all inverse systems report their chemical sink; as a result, the global mass

https://doi.org/10.5194/essd-2019-128
Preprint. Discussion started: 19 August 2019

imbalance for the top-down budget is derived as the difference between individual modelled sources and sinks (when available).

The last year of reported inversion results is 2017 (inversions until mid 2018), which represents a two year-lag with the present, which is a two-year shorter lag than for the last release (Saunois et al., 2016). Satellite observations are linked to operational data chains and are generally available days to weeks after the recording of the spectra. Surface observations can lag from months to years because of the time for flask analyses and data checks in (mostly) non-operational chains. With operational networks such as ICOS in Europe, these lags will be reduced in the future with the daily production of Near-Real time data. In addition, the final six months of inversions are generally ignored (spin down) because the estimated fluxes are not constrained by as many observations as the previous months. Also, the long inversion runs and analyses can take months to be performed. The GCP-CH_4 budget aims to represent the most recent years by reducing the analysis time and shortening the in-situ atmospheric observation release, so that the last year of the budget presents no more than a 2-year lag with the release date of the budget, as for this release.

5 Methane budget: top-down and bottom-up comparison

5.1 Global methane budget

5.1.1 Global budget of total methane emissions

Top-down estimates. At the global scale, the total emissions inferred by the ensemble of 22 inversions is 572 Tg CH_4 yr^{-1} [538-593] for the 2008-2017 decade (Table 3), with the highest ensemble mean emission of 591 Tg CH_4 yr^{-1} [552-614] for 2017. Global emissions for 2000-2009 (545 Tg CH_4 yr^{-1}) are consistent with Saunois et al. (2016) and the range of uncertainties for global emissions, 522-559 Tg CH_4 yr^{-1} is in line with Saunois et al. (2016) (535-569), although the ensemble of inverse systems contributing to this budget is different than for Saunois et al. (2016). Indeed, only six inverse systems of the nine examined here (Table S7) contributed to the Saunois et al. (2016) budget . The range reported are the minimum and maximum values among studies and do not reflect the individual full uncertainties.

Bottom-up estimates. The estimates made via the bottom-up approaches considered here are quite different from the top-down results, with global emissions about 25% larger, 737 Tg CH_4 yr^{-1} [593-880] for 2008-2017 (Table 3). Moreover, the range estimated using bottom up approaches does not overlap with that of the top-down estimates. The bottom-up estimates are given by the sum of individual anthropogenic and natural processes, with no constraint to the total. For the period 2000-2009, the discrepancy between bottom-up and top down was 30% of the top-down estimates in Saunois et al. (2016) (167 Tg CH_4 yr^{-1}); this has been reduced by only 5 % (now 158 Tg CH_4 yr^{-1} for the same period). This reduction is due to 1) a

https://doi.org/10.5194/essd-2019-128
Preprint. Discussion started: 19 August 2019

better agreement in the anthropogenic emissions (top-down and bottom-up difference reducing from 19 Tg CH_4 yr^{-1} to 3 Tg CH_4 yr^{-1}); 2) a reduction in the estimates of some natural sources other than wetlands based on recent literature (7 Tg CH_4 yr^{-1} from geological sources, 8 Tg CH_4 yr^{-1} from wild animals, and 3 Tg CH_4 yr^{-1} from allocation of wildfires to biomass & biofuel burning, see Table 3) and 3) a reduction of 35 Tg CH_4 yr^{-1} in the bottom-up estimates of wetland emissions by models when excluding lakes and paddies as wetlands (see Sect. 5.1.2 below). These reductions (-69 Tg CH_4 yr^{-1}) in the bottom-up budget are negated by revised freshwater emissions to higher values (+ 37 Tg CH_4 yr^{-1}) resulting from the integration of a recent study on lake, pond and reservoir emissions (DelSontro et al., 2018, see Sect. 3.2.2) and the integration of estuary emissions in this budget (+4 Tg CH_4 yr^{-1}). Also, the uncertainty range of some emissions has decreased in this study compared to Kirschke et al. (2013) and Saunois et al. (2016), for example for oceans, termites, wild animals, and geological sources. However, the uncertainty in the global budget is still high because of the large range reported for emissions from freshwater systems. Still, as noted in Kirschke et al. (2013), such large global emissions from the bottom-up approaches are not consistent with atmospheric constraints brought by OH optimization and are very likely overestimated. This overestimation likely results from errors related to up-scaling and/or double counting of some natural sources (e.g. wetlands, other inland water systems, see Sect. 5.1.2).

5.1.2 Global methane emissions per source category

The global methane budget for five source categories (see Sect. 2.3) for 2008-2017 is presented in Fig. 5, Fig. 6, and Table 3. Top-down estimates attribute about 60% of total emissions to anthropogenic activities (range of [55-70] %), and 40% to natural emissions. As natural emissions from bottom-up models are much larger, the anthropogenic versus natural emission ratio is more balanced in the bottom-up budget (~50% each). A current predominant role of anthropogenic sources of methane emissions is consistent with and strongly supported by available ice core and atmospheric methane records. These data indicate that atmospheric methane varied around 700 ppb during the last millennium before increasing by a factor of 2.6 to ~1800 ppb since pre-industrial times. Accounting for the decrease in mean-lifetime over the industrial period, Prather et al. (2012) estimated from these data a total source of 554 ±56 Tg-CH_4 in 2010 of which about 64% (352±45 Tg-CH_4) of anthropogenic origin, consistent with the range of our synthesis.

Wetlands. For 2008-2017, the top-down and bottom-up derived estimates of 178 Tg CH_4 yr^{-1} (range 155-200) and 149 Tg CH_4 yr^{-1} (range 102-182), respectively, are statistically consistent. Bottom-up mean wetland emissions for the 2000-2009 period are smaller in this study than those of Saunois et al. (2016). Conversely, the current 2000-2009 mean top-down wetland estimates are larger than those of Saunois et al. (2016) (Table 3). The reduction in wetland emissions from bottom-up models is related to an updated

https://doi.org/10.5194/essd-2019-128
Preprint. Discussion started: 19 August 2019

wetland extent data set (WAD2M, see Sect. 3.2.1). Interestingly, while top-down wetlands emissions estimates are higher than in Saunois et al. (2016), the range has been reduced by about 50 %. As reported in Saunois et al. (2016), all biogeochemical wetland models were forced with the same wetland extent and climate forcing (see Sect 3.2.1), with the result that the amplitude of the range of emissions of 102-179 is similar to that in Saunois et al. (2016) (151-222 for 2000-2009), and narrowed by a third compared to the previous estimates from Melton et al. (2013) (141-264) and from Kirschke et al. (2013) (177-284). This suggests that differences in wetland extent explain about a third (30-40%) of the former range of the emission estimates of global natural wetlands. The remaining range is due to differences in model structures and parameters. Bottom-up and top-down estimates differ more in this study (~30 Tg yr^{-1} for the mean) than in Saunois et al. (2016) (~17 Tg yr^{-1}), due to reduced estimates from the bottom-up models and increased estimates from the top-down models. Natural emissions from freshwater systems are not included in the prior fluxes entering the top-down approaches. However, emissions from these non-wetland systems may be accounted for in the posterior estimates of the top-down models, as these two sources are close and probably overlap at the rather coarse resolution of the top-down models. In the top-down budget, natural wetlands represent 30% on average of the total methane emissions but only 22% in the bottom-up budget (because of higher total emissions inferred). Neither bottom-up nor top-down approaches included in this study derive significant changes in wetland emissions between the two decades 2000-2009 and 2008-2017 at the global scale.

Other natural emissions. The discrepancy between top-down and bottom-up budgets is the largest for the natural emission total, which is 371 Tg CH_4 yr^{-1} [245-488] for bottom-up and only 215 Tg CH_4 yr^{-1} [176-248] for top-down over the 2008-2017 decade. Sources other than wetlands (Fig. 5 and 6), namely freshwater systems, geological sources, termites, oceans, wild animals, and permafrost, are more likely to explain this large discrepancy. For the 2008-2017 decade, top-down inversions infer non-wetland emissions of 37 Tg CH_4 yr^{-1} [21-50], whereas the sum of the individual bottom-up emissions is 199 Tg CH_4 yr^{-1} [64-284]. Atmospheric inversions infer about the same amount over the decade 2000-2009, which is almost half of the value reported in Saunois et al. (2016) (64 [21-132] Tg CH_4 yr^{-1}). This is either due to 1) a more consistent way of considering other natural emission in the various inverse systems or 2) difference in the ensemble of top-down inversions reported here. Regarding the bottom-up budget, the two main contributors to the larger bottom-up total are freshwaters (~75%) and geological emissions (~15%), both of which have large uncertainties and lack of spatially explicit representation (for freshwaters). Because of the discrepancy, this category represents 7% of total emissions in the top-down budget, but up to 25% in the bottom-up budget.

Improved area estimates of the different freshwater systems would be beneficial. For example, stream fluxes are difficult to assess because of the high-expected spatial and temporal variability (Natchimuthu et

https://doi.org/10.5194/essd-2019-128
Preprint. Discussion started: 19 August 2019

al., 2017) and very uncertain areas of headwater streams where methane-rich groundwater may be rapidly degassed. There are also uncertainties in the geographical distinction between wetlands, small lakes (e.g. thermokarst lakes), and floodplains that need more attention to avoid double counting. In addition, major uncertainty is still associated with the representation of ebullition. The intrinsic nature of this large but very locally distributed flux highlights the need for cost-efficient high-resolution techniques for resolving the spatio-temporal variations of these fluxes. In this context of observational gaps in space and time, freshwater fluxes are considered biased until measurement techniques designed to properly account for ebullition become more common (Wik et al., 2016a). On the contrary, global estimates for freshwater emissions rely on up-scaling of uncertain emission factors and emitting areas, with probable overlapping with wetland emissions (Kirschke et al., 2013; Saunois et al., 2016), which may also lead to an overestimate. More work is needed, both for flux densities and emission areas, based on observations and process modelling, to overcome these uncertainties.

For geological emissions, relatively large uncertainties come from the extrapolation of only a subset of direct measurements to estimate the global fluxes. Moreover, marine seepage emissions are still widely debated (Berchet et al., 2016), and particularly diffuse emissions from microseepages are highly uncertain. However, summing up all bottom-up fossil-CH_4 related sources (including the anthropogenic emissions) leads to a total of 172 Tg CH_4 yr^{-1} [129-219] in 2008-2017, which is about 30% (23%) of global methane emissions inferred by top-down (bottom-up) approaches. Our results are in agreement with the value inferred from ^{14}C atmospheric isotopic analyses 30% contribution of fossil-CH_4 to global emissions (Lassey et al., 2007b; Etiope et al., 2008). Uncertainties on bottom-up estimates of natural emissions lead to probably overestimated total methane emissions resulting in a lower contribution compared to Lassey et al. (2007b). All non-geological and non-wetland land source categories (wild animals, termites, permafrost) have been evaluated at a lower level than in Kirschke et al. (2013) and Saunois et al. (2016), and contribute only 13 Tg CH_4 yr^{-1} [4-19] to global emissions. From a top-down point of view, the sum of all natural sources is more robust than the partitioning between wetlands and other natural sources. To reconcile top-down inversions and bottom-up estimates, the estimation and proper partition of methane emissions between wetlands and freshwater systems should still receive a high priority. Also, including all known spatio-temporal distribution of natural emissions in top-down prior fluxes would be a step forward to consistently comparing natural versus anthropogenic total emissions between top-down and bottom-up approaches.

Anthropogenic emissions. Total anthropogenic emissions for the period 2008-2017 were assessed to be statistically consistent between top-down (357 Tg CH_4 yr^{-1}, range [334-375]) and bottom-up approaches (366 Tg CH_4 yr^{-1}, range [348-392]). The partitioning of anthropogenic emissions between agriculture and waste, fossil fuels extraction and use, and biomass and biofuel burning, also shows good consistency

https://doi.org/10.5194/essd-2019-128
Preprint. Discussion started: 19 August 2019

between top-down and bottom-up approaches, though top-down approaches suggest less fossil fuel and more agriculture and waste emissions than bottom-up estimates (Table 3 and Fig. 5 and 6). For 2008-2017, agriculture and waste contributed 219 Tg CH_4 yr^{-1} [175-239] for the top-down budget and 206 Tg CH_4 yr^{-1} [191-223] for the bottom-up budget. Fossil fuel emissions contributed 109 Tg CH_4 yr^{-1} [79-168] for the top-down budget and 127 Tg CH_4 yr^{-1} [111-154] for the bottom-up budget. Biomass and biofuel burning contributed 30 Tg CH_4 yr^{-1} [22-36] for the top-down budget and 29 Tg CH_4 yr^{-1} [25-39] for the bottom-up budget. Biofuel methane emissions rely on very few estimates at the moment (Wuebbles and Hayhoe (2002), GAINS model). Although biofuel is a small source globally (~12 Tg CH_4 yr^{-1}), more estimates are needed to allow a proper uncertainty assessment. Overall for top-down inversions the global fraction of total emissions for the different source categories is 38% for agriculture and waste, 19% for fossil fuels, and 5% for biomass and biofuel burnings. With the exception of biofuel emissions, the uncertainty associated with global anthropogenic emissions appears to be smaller than that of natural sources but with asymmetric uncertainty distribution (mean significantly different than median). In poorly observed regions, top-down inversions rely on the prior estimates and bring little or no additional information to constrain (often) spatially overlapping emissions (e.g. in India, China). Therefore, the relative agreement between top-down and bottom-up approaches may indicate the limited capability of the inversion to separate the emissions, and should therefore be treated with caution.

5.1.3 Global budget of total methane sinks

Top-down estimates. The CH_4 chemical removal from the atmosphere is estimated to 518 Tg CH_4 yr^{-1} over the period 2008-2017, with an uncertainty of about 5% (range 474-532 Tg CH_4 yr^{-1}). All the inverse models account for CH_4 oxidation by OH and $O(^1D)$, and some include stratospheric chlorine oxidation (Table S6). In addition, most of the top-down models use OH distribution from the TRANSCOM experiment (Patra et al., 2011), probably explaining the rather low uncertainty compared to bottom-up estimates (see below). Differences between transport models affect the chemical removal of CH_4, leading to different chemical loss, even with the same OH distribution. However, uncertainties in the OH distribution and magnitude (Zhao et al., 2019) are not fully taken into account here, while it could contribute to a significant change in the chemical sink (and then in the derived posterior emissions). The chemical sink represents more than 90% of the total sink, the rest being due to soil uptake (38 [27-45] Tg CH_4 yr^{-1}). Half of the top-down models use the climatological soil uptake magnitude (37-38 Tg CH_4 yr^{-1}) and distribution from Ridgwell et al. (1999), while half of the models use an estimate from the biogeochemical model VISIT (Ito and Inatomi, 2012), which calculates varying uptake between 31 and 38 Tg CH_4 yr^{-1} over the 2000-2017 period. These model input estimates are somewhat higher than the central value for bottom-up estimates of the soil sink cited in Sec. 3.3.4, leading to a correspondingly larger top-

https://doi.org/10.5194/essd-2019-128
Preprint. Discussion started: 19 August 2019

down central estimate. For overall consistency in the CH_4 budget, future top-down estimates should take the updated range of bottom-up estimates into consideration.

Bottom-up estimates. The total chemical loss for the 2000s reported here is 595 Tg CH_4 yr^{-1} with an uncertainty of 22%. The chemistry climate models show an uncertainty of about 20% on the CH_4 chemical sink (tropospheric OH plus stratospheric loss). Differences in chemical schemes (especially in the stratosphere) and in the volatile organic compound treatment probably explain most of the discrepancies among models (Zhao et al., 2019). More work is still needed to better understand the derived range in CH_4 chemical lifetime and to narrow it down in order to better assess the methane budget and the future climate projections. Recent studies have also highlighted the large uncertainty on the tropospheric chlorine source (see Sect. 3.3.3). The impact of tropospheric chlorine on methane needs to be better assessed, and then tested in the top-down systems. While the bottom-up mean estimate of the soil uptake is currently at 30 Tg CH_4 yr^{-1}, most of the top-down models use higher prior values. Due to mass-balance, decreasing the soil uptake in the top-down simulations would decrease the derived total surface methane emissions, thus further increasing the discrepancy between bottom up and top down approaches.

5.2 Latitudinal methane budget

5.2.1 Latitudinal budget of total methane emissions

The latitudinal breakdown of emissions inferred from atmospheric inversions reveals a dominance of tropical emissions at 366 Tg CH_4 yr^{-1} [321-399], representing 64% of the global total (Table 5). Thirty-two per cent of the emissions are from the mid-latitudes (185 Tg CH_4 yr^{-1} [166-204]) and 4% from high latitudes (above 60°N). The ranges around the mean latitudinal emissions are larger than for the global methane sources. While the top-down uncertainty is about 5% at the global scale, it increases to 10% for the tropics and the northern mid-latitudes to more than 25% in the northern high-latitudes (for 2008-2017, Table 5). Both top-down and bottom-up approaches show that methane emissions have increased by 20 Tg CH_4 yr^{-1} and 18 Tg CH_4 yr^{-1} in the tropics and in the northern mid-latitudes between 2000-2009 and 2008-2017, respectively.

For the 2008-2017 budget, different inversions assimilated either satellite or ground-based observations. It is of interest to determine whether these two different types of data provide consistent surface emissions. To do so, we calculated the global and hemispheric methane emissions using satellite-based inversions and ground-based inversions separately for the 2010-2017 time period, which is the longest time period for which results from both GOSAT satellite-based and surface-based inversions were available. At the global scale, satellite-based inversions infer almost identical emissions to ground-based inversions (difference of 3 [0-7] Tg CH4 yr-1), when comparing consistently surface versus satellite-based inversions for each system.

https://doi.org/10.5194/essd-2019-128
Preprint. Discussion started: 19 August 2019

This difference is lower that in Saunois et al. (2016) where satellite-based inversions reported 12 Tg higher global methane emissions compared to surface-based inversions. Differences in the ensemble (no SCIAMACHY retrieval used here) and the treatment of satellite data within each system compared to Saunois et al. (2016) explain the contrasting results. Averaged across the inversions, the global difference between satellite and surface-based inversions (3 [0-7] Tg CH_4 yr^{-1}) is not significant compared to the range derived from the different systems (range of 20 Tg CH_4 yr^{-1} using surface or satellite observations only). At the latitudinal scale, emissions vary between the satellite-based and surface-based inversions. Large absolute differences (satellite-based minus surface-based inversions) are observed over the tropical region, between -13 and +26 Tg CH_4 yr^{-1} below 30°N, and in the northern mid-latitudes (between -20 and +15 Tg CH_4 yr^{-1}). Satellite data provide stronger constraints on fluxes in tropical regions than surface data, due to a much larger spatial coverage. It is therefore not surprising that differences between these two types of observations are found in the tropical band, and consequently in the northern mid-latitudes to balance total emissions, thus affecting north-south gradient of emissions. The results presented here clearly show that the models differ in the regional attribution of methane emissions when using satellite observations compared to surface-based inversions. However, the differences are not systematically consistent in sign among the different systems (some showing positive/negative differences for the Tropics and the opposite in the northern mid-latitudes), and depend on whether of not a bias correction is applied to the satellite data based on surface observations. Also, the way the stratosphere is treated in the atmospheric models used to produce atmospheric methane columns from remote-sensing measurements (e.g. GOSAT or TCCON) also requires further investigation (Locatelli et al., 2015; Monteil et al., 2011; Bergamaschi et al., 2009; Saad et al., 2016; Houweling et al., 2017). Some studies have developed methodologies to extract tropospheric partial column abundances from the TCCON data (Saad et al., 2014; Wang et al., 2014). Such partitioning could help to explain the discrepancies between atmospheric models and satellite data.

5.2.2 Latitudinal methane emissions per source category

The analysis of the latitudinal methane budget per source category (Fig. 7) can be performed both for bottom-up and top-down approaches but with limitations. On the bottom-up side, some natural emissions are not (yet) available at regional scale (mainly inland waters). Therefore, for freshwater emissions, we applied the latitudinal contribution of Bastviken et al. (2011) to the global reported value. Further details are provided in the Supplementary to explain how the different bottom-up sources were handled. On the top-down side, as already noted, the partition of emissions per source category has to be considered with caution. Indeed, using only atmospheric methane observations to constrain methane emissions makes this partition largely dependent on prior emissions. However, differences in spatial patterns and seasonality of

https://doi.org/10.5194/essd-2019-128
Preprint. Discussion started: 19 August 2019

emissions can be utilized to constrain emissions from different categories by atmospheric methane observations (for those inversions solving for different sources categories, see Sect. 2.3).

Agriculture and waste are the largest sources of methane emissions in the tropics (130 [121-137] Tg CH_4 yr^{-1} for the bottom-up budget and 139 [127-157] for the top-down budget, about 38% of total methane emissions in this region). Although, wetland emissions are nearly as large with 115 [71-146] Tg CH_4 yr^{-1} for the bottom-up budget and 132 [102-155] Tg CH_4 yr^{-1} for the top-down budget. One top-down model suggests lower emissions from agriculture and waste compared to the ensemble but suggests higher emissions from fossil fuel: this recalls the necessary caution when discussing sectorial partitioning when using top-down inversions. Anthropogenic emissions dominate in the northern mid-latitudes, with a highest contribution from agriculture and waste emissions (42% of total emissions), closely followed by fossil fuel emissions (31% of total emissions). Boreal regions are largely dominated by wetland emissions (60% of total emissions).

The uncertainty on wetland emissions is larger in the bottom-up models than in the top-down models, while uncertainty in anthropogenic emissions is larger in the top-down models than in the inventories. The large uncertainty in tropical wetland emissions (65%) results from a heterogeneous spread among the bottom-up land-surface models. Although they are using the same wetland extent, their responses in terms of flux density show different sensitivity to temperature, vapour pressure, precipitation, and radiation.

More regional discussions were developed in Saunois et al. (2016) and are updated in Stavert et al. (2019).

6 Future developments, missing elements, and remaining uncertainties

Kirschke et al. (2013) and Saunois et al. (2016) identified four main shortcomings in the assessment of regional to global CH_4 budgets. Although progress has been made, they are still relevant and we revisit them here.

Annual to decadal CH_4 emissions from natural sources (wetlands, freshwater, geological) are highly uncertain. Since Saunois et al., (2016), several workshops (e.g. Turner et al., 2019) and publications (e.g. Thornton et al., 2016b; Knox and al., 2019) contributed to develop previous recommendations and strategies to reduce uncertainties of methane emissions due to wetlands and other freshwater systems. The main outcomes of these activities include i) the reduced estimate (by ~20%, i.e. 35 Tg CH_4 yr^{-1}) of the global wetland emissions, due to a refined wetland extent analysis and modifications of land surface model calibration, ii) the initiation of international efforts to develop a high-resolution (typically tens of meters) classification of saturated soils and inundated surfaces based on satellite data (visible and microwave), surface inventories, and expert knowledge, avoiding double counting between wetlands and other

https://doi.org/10.5194/essd-2019-128
Preprint. Discussion started: 19 August 2019

freshwater systems, iii) further development of an on-going effort to collect flux measurements within the FLUXNET activity (FLUXNET-CH_4, Knox et al., 2019) and use them to provide global flux maps based on machine learning approaches and to constrain land surface models. More flux measurements in the tropics and measurements of the isotopic atmospheric composition of the various ecosystems (bogs/swamps, C3/C4 vegetation…) will also help to better constrain methane fluxes as well as their isotopic signature in wetland models. Together with FLUXNET-CH_4 data, it will allow further refinement of parameterizations of the land surface models (Turetsky et al., 2014; Glagolev et al., 2011). There is still a need for more systematic measurements from sites reflecting the diversity of lake morphologies to better understand the short-term biological control on ebullition variability, which remains poorly known (Wik et al., 2014, 2016). Similarly, more local measurements of CH_4 and its isotopes, using continuous laser based techniques, would allow confirmation of the estimation of geological methane emissions. Further efforts are still needed in: i) extending the monitoring of the methane emissions all year round from the different natural sources (wetlands, freshwaters and geological) complemented with key environmental variables to allow proper interpretation (e.g. soil temperature and moisture, vegetation types, water temperature, acidity, nutrient concentrations, NPP, soil carbon density); ii) finalizing the on-going efforts to develop process–based modelling approaches to estimate freshwater emissions instead of data-driven up scaling of unevenly-distributed and local flux observations; and iii) again, finalizing the global high resolution classification of saturated soils and inundated surfaces which will prevent double counting between wetlands and freshwater systems. The remaining large uncertainties strongly suggest the need to develop more integrated studies including the different systems (wetlands, ponds, lakes, reservoirs, streams, rivers, estuaries, and marine systems), to avoid double counting issues but also to account for lateral fluxes.

The partitioning of CH_4 emissions and sinks by region and process is not sufficiently constrained by atmospheric observations in top-down models. In this work, we report inversions assimilating satellite data from GOSAT, which bring more constraints than surface stations, especially over tropical continents. Future satellite instruments, if their systematic errors can be as low as few ppb, will significantly enhance the capabilities to monitor CH_4 emissions from space and will largely extend the spatial coverage of the atmospheric monitoring system. Particularly promising are new satellite missions with high spatial resolution and "imaging capabilities" (Crisp et al., 2018), such as the TROPOMI instrument on Sentinel 5P, launched in October 2017 (Hu et al., 2018). With a relatively high spatial resolution (7km x 7km), TROPOMI promises to provide much more methane data than GOSAT or GOSAT-2, reducing the impact of random errors on the retrieval of methane emissions. TROPOMI has already proven to be useful by detecting large and isolated CH_4 enhancements in South Sudan pointing to emissions from tropical wetlands (Hu et al., 2018), but still has to evaluate the magnitude of its systematic errors. In this context,

https://doi.org/10.5194/essd-2019-128
Preprint. Discussion started: 19 August 2019

intrinsic low-bias observation systems from space, such as active LIDAR techniques (Ehret et al., 2017), are promising to overcome issues of systematic errors (Bousquet et al., 2018). The extension of the CH_4 surface networks to poorly observed regions (e.g. Tropics, China, India, high latitudes) and to the vertical dimension (Aircraft regular campaigns, e.g. Sweeney et al. (2015), Paris et al. (2010); Aircore campaigns, (e.g. Membrive et al., 2017; Andersen et al., 2018); TCCON observations, e.g. (Wunch et al., 2019; Wunch et al., 2011) are still critical observations to complement satellite data that do not observe well in cloudy regions and at high latitudes, and also to evaluate and eventually correct satellite biases (Buchwitz et al., 2016). Such data already exist for China (Fang et al., 2015), India (Tiwari and Kumar, 2012; Lin et al., 2015) and Siberia (Sasakawa et al., 2010; Winderlich et al., 2010) and could be assimilated in inversions if made available more systematically to the scientific community. Observations from other tracers could help partitioning the different CH_4 emitting processes (Turner et al., 2019). Carbon monoxide (e.g. Fortems-Cheiney et al., 2011) can provide useful constraints for biomass burning emissions, and ethane for fugitive emissions (e.g. Simpson et al., 2012; Turner et al., 2019). Methane isotopes can provide additional constraints to partition the different CH_4 sources and sinks, if isotopic signatures can be better known spatially and temporally (Ganesan et al., 2018): radiocarbon for fossil / non-fossil emissions (Petrenko et al., 2017; Lassey et al., 2007a,b), $^{13}CH_4$ for biogenic / pyrogenic / thermogenic emissions, CH_3D for OH loss (Röckmann et al., 2011), and emerging clumped isotope measurements for biogenic/thermogenic emissions (Stolper et al., 2014) and OH loss (Haghnegahdar et al., 2017). However, additional tracers can also bring contradictory trends in emissions such as the ones suggested for the post-2007 period by ^{13}C (Schaefer et al., 2016), and ethane (Hausmann et al., 2016). Such discrepancies have to be understood and solved to be able to properly use additional tracers to constrain CH_4 emissions. Although we have used here a state-of-the-art ensemble of Chemistry Transport Models (CTM) and Climate Chemistry Models (CCM) simulations from the CCMI (Chemistry-Climate Model Initiative, Morgenstern et al., 2018); Lamarque et al., 2013), the uncertainty on the derived CH_4 chemical loss from the chemistry climate models remains the same compared to the previous intercomparison project ACMIP, and more work is still needed to investigate the reasons. In addition, the magnitude of the CH_4 loss through oxidation by tropospheric chlorine is debated in the recent literature. More modeling and instrumental studies should be devoted to reducing the uncertainty of this potential additional sink before integrating it in top-down models. The development of regional components of the global CH_4 budget is also a way to improve global totals by feeding them with regional top-down and bottom-up approaches (Stavert et al., 2019). Such efforts have started for the US (e.g. (Miller et al., 2013), Europe (e.g. (Henne et al., 2016;Bergamaschi et al., 2018b), South and East Asia Asia (Patra et al., 2013; Lin et al., 2018) and for the Arctic (e.g. Bruhwiler et al., 2015; (Thompson et al., 2017), where seasonality (e.g. Zona et al. (2016) for tundra) and magnitude (e.g. Berchet et al. (2016) and Thornton et al. (2016a) for continental shelves) of methane emissions remain poorly

https://doi.org/10.5194/essd-2019-128
Preprint. Discussion started: 19 August 2019

understood. The on-going European project VERIFY (https://verify.lsce.ipsl.fr) aims at better estimating European greenhouse gas emissions, including CH_4 emissions. The development of the RECCAP-2 project should also provide a scientific framework to further refine GHG budgets, including methane, at regional scales (https://www.reccap2-gotemba2019.org/).

Overall, synergies between observation networks with complementary capacities (surface, troposphere, remote sensing from the surface, satellites) should be favored to increase the constraints on the global methane budget, while reducing biases in satellite data assimilated in atmospheric inversions.

The ability to explain observed atmospheric trends by using changes in sectorial emission from bottom-up inventories remains limited. Most inverse groups use the EDGARv4.3.2 inventory as a prior (or the previous EDGARv4.2). EDGAR is the historical annual gridded anthropogenic inventory used in the modelling community. However, discrepancies in both regional and sectorial totals between EDGAR and other emission inventories are important. The drivers of the discrepancies are unclear but are likely to be a combination of differences in methodologies and sectorial definitions. This suggests that more extensive comparisons and exchange between the different datasets teams would favour a path towards increased consistency. More regular updates of emission inventories will also reduce the need for extending them beyond their available coverage. The consistent use of updated activity data within each inventory will also help track the most recent changes and assess temporal and regional emissions changes.

Uncertainties in the modelling of atmospheric transport and chemistry limit the optimal assimilation of atmospheric observations and increase the uncertainties of the inversion-derived flux estimates. The TRANSCOM experiment synthesized in Patra et al. (2011) showed a large sensitivity of the representation of atmospheric transport on methane concentrations in the atmosphere. As an illustration, in their study, the modelled CH_4 budget appeared to depend strongly on the troposphere-stratosphere exchange rate and thus on the model vertical grid structure and circulation in the lower stratosphere. Locatelli et al. (2015) studied the sensitivity of inversion results to the representation of atmospheric transport and suggested that regional changes in the balance of CH_4 emissions between inversions may be due to different characteristics of the transport models used in their approach. Bruhwiler et al. (2017) questioned the strong trend inferred for the US natural gas emission from a top-down perspective (Turner et al., 2016) and showed how, among others, atmospheric transport and choice of upwind background can influence the trend in atmospheric column average methane. On the chemistry side, Nicely et al. (2017) found that the main cause of the large differences in the CTM representation of CH_4 lifetime are the variations in the chemical mechanisms implemented in the models. Using the ensemble of CTMs and CCMs from the CCMI experiment (Morgenstern et al., 2018), Zhao et al. (2019) quantified the range of CH_4 loss induced by the ensemble of

https://doi.org/10.5194/essd-2019-128
Preprint. Discussion started: 19 August 2019

OH fields to be equivalent to about half of the discrepancies between CH_4 observations and simulations as forced by the current anthropogenic inventories. These results emphasize the need to first assess, and then improve, atmospheric transport and chemistry models, especially on the vertical, and to integrate robust representation of OH fields in the atmospheric models. In addition, as stated in Sect. 3.3.4, top-down models may consider testing updated and varying soil uptake estimates, especially considering a warmer climate. Indeed, for top-down models resolving for the net flux of CH_4 at the surface integrating a larger estimate of soil uptake would allow larger emissions, and then reduce the uncertainty with the bottom-up estimates of total CH_4 sources. Finally, top-down models need to consider using the newly available updated gridded products for the different natural sources of CH_4 within their prior to be able to better compare the top-down budget with the bottom-up budget.

7 Conclusions

We have built a global methane budget by using and synthesizing a large ensemble of published methods and results with consistent approaches, including atmospheric observations and inversions (top-down models), process-based models for land surface emissions and atmospheric chemistry, and inventories of anthropogenic emissions (bottom-up models and inventories). For the 2008-2017 decade, global CH_4 emissions are 572 Tg CH_4 yr^{-1} (range of 538-593), as estimated by top-down inversions. About 60% of global emissions are anthropogenic (range of 50-70%). Bottom-up models and inventories suggest much larger global emissions (737 Tg CH_4 yr^{-1} [593-880]) mostly because of larger and more uncertain natural emissions from inland water systems, natural wetlands and geological leaks, and some likely unresolved double counting of these sources. It is also likely that some of the individual bottom-up emission estimates are too high, leading to larger global emissions from the bottom-up perspective than the atmospheric constraints suggest.

The latitudinal breakdown inferred from top-down approaches reveals a dominant role of tropical emissions (~64%) compared to mid (~32%) and high (~4%) northern latitudes (above 60°N) emissions.

Our results, including an extended set of atmospheric inversions, are compared with the previous budget syntheses of Kirschke et al. (2013) and Saunois et al. (2016), and show overall good consistency when comparing the same decade (2000-2009) at the global and latitudinal scales. While, a comparison of top-down emissions estimates determined with and without satellite data agreed well globally they differed significantly at the latitudinal scale. Most worryingly, these differences were not even consistent in sign with some models showing notable increases in a given latitudinal flux and others decreases. This suggests that while the inclusion of satellite data may, in the future, significantly increase our ability to attribute fluxes regionally this is not currently the case due to their existing inherent biases along with the

https://doi.org/10.5194/essd-2019-128
Preprint. Discussion started: 19 August 2019

inconsistent application of methods to account for these biases and differences in model stratospheric transport.

Among the different uncertainties raised in Kirschke et al. (2013), Saunois et al. (2016) estimated that 30-40% of the large range associated with modelled wetland emissions in Kirschke et al. (2013) was due to the estimation of wetland extent. Here, wetland emissions are 35 Tg CH_4 yr^{-1} smaller than previous estimates due to a refinement of wetland extent. The magnitude and uncertainty of all other natural sources have been revised and updated, leading to smaller emission estimates for oceans, geological sources, and wild animals, and higher emission estimates and their range for freshwater systems. This result places a clear priority on reducing uncertainties in emissions from inland water systems by better quantifying the emission factors of each contributing sub-systems (streams, rivers, lakes, ponds) and eliminating both uncertain up-scaling and likely double counting with wetland emissions. The development of process-based models for inland water emissions, constrained by local observations, remains a priority to reduce present uncertainties for inland water emissions. We also place importance in reducing uncertainties of the magnitude, regional distribution, inter-annual variability, and decadal trends of OH radicals in the troposphere and stratosphere, which have improved only marginally since Kirschke et al. (2013) (Zhao et al, 2019).

Our work also suggests the need for more interactions among groups developing emission inventories in order to clarify the definition of the sectorial breakdown in inventories. Such an approach would allow easier comparisons at the sub-category scale. We would also strongly benefit from on-going efforts to expand the network of atmospheric measurement stations into key tropical regions, including vertical profiles and atmospheric columns (e.g. TCCON). Finally, additional tracers (methane isotopes, ethane, CO) have the potential to constrain the global methane cycle more fully if their information content relative to methane emission trends is consistent (Schaefer et al., 2016; Hausmann et al., 2016; Thompson et al., 2018).

Building on the improvement of the points above, our aim is to update this budget synthesis as a living review paper regularly (~every two/three years). Each update will produce a more recent decadal CH_4 budget, highlight changes in emissions and trends, and incorporate newly available data and model improvements.

In addition to the decadal CH_4 budget presented in this paper, trends and year-to-year changes in the methane cycle have been thoroughly discussed in the recent literature (e.g. Nisbet et al., 2019; Turner et al., 2019). After almost a decade of stagnation in the late 1990s and early 2000s (Dlugokencky et al., 2011, Nisbet et al., 2016), a sustained atmospheric growth rate of more than +5 ppb yr^{-1} has been observed since 2007, with a further acceleration after 2014 (Nisbet et al., 2019). The last budget presented in Saunois et al. (2016) has been followed by further syntheses analysing the trends and changes in the methane sources and

https://doi.org/10.5194/essd-2019-128
Preprint. Discussion started: 19 August 2019

sinks reported in the Global Methane Budget (Saunois et al., 2017), or extended with additional constraints (Turner et al., 2019). Nevertheless, no consensus has yet been reached in explaining the CH_4 trend since 2007. A likely explanatory scenario, already discussed in Saunois et al. (2017), includes, by increasing order of uncertainty, a positive contribution from microbial and fossil sources (e.g. Nisbet et al., 2019; Schwietzke et al., 2016), a negative contribution (from biomass burning emissions before 2012 (Giglio et al., 2013; Worden et al., 2017), a downward revision of Chinese emissions (e.g. Peng et al., 2016), a negligible role of Arctic emissions (e.g. Saunois et al., 2017), a tropical dominance of the increasing emissions (e.g. Saunois et al., 2017), and an ambiguous role of OH changes that cannot explain all the observed trend but could have limited the required emission change to explain the observed atmospheric trend (e.g. Turner al., 2017; Rigby et al., 2017; Dalsøren et al., 2016; McNorton et al., 2016, 2018). The challenging increase of atmospheric CH_4 during the past decade needs additional research to be fully understood (Nisbet et al., 2019; Turner et al., 2019). The GCP will continue to take its part in analysing and synthesizing recent changes in the global to regional methane cycle based on the ensemble of top-down and bottom-up studies gathered for the budget analysis presented here.

8 Data availability

The data presented here are made available in the belief that their dissemination will lead to greater understanding and new scientific insights on the methane budget and changes to it, and helping to reduce its uncertainties. The free availability of the data does not constitute permission for publication of the data. For research projects, if the data used are essential to the work to be published, or if the conclusion or results largely depend on the data, co-authorship should be considered. Full contact details and information on how to cite the data are given in the accompanying database.

The accompanying database includes one Excel file organized in the following spreadsheets and two netcdf files defining the regions used to extend the anthropogenic inventories.

The file Global_Methane_Budget_2000-2017_v0.xlsx includes (1) a summary, (2) the methane observed mixing ratio and growth rate from the four global networks (NOAA, AGAGE, CSIRO and UCI), (3) the evolution of global anthropogenic methane emissions (including biomass burning emissions) used to produce Fig. 2, (4) the global and latitudinal budgets over 2000–2009 based on bottom-up approaches, (5) the global and latitudinal budgets over 2000–2009 based on top-down approaches, (6) the global and latitudinal budgets over 2008–2017 based on bottom-up approaches, (7) the global and latitudinal budgets over 2008– 2017 based on top-down approaches, (8) the global and latitudinal budgets for year 2017 based on bottom-up approaches, (9) the global and latitudinal budgets for year 2017 based on top-down approaches, and (10) the list of contributors to contact for further information on specific data.

https://doi.org/10.5194/essd-2019-128
Preprint. Discussion started: 19 August 2019

This database is available from ICOS (https://doi.org/10.18160/GCP-CH4-2019, Saunois et al., 2019) and the Global Carbon Project (http://www.globalcarbonproject.org).

Acknowledgements

This paper is the result of a collaborative international effort under the umbrella of the Global Carbon Project, a project of Future Earth and a research partner of the World Climate Research Programme. We acknowledge primary support for the methane budget from the Gordon and Betty Moore Foundation through Grant GBMF5439 "Advancing Understanding of the Global Methane Cycle" to Stanford University (P.I. Rob Jackson; co-P.I.s Philippe Bousquet, Marielle Saunois, Josep Canadell, Gustaf Hugelius, and Ben Poulter).

Josep G. Canadell thanks the support from the Australian National Environmental Science Program-Earth Systems and Climate Hub. Marielle Saunois and Philippe Bousquet acknowledge the computing power of LSCE for data analyses. Marielle Saunois and Philippe Bousquet acknowledge the modelling groups for making their simulations available for this analysis, the joint WCRP SPARC/IGAC Chemistry-Climate Model Initiative (CCMI) for organising and coordinating the model data analysis activity, and the British Atmospheric Data Centre (BADC) for collecting and archiving the CCMI model output. Ben Poulter acknowledges NASA support through their Terrestrial Ecology program. Peter A. Raymond acknowledges NASA award NNX17AI74G for the work on inland water systems.

Thomas Kleinen acknowledges support by the German Federal Ministry of Education and Research (BMBF) under the PalMod programme. Fortunat Joos and Jurek Mueller acknowledge support by the Swiss National Science Foundation (#200020_172476). William J. Riley and Qing Zhu acknowledge support by the US Department of Energy, BER, RGCM, RUBISCO project under contract #DE-AC02-05CH11231. Qianlai Zhuang and Licheng Liu are supported by a NASA project #NNX17AK20G). Paul A. Miller and Marielle Saunois acknowledge Adrian Gustafson for his contribution to prepare the simulations of LPJ-GUESS. Paul A. Miller, Adrian Gustafson and Wenxin Zhang acknowledge this as a contribution to the Strategic Research Area MERGE and acknowledge financial support from the Swedish Research Council (VR) and Formas project no. 2016-01201. The LPJ□GUESS simulations were performed on the Aurora resource of the Swedish National Infrastructure for Computing (SNIC) at the Lund University Centre for Scientific and Technical Computing (Lunarc), project no. 2017/1-423. Changhui Peng acknowledges the support by National Science and Engineering Research Council of Canada (NSERC) discovery grant. Nicolas Gedney acknowledges support from the Newton Fund through the Met Office Climate Science for Service Partnership Brazil (CSSP Brazil). Akihiko Ito acknowledges support by the Environment Research and Technology Development Fund (2-1710) of the Ministry of the Environment, Japan.

https://doi.org/10.5194/essd-2019-128
Preprint. Discussion started: 19 August 2019

Naveen Chandra and Prabir K. Patra are supported by the Environment Research and Technology Development Fund (2-17002) of the Ministry of the Environment, Japan. Peter Bergamaschi acknowledges the support of ECMWF providing computing resources under the special project "Improve European and global CH_4 and N_2O flux inversions (2018-2020)". Yosuke Niwa is supported by the Environment Research and Technology Development Fund (2-1701) of the Ministry of the Environment, Japan". Shamil Maksyutov acknowledges support from NIES GOSAT Project and several projects funded by the Ministry of the Environment, Japan.

FAOSTAT data collection, analysis and dissemination is funded through FAO regular budget funds. The contribution of relevant experts in member countries is gratefully acknowledged.

Goulven Laruelle is a postdoctoral fellow of the F.R.S.-FNRS at the ULB. Pierre Regnier and Glen P. Peters received funding from the VERIFY project from the European Union's Horizon 2020 research and innovation programme under grant agreement No. 776810. Simona Castaldi acknowledges project RUDN "5-100". David Bastviken acknowledges funding from the European Research Council (ERC; grant no. 725546, METLAKE), from the Swedish Research Councils VR and FORMAS, and from Linköping University. Judith Rosentreter acknowledges the support of the ARC Linkage project LP150100519. Patrick Crill acknowledges support from the Swedish Research Council VR. Thomas Weber acknowledges support from NASA grant NNX17AK11G

Robert Parker is supported by the UK National Centre for Earth Observation (nceo020005) and ESA GHG-CCI and thanks the Japanese Aerospace Exploration Agency, National Institute for Environmental Studies, and the Ministry of Environment for the GOSAT data and their continuous support as part of the Joint Research Agreement. The ALICE High Performance Computing Facility at the University of Leicester was used to produce the GOSAT retrievals. Donald R. Blake and Isobel J. Simpson (UCI) acknowledge funding support from NASA.

The operation of the Mace Head, Trinidad Head, Barbados, American Samoa, and Cape Grim AGAGE stations, and the MIT theory and inverse modeling and SIO calibration activities are supported by the National Aeronautics and Space Administration (NASA, USA) (grants NAG5-12669, NNX07AE89G, NNX11AF17G and NNX16AC98G to MIT; grants NAG5-4023, NNX07AE87G, NNX07AF09G, NNX11AF15G and NNX11AF16G to SIO), the UK Department for Business, Energy & Industrial Strategy (BEIS) contract TRN1537/06/2018 to the University of Bristol for Mace Head; the National Oceanic and Atmospheric Administration (NOAA, USA) contract RA133R15CN0008 to the University of Bristol for Barbados; and the Commonwealth Scientific and Industrial Research Organisation (CSIRO, Australia), the Bureau of Meteorology (Australia), the Department of the Environment and Energy (DoEE, Australia) and Refrigerant Reclaim Australia for Cape Grim. The CSIRO and the Australian Government Bureau of Meteorology are thanked for their ongoing long-term support of the Cape Grim station and the Cape Grim

https://doi.org/10.5194/essd-2019-128
Preprint. Discussion started: 19 August 2019

science program. The CSIRO flask network is supported by CSIRO Australia, Australian Bureau of Meteorology, Australian Institute of Marine Science, Australian Antarctic Division, NOAA USA, and the Meteorological Service of Canada. Marielle Saunois, on behalf of the atmospheric modellers, acknowledges Juha Hatakka (FMI) for making methane measurements at Pallas station and share the data to the community.

References

Abe, T., Bignell, D. E., and Higashi, M.: Termites: Evolution, Sociality, Symbioses, Ecology, Springer ed., doi: 10.1007/978-94-017-3223-9, Dordrecht, 2000.

Akagi, S. K., Yokelson, R. J., Wiedinmyer, C., Alvarado, M. J., Reid, J. S., Karl, T., Crounse, J. D., and Wennberg, P. O.: Emission factors for open and domestic biomass burning for use in atmospheric models, Atmos. Chem. Phys., 11, 4039-4072, doi:10.5194/acp-11-4039-2011, 2011.

Alexe, M., Bergamaschi, P., Segers, A., Detmers, R., Butz, A., Hasekamp, O., Guerlet, S., Parker, R., Boesch, H., Frankenberg, C., Scheepmaker, R. A., Dlugokencky, E., Sweeney, C., Wofsy, S. C., and Kort, E. A.: Inverse modelling of CH_4 emissions for 2010–2011 using different satellite retrieval products from GOSAT and SCIAMACHY, Atmos. Chem. Phys., 15, 113-133, doi:10.5194/acp-15-113-2015, 2015.

Allan, W., Lowe, D. C., Gomez, A. J., Struthers, H., and Brailsford, G. W.: Interannual variation of ^{13}C in tropospheric methane: Implications for a possible atomic chlorine sink in the marine boundary layer, Journal of Geophysical Research-Atmospheres, 110, doi:10.1029/2004JD005650, 2005.

Allan, W., Struthers, H., and Lowe, D. C.: Methane carbon isotope effects caused by atomic chlorine in the marine boundary layer: Global model results compared with Southern Hemisphere measurements, Journal of Geophysical Research-Atmospheres, 112, D04306, doi:10.1029/2006jd007369, 2007.

Allen, D. T., Torres, V. M., Thomas, J., Sullivan, D. W., Harrison, M., Hendler, A., Herndon, S. C., Kolb, C. E., Fraser, M. P., Hill, A. D., Lamb, B. K., Miskimins, J., Sawyer, R. F., and Seinfeld, J. H.: Measurements of methane emissions at natural gas production sites in the United States, Proc. Natl. Acad. Sci. USA 110, 17,768-717,773, doi:10.1073/pnas.1304880110, 2013.

Alvarez, R. A., Zavala-Araiza, D., Lyon, D. R., Allen, D. T., Barkley, Z. R., Brandt, A. R., Davis, K. J., Herndon, S. C., Jacob, D. J., Karion, A., Kort, E. A., Lamb, B. K., Lauvaux, T., Maasakkers, J. D., Marchese, A. J., Omara, M., Pacala, S. W., Peischl, J., Robinson, A. L., Shepson, P. B., Sweeney, C., Townsend-Small, A., Wofsy, S. C., and Hamburg, S. P.: Assessment of methane emissions from the U.S. oil and gas supply chain, Science, 361, 6398, pp 186-188, doi: 10.1126/science.aar7204, 2018.

https://doi.org/10.5194/essd-2019-128
Preprint. Discussion started: 19 August 2019

Andersen, T., Scheeren, B., Peters, W., and Chen, H.: A UAV-based active AirCore system for measurements of greenhouse gases, Atmos. Meas. Tech., 11, 2683-2699, https://doi.org/10.5194/amt-11-2683-2018, 2018

André, J.-C., Boucher, O., Bousquet, P., Chanin, M.-L., Chappellaz, J., and Tardieu, B.: Le méthane : d'où vient-il et quel est son impact sur le climat ?, EDP Sciences, Académie des Sciences et Technologies, Paris, 170 pp., 2014.

Andreae, M. O., and Merlet, P.: Emission of trace gases and aerosols from biomass burning, Global Biogeochemical Cycles, 15, 955–966, 2001.

Angle, J. C., Morin, T. H., Solden, L. M., Narrowe, A. B., Smith, G. J., Borton, M. A., Rey-Sanchez, C., Daly, R. A., Mirfenderesgi, G., Hoyt, D. W., Riley, W. J., Miller, C. S., Bohrer, G., and Wrighton, K. C.: Methanogenesis in oxygenated soils is a substantial fraction of wetland methane emissions, Nature Communications, 8, 1567, doi:10.1038/s41467-017-01753-4, 2017.

Aoki, S., Nakazawa, T., Murayama, S., and Kawaguchi, S.: Measurements of atmospheric methane at the Japanese Antarctic Station. Syowa., Tellus 44B, 273-281, doi:10.1034/j.1600-0889.1992.t01-3-00005.x., 1992.

Arora, V. K., Melton, J. R., and Plummer, D.: An assessment of natural methane fluxes simulated by the CLASS-CTEM model, Biogeosciences, 15, 4683-4709, https://doi.org/10.5194/bg-15-4683-2018, 2018.

Andersen, T., Scheeren, B., Peters, W., and Chen, H.: A UAV-based active AirCore system for measurements of greenhouse gases, Atmos. Meas. Tech., 11, 2683-2699, https://doi.org/10.5194/amt-11-2683-2018, 2018

Bader, W., Bovy, B., Conway, S., Strong, K., Smale, D., Turner, A. J., Blumenstock, T., Boone, C., Collaud Coen, M., Coulon, A., Garcia, O., Griffith, D. W. T., Hase, F., Hausmann, P., Jones, N., Krummel, P., Murata, I., Morino, I., Nakajima, H., O'Doherty, S., Paton-Walsh, C., Robinson, J., Sandrin, R., Schneider, M., Servais, C., Sussmann, R., and Mahieu, E.: The recent increase of atmospheric methane from 10 years of ground-based NDACC FTIR observations since 2005, Atmos. Chem. Phys., 17, 2255-2277, 10.5194/acp-17-2255-2017, 2017.

Baicich, P.: The Birds and Rice Connection, Bird Watcher's Digest. Available online at http://www.greatbirdingprojects.com/images/BWD_J-A_13_BIRDS_N_RICE.pdf (last access 10 November 2016), 2013.

Bange, H. W., Bartell, U. H., Rapsomanikis, S., and Andreae, M. O.: Methane in the Baltic and North Seas and a reassessment of the marine emissions of methane, Global Biogeochemical Cycles, 8, 465-480, doi:10.1029/94gb02181, 1994.

https://doi.org/10.5194/essd-2019-128
Preprint. Discussion started: 19 August 2019

Barba, J., Bradford, M. A., Brewer, P. E., Bruhn, D., Covey, K., van Haren, J., Megonigal, J. P., Mikkelsen, T. N., Pangala, S. R., Pihlatie, M., Poulter, B., Rivas-Ubach, A., Schadt, C. W., Terazawa, K., Warner, D. L., Zhang, Z., and Vargas, R.: Methane emissions from tree stems: a new frontier in the global carbon cycle, New Phytologist, 222, 18-28, 10.1111/nph.15582, 2019.

Bastviken, D., Cole, J., Pace, M., and Tranvik, L.: Methane emissions from lakes: Dependence of lake characteristics, two regional assessments, and a global estimate, Global Biogeochem. Cycles, 18, GB4009, doi:10.1029/2004gb002238, 2004.

Bastviken, D., Tranvik, L. J., Downing, J. A., Crill, P. M., and Enrich-Prast, A.: Freshwater Methane Emissions Offset the Continental Carbon Sink, Science, 331, 6013, doi:10.1126/science.1196808, 2011.

Bates, T. S., Kelly, K. C., Johnson, J. E., and Gammon, R. H.: A reevaluation of the open ocean source of methane to the atmosphere, Journal of Geophysical Research: Atmospheres, 101, 6953-6961, doi:10.1029/95jd03348, 1996.

Berchet, A., Bousquet, P., Pison, I., Locatelli, R., Chevallier, F., Paris, J. D., Dlugokencky, E. J., Laurila, T., Hatakka, J., Viisanen, Y., Worthy, D. E. J., Nisbet, E. G., Fisher, R. E., France, J. L., Lowry, D., and Ivakhov, V.: Atmospheric constraints on the methane emissions from the East Siberian Shelf, Atmospheric Chemistry and Physics 16, 4147–4157, doi:10.5194/acp-16-4147-2016, 2016.

Bergamaschi, P., Frankenberg, C., Meirink, J. F., Krol, M., Villani, M. G., Houweling, S., Dentener, F., Dlugokencky, E. J., Miller, J. B., Gatti, L. V., Engel, A., and Levin, I.: Inverse modeling of global and regional CH_4 emissions using SCIAMACHY satellite retrievals, Journal of Geophysical Research-Atmospheres, 114, D22301, doi:10.1029/2009jd012287, 2009.

Bergamaschi, P., Krol, M., Meirink, J. F., Dentener, F., Segers, A., van Aardenne, J., Monni, S., Vermeulen, A. T., Schmidt, M., Ramonet, M., Yver C., Meinhardt, F., Nisbet, E.G., Fisher R. E., O'Doherty, S., and Dlugokencky, E. J.: Inverse modeling of European CH_4 emissions 2001-2006. Journal of Geophysical Research, 115(D22), D22309. Doi:10.1029/2010JD014180, 2010

Bergamaschi, P., Houweling, S., Segers, A., Krol, M., Frankenberg, C., Scheepmaker, R. A., Dlugokencky, E., Wofsy, S. C., Kort, E. A., Sweeney, C., Schuck, T., Brenninkmeijer, C., Chen, H., Beck, V., and Gerbig, C.: Atmospheric CH_4 in the first decade of the 21st century: Inverse modeling analysis using SCIAMACHY satellite retrievals and NOAA surface measurements, Journal of Geophysical Research: Atmospheres, 118, 7350-7369, doi:10.1002/jgrd.50480, 2013.

Bergamaschi, P., Karstens, U., Manning, A. J., Saunois, M., Tsuruta, A., Berchet, A., Vermeulen, A. T., Arnold, T., Janssens-Maenhout, G., Hammer, S., Levin, I., Schmidt, M., Ramonet, M., Lopez, M., Lavric, J., Aalto, T., Chen, H., Feist, D. G., Gerbig, C., Haszpra, L., Hermansen, O., Manca, G., Moncrieff, J., Meinhardt, F., Necki, J., Galkowski, M., O'Doherty, S., Paramonova, N., Scheeren, H.

https://doi.org/10.5194/essd-2019-128
Preprint. Discussion started: 19 August 2019

A., Steinbacher, M., and Dlugokencky, E.: Inverse modelling of European CH_4 emissions during 2006–2012 using different inverse models and reassessed atmospheric observations, Atmos. Chem. Phys., 18, 901-920, 10.5194/acp-18-901-2018, 2018b.

Bergamaschi, P., Danila, A., Weiss, R. F., Ciais, P., Thompson, R. L., Brunner, D., Levin, I., Meijer, Y., Chevallier, F., Janssens-Maenhout, G., Bovensmann, H., Crisp, D., Basu, S., Dlugokencky, E., Engelen, R., Gerbig, C., Günther, D., Hammer, S., Henne, S., Houweling, S., Karstens, U., Kort, E., Maione, M., Manning, A. J., Miller, J., Montzka, S., Pandey, S., Peters, W., Peylin, P., Pinty, B., Ramonet, M., Reimann, S., Röckmann, T., Schmidt, M., Strogies, M., Sussams, J., Tarasova, O., van Aardenne, J., Vermeulen, A. T., and Vogel, F.: Atmospheric monitoring and inverse modelling for verification of greenhouse gas inventories, JRC111789, n°EUR 29276 EN, doi: 10.2760/759928, Publications Office of the European Union, Luxembourg, doi:10.2760/759928, 2018a

Bhatia, A., Jain, N., and Pathak, H.: Methane and nitrous oxide emissions from Indian rice paddies, agricultural soils and crop residue burning, Greenhouse Gases: Science and Technology, 3, 196-211, doi10.1002/ghg.1339, 2013.

Bian, L., Gao, Z., Sun, Y., Ding, M., Tang, J., and Schnell, R. C.: CH_4 Monitoring and Background Concentration at Zhongshan Station, Antarctica, Atmospheric and Climate Sciences, 6, 135-144 10.4236/acs.2016.61012, 2016.

Blake, D. R., and Rowland, F. S.: World-wide increase in tropospheric methane, 1978–1983, Journal of Atmospheric Chemistry, 4, 43-62, 1986.

Blake, D. R., Mayer, E. W., Tyler, S. C., Makide, Y., Montague, D. C., and Rowland, F. S.: Global Increase in Atmospheric Methane Concentrations between 1978 and 1980, Geophysical Research Letters, 9, 477-480, 1982.

Bloom, A. A., Lee□Taylor, J. , Madronich, S. , Messenger, D. J., Palmer, P. I., Reay, D. S., and McLeod, A. R.: Global methane emission estimates from ultraviolet irradiation of terrestrial plant foliage, New Phytologist, 187, 417-425, doi:10.1111/j.1469-8137.2010.03259.x, 2010.

Bogner, J., Abdelrafie Ahmed, M., Diaz, C., Faaij, A., Gao, Q., Hashimoto, S., Mareckova, K., Pipatti, R., and Zhang, T.: Waste Management, in: In Climate Change (2007), Mitigation. Contribution of Working Group III to the Fourth Assessment Report of the Intergovernmental Panel on Climate Change, edited by: Metz, B., Davidson, O. R., Bosch, P. R., Dave, R., and Meyer, L. A., Cambridge University Press, Cambridge, United Kingdom and New York, NY, USA, 2007.

Bohn, T. J., Melton, J. R., Ito, A., Kleinen, T., Spahni, R., Stocker, B. D., Zhang, B., Zhu, X., Schroeder, R., Glagolev, M. V., Maksyutov, S., Brovkin, V., Chen, G., Denisov, S. N., Eliseev, A. V., Gallego-Sala, A., McDonald, K. C., Rawlins, M. A., Riley, W. J., Subin, Z. M., Tian, H., Zhuang, Q., and

https://doi.org/10.5194/essd-2019-128
Preprint. Discussion started: 19 August 2019

Kaplan, J. O.: WETCHIMP-WSL: Ïntercomparison of wetland methane emissions models over West Siberia, Biogeosciences, 12, 3321-3349, doi:10.5194/bg-12-3321-2015, 2015.

Borges A.V. and Abril G.: Carbon Dioxide and Methane Dynamics in Estuaries, In: Editors-in-Chief: Eric Wolanski and Donald McLusky, Treatise on Estuarine and Coastal Science - Volume 5: Biogeochemistry, Academic Press, Waltham, 2011, Pages 119-161, ISBN 9780080878850, 10.1016/B978-0-12-374711-2.00504-0, 2011.

Borges, A. V., Darchambeau, F., Teodoru, C. R., Marwick, T. R., Tamooh, F., Geeraert, N., Omengo, F. O., Guerin, F., Lambert, T., Morana, C., Okuku, E., and Bouillon, S.: Globally significant greenhouse-gas emissions from African inland waters, Nature Geosci, 8, 637-642, doi:10.1038/ngeo2486, 2015.

Bousquet, P., Hauglustaine, D. A., Peylin, P., Carouge, C., and Ciais, P.: Two decades of OH variability as inferred by an inversion of atmospheric transport and chemistry of methyl chloroform, Atmospheric Chemistry and Physics, 5, 2635-2656, 2005.

Bousquet, P., Ciais, P., Miller, J. B., Dlugokencky, E. J., Hauglustaine, D. A., Prigent, C., Van der Werf, G. R., Peylin, P., Brunke, E. G., Carouge, C., Langenfelds, R. L., Lathiere, J., Papa, F., Ramonet, M., Schmidt, M., Steele, L. P., Tyler, S. C., and White, J.: Contribution of anthropogenic and natural sources to atmospheric methane variability, Nature, 443, 439-443, 2006.

Bousquet, P., Pierangelo, C., Bacour, C., Marshall, J., Peylin, P., Ayar, P. V., Ehret, G., Bréon, F.-M., Chevallier, F., Crevoisier, C., Gibert, F., Rairoux, P., Kiemle, C., Armante, R., Bès, C., Cassé, V., Chinaud, J., Chomette, O., Delahaye, T., Edouart, D., Estève, F., Fix, A., Friker, A., Klonecki, A., Wirth, M., Alpers, M., and Millet, B.: Error Budget of the MEthane Remote LIdar missioN and Its Impact on the Uncertainties of the Global Methane Budget, Journal of Geophysical Research: Atmospheres, 0, 10.1029/2018JD028907, 2018.

BP Statistical Review of World Energy, 68th edition; https://www.bp.com/en/global/corporate/energy-economics/statistical-review-of-world-energy.html (last access: 8 July 2019), 2019.

Brandt, A. R., Heath, G. A., Kort, E. A., O'Sullivan, F., Pétron, G., Jordaan, S. M., Tans, P., Wilcox, J., Gopstein, A. M., Arent, D., Wofsy, S., Brown, N. J., Bradley, R., Stucky, G. D., Eardley, D., and Harriss, R.: Methane Leaks from North American Natural Gas Systems, Science, 343, 733-735, doi:10.1126/science.1247045, 2014.

Brasseur, G., and Salomon, S.: Aeronomy of the Middle Atmosphere : Chemistry and Physics of the Stratosphere and Mesosphere, Atmospheric and Oceanographic Sciences Library, edited by: Springer, Netherlands, XII, 646 pp., 2006.

Brewer, A. W.: Evidence for a world circulation provided by the measurements of helium and water vapour distribution in the stratosphere, Quarterly Journal of the Royal Meteorological Society, 75, 351-363, 10.1002/qj.49707532603, 1949.

https://doi.org/10.5194/essd-2019-128
Preprint. Discussion started: 19 August 2019

Bridgham, S. D., Cadillo-Quiroz, H., Keller, J. K., and Zhuang, Q.: Methane emissions from wetlands: biogeochemical, microbial, and modeling perspectives from local to global scales, Global Change Biology, 19, 1325-1346, doi:10.1111/gcb.12131, 2013.

Bruhwiler, L. M., Basu, S., Bergamaschi, P., Bousquet, P., Dlugokencky, E., Houweling, S., Ishizawa, M., Kim, H. S., Locatelli, R., Maksyutov, S., Montzka, S., Pandey, S., Patra, P. K., Petron, G., Saunois, M., Sweeney, C., Schwietzke, S., Tans, P., and Weatherhead, E. C.: U.S. CH_4 emissions from oil and gas production: Have recent large increases been detected?, Journal of Geophysical Research: Atmospheres, 122, 4070-4083, doi:10.1002/2016JD026157, 2017.

Bruhwiler, L., Bousquet, P., Houweling, S., and Melton, J.: Modeling of atmospheric methane using inverse (and forward) approaches, Chapter 7 in AMAP Assessment 2015: Methane as an Arctic Climate Forcer, p. 77-89, available at http://www.amap.no/documents/doc/AMAP-Assessment-2015-Methane-as-an-Arctic-climate-forcer/1285 (last access 10 November 2016), 2015.

Buchwitz, M., de Beek, R., Burrows, J. P., Bovensmann, H., Warneke, T., Notholt, J., Meirink, J. F., Goede, A. P. H., Bergamaschi, P., Korner, S., Heimann, M., and Schulz, A.: Atmospheric methane and carbon dioxide from SCIAMACHY satellite data: initial comparison with chemistry and transport models, Atmospheric Chemistry and Physics, 5, 941-962, 2005a.

Buchwitz, M., de Beek, R., Noel, S., Burrows, J. P., Bovensmann, H., Bremer, H., Bergamaschi, P., Korner, S., and Heimann, M.: Carbon monoxide, methane and carbon dioxide columns retrieved from SCIAMACHY by WFM-DOAS: year 2003 initial data set, Atmospheric Chemistry and Physics, 5, 3313-3329, 2005b.

Buchwitz, M., de Beek, R., Noel, S., Burrows, J. P., Bovensmann, H., Schneising, O., Khlystova, I., Bruns, M., Bremer, H., Bergamaschi, P., Korner, S., and Heimann, M.: Atmospheric carbon gases retrieved from SCIAMACHY by WFM-DOAS: version 0.5 CO and CH_4 and impact of calibration improvements on CO_2 retrieval, Atmospheric Chemistry and Physics, 6, 2727-2751, 2006.

Buchwitz, M., Dils, B., Boesch, H., Crevoisier, C., Detmers, R., Frankenberg, C., Hasekamp, O., Hewson, W., Laeng, A., Noel, S., Nothold, J., Parker, R., Reuter, M., and Schneising, O.: Product Validation and Intercomparison Report (PVIR) for the Essential Climate Variable (ECV) Greenhouse Gases (GHG), ESA Climate Change Initiative (CCI), report version 4, Feb 2016, http://www.esa-ghg-cci.org/?q=webfm_send/300 (last access: 10 November 2016), 2016.

Buitenhuis E. T., Suntharalingam, P., and Le Quéré, C.: A new estimate of the ocean to atmosphere methane flux, including the first formal uncertainty estimate, in prep, 2019

Burrows, J. P., Hölzle, B., Goede, A. P. H., Visser, H., and Fricke, W.: SCIAMACHY - Scanning Imaging Absorption Spectrometer for Atmospheric Chartography, Acta Astr., 35, 445-451, 1995.

https://doi.org/10.5194/essd-2019-128
Preprint. Discussion started: 19 August 2019

Butz, A., Guerlet, S., Hasekamp, O., Schepers, D., Galli, A., Aben, I., Frankenberg, C., Hartmann, J. M., Tran, H., Kuze, A., Keppel-Aleks, G., Toon, G., Wunch, D., Wennberg, P., Deutscher, N., Griffith, D., Macatangay, R., Messerschmidt, J., Notholt, J., and Warneke, T.: Toward accurate CO_2 and CH_4 observations from GOSAT, Geophysical Research Letters, 38, L14812, doi:10.1029/2011gl047888, 2011.

Cai, Z. C., Xing, G., Yan, X., Xu, H., Tsuruta, H., Yagi, K., and Minami, K.: Methane and nitrous oxide emissions from rice paddy fields as affected by nitrous fertilizers and water management, Plant and Soil, 196, 7-14, 1997.

Campeau, A., and del Giorgio, P. A.: Patterns in CH_4 and CO_2 concentrations across boreal rivers: Major drivers and implications for fluvial greenhouse emissions under climate change scenarios, Global Change Biology, 20, 1075-1088, 10.1111/gcb.12479, 2014.

Carlson, K. M., Gerber, J. S., Mueller, N. D., Herrero, M., MacDonald, G. K., Brauman, K. A., Havlik, P., O'Connell, C. S., Johnson, J. A., Saatchi, S., and West, P. C.: Greenhouse gas emissions intensity of global croplands, Nature Climate Change, 7, 63, 10.1038/nclimate3158, 2016.

Castelán-Ortega, O. A., Carlos Ku-Vera, J., and Estrada-Flores, J. G.: Modeling methane emissions and methane inventories for cattle production systems in Mexico, Atmósfera, 27, 185-191, doi:10.1016/S0187-6236(14)71109-9, 2014.

Cathles, L., Brown, L., Taam, M., and Hunter, A.: A commentary on "The greenhouse-gas footprint of natural gas in shale formations" by R.W. Howarth, R. Santoro, and Anthony Ingraffea, Climatic Change, 113, 525-535, doi:10.1007/s10584-011-0333-0, 2012.

Caulton, D., Shepson, P. B., Santoro, R. L., Sparks, J. P., Howarth, R. W., Ingraffea, A. R., Cambaliza, M. O. L., Sweeney, C., Karion, A., Davis, K. J., Stirm, B. H., Montzka, S. A., and Miller, B. R.: Toward a better understanding and quantification of methane emissions from shale gas development, Proceedings of the National Academy of Sciences USA, 111, 6237-6242, doi:10.1073/pnas.1316546111, 2014.

CCI-Report: Comprehensive Error Characterisation Report: University of Leicester full physics XCH_4 retrieval algorithm for CRDP3 – OCFPv1.0 for the Essential Climate Variable (ECV): Greenhouse Gases (GHG), edited by : W. Hewson, Published by : ESA Climate Change Initiative (CCI), available at: http://www.esa-ghg-cci.org/index.php?q=webfm_send/283 (last access: November 10 2016), 2016.

Chang, J., Peng, P., Ciais, P., Saunois, M., Dangal, S. R.S., Herrero, M., Havlík, P., Tian, H., and Bousquet, P.: Revisiting the $\delta^{13}C$-CH_4 source signature and enteric methane emissions from domestic ruminants from shifts in C3-C4 diet composition, Nature Communications, doi:10.1038/s41467-019-11066-3, 2019.

https://doi.org/10.5194/essd-2019-128
Preprint. Discussion started: 19 August 2019

Channan, S., Collins, K., and Emanuel, W. R.: Global mosaics of the standard MODIS land cover type data., University of Maryland and the Pacific Northwest National Laboratory, College Park, Maryland, USA. , 2014.

Chappellaz, J., Bluniert, T., Raynaud, D., Barnola, J. M., Schwander, J., and Stauffert, B.: Synchronous changes in atmospheric CH_4 and Greenland climate between 40 and 8 kyr BP, Nature, 366, 443-445, 10.1038/366443a0, 1993.

Chen, H., Zhu, Q. a., Peng, C., Wu, N., Wang, Y., Fang, X., Jiang, H., Xiang, W., Chang, J., Deng, X., and Yu, G.: Methane emissions from rice paddies natural wetlands, lakes in China: Synthesis new estimate, Global Change Biology, 19, 19-32, doi:10.1111/gcb.12034, 2013.

Chen, Y. H., and Prinn, R. G.: Estimation of atmospheric methane emissions between 1996 and 2001 using a three-dimensional global chemical transport model, Journal of Geophysical Research-Atmospheres, 111, D10307, doi:10.1029/2005JD006058, 2006.

Chevallier, F., Ciais, P., Conway, T. J., Aalto, T., Anderson, B. E., Bousquet, P., Brunke, E. G., Ciattaglia, L., Esaki, Y., Frohlich, M., Gomez, A., Gomez-Pelaez, A. J., Haszpra, L., Krummel, P. B., Langenfelds, R. L., Leuenberger, M., Machida, T., Maignan, F., Matsueda, H., Morgui, J. A., Mukai, H., Nakazawa, T., Peylin, P., Ramonet, M., Rivier, L., Sawa, Y., Schmidt, M., Steele, L. P., Vay, S. A., Vermeulen, A. T., Wofsy, S., and Worthy, D.: CO_2 surface fluxes at grid point scale estimated from a global 21 year reanalysis of atmospheric measurements, J Geophys Res-Atmos, 115, 2010.

Chevallier, F., Bergamaschi, P., Brunner, D., Feng, L., Houweling, S., Kaminski, T., Knorr, W., Marshall, J., Palmer, P. I., Pandey, S., Reuter, M., Scholze, M., and Voßbeck, M.: Climate Assessment Report for the GHG-CCI project of ESA's Climate Change Initiative, version 4-28, Published by : ESA Climate Change Initiative (CCI), 96 pp, 2017.

CIA: The World Factbook. Natural gas - production. Available at https://www.cia.gov/library/publications/the-world-factbook/rankorder/2249rank.html, (last access : 10 November 2016), 2016.

Ciais, P., Sabine, C., Bala, G., Bopp, L., Brovkin, V., Canadell, J., Chhabra, A., DeFries, R., Galloway, J., M., H., Jones, C., Le Quéré, C., Myneni, R. B., Piao, S., and Thornton, P.: Carbon and Other Biogeochemical Cycles, in: In Climate Change 2013: The Physical Science Basis. Contribution of Working Group I to the Fifth Assessment Report of IPCC, edited by: Stocker, T. F., Qin, D., Plattner, G.-K., Tignor, M., Allen, S. K., Boschung, J., Nauels, A., Xia, Y., Bex, V., and Midgley, P. M., Cambridge University Press, Cambridge, 2013.

Cicerone, R. J., and Oremland, R. S.: Biogeochemical aspects of atmospheric methane, Global Biogeochemical Cycles, 2, 299-327, 1988.

https://doi.org/10.5194/essd-2019-128
Preprint. Discussion started: 19 August 2019

Cicerone, R. J., and Shetter, J. D.: Sources of atmospheric methane: Measurements in rice paddies and a discussion, Journal of Geophysical Research, 86, 7203-7209, 1981.

Collins, M., Knutti, R., Arblaster, J., Dufresne, J.-L., Fichefet, T., Friedlingstein, P., Gao, X., Gutowski, W. J., Johns, T., Krinner, G., Shongwe, M., Tebaldi, C., Weaver, A. J., and Wehner, M.: Long-term Climate Change: Projections, Commitments and Irreversibility., in: In: Climate Change 2013: The Physical Science Basis. Contribution of Working Group I to the Fifth Assessment Report of the Intergovernmental Panel on Climate Change, edited by: Stocker, T. F., Qin, D., Plattner, G.-K., Tignor, M., Allen, S. K., Boschung, J., Nauels, A., Xia, Y., Bex, V., and Midgley, P. M., Cambridge University Press, Cambridge, United Kingdom and New York, NY, USA, 2013.

Conley, S., Franco, G., Faloona, I., Blake, D. R., Peischl, J., and Ryerson, T. B.: Methane emissions from the 2015 Aliso Canyon blowout in Los Angeles, CA, Science, 351, 1317, doi:10.1126/science.aaf2348, 2016.

Conrad, R., and Seiler, W.: Influence of the surface microlayer on the flux of non-conservative trace gases (CO, H_2, CH_4, N_2O) across the ocean-atmosphere interface, Journal of Atmospheric Chemistry, 6, 83-94, 1988.

Conrad, R., Klose, M., and Claus, P.: Phosphate Inhibits Acetotrophic Methanogenesis on Rice Roots, Applied and Environmental Microbiology, 66, 828-831, 2000.

Covey, K. R., and Megonigal, J. P.: Methane production and emissions in trees and forests, New Phytologist, 222, 35-51, 10.1111/nph.15624, 2019.

Covey, K. R., Bueno de Mesquita, C. P., Oberle, B., Maynard, D., Bettigole, C., Crowther, T., Duguid, M., Steven, B., E. Zanne, A., Lapin, M., Ashton, M., Oliver, C., Lee, X., and A. Bradford, M.: Greenhouse trace gases in deadwood, Biogeochemistry, doi:10.1007/s10533-016-0253-1, 2016.

Covey, K. R., Wood, S. A., Warren, R. J., Lee, X., and Bradford, M. A.: Elevated methane concentrations in trees of an upland forest, Geophysical Research Letters, 39, L15705, doi:10.1029/2012gl052361, 2012.

Crawford, J. T., Stanley, E. H., Spawn, S. A., Finlay, J. C., Loken, L. C., and Striegl, R. G.: Ebullitive methane emissions from oxygenated wetland streams, Global Change Biology, 20, 3408–3422 doi:10.1111/gcb.12614, 2014.

Cressot, C., Chevallier, F., Bousquet, P., Crevoisier, C., Dlugokencky, E. J., Fortems-Cheiney, A., Frankenberg, C., Parker, R., Pison, I., Scheepmaker, R. A., Montzka, S. A., Krummel, P. B., Steele, L. P., and Langenfelds, R. L.: On the consistency between global and regional methane emissions inferred from SCIAMACHY, TANSO-FTS, IASI and surface measurements, Atmospheric Chemistry and Physics, 14, 577-592, doi:10.5194/acp-14-577-2014, 2014.

https://doi.org/10.5194/essd-2019-128
Preprint. Discussion started: 19 August 2019

Crevoisier, C., Nobileau, D., Fiore, A. M., Armante, R., Chedin, A., and Scott, N. A.: Tropospheric methane in the tropics - first year from IASI hyperspectral infrared observations, Atmospheric Chemistry and Physics, 9, 6337-6350, 2009.

Crisp et al., A constellation architecture for monitoring carbon dioxide and methane from space, prepared by the CEOS Atmospheric Composition Virtual Constellation Greenhouse Gas Team, available at http://ceos.org/document_management/Meetings/Plenary/32/documents/CEOS_AC-VC_White_Paper_Version_1_20181009.pdf (last access: 28 June 2019), 2018

Crutzen, P. J., Aselmann, I., and Seiler, W.: Methane production by domestic animals, wild ruminants, other herbivorous fauna, and humans, Tellus B, 38B, 271-284, 10.1111/j.1600-0889.1986.tb00193.x, 1986.

Cunnold, D. M., Steele, L. P., Fraser, P. J., Simmonds, P. G., Prinn, R. G., Weiss, R. F., Porter, L. W., O'Doherty, S., Langenfelds, R. L., Krummel, P. B., Wang, H. J., Emmons, L., Tie, X. X., and Dlugokencky, E. J.: In situ measurements of atmospheric methane at GAGE/AGAGE sites during 1985-2000 and resulting source inferences, J Geophys Res-Atmos, 107, ACH 201-ACH 20-18, doi:10.1029/2001jd001226, 2002.

Curry, C. L.: Modeling the soil consumption of atmospheric methane at the global scale, Global Biogeochemical Cycles, 21, GB4012, doi:10.1029/2006gb002818, 2007.

Dalsøren, S. B., Isaksen, I. S. A., Li, L., and Richter, A.: Effect of emission changes in Southeast Asia on global hydroxyl and methane lifetime, Tellus B, 61, 588-601, doi:10.1111/j.1600-0889.2009.00429.x, 2009.

Dalsøren, S. B., Myhre, C. L., Myhre, G., Gomez-Pelaez, A. J., Søvde, O. A., Isaksen, I. S. A., Weiss, R. F., and Harth, C. M.: Atmospheric methane evolution the last 40 years, Atmospheric Chemistry and Physics, 16, 3099-3126, doi:10.5194/acp-16-3099-2016, 2016.

Dalsøren, S. B., Myhre, G., Hodnebrog, Ø., Myhre, C. L., Stohl, A., Pisso, I., Schwietzke, S., Höglund-Isaksson, L., Helmig, D., Reimann, S., Sauvage, S., Schmidbauer, N., Read, K. A., Carpenter, L. J., Lewis, A. C., Punjabi, S., and Wallasch, M.: Discrepancy between simulated and observed ethane and propane levels explained by underestimated fossil emissions, Nature Geoscience, 11, 178-184, doi:10.1038/s41561-018-0073-0, 2018.

Damm, E., Rudels, B., Schauer, U., Mau, S., and Dieckmann, G.: Methane excess in Arctic surface water- triggered by sea ice formation and melting, Scientific Reports, 5, 16179, doi:10.1038/srep16179, 2015.

Dangal, S. R.S., Tian, H., Zhang, B., Pan, S., Lu, C., and Yang, J.: Methane emission from global livestock sector during 1890–2014: Magnitude, trends and spatiotemporal patterns, Glob Change Biol., 23, 4147–4161, doi:10.1111/gcb.13709, 2017

https://doi.org/10.5194/essd-2019-128
Preprint. Discussion started: 19 August 2019

Darmenov, A., and da Silva, A.: The Quick Fire Emissions Dataset (QFED): Documentation of versions 2.1, 2.2 and 2.4, , http://gmao.gsfc.nasa.gov/pubs/docs/Darmenov796.pdf, 2015.

Deemer, B. R., Harrison, J. A., Li, S., Beaulieu, J. J., DelSontro, T., Barros, N., Bezerra-Neto, J. F., Powers, S. M., dos Santos, M. A., and Vonk, J. A.: Greenhouse Gas Emissions from Reservoir Water Surfaces: A New Global Synthesis, BioScience, 66, 949-964, doi:10.1093/biosci/biw117, 2016.

DelSontro, T., Beaulieu, J. J., and Downing, J. A.: Greenhouse gas emissions from lakes and impoundments: Upscaling in the face of global change, Limnology and Oceanography Letters, 3, 64-75, doi:10.1002/lol2.10073, 2018.

Denman, K. L., G. Brasseur, A. Chidthaisong, P. Ciais, P.M. Cox, R.E. Dickinson, D. Hauglustaine, C. Heinze, E. Holland, D. Jacob, U. Lohmann, S Ramachandran, P.L. da Silva Dias, Wofsy, S. C., and X. Zhang: Couplings Between Changes in the Climate System and Biogeochemistry, Cambridge University Press, Cambridge, United Kingdom and New York, NY, USA., 2007.

Dentener, F., Peters, W., Krol, M., van Weele, M., Bergamaschi, P., and Lelieveld, J.: Interannual variability and trend of CH_4 lifetime as a measure for OH changes in the 1979–1993 time period, Journal of Geophysical Research, 108, 4442, doi:10.1029/2002JD002916, D15, 2003.

Desai, A. R., Xu, K., Tian, H., Weishampel, P., Thom, J., Baumann, D., Andrews, A. E., Cook, B. D., King, J. Y., and Kolka, R.: Landscape-level terrestrial methane flux observed from a very tall tower, Agricultural and Forest Meteorology, 201, 61-75, https://doi.org/10.1016/j.agrformet.2014.10.017, 2015.

Dils, B., Buchwitz, M., Reuter, M., Schneising, O., Boesch, H., Parker, R., Guerlet, S., Aben, I., Blumenstock, T., Burrows, J. P., Butz, A., Deutscher, N. M., Frankenberg, C., Hase, F., Hasekamp, O. P., Heymann, J., De Mazière, M., Notholt, J., Sussmann, R., Warneke, T., Griffith, D., Sherlock, V., and Wunch, D.: The Greenhouse Gas Climate Change Initiative (GHG-CCI): Comparative validation of GHG-CCI SCIAMACHY/ENVISAT and TANSO-FTS/GOSAT CO_2 and CH_4 retrieval algorithm products with measurements from the TCCON, Atmospheric Measurement Technologies, 7, 1723-1744, doi:10.5194/amt-7-1723-2014, 2014.

Dils, B., De Mazière, M., Müller, J. F., Blumenstock, T., Buchwitz, M., de Beek, R., Demoulin, P., Duchatelet, P., Fast, H., Frankenberg, C., Gloudemans, A., Griffith, D., Jones, N., Kerzenmacher, T., Kramer, I., Mahieu, E., Mellqvist, J., Mittermeier, R. L., Notholt, J., Rinsland, C. P., Schrijver, H., Smale, D., Strandberg, A., Straume, A. G., Stremme, W., Strong, K., Sussmann, R., Taylor, J., van den Broek, M., Velazco, V., Wagner, T., Warneke, T., Wiacek, A., and Wood, S.: Comparisons between SCIAMACHY and ground-based FTIR data for total columns of CO, CH_4, CO_2 and N_2O, Atmospheric Chemistry and Physics, 6, 1953-1976, doi:10.5194/acp-6-1953-2006, 2006.

https://doi.org/10.5194/essd-2019-128
Preprint. Discussion started: 19 August 2019

Dlugokencky, E. J., Steele, L. P., Lang, P. M., and Masarie, K. A.: The Growth-Rate and Distribution of Atmospheric Methane, Journal of Geophysical Research-Atmospheres, 99, 17,021-017,043, 1994.

Dlugokencky, E. J., Dutton, E. G., Novelli, P. C., Tans, P. P., Masarie, K. A., Lantz, K. O., and Madronich, S.: Changes in CH_4 and CO growth rates after the eruption of Mt Pinatubo and their link with changes in tropical tropospheric UV flux, Geophysical Research Letters, 23, 2761-2764, 1996.

Dlugokencky, E. J., Myers, R. C., Lang, P. M., Masarie, K. A., Crotwell, A. M., Thoning, K. W., Hall, B. D., Elkins, J. W., and Steele, L. P.: Conversion of NOAA atmospheric dry air CH_4 mole fractions to a gravimetrically prepared standard scale, Journal of Geophysical Research: Atmospheres, 110, doi:10.1029/2005JD006035, 2005.

Dlugokencky, E. J., Bruhwiler, L., White, J. W. C., Emmons, L. K., Novelli, P. C., Montzka, S. A., Masarie, K. A., Lang, P. M., Crotwell, A. M., Miller, J. B., and Gatti, L. V.: Observational constraints on recent increases in the atmospheric CH burden, Geophysical Reseasrch Letters, 36, L18803, doi:10.1029/2009GL039780, 2009.

Dlugokencky, E. J., Nisbet, E. G., Fisher, R., and Lowry, D.: Global atmospheric methane: budget, changes and dangers, Philos T R Soc A, 369, 2058-2072, 2011.

Dobson, G., W Brewer, A., and M Cwilong, B.: Meteorology of the lower stratosphere, 144-175 pp., 1946.

Downing, J. A., Prairie, Y. T., Cole, J. J., Duarte, C. M., Tranvik, L. J., Striegl, R. G., McDowell, W. H., Kortelainen, P., Caraco, N. F., Melack, J. M., and Middelburg, J. J.: The global abundance and size distribution of lakes, ponds, and impoundments, Limnology and Oceanography, 51, 2388-2397, doi:10.4319/lo.2006.51.5.2388, 2006.

Dueck, T. A., de Visser, R., Poorter, H., Persijn, S., A. Gorissen, A., W. de Visser, W., Schapendonk, A., Verhagen, J., Snel, J., Harren, F. J. M., Ngai, A. K. Y., Verstappen, F., Bouwmeester, H., Voesenek, L. A. C. J., and van der Werf, A.: No evidence for substantial aerobic methane emission by terrestrial plants: a ^{13}C-labelling approach, New Phytologist, 175, 20-35, doi:10.1111/j.1469-8137.2007.02103.x, 2007.

Dutaur, L., and Verchot, L. V.: A global inventory of the soil CH_4 sink, Global Biogeochem Cycles 21, GB4012, doi:10.1029/2006GB002734, 2007.

EDGARv4.2: European Commission, Joint Research Centre (JRC)/Netherlands Environmental Assessment Agency (PBL). Emission Database for Global Atmospheric Research (EDGAR), release version 4.2. http://edgar.jrc.ec.europa.eu (last acess: 10 November 2016), 2011.

Egger, M., Riedinger, N., Mogollón, J. M., and Jørgensen, B. B.: Global diffusive fluxes of methane in marine sediments, Nature Geoscience, 11, 421-425, doi:10.1038/s41561-018-0122-8, 2018.

https://doi.org/10.5194/essd-2019-128
Preprint. Discussion started: 19 August 2019

Ehhalt, D. H.: The atmospheric cycle of methane, Tellus, 26, 58-70, doi:10.1111/j.2153-3490.1974.tb01952.x, 1974.

Ehhalt, D., Prather, M., Dentener, F., Derwent, R., Dlugokencky, E., Holland, E., Isaksen, I., Katima, J., Kirchhoff, V., Matson, P., Midgley, P., and Wang, M.: Atmospheric chemistry and greenhouse gases. In: Climate Change 2001: The Scientific Basis. Contribution of Working Group I to the Third Assessment Report of the Intergovernmental Panel on Climate Change, edited by Houghton, J.T., Houghton, J. T., Ding, Y., Griggs, D. J., Noguer, M., van der Linder, P. J., Dai, X., Maskell, K., and Johnson, C. A., Cambridge University Press, Cambridge, United Kingdom and New York, NY, USA, 239-287, 2001.

Ehret, G., Bousquet, P., Pierangelo, C., Alpers, M., Millet, B., Abshire, J. B., Bovensmann, H., Burrows, J. P., Chevallier, F., Ciais, P., Crevoisier, C., Fix, A., Flamant, P., Frankenberg, C., Gibert, F., Heim, B., Heimann, M., Houweling, S., Hubberten, H. W., Jockel, P., Law, K., Low, A., Marshall, J., Agusti-Panareda, A., Payan, S., Prigent, C., Rairoux, P., Sachs, T., Scholze, M., and Wirth, M.: MERLIN: A French-German Space Lidar Mission Dedicated to Atmospheric Methane, Remote Sensing, 9, 2017.

EIA: The Annual Energy Outlook 2019 with projection to 2050, DOE/EIA-0383, U.S. Energy Information Administration, Office of Integrated and International Energy Analysis, available at: https://www.eia.gov/outlooks/aeo/ (last access: 28 June 2019), 2019.

Elvidge, C. D., Zhizhin, M., Baugh, K., Hsu, F.-C., and Ghosh, T.: Methods for Global Survey of Natural Gas Flaring from Visible Infrared Imaging Radiometer Suite Data, Energies, 9, 1-15, doi:10.3390/en9010014, 2016.

Elvidge, C., Ziskin, D., Baugh, K., Tuttle, B., Ghosh, T., Pack, D., Erwin, E., and Zhizhin, M.: A Fifteen Year Record of Global Natural Gas Flaring Derived from Satellite Data, Energies, 2, 595-622, 2009.

Etiope, G., and Schwietzke, S.: Global geological methane emissions: an update of top-down and bottom-up estimates, Proceedings of 8th International Symposium on Non-CO_2 Greenhouse Gases (NCGG8), Amsterdam, 12-14 June 2019, 2019.

Etiope, G., Ciotoli, G., Schwietzke, S., and Schoell, M.: Gridded maps of geological methane emissions and their isotopic signature, Earth Syst. Sci. Data, 11, 1-22, doi:10.5194/essd-11-1-2019, 2019.

Etiope, G., Lassey, K. R., Klusman, R. W., and Boschi, E.: Reappraisal of the fossil methane budget and related emission from geologic sources, Geophysical Research Letters, 35, L09307, doi:10.1029/2008gl033623, 2008.

Etiope, G.: Natural Gas Seepage. The Earth's Hydrocarbon Degassing, Springer International Publishing, 199 pp., doi:10.1007/978-3-319-14601-0, 2015.

https://doi.org/10.5194/essd-2019-128
Preprint. Discussion started: 19 August 2019

Etminan, M., Myrhe, G., Highwood, E.J., and Shine, K.P.: Radiative forcing of carbon dioxide, methane, and nitrousu oxide: A significant revision of the methane radiative forcing, Geophys Res. Let., 43, 12614-12623, 2016.

EU-Landfill-Directive: http://ec.europa.eu/environment/waste/landfill_index.htm (last access: 10 November 2016), 1999.

Fang, S., Tans, P. P., Dong, F., Zhou, H., and Luan, T.: Characteristics of atmospheric CO_2 and CH_4 at the Shangdianzi regional background station in China, Atmospheric Environment, 131, 1-8, doi:10.1016/j.atmosenv.2016.01.044, 2015.

FAO, FAOSTAT Emissions Land Use database. Food and Agriculture Organization of the United Nations. Statistical Division. Available at: http://www.fao.org/faostat/en/#data/GL (last access: April 2019), 2019.

Fiedler, S., and Sommer, M.: Methane emissions, groundwater levels and redox potentials of common wetland soils in a temperate-humid climate, Global Biogeochemical Cycles, 14, 1081-1093, doi:10.1029/1999GB001255, 2000.

Fisher, R. E., Sriskantharajah, S., Lowry, D., Lanoiselle, M., Fowler, C. M. R., James, R. H., Hermansen, O., Myhre, C. L., Stohl, A., Greinert, J., Nisbet-Jones, P. B. R., Mienert, J., and Nisbet, E. G.: Arctic methane sources: Isotopic evidence for atmospheric inputs, Geophysical Research Letters, 38, L21803, doi:10.1029/2011gl049319, 2011.

Flores, E., Rhoderick, G. C., Viallon, J., Moussay, P., Choteau, T., Gameson, L., Guenther, F. R., and Wielgosz, R. I.: Methane Standards Made in Whole and Synthetic Air Compared by Cavity Ring Down Spectroscopy and Gas Chromatography with Flame Ionization Detection for Atmospheric Monitoring Applications, Analytical Chemistry, 87, 3272-3279, 10.1021/ac5043076, 2015.

Federici, S., Tubiello, F. N., Salvatore, M., Jacobs, H., and Schmidhuber, J.: New estimates of CO_2 forest emissions and removals: 1990–2015, Forest Ecology and Management, 352, 89-98, https://doi.org/10.1016/j.foreco.2015.04.022, 2015.

Forster, P., Ramaswamy, V., Artaxo, P., Berntsen, T., Betts, B., Fahey, D. W., Haywood, J., Lean, J., Lowe, D. C., Myhre, G., Nganga, J., Prinn, R., Raga, G., Schulz, M., and Van Dorland, R.: Changes in Atmospheric Constituents and in Radiative Forcing., Cambridge University Press, Cambridge, United Kingdom and New York, NY, USA., 2007.

Fortems-Cheiney, A., Chevallier, F., Pison, I., Bousquet, P., Szopa, S., Deeter, M. N., and Clerbaux, C.: Ten years of CO emissions as seen from Measurements of Pollution in the Troposphere (MOPITT), Journal of Geophysical Research-Atmospheres, 116, D05304, 2011.

https://doi.org/10.5194/essd-2019-128
Preprint. Discussion started: 19 August 2019

Francey, R. J., Steele, L. P., Langenfelds, R. L., and Pak, B. C.: High precision long-term monitoring of radiatively active and related trace gases at surface sites and from aircraft in the southern hemisphere atmosphere, Journal of the Atmospheric Sciences, 56, 279-285, 1999.

Frankenberg, C., Aben, I., Bergamaschi, P., Dlugokencky, E. J., van Hees, R., Houweling, S., van der Meer, P., Snel, R., and Tol, P.: Global column-averaged methane mixing ratios from 2003 to 2009 as derived from SCIAMACHY: Trends and variability, Journal of Geophysical Research-Atmospheres, 116, D04302, doi:10.1029/2010jd014849, 2011.

Frankenberg, C., Meirink, J. F., Bergamaschi, P., Goede, A. P. H., Heimann, M., Korner, S., Platt, U., van Weele, M., and Wagner, T.: Satellite chartography of atmospheric methane from SCIAMACHY on board ENVISAT: Analysis of the years 2003 and 2004, Journal of Geophysical Research-Atmospheres, 111, D07303, doi: 10.1029/2005JD006235, 2006.

Frankenberg, C., Meirink, J. F., van Weele, M., Platt, U., and Wagner, T.: Assessing methane emissions from global space-borne observations, Science, 308, 1010-1014, 2005.

Fraser, A., Palmer, P. I., Feng, L., Boesch, H., Cogan, A., Parker, R., Dlugokencky, E. J., Fraser, P. J., Krummel, P. B., Langenfelds, R. L., O'Doherty, S., Prinn, R. G., Steele, L. P., van der Schoot, M., and Weiss, R. F.: Estimating regional methane surface fluxes: the relative importance of surface and GOSAT mole fraction measurements, Atmospheric Chemistry and Physics, 13, 5697-5713, doi:10.5194/acp-13-5697-2013, 2013.

Fraser, P. J., Rasmussen, R. A., Creffield, J. W., French, J. R., and Khalil, M. A. K.: Termites and global methane – Another assessment, Journal of Atmospheric Chemistry, 4, 295-310, 1986.

Fraser, W. T., Blei, E., Fry, S. C. , Newmann, M. F., Reay, D. S., Smith, K.A., and McLeod, A. R.: Emission of methane, carbon monoxide, carbon dioxide and short-chain hydrocarbons from vegetation foliage under ultraviolet irradiation, Plant, Cell and Environment, 38, 980-989, doi:10.1111/pce.12489, 2015

Friedl, M. A., Sulla-Menashe, D., Tan, B., Schneider, A., Ramankutty, N., Sibley, A., and Huang, X.: MODIS Collection 5 global land cover: Algorithm refinements and characterization of new datasets, Remote Sensing of Environment, 114, 168-182, https://doi.org/10.1016/j.rse.2009.08.016, 2010.

GAEZv3.0: Global Agro-Ecological Zones, available at: http://www.gaez.iiasa.ac.at/ (last access : 10 November 2016), 2012.

Ganesan, A. L., Stell, A. C., Gedney, N., Comyn-Platt, E., Hayman, G., Rigby, M., Poulter, B., and Hornibrook, E. R. C.: Spatially Resolved Isotopic Source Signatures of Wetland Methane Emissions, Geophysical Research Letters, 45, 3737-3745, doi:10.1002/2018GL077536, 2018.

Garcias-Bonet, N., and Duarte, C. M.: Methane Production by Seagrass Ecosystems in the Red Sea, Frontiers in Marine Science, 4, 340, 2017.

https://doi.org/10.5194/essd-2019-128
Preprint. Discussion started: 19 August 2019

Gidden, M. J., Riahi, K., Smith, S. J., Fujimori, S., Luderer, G., Kriegler, E., van Vuuren, D. P., van den Berg, M., Feng, L., Klein, D., Calvin, K., Doelman, J. C., Frank, S., Fricko, O., Harmsen, M., Hasegawa, T., Havlik, P., Hilaire, J., Hoesly, R., Horing, J., Popp, A., Stehfest, E., and Takahashi, K.: Global emissions pathways under different socioeconomic scenarios for use in CMIP6: a dataset of harmonized emissions trajectories through the end of the century, Geosci. Model Dev., 12, 1443-1475,doi:10.5194/gmd-12-1443-2019, 2019.

Giglio, L., Randerson, J. T., and van der Werf, G. R.: Analysis of daily, monthly, and annual burned area using the fourth-generation global fire emissions database (GFED4), Journal of Geophysical Research - Biogeosciences, 118, 317-328, doi:10.1002/jgrg.20042, 2013.

Glagolev, M., Kleptsova, I., Filippov, I., Maksyutov, S., and Machida, T.: Regional methane emission from West Siberia mire landscapes, Environmental Research Letters, 6, 045214, doi:10.1088/1748-9326/6/4/045214, 2011.

Gómez-Sanabria, A., Höglund-Isaksson, L., Rafaj, P., and Schöpp, W.: Carbon in global waste and wastewater flows – its potential as energy source under alternative future waste management regimes, Adv. Geosci., 45, 105-113, doi:10.5194/adgeo-45-105-2018, 2018.

Grinham, A., Albert, S., Deering, N., Dunbabin, M., Bastviken, D., Sherman, B., Lovelock, C. E., and Evans, C. D.: The importance of small artificial water bodies as sources of methane emissions in Queensland, Australia, Hydrol. Earth Syst. Sci., 22, 5281-5298, doi:10.5194/hess-22-5281-2018, 2018.

Gromov, S., Brenninkmeijer, C. A. M., and Jöckel, P.: A very limited role of tropospheric chlorine as a sink of the greenhouse gas methane, Atmos. Chem. Phys., 18, 9831-9843, doi:10.5194/acp-18-9831-2018, 2018.

Guérin, F., Abril, G., Richard, S., Burban, B., Reynouard, C., Seyler, P., and Delmas, R.: Methane and carbon dioxide emissions from tropical reservoirs: Significance of downstream rivers, Geophysical Research Letters, 33, L21407, 10.1029/2006GL027929, 2006.

Guérin, F., Deshmukh, C., Labat, D., Pighini, S., Vongkhamsao, A., Guédant, P., Rode, W., Godon, A., Chanudet, V., Descloux, S., and Serça, D.: Effect of sporadic destratification, seasonal overturn and artificial mixing on CH_4 emissions at the surface of a subtropical hydroelectric reservoir (Nam Theun 2 Reservoir, Lao PDR), Biogeosciences, 13, 3647-3663, doi:10.5194/bg-13-3647-2016, 2016.

Gumbricht, T., Roman-Cuesta, R. M., Verchot, L., Herold, M., Wittmann, F., Householder, E., Herold, N., and Murdiyarso, D.: An expert system model for mapping tropical wetlands and peatlands reveals South America as the largest contributor, Global Change Biology, 23, 3581-3599, doi:10.1111/gcb.13689, 2017.

https://doi.org/10.5194/essd-2019-128
Preprint. Discussion started: 19 August 2019

Gurney, K. R., Law, R. M., Denning, A. S., Rayner, P. J., Pak, B. C., Baker, D., Bousquet, P., Bruhwiler, L., Chen, Y. H., Ciais, P., Fung, I. Y., Heimann, M., John, J., Maki, T., Maksyutov, S., Peylin, P., Prather, M., and Taguchi, S.: Transcom 3 inversion intercomparison: Model mean results for the estimation of seasonal carbon sources and sinks, Global Biogeochemical Cycles, 18, GB2010, doi:10.1029/2003gb002111, 2004.

Haghnegahdar, M. A., Schauble, E. A., and Young, E. D.: A model for $^{12}CH_2D_2$ and $^{13}CH_3D$ as complementary tracers for the budget of atmospheric CH_4, Global Biogeochemical Cycles, 31, 1387-1407, doi:10.1002/2017GB005655, 2017.

Harris, I. C.: CRU JRA v1.1: A forcings dataset of gridded land surface blend of Climatic Research Unit (CRU) and Japanese reanalysis (JRA) data; Jan.1901 - Dec.2017. Published by : University of East Anglia Climatic Research Unit, Centre for Environmental Data Analysis, doi:10.5285/13f3635174794bb98cf8ac4b0ee8f4ed, Accessible at: http://dx.doi.org/10.5285/13f3635174794bb98cf8ac4b0ee8f4ed, 2019.

Harris, S., French, H., A. Heginbottom, J., H. Johnston, G., Ladanyi, B., Sego, D., and O. Van Everdingen, R.: Glossary of Permafrost and Related Ground-Ice Terms, doi:10.4224/20386561, 1988.

Hausmann, P., Sussmann, R., and Smale, D.: Contribution of oil and natural gas production to renewed increase in atmospheric methane (2007–2014): top–down estimate from ethane and methane column observations, Atmospheric Chemistry and Physics, 16, 3227-3244, doi:10.5194/acp-16-3227-2016, 2016.

Hayashida, S., Ono, A., Yoshizaki, S., Frankenberg, C., Takeuchi, W., and Yan, X.: Methane concentrations over Monsoon Asia as observed by SCIAMACHY: Signals of methane emission from rice cultivation, Remote Sensing of Environment, 139, 246-256, doi:10.1016/j.rse.2013.08.008, 2013.

Hayman, G. D., O'Connor, F. M., Dalvi, M., Clark, D. B., Gedney, N., Huntingford, C., Prigent, C., Buchwitz, M., Schneising, O., Burrows, J. P., Wilson, C., Richards, N., and Chipperfield, M.: Comparison of the HadGEM2 climate-chemistry model against in situ and SCIAMACHY atmospheric methane data, Atmospheric Chemistry and Physics, 14, 13257-13280, doi:10.5194/acp-14-13257-2014, 2014.

Henne, S., Brunner, D., Oney, B., Leuenberger, M., Eugster, W., Bamberger, I., Meinhardt, F., Steinbacher, M., and Emmenegger, L.: Validation of the Swiss methane emission inventory by atmospheric observations and inverse modelling, Atmos. Chem. Phys., 16, 3683-3710, doi:10.5194/acp-16-3683-2016, 2016.

Herrero, M., Havlík, P., Valin, H., Notenbaert, A., Rufino, M. C., Thornton, P. K., Blümmel, M., Weiss, F., Grace, D., and Obersteiner, M.: Global livestock: Biomass use, production, & GHG, Proceedings of the National Academy of Sciences, 110, 52, 20888-20893; doi:10.1073/pnas.1308149110, 2013

https://doi.org/10.5194/essd-2019-128
Preprint. Discussion started: 19 August 2019

Hoesly, R. M., Smith, S. J., Feng, L., Klimont, Z., Janssens-Maenhout, G., Pitkanen, T., Seibert, J. J., Vu, L., Andres, R. J., Bolt, R. M., Bond, T. C., Dawidowski, L., Kholod, N., Kurokawa, J. I., Li, M., Liu, L., Lu, Z., Moura, M. C. P., O'Rourke, P. R., and Zhang, Q.: Historical (1750–2014) anthropogenic emissions of reactive gases and aerosols from the Community Emissions Data System (CEDS), Geosci. Model Dev., 11, 369-408, 10.5194/gmd-11-369-2018, 2018.

Höglund-Isaksson, L., Thomson, A., Kupiainen, K., Rao, S., and Janssens-Maenhout, G.: Anthropogenic methane sources, emissions and future projections, Chapter 5 in AMAP Assessment 2015: Methane as an Arctic Climate Forcer, p. 39-59, available at http://www.amap.no/documents/doc/AMAP-Assessment-2015-Methane-as-an-Arctic-climate-forcer/1285 (last access : 10 November 2016), 2015.

Höglund-Isaksson, L.: Global anthropogenic methane emissions 2005-2030: Technical mitigation potentials and costs, Atmospheric Chemistry and Physics, 12, 9079-9096, doi:10.5194/acp-12-9079-2012, 2012.

Höglund-Isaksson, L.: Bottom-up simulations of methane and ethane emissions from global oil and gas systems 1980 to 2012, Environmental Research Letters, 12, 024007, doi:10.1088/1748-9326/aa583e, 2017.

Holgerson, M. A., and Raymond, P. A.: Large contribution to inland water CO_2 and CH_4 emissions from very small ponds, Nature Geoscience, 9, 222, doi:10.1038/ngeo2654, 2016.

Holton, J. R.: Meridional distribution of stratospheric trace constituents, Journal of the Atmospheric Sciences, 43, 1238–1242, 1986.

Hoor, P., Gurk, C., Brunner, D., Hegglin, M. I., Wernli, H., and Fischer, H.: Seasonality and extent of extratropical TST derived from in-situ CO measurements during SPURT, Atmos. Chem. Phys., 4, 1427-1442, doi:10.5194/acp-4-1427-2004, 2004.

Hornafius, J. S., Quigley, D., and Luyendyk, B. P.: The world's most spectacular marine hydrocarbon seeps (Coal Oil Point, Santa Barbara Channel, California): Quantification of emissions, Journal of Geophysical Research: Oceans, 104, 20703-20711, doi:10.1029/1999JC900148, 1999.

Hossaini, R., Chipperfield, M. P., Saiz-Lopez, A., Fernandez, R., Monks, S., Feng, W., Brauer, P., and von Glasow, R.: A global model of tropospheric chlorine chemistry: Organic versus inorganic sources and impact on methane oxidation, Journal of Geophysical Research: Atmospheres, 121, 14,271-214,297, doi:10.1002/2016JD025756, 2016.

Houweling, S., Krol, M., Bergamaschi, P., Frankenberg, C., Dlugokencky, E. J., Morino, I., Notholt, J., Sherlock, V., Wunch, D., Beck, V., Gerbig, C., Chen, H., Kort, E. A., Röckmann, T., and Aben, I.: A multi-year methane inversion using SCIAMACHY, accounting for systematic errors using TCCON

https://doi.org/10.5194/essd-2019-128
Preprint. Discussion started: 19 August 2019

measurements, Atmospheric Chemistry and Physics, 14, 3991-4012, doi:10.5194/acp-14-3991-2014, 2014.

Houweling, S., Bergamaschi, P., Chevallier, F., Heimann, M., Kaminski, T., Krol, M., Michalak, A. M., and Patra, P.: Global inverse modeling of CH_4 sources and sinks: an overview of methods, Atmos. Chem. Phys., 17, 235-256, 10.5194/acp-17-235-2017, 2017.

Howarth, R. W., Ingraffea, A., and Engelder, T.: Natural gas: Should fracking stop?, Nature, 477, 271-275, 2011b.

Howarth, R., Santoro, R., and Ingraffea, A.: Methane and the greenhouse-gas footprint of natural gas from shale formations, Climatic Change, 106, 679-690, doi:10.1007/s10584-011-0061-5, 2011a.

Hu, H., Landgraf, J., Detmers, R., Borsdorff, T., Aan de Brugh, J., Aben, I., Butz, A., and Hasekamp, O.: Toward Global Mapping of Methane With TROPOMI: First Results and Intersatellite Comparison to GOSAT, Geophysical Research Letters, 45, 3682-3689, doi:10.1002/2018GL077259, 2018.

Huang, J., and Prinn, R. G.: Critical evaluation of emissions of potential new gases for OH estimation, Journal of Geophysical Research, 107, 4784, doi:10.1029/2002jd002394, 2002.

Hugelius, G., Strauss, J., Zubrzycki, S., Harden, J. W., Schuur, E. A. G., Ping, C. L., Schirrmeister, L., Grosse, G., Michaelson, G. J., Koven, C. D., O'Donnell, J. A., Elberling, B., Mishra, U., Camill, P., Yu, Z., Palmtag, J., and Kuhry, P.: Estimated stocks of circumpolar permafrost carbon with quantified uncertainty ranges and identified data gaps, Biogeosciences, 11, 6573-6593, doi:10.5194/bg-11-6573-2014, 2014.

IEA: International Energy Agency. Annual Report. Available at: https://www.iea.org/statistics/electricity/ (last accessed: 8 July 2019), 2018.

Inoue, M., Morino, I., Uchino, O., Nakatsuru, T., Yoshida, Y., Yokota, T., Wunch, D., Wennberg, P. O., Roehl, C. M., Griffith, D. W. T., Velazco, V. A., Deutscher, N. M., Warneke, T., Notholt, J., Robinson, J., Sherlock, V., Hase, F., Blumenstock, T., Rettinger, M., Sussmann, R., Kyrö, E., Kivi, R., Shiomi, K., Kawakami, S., De Mazière, M., Arnold, S. G., Feist, D. G., Barrow, E. A., Barney, J., Dubey, M., Schneider, M., Iraci, L. T., Podolske, J. R., Hillyard, P. W., Machida, T., Sawa, Y., Tsuboi, K., Matsueda, H., Sweeney, C., Tans, P. P., Andrews, A. E., Biraud, S. C., Fukuyama, Y., Pittman, J. V., Kort, E. A., and Tanaka, T.: Bias corrections of GOSAT SWIR XCO_2 and XCH_4 with TCCON data and their evaluation using aircraft measurement data, Atmos. Meas. Tech., 9, 3491-3512, doi:10.5194/amt-9-3491-2016, 2016.

IPCC: Good Practice Guidance and Uncertainty Management in National Greenhouse Gas Inventories. Intergovernmental Panel on Climate Change, National Greenhouse Gas Inventories Programme. Montreal, IPCC-XVI/Doc.10(1.IV.2000), May 2000.ISBN 4-88788-000-6, 2000.

https://doi.org/10.5194/essd-2019-128
Preprint. Discussion started: 19 August 2019

IPCC: Climate change 2001: The scientific basis. Contribution of working group I to the third assessment report of the Intergovernmental Panel on Climate Change, Cambridge University Press, Cambridge, United Kingdom and New York, NY, USA, 881, 2001.

IPCC: IPCC Guidelines for National Greenhouse Gas Inventories. The National Greenhouse Gas Inventories Programme, Eggleston H.S., Buendia L., Miwa K., Ngara T. and Tanabe K. (eds). The Intergovernmental Panel on Climate Change, IPCC TSU NGGIP, IGES. Institute for Global Environmental Strategy, Hayama, Kanagawa, Japan. Available online at: http://www.ipcc-nggip.iges.or.jp/support/Primer_2006GLs.pdf (last access: 10 November 2016), 2006.

IPCC: Climate Change 2014: Mitigation of Climate Change. Contribution of Working Group III to the Fifth Assessment Report of the Intergovernmental Panel on Climate Change. Edenhofer, O., R. Pichs-Madruga, Y. Sokona, E. Farahani, S. Kadner, K. Seyboth, A. Adler, I. Baum, S. Brunner, P. Eickemeier, B. Kriemann, J. Savolainen, S. Schlömer, C. von Stechow, T. Zwickel and J.C. Minx (eds.). Cambridge University Press, 2014.

Ishizawa, M., Mabuchi, K., Shirai, T., Inoue, M., Morino, I., Uchino, O., Yoshida, Y., Maksyutov, S., and Belikov, D.: Inter-annual variability of CO2 exchange in Northern Eurasia inferred from GOSAT XCO_2, Environ. Res. Lett., 11, 105001, doi:10.1088/1748-9326/11/10/105001, 2016.

Ito, A., and Inatomi, M.: Use of a process-based model for assessing the methane budgets of global terrestrial ecosystems and evaluation of uncertainty, Biogeosciences, 9, 759-773, doi:10.5194/bg-9-759-2012, 2012.

Jackson, R. B., Down, A., Phillips, N. G., Ackley, R. C., Cook, C. W., Plata, D. L., and Zhao, K.: Natural gas pipeline leaks across Washington, D.C, Environmental Science and Technology, 48, 2051-2058, doi:10.1021/es404474x, 2014a.

Jackson, R. B., Vengosh, A., Carey, J. W., Davies, R. J., Darrah, T. H., O'Sullivan, F., and Pétron, G.: The Environmental Costs and Benefits of Fracking, Annual Review of Environment and Resources, 39, 327-362, doi:10.1146/annurev-environ-031113-144051, 2014b.

Jacob, D. J., Turner, A. J., Maasakkers, J. D., Sheng, J., Sun, K., Liu, X., Chance, K., Aben, I., McKeever, J., and Frankenberg, C.: Satellite observations of atmospheric methane and their value for quantifying methane emissions, Atmos. Chem. Phys., 16, 14371-14396, doi:10.5194/acp-16-14371-2016, 2016.

James, R. H., Bousquet, P., Bussmann, I., Haeckel, M., Kipfer, R., Leifer, I., Niemann, H., Ostrovsky, I., Piskozub, J., Rehder, G., Treude, T., Vielstädte, L., and Greinert, J.: Effects of climate change on methane emissions from seafloor sediments in the Arctic Ocean: A review, Limnology and Oceanography, 61, S283-S299, doi:10.1002/lno.10307, 2016.

https://doi.org/10.5194/essd-2019-128
Preprint. Discussion started: 19 August 2019

Janssens-Maenhout, G., Crippa, M., Guizzardi, D., Muntean, M., Schaaf, E., Dentener, F., Bergamaschi, P., Pagliari, V., Olivier, J., Peters, J., van Aardenne, J., Monni, S., Doering, U., Petrescu, R., Solazzo, E., and Oreggioni, G.: EDGAR v4.3.2 Global Atlas of the three major Greenhouse Gas Emissions for the period 1970-2012, Earth Syst. Sci. Data, 11, 959-1002, https://doi.org/10.5194/essd-11-959-2019, 2019.

Jensen, K., McDonald, K.: Surface water microwave product series version 3: A near-real time and 25-year historical global inundated area fraction time series from active and passive microwave remote sensing, IEEE Geoscience and Remote Sensing Letters, doi: 10.1109/LGRS.2019.2898779, 2019

JAXA, Launch Results of the H-IIA F40 Encapsulating GOSAT-2 and KhalifaSat : https://global.jaxa.jp/press/2018/10/20181029_h2af40.html, 2019.

Jiang, Y, Groenigen, KJ, Huang, S, Hungate, B. A., van Kessel, K., Hu, S., Zhang, J.,Wu L., Yan, X., Wang, L., Chen, J., Hang, X, Zhang, Y., Horwath, W. R., Ye, R., Linquist, B. A., Song Z., Zheng, C., Deng, A., and Zhang, W.: Higher yields and lower methane emissions with new rice cultivars, Glob Change Biol, 23, 4728– 4738. Doi:10.1111/gcb.13737, 2017

Johnson, D. E., Phetteplace, H. W., and Seidl, A. F.: Methane, nitrous oxide and carbon dioxide emissions from ruminant livestock production systems, GHGs and animal agriculture. Proceedings of the 1th International Conference on GHGs and Animal Agriculture, 7-11 November Obihiro, Japan, 77–85, 2002.

Jones, R. L., and A. Pyle, J.: Observations of CH_4 and N_2O by the NIMBUS 7 SAMS: A comparison with in situ data and two-dimensional numerical model calculations, Journal of Geophysical Research: Atmospheres, 89, 5263-5279, doi:10.1029/JD089iD04p05263, 1984.

Jung, M., Reichstein, M., and Bondeau, A.: Towards global empirical upscaling of FLUXNET eddy covariance observations: validation of a model tree ensemble approach using a biosphere model, Biogeosciences, 6, 2001-2013, doi:10.5194/bg-6-2001-2009, 2009.

Jung, M., Reichstein, M., Margolis, H. A., Cescatti, A., Richardson, A. D., Arain, M. A., Arneth, A., Bernhofer, C., Bonal, D., Chen, J., Gianelle, D., Gobron, N., Kiely, G., Kutsch, W., Lasslop, G., Law, B. E., Lindroth, A., Merbold, L., Montagnani, L., Moors, E. J., Papale, D., Sottocornola, M., Vaccari, F., and Williams, C.: Global patterns of land-atmosphere fluxes of carbon dioxide, latent heat, and sensible heat derived from eddy covariance, satellite, and meteorological observations, Journal of Geophysical Research: Biogeosciences, 116, doi:10.1029/2010JG001566, 2011.

Kai, F. M., Tyler, S. C., Randerson, J. T., and Blake, D. R.: Reduced methane growth rate explained by decreased Northern Hemisphere microbial sources, Nature, 476, 194-197, 2011.

Kaiser, J. W., Heil, A., Andreae, M. O., Benedetti, A., Chubarova, N., Jones, L., Morcrette, J. J., Razinger, M., Schultz, M. G., Suttie, M., and van der Werf, G. R.: Biomass burning emissions

https://doi.org/10.5194/essd-2019-128
Preprint. Discussion started: 19 August 2019

estimated with a global fire assimilation system based on observed fire radiative power, Biogeosciences, 9, 527-554, doi:10.5194/bg-9-527-2012, 2012.

Kang, Y., Pan, D., Bai, Y., He, X., Chen, X., Chen, C.T.A. and Wang, D. Area of the Global Major River Plumes. Acta Oceanologica Sinica , 32, 79-88, 2013.

Karion, A., Sweeney, C., Pétron, G., Frost, G., Michael Hardesty, R., Kofler, J., Miller, B. R., Newberger, T., Wolter, S., Banta, R., Brewer, A., Dlugokencky, E., Lang, P., Montzka, S. A., Schnell, R., Tans, P., Trainer, M., Zamora, R., and Conley, S.: Methane emissions estimate from airborne measurements over a western United States natural gas field, Geophysical Research Letters, 40, 4393-4397, doi:10.1002/grl.50811, 2013.

Keppler, F., Hamilton, J. T. G., Brass, M., and Rockmann, T.: Methane emissions from terrestrial plants under aerobic conditions, Nature, 439, 187-191, 2006.

Kirschke, S., Bousquet, P., Ciais, P., Saunois, M., Canadell, J. G., Dlugokencky, E. J., Bergamaschi, P., Bergmann, D., Blake, D. R., Bruhwiler, L., Cameron-Smith, P., Castaldi, S., Chevallier, F., Feng, L., Fraser, A., Heimann, M., Hodson, E. L., Houweling, S., Josse, B., Fraser, P. J., Krummel, P. B., Lamarque, J. F., Langenfelds, R. L., Le Quere, C., Naik, V., O'Doherty, S., Palmer, P. I., Pison, I., Plummer, D., Poulter, B., Prinn, R. G., Rigby, M., Ringeval, B., Santini, M., Schmidt, M., Shindell, D. T., Simpson, I. J., Spahni, R., Steele, L. P., Strode, S. A., Sudo, K., Szopa, S., van der Werf, G. R., Voulgarakis, A., van Weele, M., Weiss, R. F., Williams, J. E., and Zeng, G.: Three decades of global methane sources and sinks, Nature Geoscience, 6, 813-823, doi:10.1038/ngeo1955, 2013.

Klauda, J. B., and Sandler, S. I.: Global distribution of methane hydrate in ocean sediment, Energy and Fuels, 19, 459-470, 2005.

Kleinen, T., Brovkin, V., and Schuldt, R. J.: A dynamic model of wetland extent and peat accumulation: results for the Holocene, Biogeosciences, 9, 235-248, doi:10.5194/bg-9-235-2012, 2012.

Knox, S., Jackson, R. B., Poulter, B., McNicol, G., Fluet-Chouinard, E., Zhnag, Z., Hugelius, G., Bousuqet, P., canadell, J. G., Saunois , M., Papale, D., Chu, H., Keenan, T., Baldocchi, D., Tom, M. S., Trotta, C., Mammarella, I., Aurela, M., Bohrer, G., Campbell, D., Cescatti, A., Chamberlain, S., Chen, J., Chen, W., Dengel, S., Desai, A. R., Euskirchen, E., Friborg, T., Gasbarra, D., Goded, I., Goeckede, M., Heimann, M., Helbig, M., Hirano, T., Hollinger, D. Y., Iwata, H., Kang, M., Klatt, J., Kraus, K. W., Kutzbach, L. Lohila, A., Mitra, B., Morin, T. H., Nilsson, M. B., Niu, S., Noomets, A., Oechel, W. C., Peichl, M., Peltola, O., Reba, M. L., Runkle, B. R. K., Richardson, A. D., Ryu, Y., Sachs, T., Shcäfer, K. V. R., Scmid, H. P., Shurpali, N., Sonnentag, O., Tang, A. C. I., Ueyama, M., Vargas, R., Vesala, T., Ward, E. J., Windham-Myers, L., Wohlfahrt, G., and Zona, D.: FLUXNET-CH_4 Synthesis Activity: Objectives, Observations, and Future Directions, Bulletin of the American Meteorological Society, 2019, in press.

https://doi.org/10.5194/essd-2019-128
Preprint. Discussion started: 19 August 2019

Kock, A., and Bange, H. W.: Counting the ocean's greenhouse gas emissions,, EoS, 96, doi: 10.1029/2015EO023665, 2015.

Kohnert, K., Serafimovich, A., Metzger, S., Hartmann, J., and Sachs, T.: Strong geologic methane emissions from discontinuous terrestrial permafrost in the Mackenzie Delta, Canada, Scientific Reports, 7, 5828, doi: 10.1038/s41598-017-05783-2, 2017.

Koven, C. D., Lawrence, D. M., and Riley, W. J.: Permafrost C feedback:Deep soil C and N dynamics, Proceedings of the National Academy of Sciences, 112, 12, 3752-3757, doi:10?1073/pnas.1415123112, 2015.

Kretschmer, K., Biastoch, A., Rüpke, L., and Burwicz, E.: Modeling the fate of methane hydrates under global warming, Global Biogeochem Cycles, 29, 610-625, 1002/2014GB005011, 2015.

Kuhn, M., Lundin, E. J., Giesler, R., Johansson, M., and Karlsson, J.: Emissions from thaw ponds largely offset the carbon sink of northern permafrost wetlands, Scientific Reports, 8, 9535, doi:10.1038/s41598-018-27770-x, 2018.

Kvenvolden, K. A., and Rogers, B. W.: Gaia's breath - Global methane exhalations, Marine and Petroleum Geology, 22, 579-590, doi:10.1016/j.marpetgeo.2004.08.004, 2005.

Kvenvolden, K. A., Reeburgh, W. S., and Lorenson, T. D.: Attention turns to naturally occurring methane seepages, EOS Transactions, AGU, 82, p. 457, 2001.

Lamarque, J. F., Shindell, D. T., Josse, B., Young, P. J., Cionni, I., Eyring, V., Bergmann, D., Cameron-Smith, P., Collins, W. J., Doherty, R., Dalsoren, S., Faluvegi, G., Folberth, G., Ghan, S. J., Horowitz, L. W., Lee, Y. H., MacKenzie, I. A., Nagashima, T., Naik, V., Plummer, D., Righi, M., Rumbold, S. T., Schulz, M., Skeie, R. B., Stevenson, D. S., Strode, S., Sudo, K., Szopa, S., Voulgarakis, A., and Zeng, G.: The Atmospheric Chemistry and Climate Model Intercomparison Project (ACCMIP): overview and description of models, simulations and climate diagnostics, Geoscientific Model Development, 6, 179-206, doi:10.5194/gmd-6-179-2013, 2013.

Lamb, B. K., Edburg, S. L., Ferrara, T. W., Howard, T., Harrison, M. R., Kolb, C. E., Townsend-Small, A., Dyck, W., Possolo, A., and Whetstone, J. R.: Direct Measurements Show Decreasing Methane Emissions from Natural Gas Local Distribution Systems in the United States, Environmental Science & Technology, 49, 5161-5169, doi:10.1021/es505116p, 2015.

Lambert, G., and Schmidt, S.: Reevaluation of the oceanic flux of methane: Uncertainties and long term variations, Chemosphere, 26, 579-589, doi:10.1016/0045-6535(93)90443-9., 1993.

Lamontagne, R. A., Swinnerton, J. W., Linnenbom, V. J., and Smith, W. D.: Methane concentrations in various marine environments, Journal of Geophysical Research, 78, 5317-5324, doi:10.1029/JC078i024p05317, 1973.

https://doi.org/10.5194/essd-2019-128
Preprint. Discussion started: 19 August 2019

Lan, X., Tans, P., Sweeney, C., Andrews, A., Dlugokencky, E., Schwietzke, S., Kofler , J., McKain K., Thoning, K., Crotwell, M., Montzka, S., Miller, B. R., and Biraud, S. C.: Long□term measurements show little evidence for large increases in total U.S. methane emissions over the past decade. Geophysical Research Letters, 46, 4991– 4999, doi:10.1029/2018GL081731, 2019

Laruelle, G. G., Dürr, H. H., Lauerwald, R., Hartmann, J., Slomp, C. P., Goossens, N., and Regnier, P. A. G.: Global multi-scale segmentation of continental and coastal waters from the watersheds to the continental margins, Hydrol. Earth Syst. Sci., 17, 2029-2051, https://doi.org/10.5194/hess-17-2029-2013, 2013.

Lassey, K. R., Etheridge, D. M., Lowe, D. C., Smith, A. M., and Ferretti, D. F.: Centennial evolution of the atmospheric methane budget: what do the carbon isotopes tell us?, Atmospheric Chemistry and Physics, 7, 2119-2139, 2007a.

Lassey, K. R., Lowe, D. C., and Smith, A. M.: The atmospheric cycling of radiomethane and the "fossil fraction" of the methane source, Atmospheric Chemistry and Physics, 7, 2141-2149, 2007b.

Le Quéré, C., Buitenhuis, E. T., Moriarty, R., Alvain, S., Aumont, O., Bopp, L., Chollet, S., Enright, C., Franklin, D. J., Geider, R. J., Harrison, S. P., Hirst, A. G., Larsen, S., Legendre, L., Platt, T., Prentice, I. C., Rivkin, R. B., Sailley, S., Sathyendranath, S., Stephens, N., Vogt, M., and Vallina, S. M.: Role of zooplankton dynamics for Southern Ocean phytoplankton biomass and global biogeochemical cycles, Biogeosciences, 13, 4111-4133, doi:10.5194/bg-13-4111-2016, 2016.

le Texier, H., Solomon, S., and Garcia, R. R.: The role of molecular hydrogen and methane oxidation in the water vapour budget of the stratosphere, Quarterly Journal of the Royal Meteorological Society, 114, 281-295, doi:10.1002/qj.49711448002, 1988.

Lehner, B., and Döll, P.: Development and validation of a global database of lakes, reservoirs and wetlands, Journal of Hydrology, 296, 1-22, doi:10.1016/j.jhydrol.2004.03.028, 2004.

Lelieveld, J., Crutzen, P. J., and Dentener, F. J.: Changing concentration, lifetime and climate forcing of atmospheric methane, Tellus Series B-Chemical and Physical Meteorology, 50, 128-150, doi:10.1034/j.1600-0889.1998.t01-1-00002.x, 1998.

Lelieveld, J., Peters, W., Dentener, F. J., and Krol, M. C.: Stability of tropospheric hydroxyl chemistry, Journal of Geophysical Research-Atmospheres, 107, 4715, doi:10.1029/2002jd002272, 2002.

Lelieveld, J., Dentener, F. J., Peters, W., and Krol, M. C.: On the role of hydroxyl radicals in the self-cleansing capacity of the troposphere, Atmospheric Chemistry and Physics, 4, 337-2344, 2004.

Lelieveld, J., Lechtenbohmer, S., Assonov, S. S., Brenninkmeijer, C. A. M., Dienst, C., Fischedick, M., and Hanke, T.: Greenhouse gases: Low methane leakage from gas pipelines, Nature, 434, 841-842, doi:10.1038/434841a, 2005.

https://doi.org/10.5194/essd-2019-128
Preprint. Discussion started: 19 August 2019

Lelieveld, J., Gromov, S., Pozzer, A., and Taraborrelli, D.: Global tropospheric hydroxyl distribution, budget and reactivity, Atmos. Chem. Phys., 16, 12477–12493, doi:10.5194/acp-16-12477-2016, 2016.

Lenhart, K., Klintzsch, T., Langer, G., Nehrke, G., Bunge, M., Schnell, S., and Keppler, F.: Evidence for methane production by the marine algae *Emiliania huxleyi*, Biogeosciences, 13, 3163-3174, https://doi.org/10.5194/bg-13-3163-2016, 2016.

Li, C., Frolking, S., Xiao, X., Moore, B., Boles, S., Qiu, J., Huang, Y., Salas, W., and Sass, R.: Modeling impacts of farming management alternatives on CO_2, CH_4, and N_2O emissions: A case study for water management of rice agriculture of China, Global Biogeochemical Cycles, 19, GB3010, doi:10.1029/2004gb002341, 2005.

Liang, Q., Chipperfield, M. P., Fleming, E. L., Abraham, N. L., Braesicke, P., Burkholder, J. B., Daniel, J. S., Dhomse, S., Fraser, P. J., Hardiman, S. C., Jackman, C. H., Kinnison, D. E., Krummel, P. B., Montzka, S. A., Morgenstern, O., McCulloch, A., Mühle, J., Newman, P. A., Orkin, V. L., Pitari, G., Prinn, R. G., Rigby, M., Rozanov, E., Stenke, A., Tummon, F., Velders, G. J. M., Visioni, D., and Weiss, R. F.: Deriving Global OH Abundance and Atmospheric Lifetimes for Long-Lived Gases: A Search for CH3CCl3 Alternatives, Journal of Geophysical Research: Atmospheres, 122, 11,914-911,933, doi:10.1002/2017JD026926, 2017.

Lin, X., Ciais, P., Bousquet, P., Ramonet, M., Yin, Y., Balkanski, Y., Cozic, A., Delmotte, M., Evangeliou, N., Indira, N. K., Locatelli, R., Peng, S., Piao, S., Saunois, M., Swathi, P. S., Wang, R., Yver-Kwok, C., Tiwari, Y. K., and Zhou, L.: Simulating CH_4 and CO_2 over South and East Asia using the zoomed chemistry transport model LMDz-INCA, Atmos. Chem. Phys., 18, 9475-9497, doi:10.5194/acp-18-9475-2018, 2018.

Lin, X., Indira, N. K., Ramonet, M., Delmotte, M., Ciais, P., Bhatt, B. C., Reddy, M. V., Angchuk, D., Balakrishnan, S., Jorphail, S., Dorjai, T., Mahey, T. T., Patnaik, S., Begum, M., Brenninkmeijer, C., Durairaj, S., Kirubagaran, R., Schmidt, M., Swathi, P. S., Vinithkumar, N. V., Yver Kwok, C., and Gaur, V. K.: Long-lived atmospheric trace gases measurements in flask samples from three stations in India, Atmospheric Chemistry and Physics, 15, 9819-9849, doi:10.5194/acp-15-9819-2015, 2015.

Liu, J., Chen, H., Zhu, Q., Shen, Y., Wang, X., Wang, M., and Peng, C.: A novel pathway of direct methane production and emission by eukaryotes including plants, animals and fungi: An overview, Atmospheric Environment, 115, 26-35, https://doi.org/10.1016/j.atmosenv.2015.05.019, 2015.

Locatelli, R., Bousquet, P., Saunois, M., Chevallier, F., and Cressot, C.: Sensitivity of the recent methane budget to LMDz sub-grid-scale physical parameterizations, Atmospheric Chemistry and Physics, 15, 9765-9780, doi:10.5194/acp-15-9765-2015, 2015.

Lohila, A., Aalto, T., Aurela, M., Hatakka, J., Tuovinen, J.-P., Kilkki, J., Penttilä, T., Vuorenmaa, J., Hänninen, P., Sutinen, R., Viisanen, Y., and Laurila, T.: Large contribution of boreal upland forest

https://doi.org/10.5194/essd-2019-128
Preprint. Discussion started: 19 August 2019

soils to a catchment-scale CH_4 balance in a wet year, Geophysical Research Letters, 43, 2946-2953, doi:10.1002/2016gl067718, 2016.

Maasakkers, J. D., Jacob, D. J., Sulprizio, M. P., Scarpelli, T. R., Nesser, H., Sheng, J. X., Zhang, Y., Hersher, M., Bloom, A. A., Bowman, K. W., Worden, J. R., Janssens-Maenhout, G., and Parker, R. J.: Global distribution of methane emissions, emission trends, and OH concentrations and trends inferred from an inversion of GOSAT satellite data for 2010–2015, Atmos. Chem. Phys., 19, 7859-7881, doi:10.5194/acp-19-7859-2019, 2019.

Maavara, T., Lauerwald, R., Laruelle, G. G., Akbarzadeh, Z., Bouskill, N. J., Van Cappellen, P., and Regnier, P.: Nitrous oxide emissions from inland waters: Are IPCC estimates too high?, Global Change Biology, 25, 473-488, doi:10.1111/gcb.14504, 2019.

Maksyutov, S., Oda, T., Saito, M., Janardanan, R., Belikov, D., Kaiser, J. W., Zhuravlev, R., Ganshin, A., and Valsala, V.: Technical note: High resolution inverse modelling technique for estimating surface CO_2 fluxes based on coupled NIES-TM - Flexpart transport model and its adjoint, Atmos. Chem. Phys. Discuss., in prep., 2019.

Matthews, E., and Fung, I.: Methane emission from natural wetlands: Global distribution, area, and environmental characteristics of sources, Global Biogeochemical Cycles, 1, 61-86, doi:10.1029/GB001i001p00061, 1987.

McCalley, C. K., Woodcroft, B. J., Hodgkins, S. B., Wehr, R. A., Kim, E.-H., Mondav, R., Crill, P. M., Chanton, J. P., Rich, V. I., Tyson, G. W., and Saleska, S. R.: Methane dynamics regulated by microbial community response to permafrost thaw, Nature, 514, 478-481, doi:10.1038/nature13798, 2014.

McCarthy, M., Boering, K. A., Rice, A. L., Tyler, S., Connell, P., and Atlas, E.: Carbon and hydrogen isotopic compositions of stratospheric methane: 2. Two-dimensional model results and implications for kinetic isotope effects, Journal of Geophysical Research: Atmospheres, 108, doi:10.1029/2002JD003183, 2003.

McGinnis, D. F., Kirillin, G., Tang, K. W., Flury, S., Bodmer, P., Engelhardt, C., Casper, P., and Grossart, H.-P.: Enhancing Surface Methane Fluxes from an Oligotrophic Lake: Exploring the Microbubble Hypothesis, Environmental Science and Technology, 49, 873-880, doi:10.1021/es503385d, 2015.

McGinnis, D., Greinert, J., Artemov, Y., Beaubien, S. E., and Wuest, A.: Fate of rising methane bubbles in stratified waters: How much methane reaches the atmosphere?, Journal of Geophysical Research: Atmospheres, 111, doi:10.1029/2005JC003183, 2006.

McGuire, A. D., Christensen, T. R., Hayes, D., Heroult, A., Euskirchen, E., Kimball, J. S., Koven, C., Lafleur, P., Miller, P. A., Oechel, W., Peylin, P., Williams, M., and Yi, Y.: An assessment of the

https://doi.org/10.5194/essd-2019-128
Preprint. Discussion started: 19 August 2019

carbon balance of Arctic tundra: comparisons among observations, process models, and atmospheric inversions, Biogeosciences, 9, 3185-3204, doi:10.5194/bg-9-3185- 2012, 2012.

McKain, K., Down, A., Raciti, S. M., Budney, J., Hutyra, L. R., Floerchinger, C., Herndon, S. C., Nehrkorn, T., Zahniser, M. S., Jackson, R. B., Phillips, N., and Wofsy, S. C.: Methane emissions from natural gas infrastructure and use in the urban region of Boston, Massachusetts, Proceedings of the National Academy of Sciences, 112, 1941-1946, doi:10.1073/pnas.1416261112, 2015.

McLeod, E., Chmura, G. L., Bouillon, S., Salm, R., Björk, M., Duarte, C. M., Lovelock, C. E., Schlesinger, W. H., and Silliman, B. R.: A blueprint for blue carbon: toward an improved understanding of the role of vegetated coastal habitats in sequestering CO_2, Frontiers in Ecology and the Environment, 9, 552-560, doi:10.1890/110004, 2011.

McNorton, J., Chipperfield, M. P., Gloor, M., Wilson, C., Feng, W., Hayman, G. D., Rigby, M., Krummel, P. B., O'Doherty, S., Prinn, R. G., Weiss, R. F., Young, D., Dlugokencky, E., and Montzka, S. A.: Role of OH variability in the stalling of the global atmospheric CH_4 growth rate from 1999 to 2006, Atmospheric Chemistry and Physics Discussion, 2016, 1-24, doi:10.5194/acp-2015-1029, 2016.

McNorton, J., Wilson, C., Gloor, M., Parker, R. J., Boesch, H., Feng, W., Hossaini, R., and Chipperfield, M. P.: Attribution of recent increases in atmospheric methane through 3-D inverse modelling, Atmos. Chem. Phys., 18, 18149-18168, https://doi.org/10.5194/acp-18-18149-2018, 2018.

Melton, J. R., and Arora, V. K.: Competition between plant functional types in the Canadian Terrestrial Ecosystem Model (CTEM) v. 2.0, Geoscientific Model Development, 9, 323-361, doi:10.5194/gmd-9-323-2016, 2016.

Melton, J. R., Wania, R., Hodson, E. L., Poulter, B., Ringeval, B., Spahni, R., Bohn, T., Avis, C. A., Beerling, D. J., Chen, G., Eliseev, A. V., Denisov, S. N., Hopcroft, P. O., Lettenmaier, D. P., Riley, W. J., Singarayer, J. S., Subin, Z. M., Tian, H., Zürcher, S., Brovkin, V., van Bodegom, P. M., Kleinen, T., Yu, Z. C., and Kaplan, J. O.: Present state of global wetland extent and wetland methane modelling: conclusions from a model intercomparison project (WETCHIMP), Biogeosciences, 10, 753-788, doi:10.5194/bg-10-753-2013, 2013.

Membrive, O., Crevoisier, C., Sweeney, C., Danis, F., Hertzog, A., Engel, A., Bönisch, H., and Picon, L.: AirCore-HR: a high-resolution column sampling to enhance the vertical description of CH_4 and CO_2, Atmos. Meas. Tech., 10, 2163-2181, doi:10.5194/amt-10-2163-2017, 2017.

Mercado, L. M., Bellouin, N., Sitch, S., Boucher, O., Huntingford, C., Wild, M., and Cox, P. M.: Impact of changes in diffuse radiation on the global land carbon sink, Nature, 458, 1014, doi:10.1038/nature07949, 2009.

https://doi.org/10.5194/essd-2019-128
Preprint. Discussion started: 19 August 2019

Messager, M. L., Lehner, B., Grill, G., Nedeva, I., and Schmitt, O.: Estimating the volume and age of water stored in global lakes using a geo-statistical approach, Nature Communications, 7, 13603, doi:10.1038/ncomms13603, 2016.

Middelburg, J.J., Nieuwenhuize, J., Iversen, N., Høgh, N., de Wilde, H., Helder, W., Seifert, R., Christof, O. Methane distribution in tidal estuaries, Biogeochemistry 59, 95–119, 2002.

Mijling, B., van der A, R. J., and Zhang, Q.: Regional nitrogen oxides emission trends in East Asia observed from space, Atmos. Chem. Phys., 13, 12003-12012, doi:10.5194/acp-13-12003-2013, 2013.

Mikaloff Fletcher, S. E. M., Tans, P. P., Bruhwiler, L. M., Miller, J. B., and Heimann, M.: CH_4 sources estimated from atmospheric observations of CH_4 and its $^{13}C/^{12}C$ isotopic ratios: 1. Inverse modeling of source processes, Global Biogeochemical Cycles, 18, GB4004, doi:10.1029/2004GB002223, 2004.

Milkov, A. V.: Molecular and stable isotope compositions of natural gas hydrates: A revised global dataset and basic interpretations in the context of geological settings, Organic Geochemistry, 36, 681-702, 2005.

Miller, L. G., Sasson, C., and Oremland, R. S.: Difluoromethane, a new and improved inhibitor of methanotrophy, Applied and Environmental Microbiology, 64, 4357–4362, 1998.

Miller, S. M., Wofsy, S. C., Michalak, A. M., Kort, E. A., Andrews, A. E., Biraud, S. C., Dlugokencky, E. J., Eluszkiewicz, J., Fischer, M. L., Janssens-Maenhout, G., Miller, B. R., Miller, J. B., Montzka, S. A., Nehrkorn, T., and Sweeney, C.: Anthropogenic emissions of methane in the United States, Proceedings of the National Academy of Sciences of the United States of America, 110, 20,018-020,022, doi:10.1073/pnas.1314392110, 2013.

Minkkinen, K., and Laine, J.: Vegetation heterogeneity and ditches create spatial variability in methane fluxes from peatlands drained for forestry, Plant and Soil, 285, 289-304, doi:10.1007/s11104-006-9016-4, 2006.

Monteil, G., Houweling, S., Butz, A., Guerlet, S., Schepers, D., Hasekamp, O., Frankenberg, C., Scheepmaker, R., Aben, I., and Röckmann, T.: Comparison of CH_4 inversions based on 15 months of GOSAT and SCIAMACHY observations, J Geophys Res-Atmos, 118, 11,807-811,823, doi:10.1002/2013jd019760, 2013.

Monteil, G., Houweling, S., Dlugockenky, E. J., Maenhout, G., Vaughn, B. H., White, J. W. C., and Rockmann, T.: Interpreting methane variations in the past two decades using measurements of CH_4 mixing ratio and isotopic composition, Atmospheric Chemistry and Physics, 11, 9141-9153, doi:10.5194/acp-11-9141-2011, 2011.

Montzka, S. A., and Fraser, P. J.: Controlled Substances and Other Source Gases, Genewa, Switzerland, 1.1-1.83, World Meterological Organization, 2003.

https://doi.org/10.5194/essd-2019-128
Preprint. Discussion started: 19 August 2019

Montzka, S. A., Krol, M., Dlugokencky, E., Hall, B., Jockel, P., and Lelieveld, J.: Small Interannual Variability of Global Atmospheric Hydroxyl, Science, 331, 67-69, 2011.

Moore, C. W., Zielinska, B., Pétron, G., and Jackson, R. B.: Air impacts of increased natural gas acquisition, processing, and use: a critical review, Environmental Science and Technology 48, 8349–8359, doi:10.1021/es4053472, 2014.

Morgenstern, O., Hegglin, M. I., Rozanov, E., O'Connor, F. M., Abraham, N. L., Akiyoshi, H., Archibald, A. T., Bekki, S., Butchart, N., Chipperfield, M. P., Deushi, M., Dhomse, S. S., Garcia, R. R., Hardiman, S. C., Horowitz, L. W., Jöckel, P., Josse, B., Kinnison, D., Lin, M., Mancini, E., Manyin, M. E., Marchand, M., Marécal, V., Michou, M., Oman, L. D., Pitari, G., Plummer, D. A., Revell, L. E., Saint-Martin, D., Schofield, R., Stenke, A., Stone, K., Sudo, K., Tanaka, T. Y., Tilmes, S., Yamashita, Y., Yoshida, K., and Zeng, G.: Review of the global models used within phase 1 of the Chemistry–Climate Model Initiative (CCMI), Geosci. Model Dev., 10, 639-671, doi:10.5194/gmd-10-639-2017, 2017.

Morgenstern, O., Stone, K. A., Schofield, R., Akiyoshi, H., Yamashita, Y., Kinnison, D. E., Garcia, R. R., Sudo, K., Plummer, D. A., Scinocca, J., Oman, L. D., Manyin, M. E., Zeng, G., Rozanov, E., Stenke, A., Revell, L. E., Pitari, G., Mancini, E., Di Genova, G., Visioni, D., Dhomse, S. S., and Chipperfield, M. P.: Ozone sensitivity to varying greenhouse gases and ozone-depleting substances in CCMI-1 simulations, Atmos. Chem. Phys., 18, 1091-1114, doi:10.5194/acp-18-1091-2018, 2018.

Morino, I., Uchino, O., Inoue, M., Yoshida, Y., Yokota, T., Wennberg, P. O., Toon, G. C., Wunch, D., Roehl, C. M., Notholt, J., Warneke, T., Messerschmidt, J., Griffith, D. W. T., Deutscher, N. M., Sherlock, V., Connor, B., Robinson, J., Sussmann, R., and Rettinger, M.: Preliminary validation of column-averaged volume mixing ratios of carbon dioxide and methane retrieved from GOSAT short-wavelength infrared spectra, Atmos. Meas. Tech., 4, 1061-1076, doi:10.5194/amt-4-1061-2011, 2011.

Murguia-Flores, F., Arndt, S., Ganesan, A. L., Murray-Tortarolo, G., and Hornibrook, E. R. C.: Soil Methanotrophy Model (MeMo v1.0): a process-based model to quantify global uptake of atmospheric methane by soil, Geosci. Model Dev., 11, 2009-2032, doi:10.5194/gmd-11-2009-2018, 2018.

Myhre, G., Shindell, D., Bréon, F.-M., Collins, W., Fuglestvedt, J., Huang, J., Koch, D., Lamarque, J.-F., Lee, D., Mendoza, B., Nakajima, T., Robock, A., Stephens, G., Takemura, T., and Zhang, H.: Anthropogenic and Natural Radiative Forcing., in: In Climate Change 2013: The Physical Science Basis. Contribution of Working Group I to the Fifth Assessment Report of the Intergovernmental Panel on Climate Change, edited by: Stocker, T. F., D. Qin, D., Plattner, G.-K., Tignor, M., Allen, S. K., Boschung, J., Nauels, A., Xia, Y., Bex, V., and Midgley, P. M., Cambridge University Press, Cambridge, United Kingdom and New York, NY, USA, 2013.

https://doi.org/10.5194/essd-2019-128
Preprint. Discussion started: 19 August 2019

Naik, V., Voulgarakis, A., Fiore, A. M., Horowitz, L. W., Lamarque, J. F., Lin, M., Prather, M. J., Young, P. J., Bergmann, D., Cameron-Smith, P. J., Cionni, I., Collins, W. J., Dals√∏ren, S. B., Doherty, R., Eyring, V., Faluvegi, G., Folberth, G. A., Josse, B., Lee, Y. H., MacKenzie, I. A., Nagashima, T., van Noije, T. P. C., Plummer, D. A., Righi, M., Rumbold, S. T., Skeie, R., Shindell, D. T., Stevenson, D. S., Strode, S., Sudo, K., Szopa, S., and Zeng, G.: Preindustrial to present day changes in tropospheric hydroxyl radical and methane lifetime from the Atmospheric Chemistry and Climate Model Intercomparison Project (ACCMIP), Atmospheric Chemistry and Physics, 13, 5277-5298, doi:10.5194/acp-13-5277-2013, 2013.

Natchimuthu, S., Sundgren, I., Gålfalk, M., Klemedtsson, L., Crill, P., Danielsson, Å., and Bastviken, D.: Spatio-temporal variability of lake CH_4 fluxes and its influence on annual whole lake emission estimates, Limnology and Oceanography, 61, S13-S26, doi:10.1002/lno.10222, 2015.

Natchimuthu, S., Wallin, M. B., Klemedtsson, L., and Bastviken, D.: Spatio-temporal patterns of stream methane and carbon dioxide emissions in a hemiboreal catchment in Southwest Sweden, Scientific Reports, 7, 39729, doi:10.1038/srep39729, 2017.

Nellemann, C., Corcoran, E., Duarte, C., Valdes, L., De Young, C., Fonseca, L., and Grimsditch, G.: Blue Carbon - The Role of Healthy Oceans in Binding Carbon, GRID-Arendal, UNEP report, isbn:978-82-7701-060-1, 79, Available at : https://ccom.unh.edu/sites/default/files/publications/Nellemann_2010_BlueCarbon_book.pdf, 2009.

Nicely, J. M., Salawitch, R. J., Canty, T., Anderson, D. C., Arnold, S. R., Chipperfield, M. P., Emmons, L. K., Flemming, J., Huijnen, V., Kinnison, D. E., Lamarque, J.-F., Mao, J., Monks, S. A., Steenrod, S. D., Tilmes, S., and Turquety, S.: Quantifying the causes of differences in tropospheric OH within global models, Journal of Geophysical Research: Atmospheres, 122, 1983-2007, doi:10.1002/2016JD026239, 2017.

Nicewonger, M. R., Verhulst, K. R., Aydin, M., and Saltzman, E. S.: Preindustrial atmospheric ethane levels inferred from polar ice cores: A constraint on the geologic sources of atmospheric ethane and methane, Geophysical Research Letters, 43, 214-221, doi:10.1002/2015GL066854, 2016.

Nisbet, E. G., Fisher, R., Nimmo, R. H., Bendall, D. S., Crill, P. M., Gallego-Sala, A. V., Hornibrook, E. R. C., Lopez-Juez, E., Lowry, D., Nisbet, P. B. R., Shuckburgh, E. F., Sriskantharajah, S., Howe, C. J., and Nisbet, E. G.: Emission of methane from plants, Proceedings of the Royal Society B-Biological Sciences, 276, 1347-1354, 2009.

Nisbet, E. G., Dlugokencky, E. J., Manning, M. R., Lowry, D., Fisher, R. E., France, J. L., Michel, S. E., Miller, J. B., White, J. W. C., Vaughn, B., Bousquet, P., Pyle, J. A., Warwick, N. J., Cain, M., Brownlow, R., Zazzeri, G., Lanoisellï¿½, M., Manning, A. C., Gloor, E., Worthy, D. E. J., Brunke, E. G., Labuschagne, C., Wolff, E. W., and Ganesan, A. L.: Rising atmospheric methane: 2007–2014

https://doi.org/10.5194/essd-2019-128
Preprint. Discussion started: 19 August 2019

growth and isotopic shift, Global Biogeochemical Cycles, 30, 1356-1370, doi:10.1002/2016GB005406, 2016.

Nisbet, E. G., Manning, M. R., Dlugokencky, E. J., Fisher, R. E., Lowry, D., Michel, S. E., Myhre, C. L., Platt, S. M., Allen, G., Bousquet, P., Brownlow, R., Cain, M., France, J. L., Hermansen, O., Hossaini, R., Jones, A. E., Levin, I., Manning, A. C., Myhre, G., Pyle, J. A., Vaughn, B., Warwick, N. J., and White, J. W. C.: Very strong atmospheric methane growth in the four years 2014-2017: Implications for the Paris Agreement, Global Biogeochemical Cycles, 33, 318-342, doi:10.1029/2018GB006009, 2019.

Niwa, Y., Tomita, H., Satoh, M., Imasu, R., Sawa, Y., Tsuboi, K., Matsueda, H., Machida, T., Sasakawa, M., Belan, B., and Saigusa, N.: A 4D-Var inversion system based on the icosahedral grid model (NICAM-TM 4D-Var v1.0) – Part 1: Offline forward and adjoint transport models, Geosci. Model Dev., 10, 1157-1174, https://doi.org/10.5194/gmd-10-1157-2017, 2017a.

Niwa, Y., Fujii, Y., Sawa, Y., Iida, Y., Ito, A., Satoh, M., Imasu, R., Tsuboi, K., Matsueda, H., and Saigusa, N.: A 4D-Var inversion system based on the icosahedral grid model (NICAM-TM 4D-Var v1.0) – Part 2: Optimization scheme and identical twin experiment of atmospheric CO_2 inversion, Geosci. Model Dev., 10, 2201-2219, https://doi.org/10.5194/gmd-10-2201-2017, 2017b.

Noël, S., Weigel, K., Bramstedt, K., Rozanov, A., Weber, M., Bovensmann, H., and Burrows, J. P.: Water vapour and methane coupling in the stratosphere observed using SCIAMACHY solar occultation measurements, Atmos. Chem. Phys., 18, 4463-4476, doi:10.5194/acp-18-4463-2018, 2018.

Obu, J., Westermann, S., Bartsch, A., Berdnikov, N., Christiansen, H., Avirmed, D., Delaloye, R., Elberling, B., Etzelmüller, B., Kholodov, A., Khomutov, A., Kääb, A., Leibman, M., Lewkowicz, A., K. Panda, S., Romanovsky, V., Way, R., Westergaard-Nielsen, A., Wu, T., and Zou, D.: Northern Hemisphere permafrost map based on TTOP modelling for 2000–2016 at 1 km2 scale, Earth-Science Reviews, 193, doi:10.1016/j.earscirev.2019.04.023, 2019.

Olivier, J. G. J., and Janssens-Maenhout, G.: CO_2 Emissions from Fuel Combustion - 2012 Edition, IEA CO_2 report 2012, Part III, Greenhouse Gas Emissions, available at: http://edgar.jrc.ec.europa.eu (last access: 10 November 2016), ISBN 978-92-64-17475-7, 2012.

Olivier, J. G. J., and Janssens-Maenhout, G.: Part III: Total Greenhouse Gas Emissions, of CO_2 Emissions from Fuel Combustion (2014 ed.), International Energy Agency, Paris, ISBN-978-92-64-21709-6, 2014.

Ollivier, Q. R., Maher, D. T., Pitfield, C., and Macreadie, P. I.: Punching above their weight: Large release of greenhouse gases from small agricultural dams, Global Change Biology, 25, 721-732, doi:10.1111/gcb.14477, 2019.

https://doi.org/10.5194/essd-2019-128
Preprint. Discussion started: 19 August 2019

Osudar R, Matousu A, Alawi M, Wagner D, Bussmann I. Environmental factors affecting methane distribution and bacterial methane oxidation in the German Bight (North Sea). Estuar Coast Shelf Sci. doi:10.1016/j.ecss.2015.03.028, 2015.

Overduin, P. P., Liebner, S., Knoblauch, C., Günther, F., Wetterich, S., Schirrmeister, L., Hubberten, H.-W., and Grigoriev, M. N.: Methane oxidation following submarine permafrost degradation: Measurements from a central Laptev Sea shelf borehole, Journal of Geophysical Research - Biogeosciences, 120, 965-978, doi:10.1002/2014jg002862, 2015.

Pacala, S. W., Breidenich, C., Brewer, P. G., Fung, I., Gunson, M. R., Heddle, G., Law, B., Marland, G., Paustian, K., Prather, M., Randerson, J., T., Tans, P., and Wofsy, S. C.: Verifying Greenhouse Gas Emissions: Methods to Support International Climate Agreements, National Academies Press, edited by: N. R. Council, 124 pp., doi:10.17226/12883, 2010.

Page, S., Morrison, R., Mailins, C., Hooijer, A., Rieley, J., and Jauhiainen, J.: Review of Peat Surface Greenhouse Gas Emissions from Oil Palm Plantations in Southeast Asia, , https://www.theicct.org/sites/default/files/publications/ICCT_Peat-Emissions_Sept2011.pdf, 1-77 pp., 2011.

Pandey, S., Houweling, S., Krol, M., Aben, I., Chevallier, F., Dlugokencky, E. J., Gatti, L. V., Gloor, M., Miller, J. B., Detmers, R., Machida, T., and Röckmann, T.: Inverse modeling of GOSAT-retrieved ratios of total column CH_4 and CO_2 for 2009 and 2010, Atmos. Chem. Phys., 16, 5043–5062, doi:10.5194/acp-16-5043-2016, 2016.

Pandey, S., Houweling, S., Krol, M., Aben, I., Monteil, G., Nechita-Banda, N., Dlugokencky, E. J., Detmers, R., Hasekamp, O., Xu, X., Riley, W. J., Poulter, B., Zhang, Z., McDonald, K. C., White, J. W. C., Bousquet, P., and Röckmann, T.: Enhanced methane emissions from tropical wetlands during the 2011 La Niña, Scientific Reports, 7, 45759, doi:10.1038/srep45759, 2017.

Pangala, S. R., Enrich-Prast, A., Basso, L. S., Peixoto, R. B., Bastviken, D., Hornibrook, E. R. C., Gatti, L. V., Marotta, H., Calazans, L. S. B., Sakuragui, C. M., Bastos, W. R., Malm, O., Gloor, E., Miller, J. B., and Gauci, V.: Large emissions from floodplain trees close the Amazon methane budget, Nature, 552, 230, doi:10.1038/nature24639, 2017.

Pangala, S. R., Hornibrook, E. R. C., Gowing, D. J., and Gauci, V.: The contribution of trees to ecosystem methane emissions in a temperate forested wetland, Global Change Biology, 21, 2642-2654, doi:10.1111/gcb.12891, 2015.

Pangala, S. R., Moore, S., Hornibrook, E. R. C., and Gauci, V.: Trees are major conduits for methane egress from tropical forested wetlands, New Phytologist, 197, 524-531, doi:10.1111/nph.12031, 2013.

Paris, J.-D., Ciais, P., Nedelec, P., Stohl, A., Belan, B. D., Arshinov, M. Y., Carouge, C., Golitsyn, G. S., and Granberg, I. G.: New insights on the chemical composition of the Siberian air shed from the YAK

https://doi.org/10.5194/essd-2019-128
Preprint. Discussion started: 19 August 2019

AEROSIB aircraft campaigns, Bulletin of the American Meteorological Society, 91, 625-641, doi:10.1175/2009BAMS2663.1., 2010.

Parker, R., Boesch, H., Cogan, A., Fraser, A., Feng, L., Palmer, P. I., Messerschmidt, J., Deutscher, N., Griffith, D. W. T., Notholt, J., Wennberg, P. O., and Wunch, D.: Methane observations from the Greenhouse Gases Observing SATellite: Comparison to ground-based TCCON data and model calculations, Geophysical Research Letters, 38, L15807, doi:10.1029/2011gl047871, 2011.

Pathak, H., Li, C., and Wassmann, R.: Greenhouse gas emissions from Indian rice fields: calibration and upscaling using the DNDC model, Biogeosciences, 1, 1-11, 2005.

Patra, P. K., Houweling, S., Krol, M., Bousquet, P., Belikov, D., Bergmann, D., Bian, H., Cameron-Smith, P., Chipperfield, M. P., Corbin, K., Fortems-Cheiney, A., Fraser, A., Gloor, E., Hess, P., Ito, A., Kawa, S. R., Law, R. M., Loh, Z., Maksyutov, S., Meng, L., Palmer, P. I., Prinn, R. G., Rigby, M., Saito, R., and Wilson, C.: TransCom model simulations of CH_4 and related species: linking transport, surface flux and chemical loss with CH_4 variability in the troposphere and lower stratosphere, Atmospheric Chemistry and Physics, 11, 12,813-812,837, doi:10.5194/acp-11-12813-2011, 2011.

Patra, P. K., Canadell, J. G., Houghton, R. A., Piao, S. L., Oh, N. H., Ciais, P., Manjunath, K. R., Chhabra, A., Wang, T., Bhattacharya, T., Bousquet, P., Hartman, J., Ito, A., Mayorga, E., Niwa, Y., Raymond, P. A., Sarma, V. V. S. S., and Lasco, R.: The carbon budget of South Asia, Biogeosciences, 10, 513-527, doi:10.5194/bg-10-513-2013, 2013.

Patra, P. K., Krol, M. C. , Montzka, S. A., Arnold, T. , Atlas, E. L., Lintner, B. R. , Stephens, B. B., Xiang, B., Elkins, J. W. , Fraser, P. J., Ghosh, A., Hintsa, E. J., Hurst, D. F., Ishijima, K., Krummel, P. B., Miller, B. R., Miyazaki, K., Moore, F. L., Mühle, J., O'Doherty, S., Prinn, R. G., Steele, L. P., Takigawa, M., Wang, H. J., Weiss, R. F., Wofsy, S. C., Young, D.: Observational evidence for interhemispheric hydroxyl parity, Nature, 513, 219-223, 2014.

Patra, P. K., Saeki, T., Dlugokencky, E. J., Ishijima, K., Umezawa, T., Ito, A., Aoki, S., Morimoto, S., Kort, E. A., Crotwell, A., Ravikumar, K., and Nakazawa, T.: Regional methane emission estimation based on observed atmospheric concentrations (2002-2012), J. Meteorol. Soc. Jpn., 94, 91-113, 2016.

Patra, P. K., Takigawa, M., Watanabe, S., Chandra, N., Ishijima, K. and Yamashita, Y.: Improved Chemical Tracer Simulation by MIROC4.0-based Atmospheric Chemistry-Transport Model (MIROC4-ACTM), SOLA, 14, 91–96, doi:10.2151/sola.2018-016, 2018.

Paull, C. K., Brewer, P. G., Ussler, W., Peltzer, E. T., Rehder, G., and Clague, D.: An experiment demonstrating that marine slumping is a mechanism to transfer methane from seafloor gas-hydrate deposits into the upper ocean and atmosphere, Geo-Marine Letters, 22, 198-203, doi:10.1007/s00367-002-0113-y, 2002.

https://doi.org/10.5194/essd-2019-128
Preprint. Discussion started: 19 August 2019

Pechony, O., Shindell, D. T., and Faluvegi, G.: Direct top-down estimates of biomass burning CO emissions using TES and MOPITT versus bottom-up GFED inventory, Journal of Geophysical Research: Atmospheres, 118, 8054-8066, doi:10.1002/jgrd.50624, 2013.

Peischl, J., Ryerson, T. B., Aikin, K. C., de Gouw, J. A., Gilman, J. B., Holloway, J. S., Lerner, B. M., Nadkarni, R., Neuman, J. A., Nowak, J. B., Trainer, M., Warneke, C., and Parrish, D. D.: Quantifying atmospheric methane emissions from the Haynesville, Fayetteville, and northeastern Marcellus shale gas production regions, Journal of Geophysical Research: Atmospheres, 120, 2119-2139, doi:10.1002/2014jd022697, 2015.

Pekel, J.-F., Cottam, A., Gorelick, N., and Belward, A. S.: High-resolution mapping of global surface water and its long-term changes, Nature, 540, 418, doi:10.1038/nature20584, 2016.

Peng, S. S., Piao, S. L., Bousquet, P., Ciais, P., Li, B. G., Lin, X., Tao, S., Wang, Z. P., Zhang, Y., and Zhou, F.: Inventory of anthropogenic methane emissions in Mainland China from 1980 to 2010, Atmospheric Chemistry and Physics, 16, 14545-14562,doi:10.5194/acp-16-14545-2016, 2016.

Pérez-Barbería, F. J.: Scaling methane emissions in ruminants and global estimates in wild populations, Science of The Total Environment, 579, 1572-1580, https://doi.org/10.1016/j.scitotenv.2016.11.175, 2017.

Peters, W., Jacobson, A. R., Sweeney, C., Andrews, A. E., Conway, T. J., Masarie, K., Miller, J. B., Bruhwiler, L. M. P., Pétron, G., Hirsch, A. I., Worthy, D. E. J., van der Werf, G. R., Randerson, J. T., Wennberg, P. O., Krol, M. C., and Tans, P. P.: An atmospheric perspective on North American carbon dioxide exchange: CarbonTracker, Proceedings of the National Academy of Sciences of the United States of America, 104, 18925-18930, doi:10.1073/pnas.0708986104, 2007.

Petrenko, V. V., Smith, A. M., Schaefer, H., Riedel, K., Brook, E., Baggenstos, D., Harth, C., Hua, Q., Buizert, C., Schilt, A., Fain, X., Mitchell, L., Bauska, T., Orsi, A., Weiss, R. F., and Severinghaus, J. P.: Minimal geological methane emissions during the Younger Dryas–Preboreal abrupt warming event, Nature, 548, 443, doi:10.1038/nature23316, 2017.

Pétron, G., Karion, A., Sweeney, C., Miller, B. R., Montzka, S. A., Frost, G. J., Trainer, M., Tans, P., Andrews, A., Kofler, J., Helmig, D., Guenther, D., Dlugokencky, E., Lang, P., Newberger, T., Wolter, S., Hall, B., Novelli, P., Brewer, A., Conley, S., Hardesty, M., Banta, R., White, A., Noone, D., Wolfe, D., and Schnell, R.: A new look at methane and nonmethane hydrocarbon emissions from oil and natural gas operations in the Colorado Denver-Julesburg Basin, Journal of Geophysical Research: Atmospheres, 119, 6836-6852, doi:10.1002/2013jd021272, 2014.

Pison, I., Ringeval, B., Bousquet, P., Prigent, C., and Papa, F.: Stable atmospheric methane in the 2000s: key-role of emissions from natural wetlands, Atmos. Chem. Phys., 13, 11609–11623, doi:10.5194/acp-13-11609-2013, 2013.

https://doi.org/10.5194/essd-2019-128
Preprint. Discussion started: 19 August 2019

Pitz, S., and Megonigal, J. P.: Temperate forest methane sink diminished by tree emissions, New Phytologist, 214, 1432-1439, doi:10.1111/nph.14559, 2017.

Platt, U., Allan, W., and Lowe, D.: Hemispheric average Cl atom concentration from $^{13}C/^{12}C$ ratios in atmospheric methane, Atmos. Chem. Phys., 4, 2393-2399, doi:10.5194/acp-4-2393-2004, 2004.

Portmann, R. W., Daniel, J. S., and Ravishankara, A. R.: Stratospheric ozone depletion due to nitrous oxide: influences of other gases, Philosophical Transactions of the Royal Society of London B: Biological Sciences, 367, 1256-1264, doi:10.1098/rstb.2011.0377, 2012.

Poulter, B., Bousquet, P., Canadell, J. G., Ciais, P., Peregon, A., Saunois, M., Arora, V. K., Beerling, D. J., Brovkin, V., Jones, C. D., Joos, F., Gedney, N., Ito, A., Kleinen, T., Koven, C. D., McDonald, K., Melton, J. R., Peng, C. H., Peng, S. S., Prigent, C., Schroeder, R., Riley, W. J., Saito, M., Spahni, R., Tian, H. Q., Taylor, L., Viovy, N., Wilton, D., Wiltshire, A., Xu, X. Y., Zhang, B. W., Zhang, Z., and Zhu, Q. A.: Global wetland contribution to 2000-2012 atmospheric methane growth rate dynamics, Environmental Research Letters, 12, 10.1088/1748-9326/aa8391, 2017.

Poulter et al., in prep., 2019

Prather, M. J., Holmes, C. D., and Hsu, J.: Reactive greenhouse gas scenarios: Systematic exploration of uncertainties and the role of atmospheric chemistry, Geophysical Research Letters, 39, L09803, doi:10.1029/2012gl051440, 2012.

Prinn, R. G., Weiss, R. F., Fraser, P. J., Simmonds, P. G., Cunnold, D. M., Alyea, F. N., O'Doherty, S., Salameh, P., Miller, B. R., Huang, J., Wang, R. H. J., Hartley, D. E., Harth, C., Steele, L. P., Sturrock, G., Midgley, P. M., and McCulloch, A.: A history of chemically and radiatively important gases in air deduced from ALE/GAGE/AGAGE, Journal of Geophysical Research-Atmospheres, 105, 17,751-17,792, 2000.

Prinn, R. G., Huang, J., Weiss, R. F., Cunnold, D. M., Fraser, P. J., Simmonds, P. G., McCulloch, A., Harth, C., Salameh, P., O'Doherty, S., Wang, R. H. J., Porter, L., and Miller, B. R.: Evidence for Substantial Variations of Atmospheric Hydroxyl Radicals in the Past Two Decades, Science, doi:10.1126/science.1058673, 2001.

Prinn, R. G., Huang, J., Weiss, R. F., Cunnold, D. M., Fraser, P. J., Simmonds, P. G., McCulloch, A., Harth, C., Reimann, S., Salameh, P., O'Doherty, S., Wang, R. H. J., Porter, L. W., Miller, B. R., and Krummel, P. B.: Evidence for variability of atmospheric hydroxyl radicals over the past quarter century, Geophysical Research Letters, 32, L07809, doi:07810.01029/02004GL022228, 2005.

Prinn, R. G., R. F. Weiss, J. Arduini, T. Arnold, H. L. DeWitt, P. J. Fraser, A. L. Ganesan, J. Gasore, C. M. Harth, O. Hermansen, J. Kim, P. B. Krummel, S. Li, Z. M. Loh, C. R. Lunder, M. Maione, A. J. Manning, B. R. Miller, B. Mitrevski, J. Mühle, S. O'Doherty, S. Park, S. Reimann, M. Rigby, T. Saito, P. K. Salameh, R. Schmidt,P. G. Simmonds, L. P. Steele, M. K. Vollmer, R. H. Wang, B. Yao,

https://doi.org/10.5194/essd-2019-128
Preprint. Discussion started: 19 August 2019

Y. Yokouchi, D. Young, and L. Zhou: History of chemically and radiatively important atmospheric gases from the Advanced Global Atmospheric Gases Experiment (AGAGE), Earth Syst. Sci. Data, 10, 985-1018, https://doi.org/10.5194/essd-10-985-2018, 2018.

Ramachandran, P., Ramachandran, R., and Frenzel, P.: Plant-mediated methane emission from an Indian mangrove Purvaja, Global Change Biology, doi:10, 1825-1834, 10.1111/j.1365-2486.2004.00834.x, 2004.

Ramankutty, N., and Foley, J. A.: Estimating historical changes in global land cover: Croplands from 1700 to 1992, Global Biogeochemical Cycles, 13, 997-1027, doi:10.1029/1999GB900046, 1999.

Randel, W. J., Wu, F., Russell, J. M., Roche, A., and Waters, J. W.: Seasonal Cycles and QBO Variations in Stratospheric CH_4 and H_2O Observed in UARS HALOE Data, Journal of the Atmospheric Sciences, 55, 163-185, doi:10.1175/1520-0469(1998)055<0163:SCAQVI>2.0.CO;2, 1998.

Randerson, J. T., Chen, Y., van der Werf, G. R., Rogers, B. M., and Morton, D. C.: Global burned area and biomass burning emissions from small fires, Journal of Geophysical Research: Biogeosciences, 117, G04012, doi:10.1029/2012jg002128, 2012.

Raymond, P. A., Hartmann, J., Lauerwald, R., Sobek, S., McDonald, C., Hoover, M., Butman, D., Striegl, R., Mayorga, E., Humborg, C., Kortelainen, P., Dürr, H., Meybeck, M., Ciais, P., and Guth, P.: Global carbon dioxide emissions from inland waters, Nature, 503, doi:10.1038/nature12760, 2013.

Reeburgh, W. S., and Heggie, D. T.: Microbial methane consumption reactions and their effect on methane distributions in freshwater and marine environments, Limnology and Oceanography, 22, 1-9, doi:10.4319/lo.1977.22.1.0001, 1977.

Reeburgh, W. S.: Oceanic Methane Biogeochemistry, Chemical Reviews, 107, 486-513, doi:10.1021/cr050362v, 2007.

Ren, W. E. I., Tian, H., Xu, X., Liu, M., Lu, C., Chen, G., Melillo, J., Reilly, J., and Liu, J.: Spatial and temporal patterns of CO2 and CH4 fluxes in China's croplands in response to multifactor environmental changes, Tellus B, 63, 222-240, doi:10.1111/j.1600-0889.2010.00522.x, 2011.

Repeta, D. J., Ferrón, S., Sosa, O. A., Johnson, C. G., Repeta, L. D., Acker, M., DeLong, E. F., and Karl, D. M.: Marine methane paradox explained by bacterial degradation of dissolved organic matter, Nature Geoscience, 9, 884, doi:10.1038/ngeo2837, 2016.

Rhee, T. S., Kettle, A. J., and Andreae, M. O.: Methane and nitrous oxide emissions from the ocean: A reassessment using basin-wide observations in the Atlantic, Journal of Geophysical Research-Atmospheres, 114, D12304, doi:10.1029/2008jd011662, 2009.

Rice, A. L., Butenhoff, C. L., Shearer, M. J., Teama, D., Rosenstiel, T. N., and Khalil, M. A. K.: Emissions of anaerobically produced methane by trees, Geophysical Research Letters, 37, L03807, doi:10.1029/2009GL041565, 2010.

https://doi.org/10.5194/essd-2019-128
Preprint. Discussion started: 19 August 2019

Rice, A. L., Butenhoff, C. L., Teama, D. G., Röger, F. H., Khalil, M. A. K., and Rasmussen, R. A.: Atmospheric methane isotopic record favors fossil sources flat in 1980s and 1990s with recent increase, Proceedings of the National Academy of Sciences, doi:201522923, 10.1073/pnas.1522923113, 2016.

Ridgwell, A. J., Marshall, S. J., and Gregson, K.: Consumption of atmospheric methane by soils: A process-based model, Global Biogeochemical Cycles, 13, 59-70, doi:10.1029/1998gb900004, 1999.

Rigby, M., Prinn, R. G., Fraser, P. J., Simmonds, P. G., Langenfelds, R. L., Huang, J., Cunnold, D. M., Steele, L. P., Krummel, P. B., Weiss, R. F., O'Doherty, S., Salameh, P. K., Wang, H. J., Harth, C. M., Mühle, J., and Porter, L. W.: Renewed growth of atmospheric methane, Geophysical Research Letters, 35, L22805, doi:10.1029/2008gl036037, 2008.

Rigby, M., Montzka, S. A., Prinn, R. G., White, J. W. C., Young, D., O'Doherty, S., Lunt, M. F., Ganesan, A. L., Manning, A. J., Simmonds, P. G., Salameh, P. K., Harth, C. M., Mühle, J., Weiss, R. F., Fraser, P. J., Steele, L. P., Krummel, P. B., McCulloch, A., and Park, S.: Role of atmospheric oxidation in recent methane growth, Proceedings of the National Academy of Sciences, 114, 5373, 2017.

Riley, W. J., Subin, Z. M., Lawrence, D. M., Swenson, S. C., Torn, M. S., Meng, L., Mahowald, N. M., and Hess, P.: Barriers to predicting changes in global terrestrial methane fluxes: analyses using CLM4Me, a methane biogeochemistry model integrated in CESM, Biogeosciences, 8, 1925-1953, doi:10.5194/bg-8-1925-2011, 2011.

Ringeval, B., Friedlingstein, P., Koven, C., Ciais, P., de Noblet-Ducoudre, N., Decharme, B., and Cadule, P.: Climate-CH_4 feedback from wetlands and its interaction with the climate-CO_2 feedback, Biogeosciences, 8, 2137-2157, doi:10.5194/bg-8-2137-2011, 2011.

Ringeval, B., Houweling, S., van Bodegom, P. M., Spahni, R., van Beek, R., Joos, F., and Röckmann, T.: Methane emissions from floodplains in the Amazon Basin: challenges in developing a process-based model for global applications, Biogeosciences, 11, 1519-1558, doi:10.5194/bg-11-1519-2014, 2014.

Röckmann, T., Brass, M., Borchers, R., and Engel, A.: The isotopic composition of methane in the stratosphere: high-altitude balloon sample measurements, Atmospheric Chemistry and Physics, 11, 13,287-213,304, doi:10.5194/acp-11-13287-2011, 2011.

Rosentreter, J. A., Maher, D. T., Erler, D. V., Murray, R. H., and Eyre, B. D.: Methane emissions partially offset "blue carbon" burial in mangroves, Science Advances, 4, eaao4985, doi:10.1126/sciadv.aao4985, 2018.

Rossi, S., Tubiello, F. N., Prosperi, P., Salvatore, M., Jacobs, H., Biancalani, R., House, J. I., and Boschetti, L.: FAOSTAT estimates of greenhouse gas emissions from biomass and peat fires, Climatic Change, 135, 699-711, doi:10.1007/s10584-015-1584-y, 2016.

https://doi.org/10.5194/essd-2019-128
Preprint. Discussion started: 19 August 2019

Saad, K. M., Wunch, D., Deutscher, N. M., Griffith, D. W. T., Hase, F., De Mazière, M., Notholt, J., Pollard, D. F., Roehl, C. M., Schneider, M., Sussmann, R., Warneke, T., and Wennberg, P. O.: Seasonal variability of stratospheric methane: implications for constraining tropospheric methane budgets using total column observations, Atmos. Chem. Phys., 16, 14003-14024, doi:10.5194/acp-16-14003-2016, 2016.

Saad, K. M., Wunch, D., Toon, G. C., Bernath, P., Boone, C., Connor, B., Deutscher, N. M., Griffith, D. W. T., Kivi, R., Notholt, J., Roehl, C., Schneider, M., Sherlock, V., and Wennberg, P. O.: Derivation of tropospheric methane from TCCON CH_4 and HF total column observations, Atmospheric Measurement Technologies, 7, 2907-2918, doi:10.5194/amt-7-2907-2014, 2014.

Sanderson, M. G.: Biomass of termites and their emissions of methane and carbon dioxide: A global database, Global Biogeochemical Cycles, 10, 543-557, doi:10.1029/96gb01893, 1996.

Santini, M., and Di Paola, A.: Changes in the world rivers' discharge projected from an updated high resolution dataset of current and future climate zones, Journal of Hydrology, 531, 768-780, 2015.

Sasakawa, M., Shimoyama, K., Machida, T., Tsuda, N., Suto, H., Arshinov, M., Davydov, D., Fofonov, A., Krasnov, O., Saeki, T., Koyama, Y., and Maksyutov, S.: Continuous measurements of methane from a tower network over Siberia, Tellus B, 62, 403-416, doi:10.1111/j.1600-0889.2010.00494.x, 2010.

Sasakawa, M., Tsunogai, U., Kameyama, S., Nakagawa, F., Nojiri, Y., and Tsuda, A.: Carbon isotopic characterization for the origin of excess methane in subsurface seawater, Journal of Geophysical Research: Oceans, 113, C03012, doi:10.1029/2007jc004217, 2008.

Saunois, M., Bousquet, P., Poulter, B., Peregon, A., Ciais, P., Canadell, J. G., Dlugokencky, E. J., Etiope, G., Bastviken, D., Houweling, S., Janssens-Maenhout, G., Tubiello, F. N., Castaldi, S., Jackson, R. B., Alexe, M., Arora, V. K., Beerling, D. J., Bergamaschi, P., Blake, D. R., Brailsford, G., Brovkin, V., Bruhwiler, L., Crevoisier, C., Crill, P., Covey, K., Curry, C., Frankenberg, C., Gedney, N., Höglund-Isaksson, L., Ishizawa, M., Ito, A., Joos, F., Kim, H. S., Kleinen, T., Krummel, P., Lamarque, J. F., Langenfelds, R., Locatelli, R., Machida, T., Maksyutov, S., McDonald, K. C., Marshall, J., Melton, J. R., Morino, I., Naik, V., O'Doherty, S., Parmentier, F. J. W., Patra, P. K., Peng, C., Peng, S., Peters, G. P., Pison, I., Prigent, C., Prinn, R., Ramonet, M., Riley, W. J., Saito, M., Santini, M., Schroeder, R., Simpson, I. J., Spahni, R., Steele, P., Takizawa, A., Thornton, B. F., Tian, H., Tohjima, Y., Viovy, N., Voulgarakis, A., van Weele, M., van der Werf, G. R., Weiss, R., Wiedinmyer, C., Wilton, D. J., Wiltshire, A., Worthy, D., Wunch, D., Xu, X., Yoshida, Y., Zhang, B., Zhang, Z., and Zhu, Q.: The global methane budget 2000–2012, Earth Syst. Sci. Data, 8, 697-751, doi :10.5194/essd-8-697-2016, 2016.

https://doi.org/10.5194/essd-2019-128
Preprint. Discussion started: 19 August 2019

Saunois, M., Bousquet, P., Poulter, B., Peregon, A., Ciais, P., Canadell, J. G., Dlugokencky, E. J., Etiope, G., Bastviken, D., Houweling, S., Janssens-Maenhout, G., Tubiello, F. N., Castaldi, S., Jackson, R. B., Alexe, M., Arora, V. K., Beerling, D. J., Bergamaschi, P., Blake, D. R., Brailsford, G., Bruhwiler, L., Crevoisier, C., Crill, P., Covey, K., Frankenberg, C., Gedney, N., Höglund-Isaksson, L., Ishizawa, M., Ito, A., Joos, F., Kim, H. S., Kleinen, T., Krummel, P., Lamarque, J. F., Langenfelds, R., Locatelli, R., Machida, T., Maksyutov, S., Melton, J. R., Morino, I., Naik, V., O'Doherty, S., Parmentier, F. J. W., Patra, P. K., Peng, C., Peng, S., Peters, G. P., Pison, I., Prinn, R., Ramonet, M., Riley, W. J., Saito, M., Santini, M., Schroeder, R., Simpson, I. J., Spahni, R., Takizawa, A., Thornton, B. F., Tian, H., Tohjima, Y., Viovy, N., Voulgarakis, A., Weiss, R., Wilton, D. J., Wiltshire, A., Worthy, D., Wunch, D., Xu, X., Yoshida, Y., Zhang, B., Zhang, Z., and Zhu, Q.: Variability and quasi-decadal changes in the methane budget over the period 2000–2012, Atmos. Chem. Phys., 17, 11135-11161, doi:10.5194/acp-17-11135-2017, 2017.

Saunois, M., Stavert, A., Poulter, B., Bousquet, P., Canadell, J. G., Jackson, R. B., Raymond, P.A., Dlugokencky, E.J., Houweling, S., Patra, P.K., Ciais., P., Arora, V. K., Bastviken, D., Bergamaschi, P., Blake, D. R., Brailsford, G., Bruhwiler, L., Carlson, K. M., Carrol, M., Castaldi, S., Chandra, N., Crevoisier, C., Crill, P.M., Covey, K., Curry, C.L., Etiope, G., Frankenberg, C., Gedney, N., Hegglin, M.I., Höglund-Isaksson, L., Hugelius, G., Ishizawa M., Ito, A., Janssens-Maenhout, G., Jensen, K. M. Joos, F., Kleinen, T., Krummel, P. B., Langenfelds, R. L., Laruelle, G.G, Liu, L., Machida, T., Maksyutov, S., McDonald, K. C., McNorton, J., Miller, P.A., Melton, J.R., Morino, I., Müller, J., Murguia-Flores, F., Naik, V., Niwa, Y., Noce, S., O'Doherty, S., Parker, R.J., Peng, C., Peng, S., Peters, G.P., Prigent, C., Prinn, R., Ramonet, M., Regnier, P., Riley, W. J., Rosentreter, J.A., Segers, A., Simpson, I. J., Shi, H., Smith, S.J, Steele, P.L., Thornton, B.F., Tian, H., Tohjima, Y., Tubiello, F. N., Tsuruta, A., Viovy, N., Voulgarakis, A., Weber, T. S., van Weele, M., van der Werf, G.R., Weiss, R., Worthy, D., Wunch, D., Yin, Y., Yoshida, Y., ZhangW., Zhang, Z., Zhao, Y., Zheng, B., Zhu, Q., Zhu, Q., and Zhuang, Q.: Global Methane Bugdet 2000-2017, doi: 10.18160/GCP-CH4-2019,version 1.0, 2019

Schaefer, H., Fletcher, S. E. M., Veidt, C., Lassey, K. R., Brailsford, G. W., Bromley, T. M., Dlugokencky, E. J., Michel, S. E., Miller, J. B., Levin, I., Lowe, D. C., Martin, R. J., Vaughn, B. H., and White, J. W. C.: A 21st century shift from fossil-fuel to biogenic methane emissions indicated by $^{13}CH_4$, Science, 352, 80-84, doi:10.1126/science.aad2705, 2016.

Schepers, D., Guerlet, S., Butz, A., Landgraf, J., Frankenberg, C., Hasekamp, O., Blavier, J. F., Deutscher, N. M., Griffith, D. W. T., Hase, F., Kyro, E., Morino, I., Sherlock, V., Sussmann, R., and Aben, I.: Methane retrievals from Greenhouse Gases Observing Satellite (GOSAT) shortwave

https://doi.org/10.5194/essd-2019-128
Preprint. Discussion started: 19 August 2019

infrared measurements: Performance comparison of proxy and physics retrieval algorithms, Journal of Geophysical Research: Atmospheres, 117, D10307, doi:10.1029/2012jd017549, 2012.

Schneising, O., Burrows, J. P., Dickerson, R. R., Buchwitz, M., Reuter, M., and Bovensmann, H.: Remote sensing of fugitive methane emissions from oil and gas production in North American tight geologic formations, Earth's Future, 2, 548-558, doi:10.1002/2014EF000265, 2014.

Schroeder, R., McDonald, K. C., Chapman, B., Jensen, K., Podest, E., Tessler, Z., Bohn, T. J., and Zimmerman, R.: Development and evaluation of a multi-year inundated land surface data set derived from active/passive microwave remote sensing data, Remote Sensing, 7, 16,668-616,732, doi:10.3390/rs71215843, 2015.

Schuur, E. A. G., McGuire, A. D., Schadel, C., Grosse, G., Harden, J. W., Hayes, D. J., Hugelius, G., Koven, C. D., Kuhry, P., Lawrence, D. M., Natali, S. M., Olefeldt, D., Romanovsky, V. E., Schaefer, K., Turetsky, M. R., Treat, C. C., and Vonk, J. E.: Climate change and the permafrost carbon feedback, Nature, 520, 171-179, doi:10.1038/nature14338, 2015.

Schwietzke, S., Sherwood, O. A., Bruhwiler, L. M. P., Miller, J. B., Etiope, G., Dlugokencky, E. J., Michel, S. E., Arling, V. A., Vaughn, B. H., White, J. W. C. and Tans, P. P.: Upward revision of global fossil fuel methane emissions based on isotope database, Nature, 538,88-91, doi: 10.1038/nature19797, 2016.

Segers, A.J., & Houweling, S.: Description of the CH_4 Inversion Production Chain, CAMS (Copernicus Atmospheric Monitoring Service) Report, latest version: https://atmosphere.copernicus.eu/sites/default/files/2018-11/CAMS73_2015SC3_D73.2.5.5-2018_201811_production_chain_v1_0.pdf, 2018

Shakhova, N., Semiletov, I., Salyuk, A., Yusupov, V., Kosmach, D., and Gustafsson, Ö.: Extensive Methane Venting to the Atmosphere from Sediments of the East Siberian Arctic Shelf, Science, 327, 1246-1250, doi:10.1126/science.1182221, 2010.

Shakhova, N., Semiletov, I., Leifer, I., Sergienko, V., Salyuk, A., Kosmach, D., Chernykh, D., Stubbs, C., Nicolsky, D., Tumskoy, V., and Gustafsson, O.: Ebullition and storm-induced methane release from the East Siberian Arctic Shelf, Nature Geoscience, 7, 64-70, doi:10.1038/ngeo2007, 2014.

Shakhova, N., Semiletov, I., Sergienko, V., Lobkovsky, L., Yusupov, V., Salyuk, A., Salomatin, A., Chernykh, D., Kosmach, D., Panteleev, G., Nicolsky, D., Samarkin, V., Joye, S., Charkin, A., Dudarev, O., Meluzov, A., and Gustafsson, O.: The East Siberian Arctic Shelf: towards further assessment of permafrost-related methane fluxes and role of sea ice, Philosophical Transactions of the Royal Society of London A: Mathematical, Physical and Engineering Sciences, Philos. T. Roy. Soc. A, 373, 20140451, doi:10.1098/rsta.2014.0451, 2015.

https://doi.org/10.5194/essd-2019-128
Preprint. Discussion started: 19 August 2019

Shindell, D., Kuylenstierna, J. C. I., Vignati, E., van Dingenen, R., Amann, M., Klimont, Z., Anenberg, S. C., Muller, N., Janssens-Maenhout, G., Raes, F., Schwartz, J., Faluvegi, G., Pozzoli, L., Kupiainen, K., Höglund-Isaksson, L., Emberson, L., Streets, D., Ramanathan, V., Hicks, K., Oanh, N. T. K., Milly, G., Williams, M., Demkine, V., and Fowler, D.: Simultaneously Mitigating Near-Term Climate Change and Improving Human Health and Food Security, Science, 335, 183-189, doi:10.1126/science.1210026, 2012.

Shorter, J. H., Mcmanus, J. B., Kolb, C. E., Allwine, E. J., Lamb, B. K., Mosher, B. W., Harriss, R. C., Partchatka, U., Fischer, H., Harris, G. W., Crutzen, P. J., and Karbach, H.-J.: Methane emission measurements in urban areas in Eastern Germany, Journal of Atmospheric Chemistry, 124, 121-140, 1996.

Simpson, I. J., Sulbaek Andersen, M. P., Meinardi, S., Bruhwiler, L., Blake, N. J., Helmig, D., Rowland, F. S., and Blake, D. R.: Long-term decline of global atmospheric ethane concentrations and implications for methane, Nature, 488, 490-494, doi:10.1038/nature11342, 2012.

Simpson, I. J., Thurtell, G. W., Kidd, G. E., Lin, M., Demetriades-Shah, T. H., Flitcroft, I. D., Kanemasu, E. T., Nie, D., Bronson, K. F., and Neue, H. U.: Tunable diode laser measurements of methane fluxes from an irrigated rice paddy field in the Philippines, Journal of Geophysical Research: Atmospheres, 100, 7283-7290, doi:10.1029/94jd03326, 1995.

Smith, L. K., and Lewis, W. M.: Seasonality of methane emissions from five lakes and associated wetlands of the Colorado Rockies, Global Biogeochem Cycles, 6, 323-338, 1992.

Spahni, R., Wania, R., Neef, L., van Weele, M., Pison, I., Bousquet, P., Frankenberg, C., Foster, P. N., Joos, F., Prentice, I. C., and van Velthoven, P.: Constraining global methane emissions and uptake by ecosystems, Biogeosciences, 8, 1643-1665, doi:10.5194/bg-8-1643-2011, 2011.

Stanley, E. H., Casson, N. J., Christel, S. T., Crawford, J. T., Loken, L. C., and Oliver, S. K.: The ecology of methane in streams and rivers: patterns, controls, and global significance, Ecological Monographs, 86, 146-171, doi:10.1890/15-1027, 2016.

Stanley, K. M., Grant, A., O'Doherty, S., Young, D., Manning, A. J., Stavert, A. R., Spain, T. G., Salameh, P. K., Harth, C. M., Simmonds, P. G., Sturges, W. T., Oram, D. E., and Derwent, R. G.: Greenhouse gas measurements from a UK network of tall towers: technical description and first results, Atmos. Meas. Tech., 11, 1437-1458, doi:10.5194/amt-11-1437-2018, 2018.

Stavert, A.et al., in prep, 2019.

Steele, L. P., Fraser, P. J., Rasmussen, R. A., Khalil, M. A. K., Conway, T. J., Crawford, A. J., Gammon, R. H., Masarie, K. A., and Thoning, K. W.: The global distribution of methane in the troposphere, Journal of Atmospheric Chemistry, 5, 125–171, 1987.

https://doi.org/10.5194/essd-2019-128
Preprint. Discussion started: 19 August 2019

Stocker, B. D., Spahni, R., and Joos, F.: DYPTOP: a cost-efficient TOPMODEL implementation to simulate sub-grid spatio-temporal dynamics of global wetlands and peatlands, Geoscientific Model Development, 7, 3089-3110, doi:10.5194/gmd-7-3089-2014, 2014.

Stolper, D. A., Sessions, A. L., Ferreira, A. A., Santos Neto, E. V., Schimmelmann, A., Shusta, S. S., Valentine, D. L., and Eiler, J. M.: Combined 13C–D and D–D clumping in methane: Methods and preliminary results, Geochimica et Cosmochimica Acta, 126, 169-191, doi:10.1016/j.gca.2013.10.045, 2014.

Sweeney, C., Karion, A., Wolter, S., Newberger, T., Guenther, D., Higgs, J. A., Andrews, A. E., Lang, P. M., Neff, D., Dlugokencky, E., Miller, J. B., Montzka, S. A., Miller, B. R., Masarie, K. A., Biraud, S. C., Novelli, P. C., Crotwell, M., Crotwell, A. M., Thoning, K., and Tans, P. P.: Seasonal climatology of CO_2 across North America from aircraft measurements in the NOAA/ESRL Global Greenhouse Gas Reference Network, Journal of Geophysical Research: Atmospheres, 120, 5155-5190, doi:10.1002/2014jd022591, 2015.

Swinnerton, J. W., and Linnenbom, V. J.: Gaseous Hydrocarbons in Sea Water: Determination, Science, 156, 1119-1120, doi:10.1126/science.156.3778.1119, 1967.

Tan, Z and Zhuang, Q. Arctic lakes are continuous methane sources to the atmosphere under warming conditions. Environ. Res. Lett.10 054016 doi:10.1088/1748-9326/10/5/054016, 2015.

Tan, Z., Q. Zhuang, D. K. Henze, C. Frankenberg, E. Dlugokencky, C. Sweeney, A. J. Turner, M. Sasakawa, and T. Machida. Inverse modeling of pan-Arctic methane emissions at high spatial resolution: what can we learn from assimilating satellite retrievals and using different process-based wetland and lake biogeochemical models? Atmos. Chem. Phys., 16, 12649-12666, 2016.

Tan, Z., Zhuang, Q., and Walter Anthony, K.: Modeling methane emissions from arctic lakes: Model development and site-level study, Journal of Advances in Modeling Earth Systems, 7, 459-483, 10.1002/2014MS000344, 2015.

Tans, P., and Zellweger, C.: 17th WMO/IAEA Meeting on Carbon Dioxide, Other Greenhouse Gases and Related Tracers Measurement Techniques, WMO/GAW report 213 (GGMT-2013), 158pp, 2014.

Taylor, P. G., Bilinski, T. M., Fancher, H. R. F., Cleveland, C. C., Nemergut, D. R., Weintraub, S. R., Wieder, W. R., and Townsend, A. R.: Palm oil wastewater methane emissions and bioenergy potential, Nature Climate Change, 4, 151, doi:10.1038/nclimate2154, 2014.

Thompson, R. L., Nisbet, E. G., Pisso, I., Stohl, A., Blake, D., Dlugokencky, E. J., Helmig, D., and White, J. W. C.: Variability in Atmospheric Methane From Fossil Fuel and Microbial Sources Over the Last Three Decades, Geophysical Research Letters, 45, 11,499-411,508, doi:10.1029/2018GL078127, 2018.

https://doi.org/10.5194/essd-2019-128
Preprint. Discussion started: 19 August 2019

Thompson, R. L., Sasakawa, M., Machida, T., Aalto, T., Worthy, D., Lavric, J. V., Lund Myhre, C., and Stohl, A.: Methane fluxes in the high northern latitudes for 2005–2013 estimated using a Bayesian atmospheric inversion, Atmos. Chem. Phys., 17, 3553-3572, doi:10.5194/acp-17-3553-2017, 2017.

Thompson, R. L., Stohl, A., Zhou, L. X., Dlugokencky, E., Fukuyama, Y., Thojima, Y., Kim, S.-Y., Lee, H., Nisbet, E.G., Fisher, R.E., Lowry, D., Weiss, R. F., Prinn, R.G., O'Doherty, S., Young, D., and White, J. W. C.: Methane emissions in East Asia for 2000–2011 estimated using an atmospheric Bayesian inversion, Journal of Geophysical Research Atmosphere, 120, 4352–4369. doi:10.1002/2014JD022394, 2015.

Thoning, K. W., Tans, P. P., and Komhyr, W. D.: Atmospheric carbon dioxide at Mauna Loa Observatory. 2. Analysis of the NOAA GMCC data, 1974,1985, Journal of Geophysical Research, 94, 8549-8565, 1989.

Thorneloe, S. A., Barlaz, M. A., Peer, R., Huff, L. C., Davis, L., and Mangino, J.: Waste management, in: Atmospheric Methane: Its Role in the Global Environment, edited by: Khalil, M., Springer-Verlag, New York, 234–262, 2000.

Thornton, B. F., M. C. Geibel, P. M. Crill, C. Humborg, and C.-M. Mörth, Methane fluxes from the sea to the atmosphere across the Siberian shelf seas, Geophys. Res. Lett., 43, doi:10.1002/ 2016GL068977, 2016a.

Thornton, B. F., M. Wik, and P. M. Crill, Double-counting challenges the accuracy of high-latitude methane inventories, Geophys. Res. Lett., 43, doi:10.1002/2016GL071772, 2016b.

Thornton, J. A., Kercher, J. P., Riedel, T. P., Wagner, N. L., Cozic, J., Holloway, J. S., Dubé, W. P., Wolfe, G. M., Quinn, P. K., Middlebrook, A. M., Alexander, B., and Brown, S. S.: A large atomic chlorine source inferred from mid-continental reactive nitrogen chemistry, Nature, 464, 271-274, doi:10.1038/nature08905, 2010.

Tian, H., Xu, X., Liu, M., Ren, W., Zhang, C., Chen, G., and Lu, C.: Spatial and temporal patterns of CH_4 and N_2O fluxes in terrestrial ecosystems of North America during 1979–2008: application of a global biogeochemistry model, Biogeosciences, 7, 2673-2694, doi:10.5194/bg-7-2673-2010, 2010.

Tian, H., Xu, X., Lu, C., Liu, M., Ren, W., Chen, G., Melillo, J., and Liu, J.: Net exchanges of CO_2, CH_4, and N_2O between China's terrestrial ecosystems and the atmosphere and their contributions to global climate warming, Journal of Geophysical Research: Biogeosciences, 116, G02011, doi:10.1029/2010jg001393, 2011.

Tian, H., Chen, G., Lu, C., Xu, X., Ren, W., Zhang, B., Banger, K., Tao, B., Pan, S., Liu, M., Zhang, C., Bruhwiler, L., and Wofsy, S.: Global methane and nitrous oxide emissions from terrestrial ecosystems due to multiple environmental changes, Ecosystem Health and Sustainability, 1, 1-20, doi:10.1890/ehs14-0015.1, 2015.

https://doi.org/10.5194/essd-2019-128
Preprint. Discussion started: 19 August 2019

Tian, H., Lu, C., Ciais, P., Michalak, A. M., Canadell, J. G., Saikawa, E., Huntzinger, D. N., Gurney, K. R., Sitch, S., Zhang, B., Yang, J., Bousquet, P., Bruhwiler, L., Chen, G., Dlugokencky, E., Friedlingstein, P., Melillo, J., Pan, S., Poulter, B., Prinn, R., Saunois, M., Schwalm, C. R., and Wofsy, S. C.: The terrestrial biosphere as a net source of greenhouse gases to the atmosphere, Nature, 531, 225-228, doi:10.1038/nature16946, 2016.

Tian, H., Yang, J., Xu, R., Lu, C., Canadell, J. G., Davidson, E. A., Jackson, R. B., Arneth, A., Chang, J., Ciais, P., Gerber, S., Ito, A., Joos, F., Lienert, S., Messina, P., Olin, S., Pan, S., Peng, C., Saikawa, E., Thompson, R. L., Vuichard, N., Winiwarter, W., Zaehle, S., and Zhang, B.: Global soil nitrous oxide emissions since the preindustrial era estimated by an ensemble of terrestrial biosphere models: Magnitude, attribution, and uncertainty, Global Change Biology, 25, 640-659, doi:10.1111/gcb.14514, 2019.

Tiwari, Y. K., and Kumar, K. R.: GHG observation programs in India, Asian GAWgreenhouse gases, 3, Korea Meteorological Administration, Chungnam, South Korea, 2012.

Tsuruta, A., Aalto, T., Backman, L., Hakkarainen, J., van der Laan-Luijkx, I. T., Krol, M. C., Spahni, R., Houweling, S., Laine, M., Dlugokencky, E., Gomez-Pelaez, A. J., van der Schoot, M., Langenfelds, R., Ellul, R., Arduini, J., Apadula, F., Gerbig, C., Feist, D. G., Kivi, R., Yoshida, Y., and Peters, W.: Global methane emission estimates for 2000–2012 from CarbonTracker Europe-CH_4 v1.0, Geosci. Model Dev., 10, 1261-1289, https://doi.org/10.5194/gmd-10-1261-2017, 2017.

Tubiello, F. N., Salvatore, M., Rossi, S., Ferrara, A., Fitton, N., and Smith, P.: The FAOSTAT database of greenhouse gas emissions from agriculture, Environmental Research Letters, 8, 015009, doi:10.1088/1748-9326/8/1/015009, 2013.

Tubiello, F. N., Salvatore, M., Rossi, S., Ferrara, A., Fitton, N., and Smith, P.: Greenhouse gas emissions due to agriculture, Environmental Research Letters, 8, 015009, doi: 10.1088/1748-9326/8/1/015009, 2019

Turetsky, M. R., Kotowska, A., Bubier, J., Dise, N. B., Crill, P., Hornibrook, E. R. C., Minkkinen, K., Moore, T. R., Myers-Smith, I. H., Nykänen, H., Olefeldt, D., Rinne, J., Saarnio, S., Shurpali, N., Tuittila, E.-S., Waddington, J. M., White, J. R., Wickland, K. P., and Wilmking, M.: A synthesis of methane emissions from 71 northern, temperate, and subtropical wetlands, Global Change Biology, 20, 2183-2197, doi:10.1111/gcb.12580, 2014.

Turner, A. J., Jacob, D. J., Benmergui, J., Wofsy, S. C., Maasakkers, J. D., Butz, A., Hasekamp, O., and Biraud, S. C.: A large increase in U.S. methane emissions over the past decade inferred from satellite data and surface observations, Geophys. Res. Lett., 43, 2218– 2224, doi:10.1002/2016GL067987, 2016.

https://doi.org/10.5194/essd-2019-128
Preprint. Discussion started: 19 August 2019

Turner, A. J., Frankenberg, C., Wennberg, P. O., and Jacob, D. J.: Ambiguity in the causes for decadal trends in atmospheric methane and hydroxyl, Proceedings of the National Academy of Sciences, doi: 10.1073/pnas.1616020114, 2017.

Turner, A. J., Fung, I., Naik, V., Horowitz, L. W., and Cohen, R. C.: Modulation of hydroxyl variability by ENSO in the absence of external forcing, Proceedings of the National Academy of Sciences, 115, 8931, doi:10.1073/pnas.1807532115, 2018.

Turner, A. J., Frankenberg, C., and Kort, E. A.: Interpreting contemporary trends in atmospheric methane, Proceedings of the National Academy of Sciences, 116, 2805, doi:10.1073/pnas.1814297116, 2019.

Upstill-Goddard, R.C., Barnes, J., Frost, T., Punshon, S., Owens, N.J.P. Methane in the Southern North Sea: low salinity inputs, estuarine removal and atmospheric flux, Global Biogeochemical Cycles 14, 1205–1217, 2000.

USEPA: Global anthropogenic non-CO_2 greenhouse gas emissions: 1990-2020. United States Environmental Protection Agency, Washington D.C., 2006.

USEPA: Office of Atmospheric Programs (6207J), Methane and Nitrous Oxide Emissions From Natural Sources, U.S. Environmental Protection Agency, EPA 430-R-10-001. Washington, DC 20460, Available online at http://nepis.epa.gov/ (last access:), 2010a

USEPA, DRAFT - Greenhouse Gas Emissions Estimation Methodologies for Biogenic Emissions from Selected Source Categories: Solid Waste Disposal Wastewater Treatment Ethanol Fermentation. Submitted by RTI International to the Sector Policies and Programs Division, Measurement Policy Group, US EPA, EPA Contract No. EP-D-06-118, available at: https://www3.epa.gov/ttnchie1/efpac/ghg/GHG_Biogenic_Report_draft_Dec1410.pdf (last access: Nov 21 2016), 2010b.

USEPA: Draft: Global Anthropogenic Non-CO_2 Greenhouse Gas Emissions: 1990-2030. EPA 430-R-03-002, United States Environmental Protection Agency, Washington D.C., 2011.

USEPA: Global Anthropogenic Non-CO_2 Greenhouse Gas Emissions 1990-2030, EPA 430-R-12-006, US Environmental Protection Agency, Washington DC., 2012.

USEPA: Draft Inventory of U.S. Greenhouse gas Emissions and Sinks: 1990-2014. EPA 430-R-16-002. February 2016. U.S. Environmental Protection Agency, Washington, DC, USA, 2016.

Valentine, D. W., Holland, E. A., and Schimel, D. S.: Ecosystem and physiological controls over methane production in northern wetlands, Journal of Geophysical Research, 99, 1563-1571, 1994.

Valentini, R., Arneth, A., Bombelli, A., Castaldi, S., Cazzolla Gatti, R., Chevallier, F., Ciais, P., Grieco, E., Hartmann, J., Henry, M., Houghton, R. A., Jung, M., Kutsch, W. L., Malhi, Y., Mayorga, E., Merbold, L., Murray-Tortarolo, G., Papale, D., Peylin, P., Poulter, B., Raymond, P. A., Santini, M., Sitch, S., Vaglio Laurin, G., van der Werf, G. R., Williams, C. A., and Scholes, R. J.: A full

https://doi.org/10.5194/essd-2019-128
Preprint. Discussion started: 19 August 2019

greenhouse gases budget of Africa: synthesis, uncertainties, and vulnerabilities, Biogeosciences, 11, 381-407, doi:10.5194/bg-11-381-2014, 2014.

van der Werf, G. R., Randerson, J. T., Giglio, L., Collatz, G. J., Mu, M., Kasibhatla, P. S., Morton, D. C., DeFries, R. S., Jin, Y., and van Leeuwen, T. T.: Global fire emissions and the contribution of deforestation, savanna, forest, agricultural, and peat fires (1997-2009), Atmospheric Chemistry and Physics, 10, 11,707-711,735, 2010.

van der Werf, G. R., Randerson, J. T., Giglio, L., van Leeuwen, T. T., Chen, Y., Rogers, B. M., Mu, M., van Marle, M. J. E., Morton, D. C., Collatz, G. J., Yokelson, R. J., and Kasibhatla, P. S.: Global fire emissions estimates during 1997–2016, Earth Syst. Sci. Data, 9, 697-720, doi:10.5194/essd-9-697-2017, 2017.

van Marle, M. J. E., Kloster, S., Magi, B. I., Marlon, J. R., Daniau, A. L., Field, R. D., Arneth, A., Forrest, M., Hantson, S., Kehrwald, N. M., Knorr, W., Lasslop, G., Li, F., Mangeon, S., Yue, C., Kaiser, J. W., and van der Werf, G. R.: Historic global biomass burning emissions for CMIP6 (BB4CMIP) based on merging satellite observations with proxies and fire models (1750–2015), Geosci. Model Dev., 10, 3329-3357, doi:10.5194/gmd-10-3329-2017, 2017.

Vardag, S., Hammer, S., O'Doherty, S., Spain, T., Wastine, B., Jordan, A., and Levin, I.: Comparisons of continuous atmospheric CH_4, CO_2 and N_2O measurements - Results from a travelling instrument campaign at Mace Head, Atmos. Chem. Phys., 14, 8403-8418, 10.5194/acp-14-8403-2014, 2014.

Verpoorter, C., Kutser, T., Seekell, D. A., and Tranvik, L. J.: A global inventory of lakes based on high-resolution satellite imagery, Geophysical Research Letters, 41, 6396-6402, doi:10.1002/2014gl060641, 2014.

Voulgarakis, A., Marlier, M. E., Faluvegi, G., Shindell, D. T., Tsigaridis, K., and Mangeon, S.: Interannual variability of tropospheric trace gases and aerosols: The role of biomass burning emissions, Journal of Geophysical Research: Atmospheres, 120, 7157-7173, doi:10.1002/2014jd022926, 2015.

Voulgarakis, A., Naik, V., Lamarque, J. F., Shindell, D. T., Young, P. J., Prather, M. J., Wild, O., Field, R. D., Bergmann, D., Cameron-Smith, P., Cionni, I., Collins, W. J., Dals√∏ren, S. B., Doherty, R. M., Eyring, V., Faluvegi, G., Folberth, G. A., Horowitz, L. W., Josse, B., MacKenzie, I. A., Nagashima, T., Plummer, D. A., Righi, M., Rumbold, S. T., Stevenson, D. S., Strode, S. A., Sudo, K., Szopa, S., and Zeng, G.: Analysis of present day and future OH and methane lifetime in the ACCMIP simulations, Atmospheric Chemistry and Physics, 13, 2563-2587, doi:10.5194/acp-13-2563-2013, 2013.

https://doi.org/10.5194/essd-2019-128
Preprint. Discussion started: 19 August 2019

Wallmann, K., Pinero, E., Burwicz, E., Haeckel, M., Hensen, C., Dale, A., and Ruepke, L.: The Global Inventory of Methane Hydrate in Marine Sediments: A Theoretical Approach, Energies, 5, 2449-2498, 2012.

Walter Anthony, K., Daanen, R., Anthony, P., Schneider von Deimling, T., Ping, C.-L., Chanton, J. P., and Grosse, G.: Methane emissions proportional to permafrost carbon thawed in Arctic lakes since the 1950s, Nature Geoscience, 9, 679, doi:10.1038/ngeo2795, 2016.

Wang, Z., Deutscher, N. M., Warneke, T., Notholt, J., Dils, B., Griffith, D. W. T., Schmidt, M., Ramonet, M., and Gerbig, C.: Retrieval of tropospheric column-averaged CH_4 mole fraction by solar absorption FTIR-spectrometry using N2O as a proxy, Atmospheric Measurement Techniques, 7, 3295-3305, doi:10.5194/amt-7-3295-2014, 2014.

Wang, Z.-P., Gu, Q., Deng, F.-D., Huang, J.-H., Megonigal, J. P., Yu, Q., Lü, X.-T., Li, L.-H., Chang, S., Zhang, Y.-H., Feng, J.-C., and Han, X.-G., Methane emissions from the trunks of living trees on upland soils, New Phytol., 211, 429-439, doi:10.1111/nph.13909, 2016.

Wang, X., Jacob, D. J., Eastham, S. D., Sulprizio, M. P., Zhu, L., Chen, Q., Alexander, B., Sherwen, T., Evans, M. J., Lee, B. H., Haskins, J. D., Lopez-Hilfiker, F. D., Thornton, J. A., Huey, G. L., and Liao, H.: The role of chlorine in global tropospheric chemistry, Atmos. Chem. Phys., 19, 3981-4003, doi:10.5194/acp-19-3981-2019, 2019a.

Wang, F., Maksyutov, S., Tsuruta, A., Janardanan, R., Ito, A., Sasakawa, M., Machida, T., Morino, I., Yoshida, Y., Kaiser, J. W., Janssens-Maenhout, G., Dlugokencky, E., Mammarella, I., Lavric, J. V., and Matsunaga, T.: Methane emission estimates by the global high-resolution inverse model using national inventories, Remote Sensing, submitted, 2019b.

Wania, R., Melton, J. R., Hodson, E. L., Poulter, B., Ringeval, B., Spahni, R., Bohn, T., Avis, C. A., Chen, G., Eliseev, A. V., Hopcroft, P. O., Riley, W. J., Subin, Z. M., Tian, H., van Bodegom, P. M., Kleinen, T., Yu, Z. C., Singarayer, J. S., Zurcher, S., Lettenmaier, D. P., Beerling, D. J., Denisov, S. N., Prigent, C., Papa, F., and Kaplan, J. O.: Present state of global wetland extent and wetland methane modelling: Methodology of a model inter-comparison project (WETCHIMP), Geoscientific Model Development, 6, 617-641, doi:10.5194/gmd-6-617-2013, 2013.

Wania, R., Ross, I., and Prentice, I. C.: Implementation and evaluation of a new methane model within a dynamic global vegetation model: LPJ-WHyMe v1.3.1, Geosci. Model Dev., 3, 565-584, doi :10.5194/gmd-3-565-2010, 2010.

Wassmann, R., Lantin, R. S., Neue, H. U., Buendia, L. V., Corton, T. M., and Lu, Y.: Characterization of methane emissions in Asia III: Mitigation options and future research needs, Nutrient Cycling in Agroecosystems, 58, 23-36, 2000.

https://doi.org/10.5194/essd-2019-128
Preprint. Discussion started: 19 August 2019

Weber, T., Wiseman, N., and Kock, A.: Global ocean methane emissions constrained by machine learning models". Authors are T. Weber, N. Wiseman, A. Kock., in review in Nature Communication, 2019.

Westbrook, G. K., Thatcher, K. E., Rohling, E. J., Piotrowski, A. M., Pälike, H., Osborne, A. H., Nisbet, E. G., Minshull, T. A., Lanoisellé, M., James, R. H., Hühnerbach, V., Green, D., Fisher, R. E., Crocker, A. J., Chabert, A., Bolton, C., Beszczynska-Möller, A., Berndt, C. and Aquilina, A.: Escape of methane gas from seabed along the West Spitsbergen continental margin, Geophysical research Letters, 36, L15608,doi:10.1029/2009GL039191, 2009.

Whalen, S. C.: Biogeochemistry of Methane Exchange between Natural Wetlands and the Atmosphere, Environmental Engineering Science, 22, 73-94, doi:10.1089/ees.2005.22.73, 2005.

Widhalm, B., Bartsch, A., and Heim, B.: A novel approach for the characterization of tundra wetland regions with C-band SAR satellite data, International Journal of Remote Sensing, 36, 5537-5556, doi:10.1080/01431161.2015.1101505, 2015.

Wiedinmyer, C., Akagi, S. K., Yokelson, R. J., Emmons, L. K., Al-Saadi, J. A., Orlando, J. J., and Soja, A. J.: The Fire INventory from NCAR (FINN): A high resolution global model to estimate the emissions from open burning, Geoscientific Model Development, 4, 625-641, doi:10.5194/gmd-4-625-2011, 2011.

Wiedinmyer, C., Tie, X., Guenther, A., Neilson, R., and Granier, C.: Future Changes in Biogenic Isoprene Emissions: How Might They Affect Regional and Global Atmospheric Chemistry?, Earth Interactions, 10, doi:10-003, doi:10.1175/EI174.1, 2006.

Wik, M., Thornton, B. F., Bastviken, D., MacIntyre, S., Varner, R. K., and Crill, P. M.: Energy input is primary controller of methane bubbling in subarctic lakes, Geophysical Research Letters, 41, 2013GL058510, doi:10.1002/2013gl058510, 2014.

Wik, M., Thornton, B. F., Bastviken, D., Uhlbäck, J., and Crill, P. M.: Biased sampling of methane release from northern lakes: A problem for extrapolation, Geophysical Research Letters, 43, 1256-1262, doi:10.1002/2015gl066501, 2016a.

Wik, M., Varner, R. K., Anthony, K. W., MacIntyre, S., and Bastviken, D.: Climate-sensitive northern lakes and ponds are critical components of methane release, Nature Geoscience, 9, 99-105, doi:10.1038/ngeo2578, 2016b.

Winderlich, J., Chen, H., Gerbig, C., Seifert, T., Kolle, O., Lavrič, J. V., Kaiser, C., Höfer, A., and Heimann, M.: Continuous low-maintenance CO_2/CH_4/H_2O measurements at the Zotino Tall Tower Observatory (ZOTTO) in Central Siberia, Atmospheric Measurement Techniques, 3, 1113-1128, doi:10.5194/amt-3-1113-2010, 2010.

https://doi.org/10.5194/essd-2019-128
Preprint. Discussion started: 19 August 2019

Woodward, G., Gessner, M. O., Giller, P. S., Gulis, V., Hladyz, S., Lecerf, A., Malmqvist, B., McKie, B. G., Tiegs, S. D., Cariss, H., Dobson, M., Elosegi, A., Ferreira, V., Graça, M. A. S., Fleituch, T., Lacoursière, J. O., Nistorescu, M., Pozo, J., Risnoveanu, G., Schindler, M., Vadineanu, A., Vought, L. B.-M., and Chauvet, E.: Continental-Scale Effects of Nutrient Pollution on Stream Ecosystem Functioning, Science, 336, 1438-1440, doi:10.1126/science.1219534, 2012.

Wooster, M. J., Roberts, G., Perry, G. L. W., and Kaufman, Y. J.: Retrieval of biomass combustion rates and totals from fire radiative power observations: FRP derivation and calibration relationships between biomass consumption and fire radiative energy release, Journal of Geophysical Research: Atmospheres, 110, D24311, doi:10.1029/2005jd006318, 2005.

Worden, J. R., Bloom, A. A., Pandey, S., Jiang, Z., Worden, H. M., Walker, T. W., Houweling, S., and Röckmann, T.: Reduced biomass burning emissions reconcile conflicting estimates of the post-2006 atmospheric methane budget, Nature Communications, 8, 2227, doi:10.1038/s41467-017-02246-0, 2017.

Wuebbles, D. J., and Hayhoe, K.: Atmospheric methane and global change, Earth-Science Reviews, 57, 177-210, 2002.

Wunch, D., Toon, G. C., Blavier, J.-F. L., Washenfelder, R. A., Notholt, J., Connor, B. J., Griffith, D. W. T., Sherlock, V., and Wennberg, P. O.: The Total Carbon Column Observing Network, Philosophical Transactions of the Royal Society A, 369, 2087-2112, doi:10.1098/rsta.2010.0240, 2011.

Wunch, D., Toon, G. C., Hedelius, J. K., Vizenor, N., Roehl, C. M., Saad, K. M., Blavier, J. F. L., Blake, D. R., and Wennberg, P. O.: Quantifying the loss of processed natural gas within California's South Coast Air Basin using long-term measurements of ethane and methane, Atmos. Chem. Phys., 16, 14091-14105, doi:10.5194/acp-16-14091-2016, 2016.

Wunch, D., Jones, D. B. A., Toon, G. C., Deutscher, N. M., Hase, F., Notholt, J., Sussmann, R., Warneke, T., Kuenen, J., Denier van der Gon, H., Fisher, J. A., and Maasakkers, J. D.: Emissions of methane in Europe inferred by total column measurements, Atmos. Chem. Phys., 19, 3963-3980, doi:10.5194/acp-19-3963-2019, 2019.

Xu, X. F., Tian, H. Q., Zhang, C., Liu, M. L., Ren, W., Chen, G. S., Lu, C. Q., and Bruhwiler, L.: Attribution of spatial and temporal variations in terrestrial methane flux over North America, Biogeosciences, 7, 3637-3655, doi:10.5194/bg-7-3637-2010, 2010.

Xu, X., and Tian, H.: Methane exchange between marshland and the atmosphere over China during 1949–2008, Global Biogeochemical Cycles, 26, GB2006, doi:10.1029/2010gb003946, 2012.

Yan, X., Akiyama, H., Yagi, K., and Akimoto, H.: Global estimations of the inventory and mitigation potential of methane emissions from rice cultivation conducted using the 2006 Intergovernmental

https://doi.org/10.5194/essd-2019-128
Preprint. Discussion started: 19 August 2019

Panel on Climate Change Guidelines, Global Biogeochemical Cycles, 23, GB2002, doi:10.1029/2008gb003299, 2009.

Yin, Y., Chevallier, F., Ciais, P., Broquet, G., Fortems-Cheiney, A., Pison, I., and Saunois, M.: Decadal trends in global CO emissions as seen by MOPITT, Atmospheric Chemistry and Physics, 15, 13433-13451, doi:10.5194/acp-15-13433-2015, 2015.

Yin, Y., Chevallier, F., Frankenberg, C., Ciais, P., Bousuqet, P., Saunois, M., Zheng, B., Worden, J. R., Bloom, A. A., Parker, R., Jacob, D., J., and Dlugokencky, E. J.: Sources from tropical wetlands and China accelerate methane growth rate since 2010, submitted to PNAS, 2019.

Yoshida, Y., Kikuchi, N., Morino, I., Uchino, O., Oshchepkov, S., Bril, A., Saeki, T., Schutgens, N., Toon, G. C., Wunch, D., Roehl, C. M., Wennberg, P. O., Griffith, D. W. T., Deutscher, N. M., Warneke, T., Notholt, J., Robinson, J., Sherlock, V., Connor, B., Rettinger, M., Sussmann, R., Ahonen, P., Heikkinen, P., Kyrö, E., Mendonca, J., Strong, K., Hase, F., Dohe, S., and Yokota, T.: Improvement of the retrieval algorithm for GOSAT SWIR XCO_2 and XCH_4 and their validation using TCCON data, Atmospheric Measurement Techniques, 6, 1533-1547, doi:10.5194/amt-6-1533-2013, 2013.

Yver Kwok, C., Laurent, O., Guemri, A., Philippon, C., Wastine, B., Rella, C. W., Vuillemin, C., Truong, F., Delmotte, M., Kazan, V., Darding, M., Lebègue, B., Kaiser, C., Xueref-Rémy, I., and Ramonet, M.: Comprehensive laboratory and field testing of cavity ring-down spectroscopy analyzers measuring H_2O, CO_2, CH_4 and CO, Atmos. Meas. Tech., 8, 3867-3892, doi:10.5194/amt-8-3867-2015, 2015.

Zavala-Araiza, D., Lyon, D. R., Alvarez, R. A., Davis, K. J., Harriss, R., Herndon, S. C., Karion, A., Kort, E. A., Lamb, B. K., Lan, X., Marchese, A. J., Pacala, S. W., Robinson, A. L., Shepson, P. B., Sweeney, C., Talbot, R., Townsend-Small, A., Yacovitch, T. I., Zimmerle, D. J., and Hamburg, S. P.: Reconciling divergent estimates of oil and gas methane emissions, Proceedings of the National Academy of Sciences USA 112, 15597-15602, doi:10.1073/pnas.1522126112, 2015.

Zhang, B., and Chen, G. Q.: China's CH_4 and CO_2 Emissions: Bottom-Up Estimation and Comparative Analysis, Ecological Indicators, 47, 112-122, doi:10.1016/j.ecolind.2014.01.022, 2014.

Zhang, G., Zhang, J., Lui, S., Ren, J., Xu, J., Zhang, F. Methane in the Changjiang (Yangtze River) Estuary and its adjacent marine area: riverine input, sediment release and atmospheric fluxes. Biogeochemistry 91, 71–84, 2008.

Zhang, B., Tian, H., Ren, W., Tao, B., Lu, C., Yang, J., Banger, K. and Pan, S.: Methane emissions from global rice fields: Magnitude, Spatiotemporal patterns and environmental controls, Global Biogeochemical Cycles, 30, 1246-1263, doi:10.1002/2016GB005381, 2016a.

https://doi.org/10.5194/essd-2019-128
Preprint. Discussion started: 19 August 2019

Zhang, Z., Zimmermann, N. E., Kaplan, J. O., and Poulter, B.: Modeling spatiotemporal dynamics of global wetlands: comprehensive evaluation of a new sub-grid TOPMODEL parameterization and uncertainties, Biogeosciences, 13, 1387-1408, https://doi.org/10.5194/bg-13-1387-2016, 2016b.

Zhang, Y., Xiao, X., Wu, X., Zhou, S., Zhang, G., Qin, Y., and Dong, J.: A global moderate resolution dataset of gross primary production of vegetation for 2000-2016, Sci Data, 4, 170165-170165, doi:10.1038/sdata.2017.165, 2017a.

Zhang, Zhen, Niklaus E. Zimmermann, Andrea Stenke, Xin Li, Elke L. Hodson, Gaofeng Zhu, Chunlin Huang, and Benjamin Poulter. "Emerging Role of Wetland Methane Emissions in Driving 21st Century Climate Change." Proceedings of the National Academy Sciences 114, no. 36 (September 5, 2017): 9647–52. https://doi.org/10.1073/pnas.1618765114, 2017b

Zhao, Y., Saunois, M., Bousquet, P., Lin, X., Hegglin, M. I., Canadell, J. G., Jackson, R. B., Hauglustaine, D. A., Szopa, S., Stavert, A. R., Abraham, N. L., Archibald, A. T., Bekki, S., Deushi, M., Jöckel, P., Josse, B., Kinnison, D., Kirner, O., Marécal, V., O'Connor, F. M., Plummer, D. A., Revell, L. E., Rozanov, E., Stenke, A., Strode, S., Tilmes, S., Dlugokencky, E. J., and Zheng, B.: Inter-model comparison of global hydroxyl radical (OH) distributions and their impact on atmospheric methane over the 2000-2016 period, Atmos. Chem. Phys. Discuss., 2019, 1-47, 10.5194/acp-2019-281, 2019.

Zheng, B., Chevallier, F., Ciais, P., Yin, Y., and Wang, Y.: On the role of the flaming to smoldering transition in the seasonal cycle of African fire emissions, Geophys. Res. Lett., doi: 10.1029/2018GL079092, 2018a.

Zheng, B., Chevallier, F., Ciais, P., Yin, Y., Deeter, M., Worden, H., Wang, Y. L., Zhang, Q., and He, K. B.: Rapid decline in carbon monoxide emissions and export from East Asia between years 2005 and 2016, Environ. Res. Lett., 13, 044007, doi: 10.1088/1748-9326/aab2b3, 2018b.

Zhu, Q., Liu, J., Peng, C., Chen, H., Fang, X., Jiang, H., Yang, G., Zhu, D., Wang, W., and Zhou, X.: Modelling methane emissions from natural wetlands by development and application of the TRIPLEX-GHG model, Geoscientific Model Development, 7, 981-999, doi:10.5194/gmd-7-981-2014, 2014.

Zhu, Q., Peng, C., Chen, H., Fang, X., Liu, J., Jiang, H., Yang, Y., and Yang, G.: Estimating global natural wetland methane emissions using process modelling: spatio-temporal patterns and contributions to atmospheric methane fluctuations, Global Ecology and Biogeography, 24, 959-972, 2015.

Zhuang, Q., Chen, M., Xu, K., Tang, J., Saikawa, E., Lu, Y., Melillo, J., Prinn, R., and McGuire, A.D..: response of global soil consumption of atmospheric methane to changes in atmospheric climate and

https://doi.org/10.5194/essd-2019-128
Preprint. Discussion started: 19 August 2019

nitrogen deposition: global soil consumption of methane, Global Biogeochemical Cycles, 27, 650-663, doi:10.1002/gbc.20057, 2013.

Zhuang, Q., J. M. Melillo, D. W. Kicklighter, R. G. Prinn, D. A. McGuire, P. A. Steudler, B. S. Felzer, S. Hu. Methane fluxes between terrestrial ecosystems and the atmosphere at northern high latitudes during the past century: A retrospective analysis with a process-based biogeochemistry model, Global Biogeochemical Cycles,18 , GB3010, doi:10.1029/2004GB002239, 2004.

Zona, D., Gioli, B., Commane, R., Lindaas, J., Wofsy, S. C., Miller, C. E., Dinardo, S. J., Dengel, S., Sweeney, C., Karion, A., Chang, R. Y.-W., Henderson, J. M., Murphy, P. C., Goodrich, J. P., Moreaux, V., Liljedahl, A., Watts, J. D., Kimball, J. S., Lipson, D. A., and Oechel, W. C.: Cold season emissions dominate the Arctic tundra methane budget, Proceedings of the National Academy of Sciences of the United States of America, 113, 40-45, doi:10.1073/pnas.1516017113, 2016.

https://doi.org/10.5194/essd-2019-128
Preprint. Discussion started: 19 August 2019

Open Access Earth System Science Data Discussions

Table 1: B-U models and inventories for anthropogenic and biomass burning inventories used in this study. *Due to its limited sectorial breakdown this dataset was not used in Table 3. ^Extended to 2017 for this study as described in Section 3.1.1.

B-U models and inventories	Contribution	Time period (resolution)	Gridded	References
CEDS (country based)	Fossil fuels, Agriculture and waste, Biofuel	1970-2015^ (yearly)	no	(Hoesly et al., 2018)
CEDS (gridded)*	Fossil fuels, Agriculture and waste, Biofuel	1970-2014 (monthly)	0.5x0.5°	(Hoesly et al., 2018)
EDGARv4.2.3	Fossil fuels, Agriculture and waste, Biofuel	1990-2012^ (yearly)	0.1x0.1°	(Janssens-Maenhout et al., 2019)
IIASA GAINS ECLIPSEv6	Fossil fuels, Agriculture and waste, Biofuel	1990-2015^ (1990-2015 yearly, >2015 5-yr interval interpolated to yearly)	0.5x0.5°	(Höglund-Isaksson, 2012)
USEPA	Fossil fuels, Agriculture and waste, Biofuel, Biomass Burning	1990-2030 (10-yr interval, interpolated to yearly)	no	(USEPA, 2012)
FAO-CH4	Agriculture, Biomass Burning	1961-2016^ 1990-2016 (Yearly)	no	(Frederici et al., 2015 ;Tubiello et al., 2014, 2019)
FINNv1.5	Biomass burning	2002-2018 (daily)	1km resolution	(Wiedinmyer et al., 2011)
GFASv1.3	Biomass burning	2003-2016 (daily)	0.1x0.1°	(Kaiser et al., 2012)
GFEDv4.1s	Biomass burning	1997-2017 (monthly)	0.25x0.25°	(Giglio et al., 2013)
QFEDv2.5	Biomass burning	2000-2017 (daily)	0.1x0.1°	(Darmenov, 2015)

https://doi.org/10.5194/essd-2019-128
Preprint. Discussion started: 19 August 2019

Open Access Earth System Science Data Discussions

Table 2: Biogeochemical models that computed wetland emissions used in this study. Runs were performed for the whole period 2000-2017. Models run with prognostic (using their own calculation of wetland areas) and/or diagnostic (using WAD2M) wetland surface areas (see Sect 3.2.1).

Model	Institution	Prognostic	Diagnostic	References
CLASS-CTEM	Environment and Climate Change Canada	y	y	Arora, Melton and Plummer (2018) Melton and Arora (2016)
DLEM	Auburn University	n	y	Tian et al., (2010;2015)
ELM	Lawrence Berkeley National Laboratory	y	y	Riley et al. (2011)
JSBACH	MPI	n	y	**XXX**
JULES	UKMO	y	y	Hayman et al. (2014)
LPJ GUESS	Lund University	n	y	McGuire et al. (2012)
LPJ MPI	MPI	n	y	Kleinen et al. (2012)
LPJ-WSL	NASA GSFC	y	y	Zhang et al. (2016b)
LPX-Bern	University of Bern	y	y	Spahni et al. (2011)
ORCHIDEE	LSCE	y	y	Ringeval et al. (2011)
TEM-MDM	Purdue University	n	y	Zhuang et al. (2004)
TRIPLEX_GHG	UQAM	n	y	Zhu et al., (2014;2015)
VISIT	NIES	y	y	Ito and Inatomi (2012)

https://doi.org/10.5194/essd-2019-128
Preprint. Discussion started: 19 August 2019

Open Access Earth System Science Data Discussions

Table 3: Global methane emissions by source type in Tg CH_4 yr^{-1} from Saunois et al. (2016) (left column pair) and for this work using bottom-up and top-down approaches). Because top-down models cannot fully separate individual processes, only five categories of emissions are provided (see text). Uncertainties are reported as [min-max] range of reported studies. Differences of 1 Tg CH_4 yr^{-1} in the totals can occur due to rounding errors.

	Saunois et al. (2016)		This work					
Period of time	**2000-2009**		**2000-2009**		**2008-2017**		**2017**	
Approaches	**bottom-up**	**top-down**	**bottom-up**	**top-down**	**bottom-up**	**top-down**	**bottom-up**	**top-down**
NATURAL SOURCES	**382** [255-519]	**234** [194-292]	**369** [245-485]	**214** [176-243]	**371** [245-488]	**215** [176-248]	**367** [243-489]	**228** [183-266]
Natural wetlands	**183** [151-222]	**166** [125-204]	**147** [102-179]	**180** [153-196]	**149** [102-182]	**178** [155-200]	**145** [100-183]	**189** [155-217]
Other natural sources	**199** [104-297]	**68** [21-130]	**222** [143-306]	**35** [21-47]	**222** [143-306]	**37** [21-50]	**222** [143-306]	**39** [21-50]
Other land sources	**185** [99-272]		**209** [134-284]					
Freshwaters [a]	122 [60-180]		159 [117-212]					
Geological (onshore)	40 [30-56]		38 [13-53]					
Wild animals	10 [5-15]		2 [1-3]					
Termites	9 [3-15]		9 [3-15]					
Wildfires	3 [1-5]		(**)					
Permafrost soils (direct)	1 [0-1]		1 [0-1]					
Vegetation	(*)		(*)					
Oceanic sources	**14** [5-25]		**13** [9-22]					
Geological (offshore)	12 [5-20]		7 [5-12]					
Biogenic open and coastal [b]	2 [0-5]		6 [4-10]					
ANTHROPOGENIC SOURCES	**338** [329-342]	**319** [255-357]	**334** [325-357]	**331** [310-346]	**366** [348-392]	**357** [334-375]	**378** [357-404]	**362** [339-379]
Agriculture and waste	**190** [174-201]	**183** [112-241]	**192** [178-206]	**202** [173-219]	**206** [191-223]	**219** [175-239]	**213** [198-233]	**227** [205-246]
Enteric ferm. & manure	103 [95-109][c]		104 [93-109]		111 [106-116]		115 [110-121]	
Landfills & waste	57 [51-61][c]		60 [55-63]		65 [60-69]		68 [64-73]	
Rice cultivation	29 [23-35][c]		28 [23-34]		30 [25-38]		30 [24-39]	
Fossil fuels	**112** [107-126]	**101** [77-126]	**110** [93-129]	**100** [70-149]	**127** [111-154]	**109** [79-168]	**134** [117-161]	**107** [90-120]
Coal mining	36 [24-43][c]		31 [24-42]		42 [29-60]		43 [31-62]	
Oil & Gas	76 [64-85][cf]		73 [59-85]		79 [66-92]		83 [69-97]	
Industry	-		2 [0-6]		3 [0-7]		3 [0-8]	
Transport	-		4 [1-11]		4 [1-12]		4 [1-13]	
Biomass & biof. burn.	**30** [26-34]	**35** [16-53]	**32** [26-46]	**29** [23-35]	**30** [26-40]	**30** [22-36]	**28** [22-37]	**28** [25-32]
Biomass burning	18 [15-20]		19 [15-32]		17 [14-26]		16 [11-24]	
Biofuel burning	12 [9-14]		12 [9-14]		12 [10-14]		12 [10-14]	
SINKS								
Total chemical loss	**604** [483-738]	**514**[d]	**595** [489-749]	**505** [459-516]		**518** [474-532]		**531** [502-540]
Tropospheric OH	528 [454-617]		553 [476-677]					
Stratospheric loss	51 [16-84]		31 [12-37]					
Tropospheric Cl	25 [13-37]		11 [1-35]					
Soil uptake	**28** [9-47]	**32** [27-38]	**30** [11-49]	**34** [27-41]		**38** [27-45]		**40** [37-47]
Sum of sources	**719** [583-861]	**552** [535-566]	**703** [570-842]	**545** [522-559]	**737** [593-880]	**572** [538-593]	**745** [600-893]	**591** [552-614]

https://doi.org/10.5194/essd-2019-128
Preprint. Discussion started: 19 August 2019

Open Access Earth System Science Data Discussions

Sum of Sinks	**632** [592-785]	**546**[d]	**625** [500-798]	**540** [486-556]	**556** [501-574]	**571** [540-585]
Imbalance		**6**[e]		**4** [-11-36]	**16** [0- 47]	**11** [0- 39]
Atmospheric growth		**6.0** [4.9-6.6]				

(*) uncertain but likely small for upland forest and aerobic emissions, potentially large for forested wetland, but likely included elsewhere

(**) We stop reporting this value to avoid potential double counting with satellite-based products of biomass burning (see Sect. 3.1.5)

a: Freshwater includes lakes, ponds, reservoirs, streams and rivers

b: includes flux from hydrates considered at 0 for this study, includes estuaries

c: For IIASA inventory the breakdown of agriculture and waste (rice, Enteric fermentation & manure, Landfills & waste) and fossil fuel (coal, oil, gas & industry) sources used the same ratios as the mean of EDGAR and USEPA inventories in Saunois et al. (2016).

d: total sink was deduced from global mass balance and not directly computed in Saunois et al. (2016).

e: computed as the difference of global sink and soil uptake in Saunois et al. (2016).

f: Industry and transport emissions were included in the Oil & Gas category in Saunois et al. (2016)

https://doi.org/10.5194/essd-2019-128
Preprint. Discussion started: 19 August 2019

Open Access Earth System Science Data Discussions

Table 4: Top-down studies used in our new analysis, with their contribution to the decadal and yearly estimates noted. For decadal means, top down studies have to provide at least 8 years of data over the decade to contribute to the estimate.

Model	Institution	Observation used	Time period	Number of inversions	2000-2009	2008-2017	2017	References
Carbon Tracker-Europe CH_4	FMI	Surface stations	2000-2017	1	y	y	y	Tsuruta et al. (2017)
Carbon Tracker-Europe CH_4	FMI	GOSAT NIES L2 v2.72	2010-2017	1	n	y	y	Tsuruta et al. (2017)
GELCA	NIES	Surface stations	2000-2015	1	y	y	n	Ishizawa et al. (2016)
LMDz-PYVAR	LSCE/CEA	Surface stations	2010-2016	2	n	y	n	Yin et al. (2019)
LMDz-PYVAR	LSCE/CEA	GOSAT Leicester	2010-2016	4	n	y	n	Yin et al. (2019)
LMDz-PYVAR	LSCE/CEA	GOSAT Leicester	2010-2017	2	n	y	y	Zheng et al. (2018a, 2018b)
MIROC4-ACTM	JAMSTEC	Surface stations	2000-2016	1	y	y	n	Patra et al. (2016; 2018)
NICAM-TM	NIES	Surface stations	2000-2017	1	y	y	y	Niwa et al. (2017a; 2017b)
NIES-TM-FLEXPART (NTF)	NIES	Surface stations	2000-2017	1	y	y	y	Maksyutov et al. (2019); Wang et al. (2019b)
NIES-TM-FLEXPART (NTF)	NIES	GOSAT NIES L2 v2.72	2010-2017	1	n	y	y	Maksyutov et al. (2019); Wang et al., (2019b)
TM5-CAMS	TNO/VU	Surface stations	2000-2017	1	y	y	y	Segers and Houwelling (2018); Bergamaschi et al. (2010; 2013), Pandey et al. (2016)
TM5-CAMS	TNO/VU	GOSAT ESA/CCI v2.3.8	2010-2017	1	n	y	y	Segers and Houwelling (2018,report); Bergamaschi et al.

https://doi.org/10.5194/essd-2019-128
Preprint. Discussion started: 19 August 2019

								(2010; 2013), Pandey et al. (2016)
TM5-4DVAR	EC-JRC	Surface stations	2000-2017	2	y	y	y	Bergamaschi et al. (2013, 2018)
TM5-4DVAR	EC-JRC	GOSAT OCPR v7.2	2010-2017	2	n	y	y	Bergamaschi et al. (2013, 2018)
TOMCAT	Uni. of Leeds	Surface stations	2003-2015	1	n	y	n	McNorton et al. (2018)

https://doi.org/10.5194/essd-2019-128
Preprint. Discussion started: 19 August 2019

Open Access Earth System Science Data Discussions

Table 5: Global and latitudinal total methane emissions in Tg CH_4 yr^{-1}, as decadal means (2000-2009 and 2008-2017) and for the year 2017, for this work using bottom-up and top-down approaches. Global emissions for 2000-2009 are also compared with Saunois et al. (2016) and Kirschke et al. (2013) for top-down and bottom-up approcahes. Latitudinal total emissions for 2000-2009 are compared with Saunois et al. (2016) for top-down studies only. Uncertainties are reported as [min-max] range. Differences of 1 Tg CH_4 yr^{-1} in the totals can occur due to rounding errors.

Period	**2000-2009**		**2008-2017**		**2017**	
Approach	**Bottom-up**	**Top-down**	**Bottom-up**	**Top-down**	**Bottom-up**	**Top-down**
Global						
This work	**703** [570-842]	**545** [522-559]	**737** [593-880]	**572** [538-593]	**745** [600-893]	**591** [552-614]
Saunois et al. (2016)	*719 [583-861]*	*552 [535-566]*	-	-	-	-
Kirschke et al. (2013)	*678 [542-852]*	*553 [526-569]*	-	-	-	-
90°S-30°N						
This work	**410** [336-522]	**346** [320-379]	**430** [357-544]	**366** [321-399]	**435** [362-552]	**379** [332-405]
Saunois et al. (2016)	-	356 [334-381]	-	-	-	-
30°N-60°N						
This work	**250** [205-330]	**178** [159-199]	**268** [223-346]	**185** [166-204]	**276** [230-352]	**187** [171-202]
Saunois et al. (2016)	-	176 [159-195]	-	-	-	-
60°N-90°N						
This work	**41** [29-65]	**23** [17- 32]	**39** [26-63]	**22** [17- 29]	**36** [24- 60]	**24** [20- 28]
Saunois et al. (2016)	-	20 [15-25]	-	-	-	-

https://doi.org/10.5194/essd-2019-128
Preprint. Discussion started: 19 August 2019

Open Access Earth System Science Data Discussions

Table 6: Latitudinal methane emissions in Tg CH_4 yr^{-1} for the last decade 2008-2017, based on top-down and bottom-up approaches. Uncertainties are reported as [min-max] range of reported studies. Differences of 1 Tg CH_4 yr^{-1} in the totals can occur due to rounding errors. For bottom-up approaches, other natural sources (as a result total methane emissions and natural emissions) are not reported here due to a lack of spatial distribution for some sources (freshwater). Bottom-up anthropogenic estimates are based only on the gridded products from EDGARv4.3.2 and GAINS.

Latitudinal band	**< 30°N**		**30°N-60°N**		**60°-90°N**	
Approach	Bottom-up	Top-Down	Bottom-up	Top-Down	Bottom-up	Top-Down
Natural Sources	227 [71-146]	158 [115-189]	115 [71- 193]	41 [29-52]	31 [18- 55]	16 [11-20]
Natural Wetland	115 [71-146]	133 [102-155]	25 [11-44]	32 [24-41]	9 [2-18]	13 [7-16]
Other natural	112 [84-194]	25 [14-36]	90 [60-149]	9 [4-14]	22 [16-37]	3 [0-4]
Anthropogenic sources	203 [202-204]	208 [186-229]	153 [152-153]	144 [117-170]	8 [8-8]	6 [2-10]
Agriculture & Waste	130 [121-137]	139 [127-157]	80 [77-84]	78 [67-87]	1 [1-1]	1 [1-2]
Fossil Fuels	42 [40-46]	47 [37-52]	65 [58-71]	60 [34-85]	7 [6-8]	4 [2-7]
Biomass & biofuel burning	20 [18-22]	22 [18-28]	8 [6-9]	6 [5-8]	1 [0-1]	1 [1-1]
Sum of sources	430 [357-544]	366 [321-399]	268 [223-346]	185 [166-204]	39 [26- 63]	22 [17- 29]

https://doi.org/10.5194/essd-2019-128
Preprint. Discussion started: 19 August 2019

Open Access Earth System Science Data Discussions

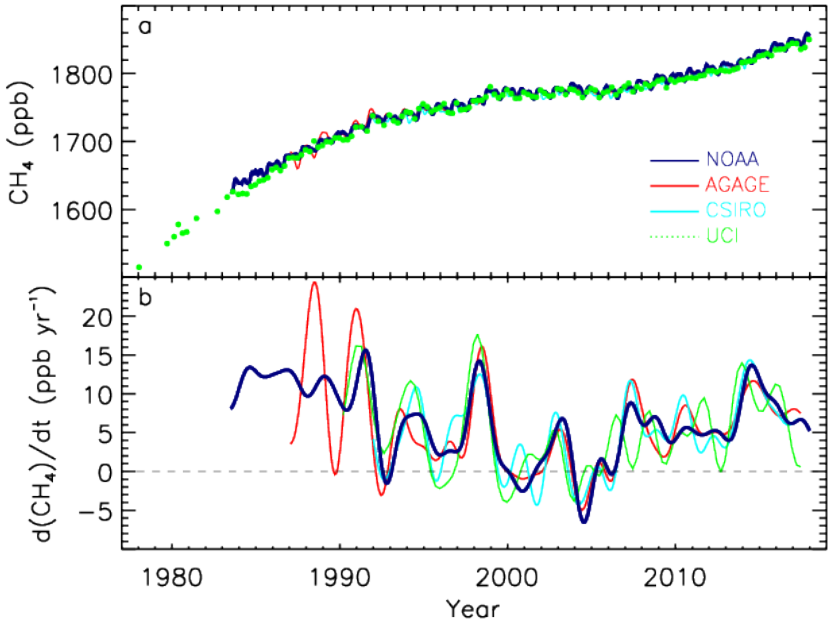

Figure 1: Globally averaged atmospheric CH_4 (ppb) (a) and its annual growth rate G_{ATM} (ppb yr^{-1}) (b) from four measurement programs, National Oceanic and Atmospheric Administration (NOAA), Advanced Global Atmospheric Gases Experiment (AGAGE), Commonwealth Scientific and Industrial Research Organisation (CSIRO), and University of California, Irvine (UCI). Detailed descriptions of methods are given in the supplementary material of Kirschke et al. (2013).

https://doi.org/10.5194/essd-2019-128
Preprint. Discussion started: 19 August 2019

Open Access Earth System Science Data Discussions

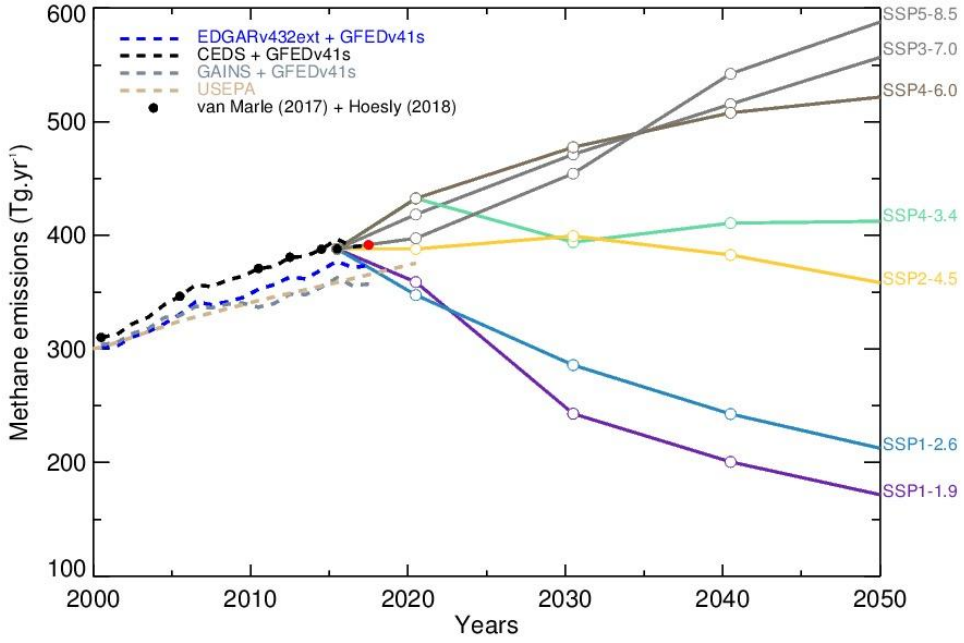

Figure 2: Global anthropogenic methane emissions (including biomass burning) from historical inventories and future projections (in Tg CH_4 yr^{-1}). USEPA and GAINS estimates have been linearly interpolated from the 5-year original products to yearly values. After 2005, USEPA original estimates are projections. The SSP scenarios used in CMIP6 are presented in Gidden et al. (2018). The red marker highlights the emissions in 2017 from the CEDS inventory extended to 2017 for this study.

https://doi.org/10.5194/essd-2019-128
Preprint. Discussion started: 19 August 2019

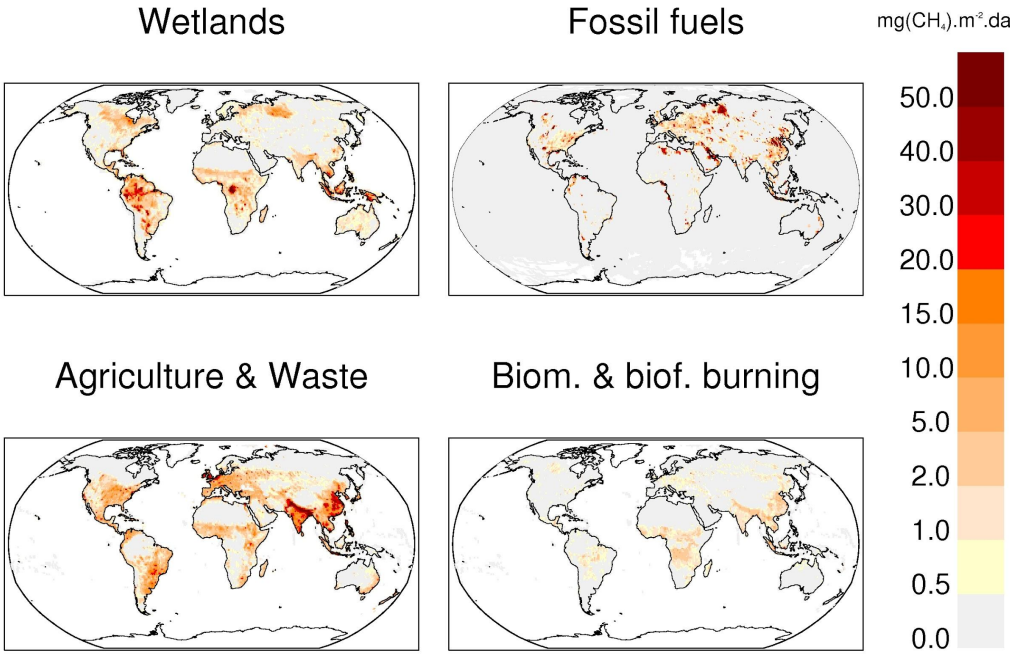

Figure 3: Methane emissions from four source categories: natural wetlands (excluding lakes, ponds, and rivers), biomass and biofuel burning, Agriculture and Waste, and Fossil fuels for the 2008-2017 decade in mg CH_4 m^{-2} day^{-1}. The wetland emission map represents the mean daily emission average over the 13 biogeochemical models listed in Table 2 and over the 2008-2017 decade. Fossil fuel and Agriculture and Waste emission maps are derived from the mean estimates of gridded CEDS, EGDARv4.3.2 and GAINS models. The biomass and biofuel burning map results from the mean of the biomass burning inventories listed in Table 1 added to the mean of the biofuel estimate from CEDS, EDGARv4.3.2 and GAINS models.

https://doi.org/10.5194/essd-2019-128
Preprint. Discussion started: 19 August 2019

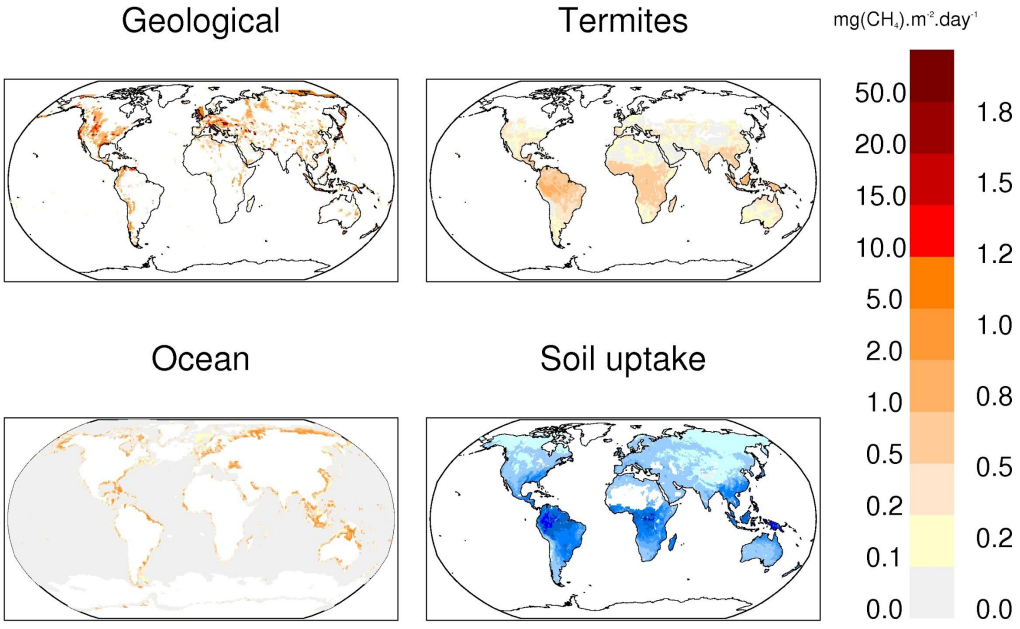

Figure 4: Methane emissions (mg CH_4 m^{-2} day^{-1}) from three natural sources: geological (Etiope et al., 2019), termites (this study) and oceans (Weber et al., 2019), and methane uptake in soils (mg CH_4 m^{-2} day^{-1}) presented in positive units, and based on Murguia-Flores et al. (2018).

https://doi.org/10.5194/essd-2019-128
Preprint. Discussion started: 19 August 2019

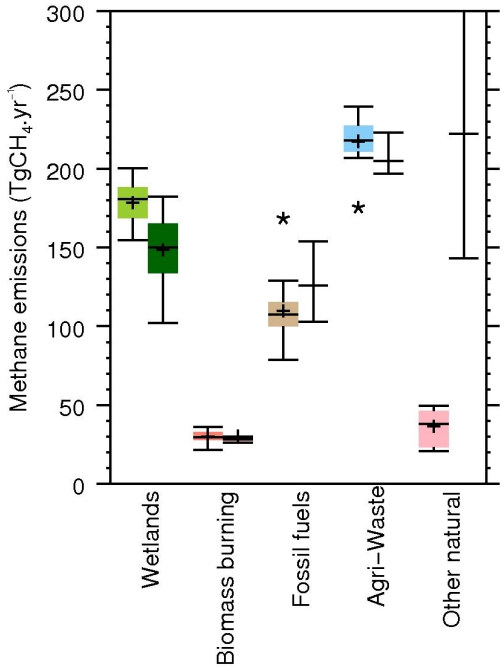

Figure 5: Methane global emissions from the five broad categories (see Sect. 2.3) for the 2008-2017 decade for T-D inversions models (left light coloured boxplots) in Tg CH_4 yr^{-1} and for B-U models and inventories (right dark coloured boxplots). Median value, first and third quartiles are presented in the boxes. The whiskers represent the minimum and maximum values when suspected outliers are removed (see Sect. 2.2). Suspected outliers are marked with stars when existing. B-U quartiles are not available for B-U estimates. Mean values are represented with "+" symbols, these are the values reported in Table 3.

https://doi.org/10.5194/essd-2019-128
Preprint. Discussion started: 19 August 2019

Open Access Earth System Science Data Discussions

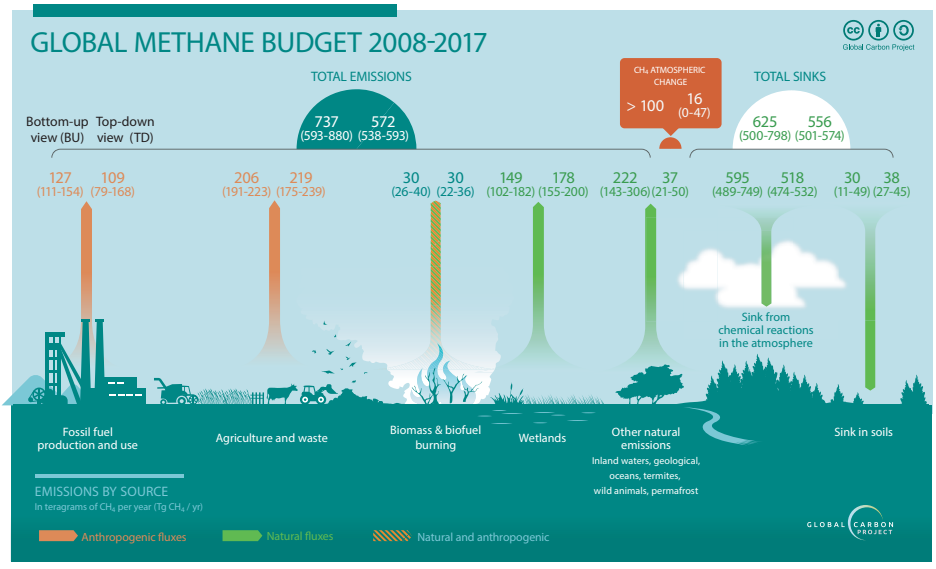

Figure 6: Global Methane Budget for the 2008-2017 decades. Both bottom-up (left) and top-down (right) estimates are provided for each emission and sink category in Tg CH_4 yr^{-1}, as well as for total emissions and total sinks.

https://doi.org/10.5194/essd-2019-128
Preprint. Discussion started: 19 August 2019

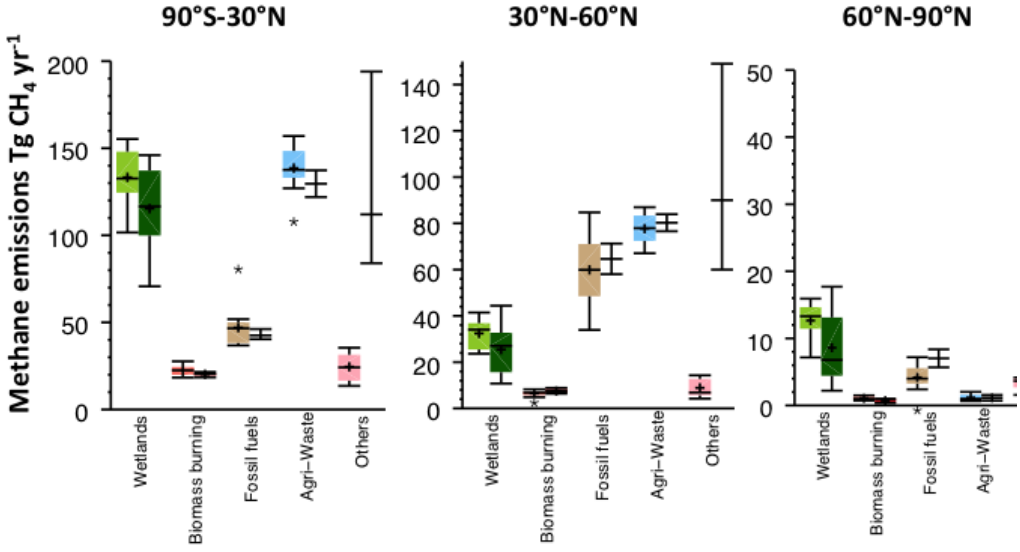

Figure 7: Methane latitudinal emissions from the five broad categories (see Sect. 2.3) for the 2008-2017 decade for top-down inversions models (left light coloured boxplots) in Tg CH_4 yr^{-1} and for bottom-up models and inventories (right dark coloured boxplots). Median value, first and third quartiles are presented in the boxes. The whiskers represent the minimum and maximum values when suspected outliers are removed (see Sect. 2.2). Suspected outliers are marked with stars as shown. B-U quartiles are not available for B-U estimates. Mean values are represented with "+" symbols, these are the values reported in Table 6.